MODELING AND ASSESSMENT OF FLOW AND TRANSPORT IN THE HUECO BOLSON, A TRANSBOUNDARY GROUNDWATER SYSTEM: THE EL PASO/CIUDAD JUAREZ CASE

A Dissertation

by

OKECHUKWU NWANESHIUDU

Submitted to the Office of Graduate Studies of
Texas A&M University
in partial fulfillment of the requirements for the degree of

DOCTOR OF PHILOSOPHY

December 2007

Major Subject: Water Management and Hydrological Sciences

MODELING AND ASSESSMENT OF FLOW AND TRANSPORT IN THE HUECO BOLSON, A TRANSBOUNDARY GROUNDWATER SYSTEM: THE EL PASO/CIUDAD JUAREZ CASE

A Dissertation

by

OKECHUKWU NWANESHIUDU

Submitted to the Office of Graduate Studies of
Texas A&M University
in partial fulfillment of the requirements for the degree of

DOCTOR OF PHILOSOPHY

Approved by:

Co-Chairs of Committee:	Yavuz Corapcioglu
	Hongbin Zhan
Committee Members:	Norris Stubbs
	Suresh Pillai
Intercollegiate Faculty Chair:	Ronald Kaiser

December 2007

Major Subject: Water Management and Hydrological Sciences

ABSTRACT

Modeling and Assessment of Flow and Transport in the Hueco Bolson, a Transboundary Groundwater System: The El Paso/Ciudad Juarez Case. (December 2007)

Okechukwu Nwaneshiudu, B.S., Temple University;

M.S., Texas A&M University

Co-Chairs of Advisory Committee: Dr. Yavuz Corapcioglu
Dr. Hongbin Zhan

Potential contamination from hazardous and solid waste landfills stemming from population increase, rapid industrialization, and the proliferation of assembly plants known as the maquiladoras, are of major concern in the U.S.-Mexican border area. Additionally, historical, current, and future stresses on the Hueco Bolson alluvial aquifer in the El Paso/Ciudad Juarez area due to excessive groundwater withdrawal can affect contaminant migration in the area. In the current study, an updated and improved three-dimensional numerical groundwater flow and transport model is developed using a current Hueco Bolson groundwater availability model as its basis. The model with contaminant transport is required to access and characterize the extent of vulnerability of the aquifer to potential contamination from landfills in the El Paso/Ciudad Juarez border area. The model developed in this study is very capable of serving as the basis of future studies for water availability, water quality, and contamination assessments in the Hueco Bolson.

The implementation of fate and transport modeling and the incorporation of the Visual MODFLOW® pre and post processor, requiring MODFLOW 2000 data

conversion, enabled significant enhancements to the numerical modeling and computing capabilities for the Hueco Bolson. The model in the current research was also developed by employing MT3DMS©, ZONEBUDGET, and Visual PEST® for automated calibrations.

Simulation results found that the Hueco Bolson released more water from storage than the aquifer was being recharged in response to increased pumping to supply the growing border area population. Hence, significant head drops and high levels of drawdown were observed in the El Paso/Ciudad Juarez area. Predictive simulations were completed representing scenarios of potential contamination from the border area sites. Fate and transport results were most sensitive to hydraulic conductivities, flow velocities, and directions at the sites. Sites that were located within the vicinity of the El Paso Valley and the Rio Grande River, where head differences and permeabilities were significant, exhibited the highest potentials for contaminant migration.

DEDICATION

I dedicate this work to God almighty for making everything possible and to my parents and siblings for providing opportunities for me and supporting me.

ACKNOWLEDGMENTS

I am forever in debt to my parents, without whom I would not be where I am currently and to my brothers and sisters for believing in me and supporting me. I would also like to acknowledge my committee co-chairs and members, Dr. Yavuz Corapcioglu, Dr. Hongbin Zhan, Dr. Suresh Pillai, and Dr. Norris Stubbs for their input and suggestions. I also would like to recognize the late Dr. Timothy Kramer, my friends and colleagues, and the praise team at Covenant Family Church in College Station, which I was a part of during my tenure, for encouraging and supporting me along the way. Finally, I would like to acknowledge the Texas A&M Association of Former Students, the Texas Water Resources Institute Research Grant Award program, and the Texas A&M Water Management and Hydrological Sciences interdisciplinary program for providing me with this golden opportunity, for their investment, and their support.

TABLE OF CONTENTS

Page

Page

Page

LIST OF FIGURES

FIGURE Page

FIGURE Page

LIST OF TABLES

1. INTRODUCTION

The challenges of binational transboundary ground and surface water management are clearly illustrated at the U.S.-Mexico border, specifically in the El Paso/Ciudad Juarez border area. Numerous studies [1, 3, 7, 8] have examined issues related to the water resources of this area from technical, political, and economic points of view. Rapid population growth, shared resources, and social conflicts in the area compound the effects of limited water resources, and exemplify the complexities of issues relating to border water management.

1.1 RESEARCH ISSUES

1.1.1 Border area groundwater issues

The U.S.-Mexico border runs approximately 2000 miles from the Gulf of Mexico to the Pacific Ocean. The border area representing the El Paso/Ciudad Juarez area, also known as "Paso del Norte," makes up 15.4 percent of the U.S.-Mexico border area's total population (about two million people) and is located in an arid region with an average annual rainfall of seven inches or less [7]. The communities in El Paso, Chihuahua (Juarez), and New Mexico (southern Dona Ana County) make up the population of the area (Fig. 1) [6]. These communities not only share air, water, land, and ecosystem resources, but do this under different institutional and societal structures and conditions which make binational environmental management complex and challenging.

This dissertation follows the style and format of Acta Odontologica Scandinavica.

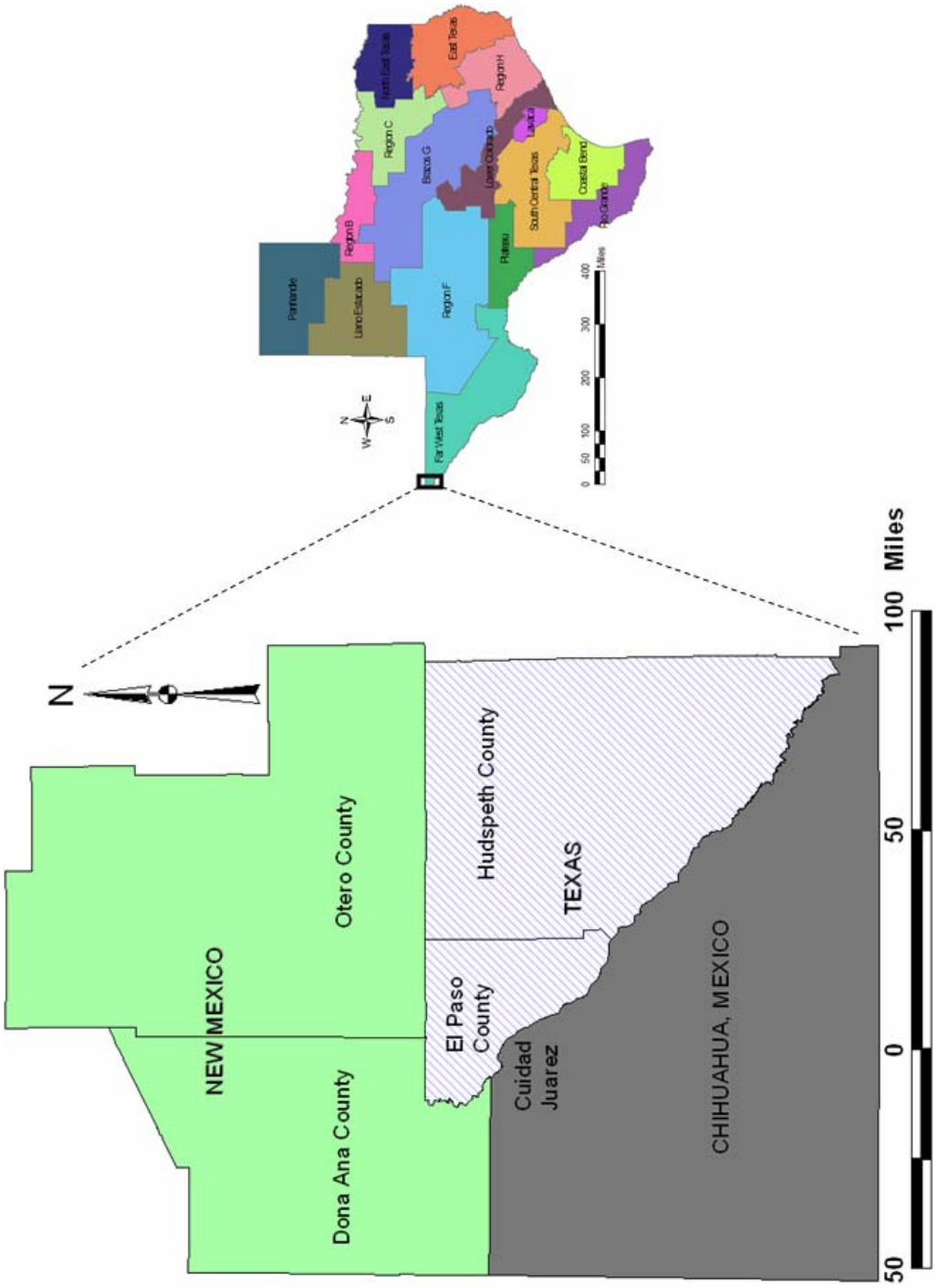

Fig. 1. Study area: Map of the border area of Mexico, Texas, and New Mexico and communities of El Paso, Ciudad Juarez, southern Dona Ana County, and Otero County in the border area [6].

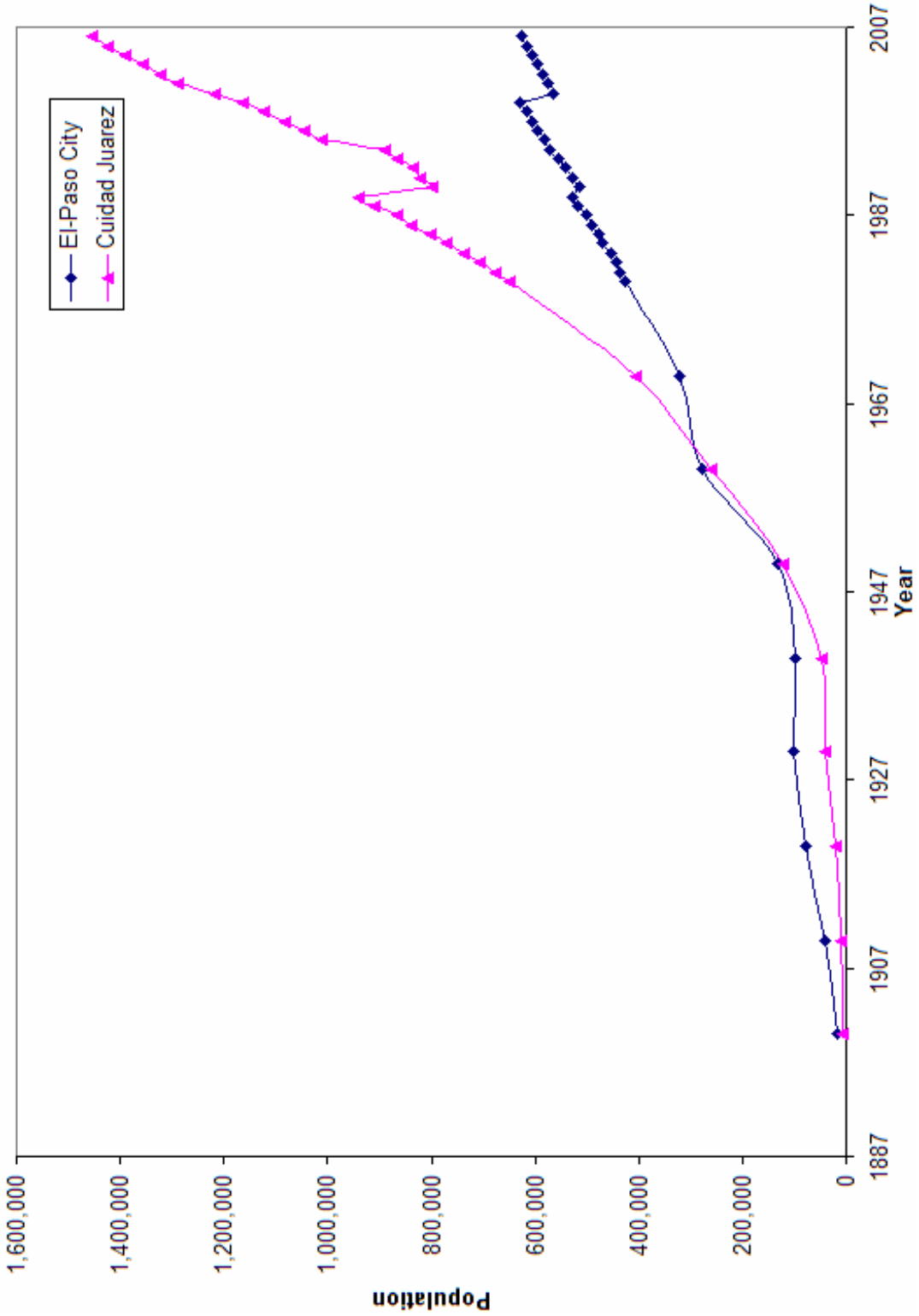

Fig. 2. Growing annual population of the El Paso/Juarez Border Area [1].

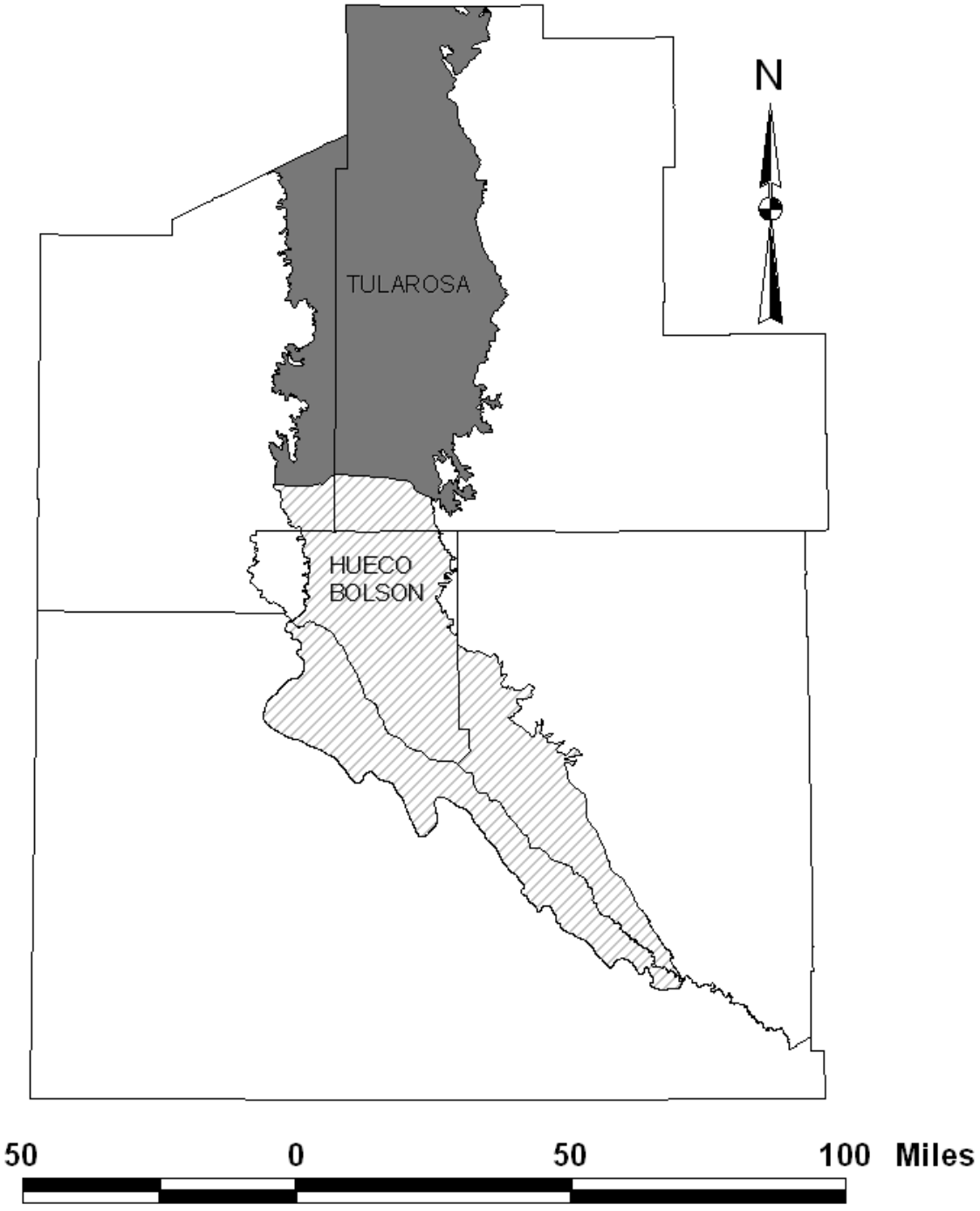

Fig. 3. Study area: Map of the Hueco Bolson and the Tularosa Basin [6]

This border region has also experienced significantly high population growth rates since the early 1900's (Fig. 2). The Hueco Bolson alluvial-aquifer system (Fig. 3), considered the southern portion of the Tularosa-Hueco Basin, which is the main supply source of groundwater to the growing population of the El Paso/Ciudad Juarez area, has been depleted at a dramatic rate [7-9]. Ciudad Juarez depends on the Bolson for the majority (almost 100 percent) of its water supply and, therefore, faces the greatest challenge of both communities. El Paso, on the other hand, has significantly increased its dependence on surface water from the Rio Grande to compliment its reliance on groundwater usage since the 1980s, but is still dependent on the groundwater.

Groundwater overdraft and aquifer depletion remain the main potential problems facing the El Paso-Juarez communities, if the current state of the aquifer is exacerbated. Groundwater overdraft can result in eventual water shortages, subsidence, limited potential for pollution dilution, and poor groundwater quality. Poor groundwater quality in production wells can also lead to the abandonment of these wells resulting in wasted resources. A numerical model in the groundwater management framework is required to properly assess quantity and availability of the Hueco Bolson.

1.1.2 Border area groundwater contamination issues

Industries located along the border area provide the majority of jobs for the border population. The high population growth rates and rapid industrialization of the U.S.-Mexico border have substantiated the need for solid and hazardous waste management infrastructure [3]. In particular, the border area's most thriving industry, the Maquiladoras, comprised of assembly plants which import raw materials into Mexico for

the assembly of finished products, has grown significantly [3]. In the U.S. – Mexico border area, there are a total of 64 landfills in operation for the final disposal of municipal solid wastes (Fig. 4). 59 of these municipal solid waste land fills are located on the U.S. side of the border region, 27 in Texas, 4 in New Mexico, 18 in California, and 10 in Arizona [3]. There are currently 5 municipal solid waste landfills located on the Mexican side of the border, one in each of the Mexican border area's major cities (Nuevo Laredo, Matamoros, Tijuana, Nogales, and Ciudad Juarez). In the El Paso/Ciudad Juarez portion of the U.S. Mexico border area, 7 municipal solid waste disposal landfills currently exist, 6 in El Paso, and 1 in Ciudad Juarez [3]. While a majority of the municipal solid waste land fills are located on the U.S. side, the U.S. EPA imposes stringent regulations on disposal of solid and hazardous waste and operations of disposal sites.

Mexico on the other hand, currently lacks permitted disposal capacity on its side of the border region and environmental laws are less stringent. Additionally, in the El Paso/Ciudad Juarez area, shortages of space in solid waste disposal sites are becoming more prevalent. Another major issue facing the El Paso/Ciudad Juarez border area is pollution from scrap tire disposal at the solid waste disposal sites. Tire pile incinerations in Paso Del Norte also occur due to space limitations at land fills [10]. Threats from air pollution and groundwater pollution are eminent in the Border area. Contamination could occur from solid waste disposal sites, thereby contaminating groundwater resources on both sides of the border. A numerical fate and transport model is required to assess and predict potential patterns of plume migration in this border area and none is currently in place.

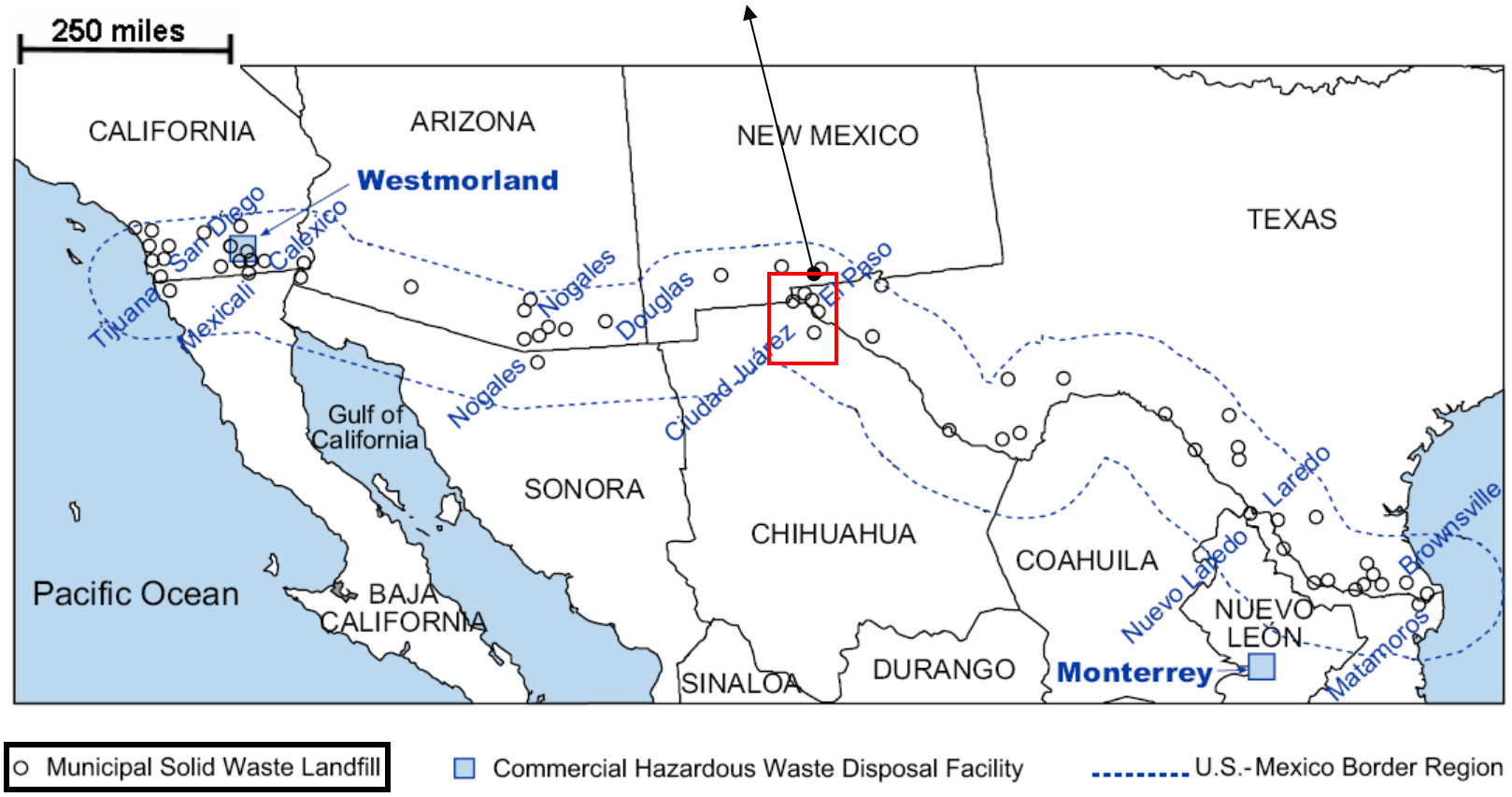

Fig. 4. Hazardous and solid waste disposal facilities in the U.S. Mexico border area (After U.S. EPA [3])

The first Texas state water plan, called "Water for Texas," was developed and adopted in 2002, as a result of the passing of Senate Bill 1, during the 75th Texas Legislature. The Texas GAM (groundwater availability modeling) program for aquifers located within Texas and transboundary aquifers were established under the state water plan. GAMs are used to quantify groundwater availability in aquifers, understand groundwater flow in aquifers, make predictions, and test scenarios. The GAMs were developed using the MODFLOW program. A GAM was developed for the Hueco Bolson aquifer. However, the incorporation of a contaminant transport model hasn't been successful since its creation. Hence, no studies currently exist which examine fate and transport of potential contamination, which could occur from the solid waste landfills located within the border area.

1.2 RESEARCH OBJECTIVES

Potential problems and issues related to groundwater availability and potential groundwater contamination facing the El Paso/Ciudad Juarez border area are addressed in this research. These issues not only involve groundwater management but involve several landfills and hazardous waste sites which are located in the area as shown (Fig. 4). The goals of this research are to assess the fate and transport of contamination which could occur within the El Paso/Ciudad Juarez border region, and assess current and future groundwater availability in the aquifer.

1.2.1 First objective: Development of a numerical groundwater flow model

An improved and updated 3-D 10 layer transient groundwater flow model with 94 annual stress periods (1903 – 1996) will be developed for the Hueco Bolson. The GAM

for the Hueco Bolson will be used as the foundation for the new model developed in this dissertation. The GAM was developed by the United States Geological Survey (USGS) by employing a modified MODFLOW 96 source code and packages due to the problem of dewatered layers. The proposed groundwater flow model seeks to resolve questions such as the following:

1) Can groundwater resources from the Hueco Bolson sustain the water demands of the El Paso/Ciudad Juarez population in the future?
2) Can the Visual MODFLOW pre and post processor and the MODFLOW 2000 code be incorporated into the Hueco Bolson GAM to update and enhance its modeling capabilities?
3) How will the aquifer respond to increased pumping to supply the water needs of the growing populations?
4) Can the proposed flow model be created and calibrated against measured data to enable predictions of future water availability over the next 50 years?

1.2.2 Second objective: Incorporation of a contaminant transport model

A contaminant transport model component will be incorporated into the groundwater flow model to assess fate and transport of potential contamination that could occur within the El Paso/Ciudad Juarez border area. This research objective will address questions such as the following:

1) Given locations of possible contaminations from landfills, can the spatio-temporal pattern of potential groundwater contamination through the year 2050 be predicted using the groundwater transport model?

2) Can possible contaminations from landfills occurring on the U.S. side affect the groundwater resources on the Mexican side or vice versa?
3) What are the driving factors behind potential contaminant plume migration in the El Paso/Ciudad Juarez border area?

1.3 RESEARCH PROCEDURE AND JUSTIFICATION

It is anticipated that accomplishment of the following objectives, which will require successful completion of the proposed groundwater flow and transport model, will involve several steps as follows:

1) Model data: Model input data in the MODFLOW 96 format will be acquired from the GAM and converted to the MODFLOW 2000 format. Additionally, outdated model files and model files not compatible with MODFLOW 2000 will be recreated using the Visual MODFLOW pre and post processor.
2) Model simulations: Preliminary model simulations will be initiated and convergence at the lowest possible criterion will be enabled.
3) Model Calibration: Model calibrations against measured data will be performed to enable valid model predictions.
4) Predictions: Model predictions will be conducted over the 53 year prediction period from 1997 to 2050.
5) Site assignments: Landfills sites will be assigned and contaminant transport simulations will be conducted at each site over the 53 year prediction period.

A new an updated model from the Heuco Bolson GAM is required because numerical models are developed to be transitory tools and should evolve in response to

more accurate information about the aquifers, increasing computational resources, updated modeling codes, and newer model packages that supersede older and out dated model packages. The restrictions of the Heuco Bolson GAM are the lack of ability to perform transport simulations as well outdated input file packages. These limitations will be improved upon in this new model.

The two main objectives of the current modeling effort, involve the implementation of fate and transport modeling, and the incorporation of the Visual MODFLOW© pre and post processor (requiring MODFLOW 2000 input data conversion). These objectives will not only enable significant enhancements to the numerical modeling and computing capabilities for the Hueco Bolson, but also provide needed investigations to access and characterize the extent of vulnerability of the aquifer to potential contamination from landfills in the El Paso/Ciudad Juarez border area.

The current study represents another effort in the line of modeling studies for the Hueco Bolson. The study is the most current modeling effort dealing with water resources and potential contamination of the Hueco Bolson. The objective at this moment was not conduct a very detailed and comprehensive fate and transport model, simply due to lack of defendable field data. However, the model developed in this study is very capable of serving as the basis of future studies, dealing with water availability or water quality that will be performed when needed data is available.

2. BACKGROUND

The Hueco Bolson, Rio Grande, and the Rio Grande alluvial aquifer, major constituents of the border area, have been studied extensively since the early 1900s and several studies [4, 5, 11-13] currently exist which characterize and examine the geology and hydrogeology of these basins.

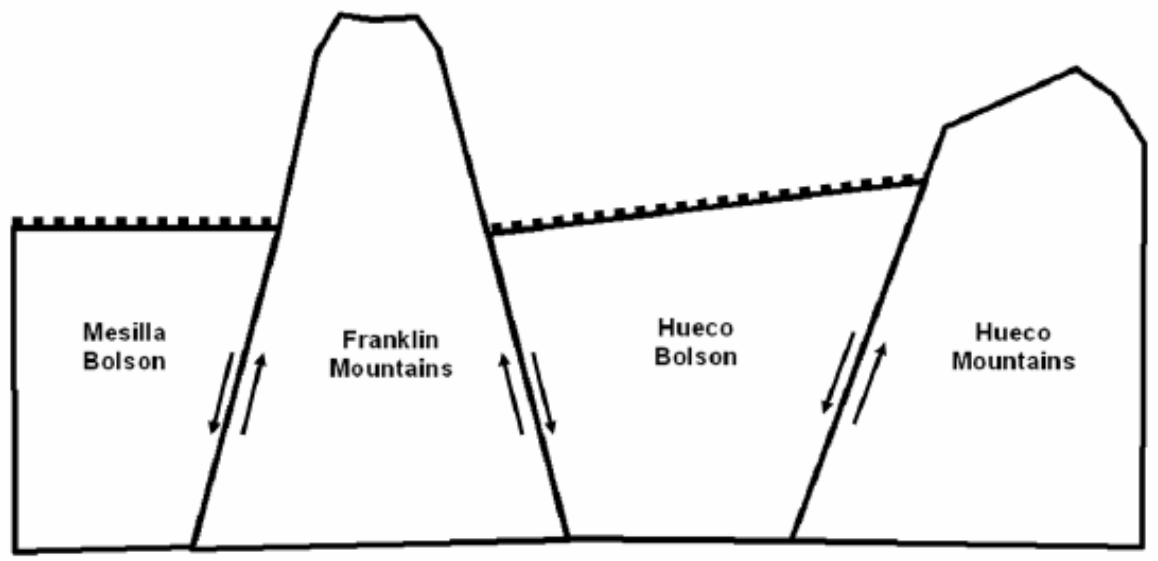

Fig. 5. Basic cross-section of the Hueco Bolson aquifer basin (after Hutchison [13])

2.1 THE HUECO BOLSON

2.1.1 Extent

The Hueco Bolson has been described as a basin-fill type aquifer of varying depth bounded by faults along the Franklin mountains on the west and by faults along the Hueco mountains on the east as can be seen in a basic and simplified cross-section of the area (Fig. 5) [13]. The Hueco Bolson aquifer, which spans an area of about 2,500 square

miles, transcends the boundaries of 3 states in two nations, namely, New Mexico, Texas, and Chihuahua.

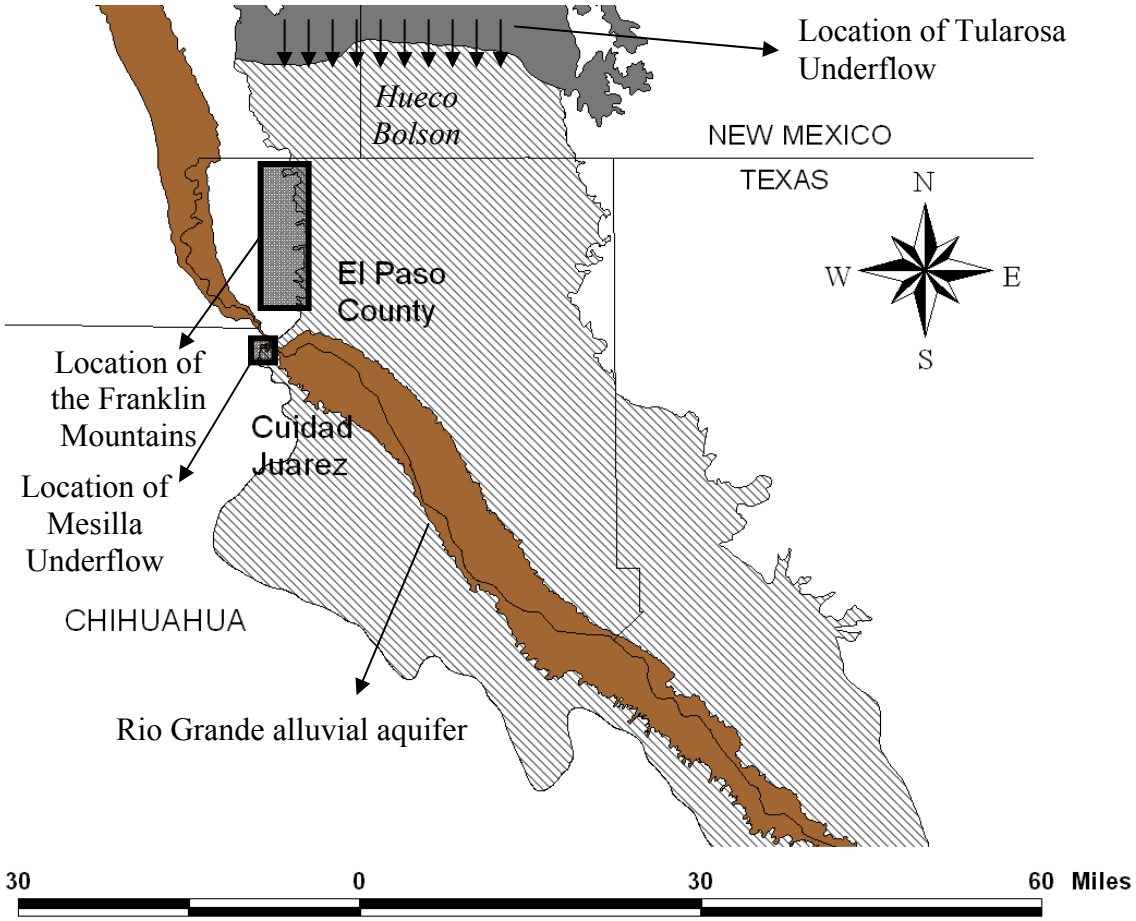

Fig. 6. Map of the Hueco Bolson, Rio Grande alluvium, and location of the Franklin mountains [6].

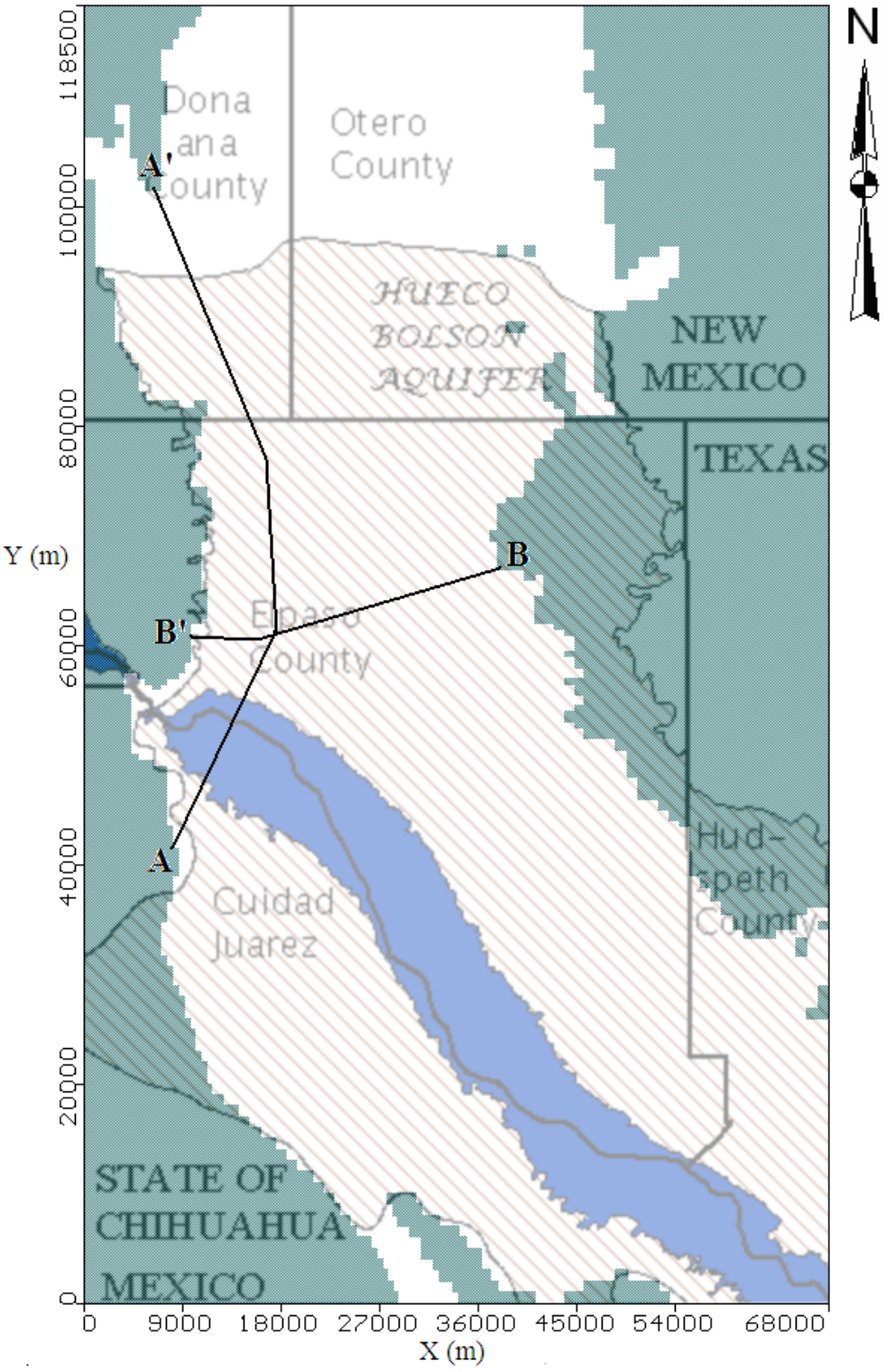

Fig. 7. A-A’ and B-B’ cross-sections of the Hueco Bolson in the model domain

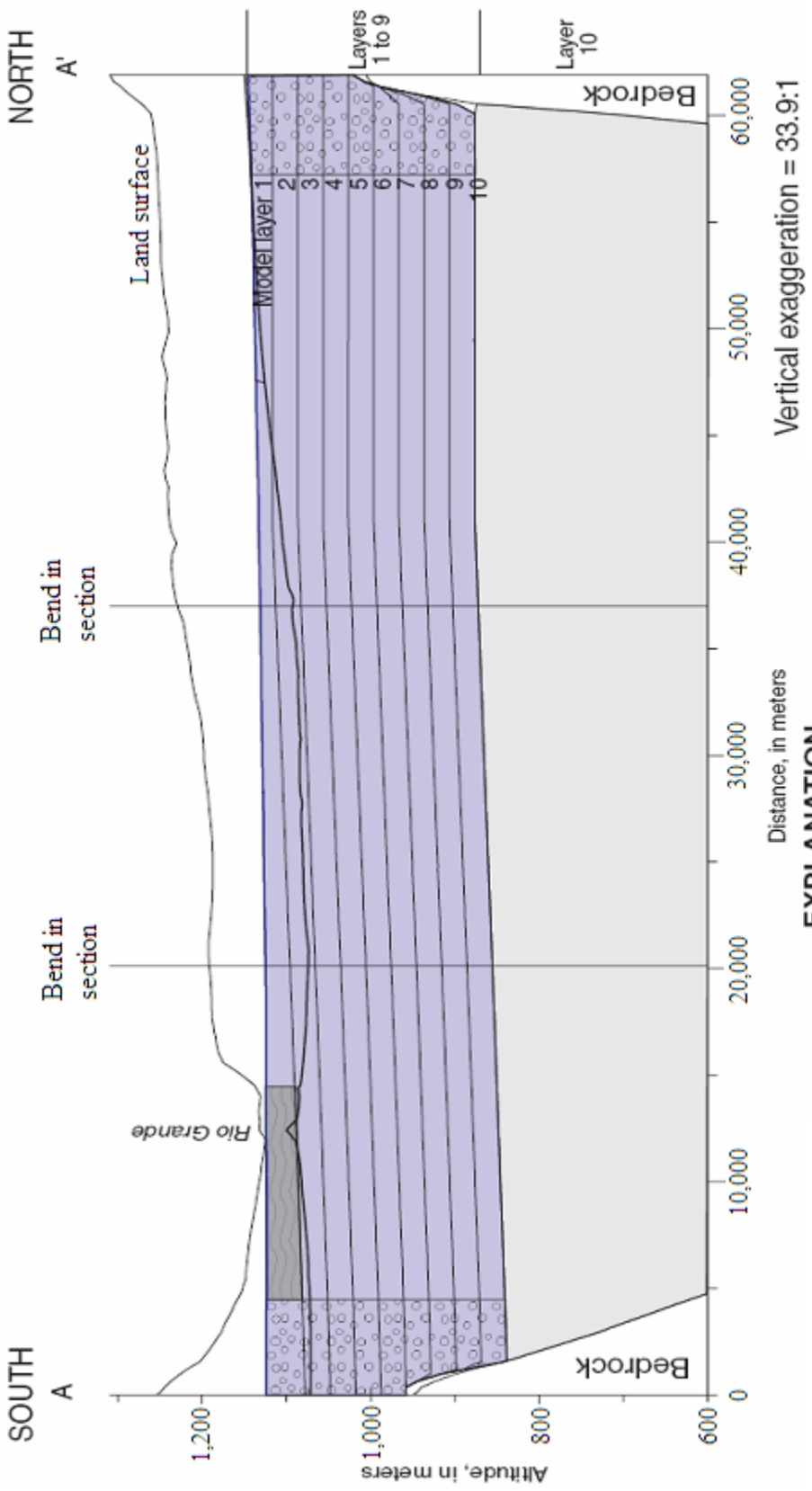

Fig. 8. Section A-A in the model domain displaying north to south cross-sections of geologic properties of the Hueco Bolson (after Heywood and Yager [5]).

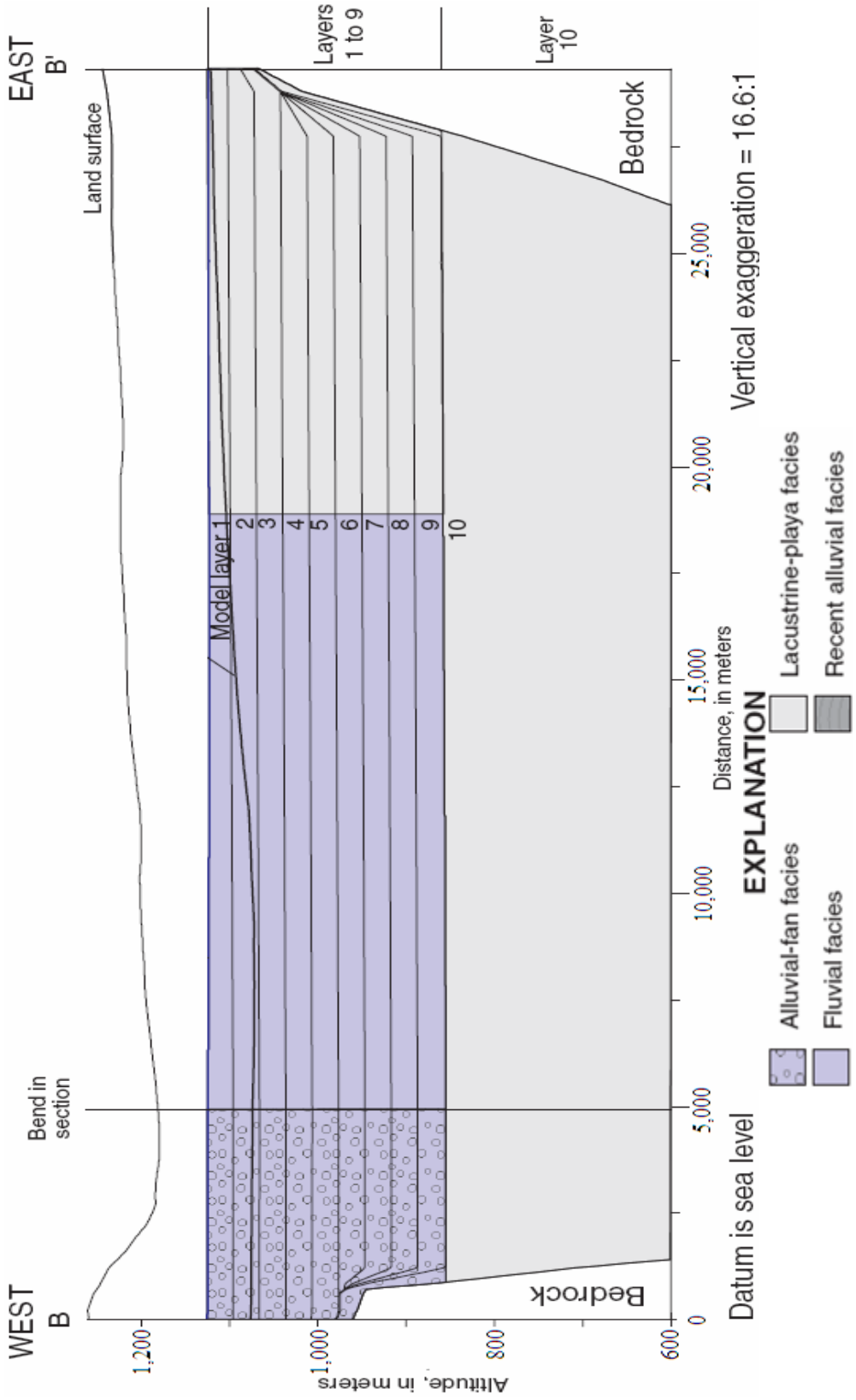

Fig. 9. Section B-B in the model domain displaying east to west cross-sections of geologic properties of the Hueco Bolson (after Heywood and Yager [5]).

2.1.2 Geology

The Basin varies in thickness from the El Paso area, where the aquifer assumes a thickness of up to 2,700 meters, to the unproductive southeastern regions were the aquifer is about 300 to 900 meters thick. The majority of the potable Heuco Bolson aquifer water is assumed to occur beneath the El Paso/Juarez area, while very little and less productive portions occur in the adjoining Hudspeth County area (Fig. 6) [14, 15].

In New Mexico, the Tularosa Basin (Fig. 6) bounds the Hueco Bolson on the north and groundwater flows from the Tularosa into the Hueco Bolson [4]. The Hueco Bolson aquifer can be described as a highly heterogeneous and anisotropic system. The aquifer is made of unconsolidated basin fill material composed of various materials (ranging from poorly sorted to well sorted) including sand, gravel, and silt in the upper zones and lower zones composed of clays and silts [14, 15].

The basin fill material, which comprises the Hueco Bolson, has been classified into four hydrogeologic facies by Heywood and Yager [5] based on historical deposition and structure. The four facies, which include fluvial facies, alluvial-fan facies, lacustrine-playa facies, and recent alluvial facies, are believed to interfinger as shown in the cross-sections (Fig. 7, Fig. 8, and Fig. 9) resulting in the gradational changes in the hydraulic conductivity at the scale of the ground water flow model [5]. The fluvial facies, which originated from the Rio Grande deposits 0.67 to 3.8 million years ago, are made of fluvial sediments and consist of fine-to-coarse grained channel sand interbedded with clay and silt. These silt and clay interbeds make up approximately one third of the fluvial sediments [5].

The alluvial fan facies, which occur predominantly in the western portion of the bolson and originate from the present-day Organ and Franklin Mountains, consist of poorly sorted gravel and coarse-to fine grained sand [5, 16]. The lacustrine-playa facies which occur predominantly at the eastern and southeastern parts of the Bolson and at depths below the alluvial-fan facies and fluvial facies are made of thick deposits of clay and silt [5]. The recent alluvial facies are formations resulting from erosion, due to the deposition of the fluvial, alluvial-fan, and lacustrine-playa facies [5, 17].

Ranges of horizontal hydraulic conductivities have been determined for the Hueco Bolson through pumping tests conducted by El Paso Water Utilities (EPWU). The pumping tests were conducted in 85 production wells located in high permeability areas such as the fluvial and alluvial-fan facies [5]. Estimated horizontal hydraulic conductivities from the tests ranged from 1 to 50 m/day with an average of about 10 ± 7 m/day. Vertical hydraulic conductivities of 6×10^{-3} to 2×10^{-2} m/day were determined from tests of undisturbed clay core samples conducted by the Colorado School of Mines. The clay core samples were collected at 5 different depth intervals near the Rio Grande [5].

A majority of the groundwater produced from the Hueco Bolson by Ciudad Juarez and the City of El Paso are used for municipal supply purposes. Significant amounts of historical pumping have lowered water levels, and reduced the overall quality of the groundwater in the Hueco Bolson. Recharge to the Hueco Bolson occurs from precipitation runoff from the Franklin Mountains, underflow from the Tularosa aquifer, and additional underflow from the Mesilla Bolson aquifer, which are located as shown

(Fig. 6). Additionally, significant recharge to the aquifer also occurs via infiltration of water from the Rio Grande (through the Rio Grande alluvium), irrigation canals, and drains [15].

The overall water quality of the Heuco Bolson varies significantly with the differing depths of the aquifer. A predominant portion of the Bolson contains groundwater of varying quality, ranging from 1 to 1000 mg/L TDS in upper zones to more than 1000 mg/L in deeper zones [14, 15]. Water quality has also been found to degrade laterally from west to east [4]. The ground water in the southeastern portion of the Bolson (southern El Paso and Hudspeth County area) (Fig. 6) was found to contain high amounts of gypsum and very limited recharge was found to occur in this area. Testing, which was performed on this portion of the aquifer, also revealed no occurrence of freshwater [15].

2.2 THE RIO GRANDE AND RIO GRANDE ALLUVIAL AQUIFER

The resources of the Rio Grande and the Rio Grande alluvial aquifer (Fig. 6) are shared by the communities of El Paso, Juarez, and southern Dona Ana County which are located along the U.S/Mexico border. Surface water for irrigation water supply needs from the Rio Grande is supplemented by groundwater pumping from the Rio Grande Alluvium. The Rio Grande flow originates from snowmelt runoff, which occurs in northern New Mexico and southern Colorado [12, 13]. The Rio Grande alluvium overlies the Heuco Bolson aquifer at the El Paso Valley, which can be defined as the area were the river is hydraulically connected to the Hueco Bolson aquifer. The valley extends

about 90 miles southeast of El Paso (Fig. 6) and assumes a horizontal thickness of about 6 to 8 miles as it meanders southeast [12].

The Rio Grande alluvial aquifer, which underlies the El Paso Valley, is relatively thin compared to the Hueco Bolson with an average vertical thickness of about 64 m and is filled with recent alluvial deposits made up of irregularly distributed clays, gravels, silts, and sands [4, 12, 13]. The Rio Grande River, which is currently a losing stream (Fig. 10), is hydraulically connected to the Rio Grande aquifer, which in turn is connected to the underlying Hueco Bolson aquifer.

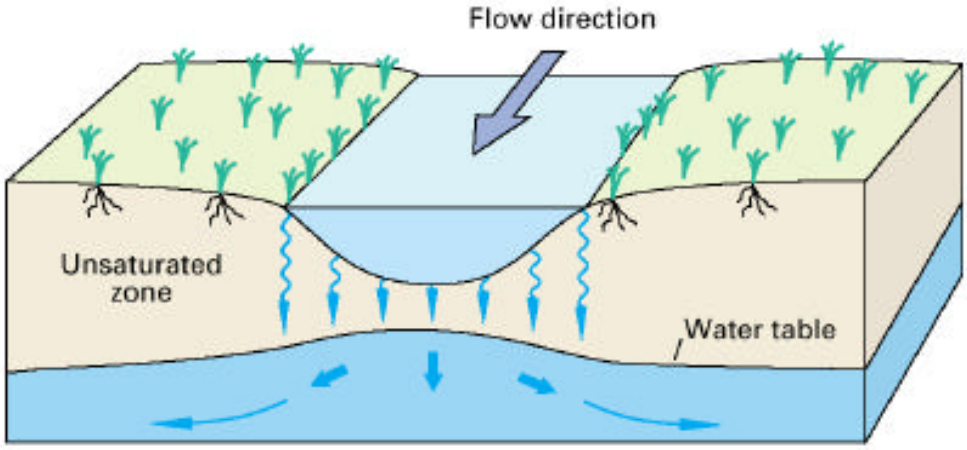

Fig. 10. The losing stream aquifer condition (after Hutchison [4])

Problems of groundwater salinization exist in the Rio Grande alluvium as a result of irrigation practices along the Rio Grande River. Irrigation water in the area, which discharges into the Rio Grande River, develops salinity during the course of discharge into the river because of the high evapotranspiration of the area. Seepage into the underlying aquifer is of concern because of the potential negative impacts on the hydraulically connected Hueco Bolson aquifer [12].

2.3 WATER RESOURCES MANAGEMENT

2.3.1 Climate change and border water management issues

Climate change and variability also pose a threat to the water resources of the El Paso/Ciudad Juarez border region. Liverman et al. [8] found that the Rio Grande river flows in the border area fluctuate significantly annually because of high interannual climate variability. The fluctuating Rio Grande river flows can cause frequent drought and problems for water use arrangements in the border area. Additionally, groundwater recharge is significantly impacted, because the Rio Grande is a major source of groundwater recharge to the aquifer. Studies suggest that global warming could also impact the water supply in the border area region in the future. Other studies have suggested that increases in greenhouse gas concentrations could significantly impact the water resources of the border area by bringing about drier and warmer climates, which will further exacerbate current dry conditions of the area [8].

Groundwater aquifers do not recognize man-made borders of land. The complexity of the U.S.-Mexican border water management issues in the El Paso/Ciudad Juarez area are intensified by rapid population growth, shared resources, and conflicts involving the limited water resources. The different legal systems of states and nations in this region add to the complexity of the water supply challenges of this region. Different laws are maintained by Texas, New Mexico, and Chihuahua in regards to the governing of groundwater rights and usage [7, 18]. In New Mexico, the state regulates its groundwater rights. In Texas, doctrines like the “right of capture” exist where a land owner has rights to the groundwater beneath his/her land. In Chihuahua, control and

regulation of groundwater rights are handled by a federal agency called the "Comision Nacional de Agua (CNA)," which translates to the "National Commission of Water" [7, 18]. The three states also maintain different definitions of groundwater rights. Additionally, in Mexico, the Mexican Constitution defines water as the property of the nation, while in the United States, state laws define groundwater rights [7, 8, 18].

Various issues dealing with the Rio Grande surface waters of this border area are currently being addressed in treaties, compacts, and agreements, but there are no such discussions that address the groundwater issues [19]. Some interstate commissions like the New Mexico-Texas Water Commission and the Rio Grande Compact Commission address issues dealing with the Rio Grande and also have impacts on the aquifers. The International Boundary and Water Commission (IBWC) implements binational agreements between the U.S. and Mexico and administers the 1944 water treaty, which governs the management of the Rio Grande and Colorado river surface water systems [9]. The IBWC also supervises and manages water that crosses from one country into the other. The IBWC has the potential to participate in issues dealing with the internationally shared aquifers, however, control and disputes over the use of these internationally shared aquifers in the U.S.- Mexico border area could potentially escalate into major problems between the United States and Mexico if not resolved [7, 9, 19].

2.3.2 El Paso supply and usage

In El Paso, surface water is supplied by the Rio Grande and a majority of the ground water is supplied by the Hueco Bolson and partially from and adjacent aquifer system, the Mesilla Bolson. El Paso Water Utilities (EPWU) is responsible for supplying

water to El Paso communities and currently supplies about 90% of all municipal usage. The current total demand in El Paso is 136 million cubic meters per year. [7, 13]

Through several successful water management strategies including conservation, incentive programs, and use of reclaimed water, drops in per capita usage have been observed. With the current total demand of 136 million cubic meters per year, a drop from 0.85 cubic meters per person per day to about 0.52 cubic meters per person per day has been successfully achieved. El Paso also maintains 79.5 million cubic meters per year in water rights from the Rio Grande. A current total supply of 186 million cubic meters per year is available to El Paso for annual consumption [4, 13]. Table 1 illustrates how much water is expected from all sources of water supply to the El Paso area under normal conditions (no drought and full supply from the Rio Grande) and potential drought-of-record conditions [13]. Significantly increased pumping is expected to occur in the Hueco Bolson during drought-of-record conditions.

Table 1
Water supply for the El Paso area from major sources under different conditions [13]

Water supply source	Normal Conditions	Drought-of-record conditions
Rio Grande	40%	6.7%
Hueco Bolson	33.3%	60%
Mesilla Bolson	23.3%	30%
Reclaimed water supply	3.3%	3.3%

2.3.3 Juarez supply and usage

In Ciudad Juarez, the Chihuahua State Central Water Utility (JCAS) oversees the Ciudad Juarez Water Utility (Junta Municipal de Agua y Saneamiento de Juarez (JMAS)), which in turn is responsible for the provision of water to Ciudad Juarez. Ciudad

Juarez relies on the Hueco Bolson for the majority its water supply. In the early 1990's, JMAS operated only 5 major production wells to serve Ciudad Juarez residents. In keeping with large population increases, JMAS increased its production well capacity to 12 wells in late 1990's [7]. However, the current water supply is not enough to provide continuous services to connected users, and the distribution network, which loses from 15 to 20 percent of the total supply, only reaches 94 to 96 percent of the residents. The water metering system also requires significant improvements to gain better income control, and also to better manage the water systems on the Mexican side more efficiently [7].

2.3.4 Current groundwater management in Texas

Senate Bill 1 changed the water planning and management processes in Texas to be primarily public focused and centered [20]. In order to increase public participation, public awareness, and public education, 16 planning groups were created and, thus, 16 regional water plans were developed by the planning groups for their different regions (Fig. 11). The Texas state water plan identifies actions required to meet the water needs of local communities during drought of record conditions, which may occur over the next 50 years, and incorporates the 16 approved regional water plans [20]. Additionally, the planning groups supply information on water demands, actions needed, and water supplies for their different planning regions. Another purpose of Senate Bill 1 was to determine the location and volume of groundwater supplies from sources that currently exist and sources which are un-delineated that may be available for future use. Thus, the location and extent of 9 major aquifers and 21 minor aquifers, which underlie

approximately 90% of the land mass in the Texas region and groundwater management areas, were delineated (Fig. 12 and Fig. 13) [2, 20].

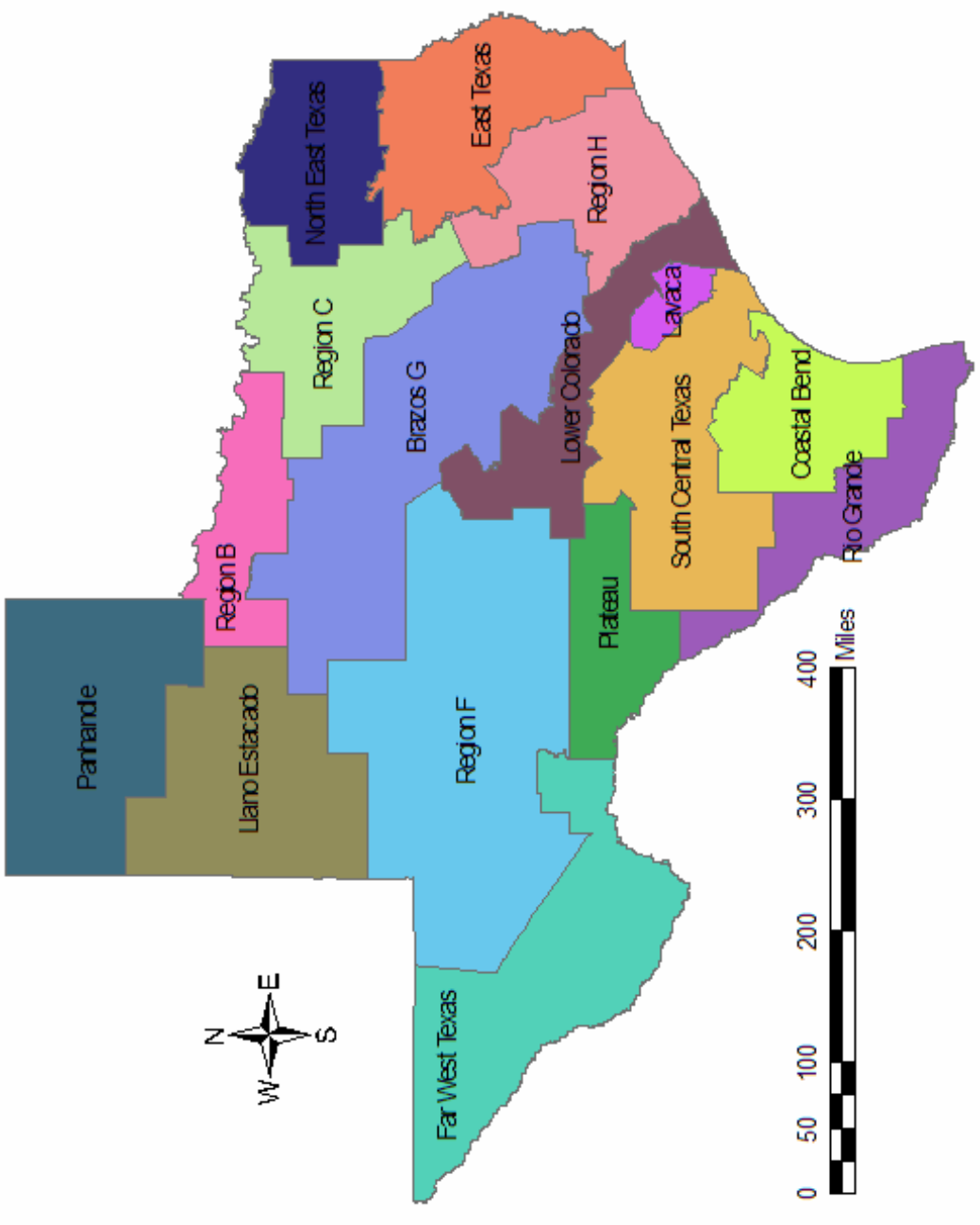

Fig. 11. 16 water planning regions in Texas [2]

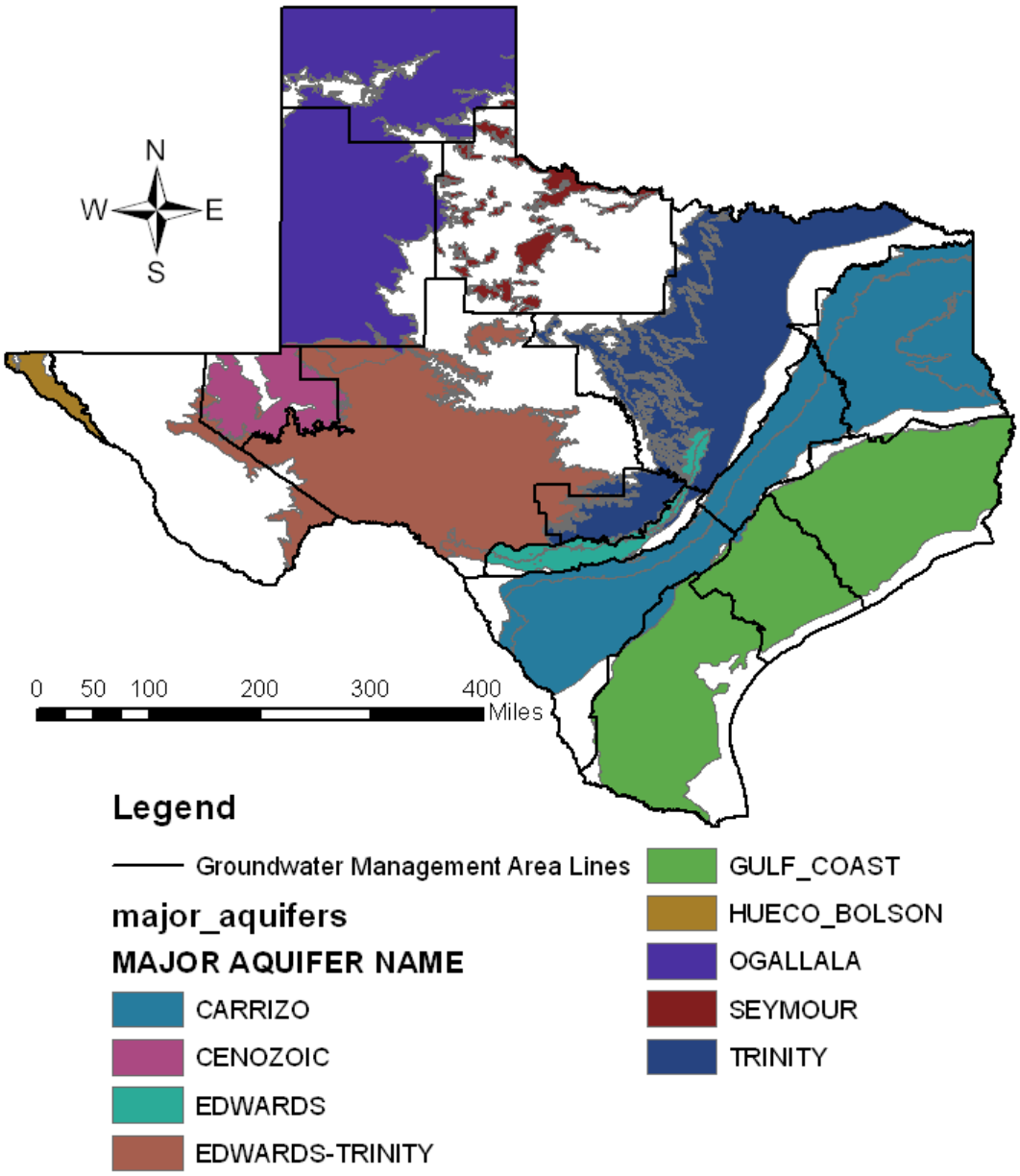

Fig. 12. Major aquifers of Texas in groundwater management areas [2].

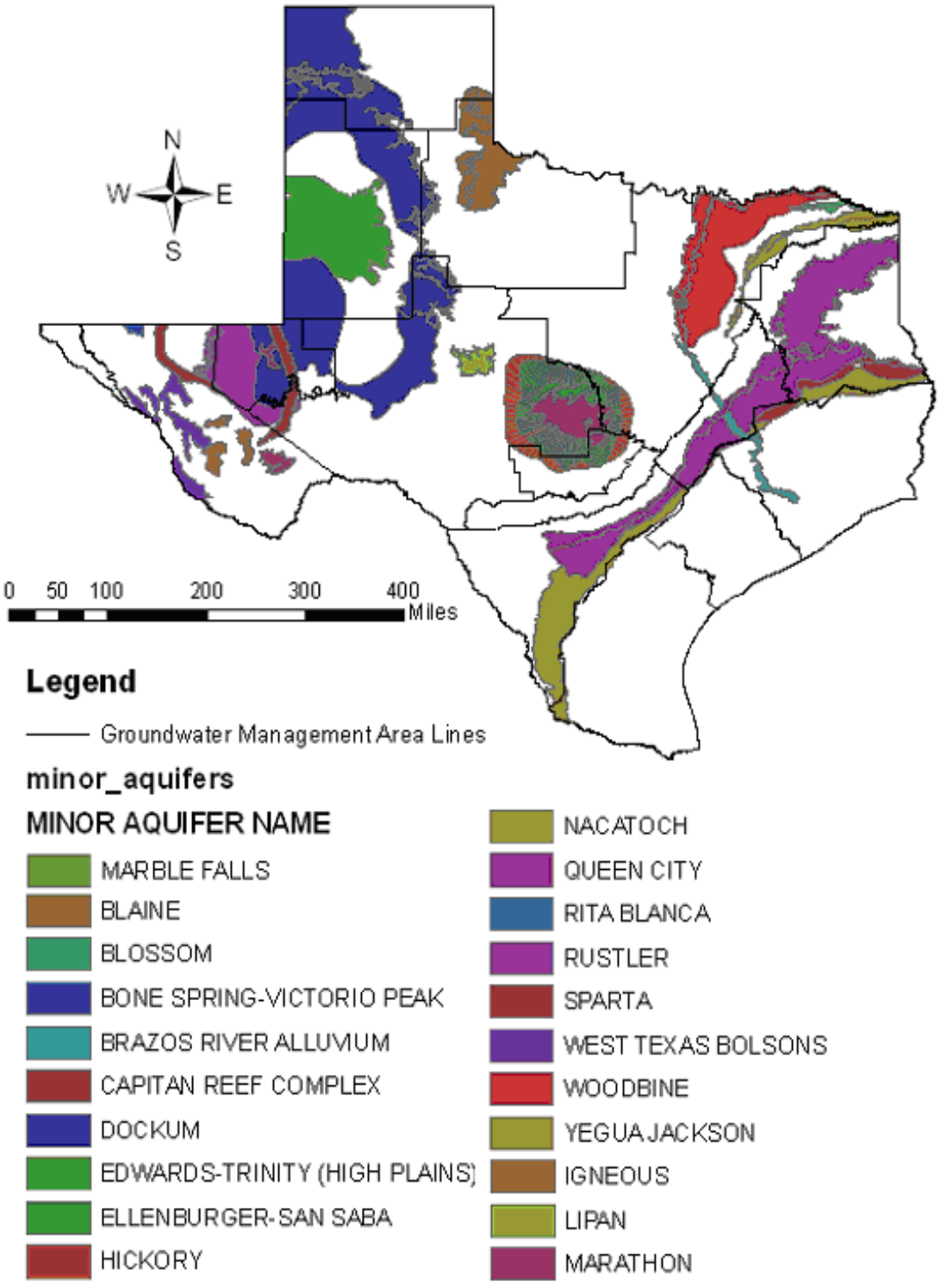

Fig. 13. Minor aquifers of Texas in groundwater management areas [2].

Table 2
Groundwater availability in aquifers in Texas

Aquifer	Groundwater availabilty in 2000 under drought conditions (million m^3/Year)
Ogallala	7895
Gulf Coast	1974
Carrizo-Wilcox	1974
Edwards-Trinity Plateau	1209
Queen City	839
West Texas Bolsons	703
Capitan	481
Edwards (BFZ)	456
Seymour	308
Hickory	296
Blaine	222
Igneous	222
Trinity	222
Pecos Alluvium	210
Spart	197
Bone Spring - Victorio	173
Hueco-Mesilla Bolson	148
Brazos Alluvium	136
Dockum	100
Lipa	60
Ellenburger - San Saba	57
Marathon	37
Woodbine	32
Marble Falls	27
Rita	7
Edawards - Trinity High Plains	6
Nacatoch	6
Rustler	5
Blossom	1

The amounts of water that can be produced or accessed using existing infrastructure are classified as groundwater supplies. Production capacities of major and minor aquifers vary significantly each year and are dependent on annual pumpage [20]. Some production capacities of major and minor aquifers in Texas are shown in Table 2. According to this data from the 2002 state water plan, the Ogallala aquifer represents the largest production capacity. Additionally, the Texas Water Development Board (TWDB)

was authorized by the Texas legislature in 2001 to develop or obtain groundwater availability models (GAM) for both minor and major aquifers located in Texas. Current GAMs were developed in close coordination with regional and local agencies like planning groups and groundwater conservation districts [21].

3. PRIOR WORK ON GROUNDWATER MODELING

Groundwater modeling efforts for the Hueco Bolson have been underway since the late 1960s, ranging from the first electric analog model developed in the late 1960's to the current Groundwater Availability Model (GAM) developed by the United States Geological Survey (USGS). This section presents a review of previous groundwater models developed for the Hueco Bolson, specifically, the models developed by Leggat and Davis [22], Meyer [23], Lee Wilson and Associates [24-26], Kernodle [27], Groschen [11], and Heywood and Yager [5].

The two-dimensional electric analog model created by Leggat and Davis [22] was employed to quantitatively evaluate the groundwater availability and resources of the Hueco Bolson. Leggat and Davis [22] developed the electric analog model by using an electrical resistor/capacitor network to simulate the hydrologic and geologic properties of the aquifer. The electric analog model created by Leggat and Davis [22] employed an analogy between groundwater flow and the flow of electricity. The aquifer media, which inhibits the flow of water, was simulated using networks of resistors of varying resistances, which obstruct the flow of current, while the aquifer storage was simulated using capacitors, which store electricity. Leggat and Davis [22] made predictions of groundwater declines due to withdrawals through 1990 and concluded that computed groundwater declines could be reduced if pumping in the Hueco Bolson would be supplemented by supplies from other sources. Meyer [23] later developed a three-dimensional two layer transient model to simulate declines in water levels and to estimate the total volume of freshwater in storage in the Hueco Bolson. The two layer model,

which simulated both the unconfined and confined parts of the aquifer system, was built using a documented code by Bredehoeft and Pinder [28].

A four layer, three dimensional, transient groundwater flow model was developed by Lee Wilson and Associates [24-26] a few years later to simulate the fresh groundwater flow in the Hueco Bolson. The model, which had 41 rows and 18 columns, was developed using MODFLOW 88, the earliest USGS Fortran based, block-centered modular groundwater flow model that quantifies and analyzes groundwater flow using the finite-difference method [29]. Kernodle [27] enhanced the Lee Wilson and Associates [24-26] finite difference model by adding an interbed-compaction and elastic/inelastic storage computational package, which further enabled the model to simulate land subsidence due to groundwater withdrawals.

Groschen [11] numerically analyzed the groundwater flow system of the Hueco Bolson by creating a groundwater flow model and a salinity transport model. The 26 row, 14 column, and 4 layer flow and transport models were created using MODFLOW 88 and HST3D (a three dimensional heat and solute transport flow model). From the simulation results, Groschen [11] determined that saline water in the Rio Grande alluvium originating from the Rio Grande was a major source of saline water intrusion into the Hueco Bolson.

The Heywood and Yager [5] groundwater flow model has been adapted as the current Groundwater availability model (GAM) for the Hueco Bolson This model is available from the Texas Water Development Board (TWDB). The GAM, which consists of 165 rows, 100 columns, and 10 layers was developed using a modified MODFLOW

96 code [30]. The GAM simulates groundwater flow using 10 packages which include: the Basic package (BAS), the Block Centered Flow Package (BCF), the Evapotranspiration package (EVT), the Drain package (DRN), the Flow and Head Boundary package (FHB), the Recharge package (RCH), and the Wells package (WEL),

Other packages used in the model include the Multi Aquifer Well package (MAW), the Interbed Storage package (IBS), the Horizontal Flow Barrier package (HFB), the Initial Head package (HDS), and the Stream package (STR) [5]. The Pre-conditioned Conjugate Gradient solver (PCG) was used to solve the model for simulations, calibrations, and predictions. The STR package and MAW package were modified due to dried model cells and upper layers to better represent historic dewatering of the Hueco Bolson due to pumping [5].

Heywood and Yager [5] enabled stream leakage to the aquifer from the topmost active cell upon drying of the upper layer by modifying the STR package. In addition, Heywood and Yager [5] mitigated dewatering, which caused layers to go dry, by modifying the MODFLOW source code and the MAW package to omit dry layers from simulations and apportioning flows to or from wells in the remaining layers [5]. The Heywood and Yager [5] GAM results that show optimum values, and their 95% confidence intervals for the Hueco Bolson are presented in Table 3. Optimum values were determined through nonlinear regression in a transient state simulation. The values included are estimates for the recharge, hydraulic conductivity (horizontal (K_x), vertical (K_z)), specific yield, specific storage, conductance, and evapotranspiration.

Table 3
Results and parameter values from GAM (after Heywood and Yager [5])

Parameter	Value	Confidence interval	Scaled sensitivity, in meters
Recharge:			
Irrigation-return flow[1]	3.8×10^4 m^3/d	2.2×10^4 - 6.5×10^4 m^3/d	0.3
Underflow from Tularosa Basin	2.0×10^4 m^3/d	1.9×10^4 - 2.2×10^4 m^3/d	7
Mountain front on alluvial fans[2]	8.0×10^2 m^3/d	0 - 2×10^3 m^3/d	2
Underflow from Mesilla Basin	3.4×10^2 m^3/d	Not estimated	N/A
Horizontal hydraulic conductivity:			
Alluvial-fan facies	6.8 m/d	6.0 - 7.7 m/d	5
Recent fluvial sediments	4.0 m/d	2.8 - 7.2 m/d	2
Fluvial and alluvial facies	6.8 m/d	6.4 - 7.2 m/d	10
Lacustrine-playa facies	0.9 m/d	0.5 - 1.4 m/d	0.3
Quaternary faults	3.8×10^{-3} m/d	1×10^{-3} - 1×10^{-2} m/d	8
Vertical hydraulic conductivity:			
Alluvial-fan facies	1.2×10^{-3} m/d	6×10^{-4} - 2×10^{-3} m/d	3
Recent fluvial sediments	1.3×10^{-1} m/d	6×10^{-2} - 6×10^{-1} m/d	2
Fluvial and alluvial facies	1.3×10^{-2} m/d	1×10^{-2} - 1.5×10^{-2} m/d	0.6
Lacustrine-playa facies	2.5×10^{-2} m/d	6×10^{-3} - 1×10^{-1} m/d	0.4
Specific yield	0.178	0.173 - 0.184	10
Specific storage - elastic	7×10^{-6} m^{-1}	2×10^{-6} - 1×10^{-5} m^{-1}	0.5
Specific storage - inelastic	7×10^{-5} m^{-1}	Not estimated	N/A
Conductance per unit length:			
Rio Grande	1.8 m/d	1.6 - 2.0 m/d	1
Agricultural drains	5.8 m/d	2 - 1.6×10^1 m/d	2
Irrigation canals	3.0 m/d	Not estimated	N/A
Evapotranspiration extinction depth	5 m	Not estimated	N/A
Maximum evapotranspiration rate	4.6×10^{-3} m/d	1×10^{-3} - 7×10^{-3} m/d	2
Manning's *n*:			
Rio Grande	0.03	Not estimated	N/A
Franklin Canal, Acequia Madre	0.004	Not estimated	N/A

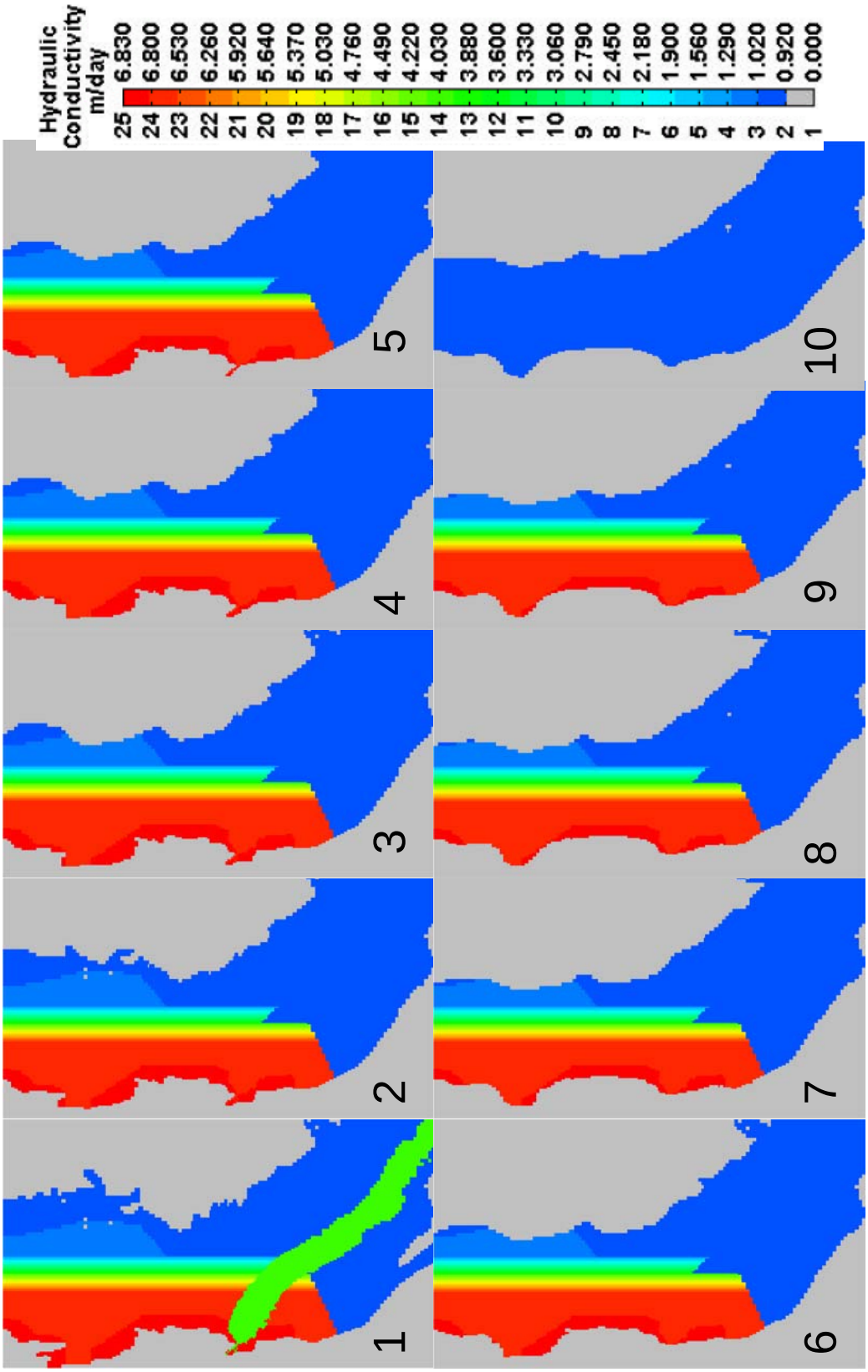

Fig. 14. Distribution of horizontal hydraulic conductivity results (after Heywood and Yager [5])

Horizontal hydraulic conductivities ranged from 0.9 to 6.8 m/day with distributions for the 10 layers as shown (Fig. 14). The GAM results show that the model is most sensitive to 4 major components of the model which are the horizontal hydraulic conductivity of the alluvial and fluvial facies (the predominant location of the majority of the production wells), the specific yield, the faults, and the underflow from the Tularosa.

4. METHODS AND PROCEDURES

In this dissertation, a three dimensional 10 layer transient groundwater flow model with 94 annual stress periods for the Hueco Bolson was developed using the current GAM as its basis. A major limitation of the Hueco Bolson GAM was the dewatering of layers, which required modifications to be made to the MODFLOW 96 source code. This issue was resolved by recreating the GAM in an improved and updated MODFLOW 2000 environment using the Visual MODFLOW© pre and post-processor.

4.1 MODELING TOOLS

Different modeling programs and tools that are commonly used in current groundwater modeling practice were utilized in the development of the proposed model. These programs include MODFLOW, and other tools such as MT3DMS©, PEST©, ZONEBUDGET, and the Visual MODFLOW© pre and post processor, which manipulate and utilize results from MODFLOW to perform additional tasks.

4.1.1 Modular groundwater flow model (MODFLOW)

MODFLOW, the modular groundwater flow modeling tool, which was developed by the USGS, is a FORTRAN based, block-centered flow model which quantifies and analyzes groundwater flow using the finite-difference method and input data from field measurements [29]. The MODFLOW program will be used in the current endeavor. MODFLOW uses the finite-difference method to solve a form of the groundwater flow equation:

$$\frac{\partial}{\partial x}\left[K_{XX}\frac{\partial h}{\partial x}\right]+\frac{\partial}{\partial y}\left[K_{YY}\frac{\partial h}{\partial y}\right]+\frac{\partial}{\partial z}\left[K_{ZZ}\frac{\partial h}{\partial z}\right]-W=\frac{\partial h}{\partial t}S_S \quad (1)$$

where K_{XX}, K_{YY}, and K_{ZZ} are the principal components of the hydraulic-conductivity tensor, LT^{-1}; h is the hydraulic head, L; W represents sources or sinks; t is time, T; S_S is the specific storage coefficient, L^{-1}. A main program and series of packages carry out the implementation of the finite difference method in MODFLOW.

These packages, which are usually problem specific, are made up of a series of independent subroutines called modules that are employed by the main program to deal with specific aspects of the simulation. Available packages include: the basic package, which contains and deals with model spatial and temporal data; the well package, which simulates the effects of injection and pumping wells; and the recharge package, which simulates the effects of natural recharge. Other optional packages that simulate evapotranspiration, drains, head boundary conditions, and different solution procedures may or may not be required, depending on the problem being simulated [30, 31].

The GAM for the Hueco Bolson in the El Paso/Ciudad Juarez area, which is currently in use, runs only on a modified MODFLOW 96 code and the issue of dried model cells and dewatering in MODFLOW 96 still remains. Additionally, several input packages used in MODFLOW 96 for the GAM have either been updated or are no longer in use. An updated version, MODFLOW 2000, has several updates and enhancements which include the addition of calibration capabilities, implementation of vertical flow calculation under dewatered conditions, and dry cell re-wetting. Dry cell re-wetting is accomplished using automated conversions from dry cells, which is when calculated

heads in cells become smaller than the bottom elevations of the cells during a simulation) to wet during simulations [32]. These improvements in the MODFLOW 2000 version enable effective simulations that don't require the cumbersome tasks of the removal of dewatered cells or layers from the simulations or modifications to a MODFLOW source code or modifications to its packages. Therefore, a transition of the Hueco Bolson GAM developed in the modified MODFLOW 96 environment to a MODFLOW 2000 environment will enable significant improvements to the simulation and modeling capabilities of the GAM for future usage.

4.1.2 Modular 3-dimensional transport model (MT3D)

MT3D is a three-dimensional transport model commonly used in groundwater and remediation assessment studies for contaminant and mass transport modeling. MT3D facilitates simulation of transport processes such as dispersion, diffusion, advection, and chemical reactions of contaminants in groundwater. In addition, MT3D simulates changes in concentrations of contaminants over time by not only taking advection, dispersion and diffusion into consideration, but also various types of boundary conditions, such as external concentration sources or sinks [33]. MT3D utilizes the governing partial differential equation, which describes the fate and transport of contaminants in three-dimensional, transient groundwater flow systems:

$$\frac{\partial(\theta C^k)}{\partial t} = \frac{\partial}{\partial x_i}\left[\theta D_{ij}\frac{\partial C^k}{\partial x_j}\right] - \frac{\partial}{\partial x_i}\left[\theta v_i C^k\right] + q_s C_c^k + \sum R_n \qquad (2)$$

where θ is the porosity of the subsurface medium, dimensionless; t is time, T; C^k is the dissolved concentration of species k, ML^{-3}; x_i is the distance along the respective

Cartesian coordinate axis, L; D_{ij} is the hydrodynamic dispersion coefficient tensor, L^2T^{-1}; v_i is the seepage or linear pore water velocity (related to the specific discharge or Darcy flux by $v = q_i/\theta$), LT^{-1}; q_s is the volumetric flow rate per unit volume of aquifer representing fluid sources sinks (negative) and sources (positive), T^{-1}; $\sum R_n$ is the chemical reaction term, $ML^{-3}T^{-1}$; C_s^k is the concentration of the source or sink flux for species k, ML^{-3}.

This equation is solved in MT3D employing a user-directed choice of three major classes of solution techniques, including the finite-difference method, the particle-tracking-based Eulerian-Lagrangian method, and the higher-order finite-volume method. A latest release, the Modular three-Dimensional Transport model for Multi-Species (MTRDMS), will be used in the current endeavor for the contaminant transport simulations [34].

4.1.3 Parameter estimation (PEST)

In addition to the MODFLOW program, PEST©, a widely used program for calibration of non-linear models, was used to calibrate the new model to ensure that results generated by the model, such as head and concentration, corroborated field-measured observations. PEST© is generally used to adjust model parameters that are considered difficult, expensive, or perhaps impossible to obtain with precision from the field such as conductivities, storage, and recharge. The parameter adjustment process in PEST© is performed by adjusting model parameters in an iterative process [35]. The iterative process involves using recurring model runs in progressive optimization

sequences until discrepancies between model-generated results and field measurements are minimized, specifically when a minimum of the weighted sum of squares differences between the two is achieved [35]. Input specifications, such as parameter change ranges, initial parameter values (from the un-calibrated model), parameter change increments, and weights of field-measured observations, are provided by the user.

The optimizations are performed by the linearization of the relationship between the model's outputs at observation points and its parameters. During each optimization attempt, linearization is achieved by using a Taylor series expansion to calculate the partial derivatives of each model output with respect to each parameter [35]. The minimum of the weighted sum of square differences is achieved in PEST© by the calculation of an objective function. The calculation is accomplished by employing the Gauss-Marquardt-Levenberg algorithm using the objective function:

$$\Phi = (c - c_O - J(b - b_O))^t Q(c - c_O - J(b - b_O)) \quad (3)$$

where upgraded parameters at each optimization attempt are determined using

$$(b - b_O) = ((J^t QJ + \alpha I)^{-1} J^t Qr) \quad (4)$$

and Φ is the objective function (sum of squared of the weighted residuals); J is the Jacobian which is comprised of the derivatives of individual measured observations with respect to each parameter being updated; Q is a diagonal matrix which is comprised of the squares of the weight assigned to the measured observation; (b - b_O) is a vector which defines the discrepancy between the initial parameters b_O and the updated parameters b; (c – c_O) is a vector which defines the discrepancy between model calculated results c_O and measured observations c; I is the identity matrix; r is a vector of residuals for a

parameter set in an iteration; α is the Marquardt parameter [35]. In the current endeavor an implementation of PEST© known as Visual PEST© is used, which enabled real-time monitoring of the optimization processes to be viewed in a graphical windows environment.

4.1.4 ZONEBUDGET

ZONEBUDGET was developed by the USGS and quantifies inflows, outflows, and storage changes of an entire model domain, or within a specific area located within the model domain, using results from a MODFLOW simulation. ZONEBUDGET was also used in this model to display mass balance results and quantify groundwater availability in storage [36].

4.1.5 Visual MODFLOW pre and post processor

Pre and post processor applications in groundwater modeling are becoming more wide-spread. Pre and post-processors can be described as programs created using Visual BASIC, C, or other programming languages which expand the capabilities of computational modeling programs. Pre and post processors provide graphical user interfaces (GUIs), pre processor programs (for preparing, acquiring, manipulating, analyzing, and managing model input data), and post processor programs (for analyzing, managing, summarizing, interpreting, communicating, and displaying modeling results) [37]. Most pre and post processors are commercially available and provide different ranges of capabilities. The pre and post processor that will be used in this project is Visual MODFLOW© (Waterloo Hydrogeologic, Inc), a widely used pre and post

processor that implements the USGS MODFLOW program along with many others such as MT3DMS© (solute transport modeling), PEST© (parameter estimation), and ZONEBUDGET [38].

4.2 DATA COMPILATION

The Hueco Boslon aquifer has been studied extensively since the early 1900's. Related developments of groundwater and solute transport models have been underway since the late 1960's. Earlier modeling efforts and studies have performed tests on the aquifer and collected data related to its geology and regional groundwater flow. This model is an extension of the current model, the Hueco Bolson GAM, therefore the necessary data was acquired from input files from the Hueco Bolson GAM. The conceptual model used in this research also closely mirrors the conceptual model used in the current Hueco Bolson GAM.

4.3 MODEL DATA CONVERSION AND IMPORT

A specialized utility program developed by the USGS, called the MODFLOW 96 to 2K conversion tool (MF96TO2K), was used to convert the Hueco Bolson MODFLOW 96 model files to MODFLOW 2000 input files [32]. During the conversion process, three input files, namely, the name (NAM) file, the basic file (BAS), and the block-centered flow package (BCF) file were recreated and modified while all other model files remained unchanged. The NAM file cataloged all the available input and output files for the model, the BAS file contained information about model grid data and layers, and the BCF file contained information related to the physical properties of the aquifer medium

such as conductivity, storage, layer elevations. [32]. Four file packages compatible with MODFLOW 2000 were generated in the conversion process. These files were the new BAS, BCF, NAM, and the DIS (discretization) file. The MF96TO2K conversion program extracted elevation data from the BCF file and other model data from the BAS file, and used the extracted data to create the new DIS file. The NAM file was also modified to contain the new DIS file [32]. The converted model input file packages that were created using the MF96TO2K converter were imported into the Visual MODFLOW© interface using the Visual MODFLOW© import utility.

4.4 SPATIAL DISCRETIZATION

The model domain, a finite-difference model grid, is made up of 100 columns, 165 rows, and 10 layers. The variable grid spacing ranged from 500 meters by 500 meters to 1000 meters by 1000 meters. The finer grids were used in the El Paso/Ciudad Juarez area, these being the areas of interest (Fig. 15). Horizontal anisotropy was specified as equal in the X and Y directions (a horizontal anisotropy ratio of 1). The map of the study area was superimposed on the model domain using geo-referencing methods in the Visual MODFLOW© pre and post processor. The model domain (the active grid cells) covers an area of about 3,839 km^2 and is surrounded by no-flow boundaries (the inactive grid cells), which cover an area of about 5,099km^2 (Fig. 16 and Fig. 17) [5]. Inactive zones and no-flow boundaries illustrate fault bounded regions, and are represented by the Franklin Mountains on the west and the Hueco Mountains on the east (Fig. 16 and Fig. 18).

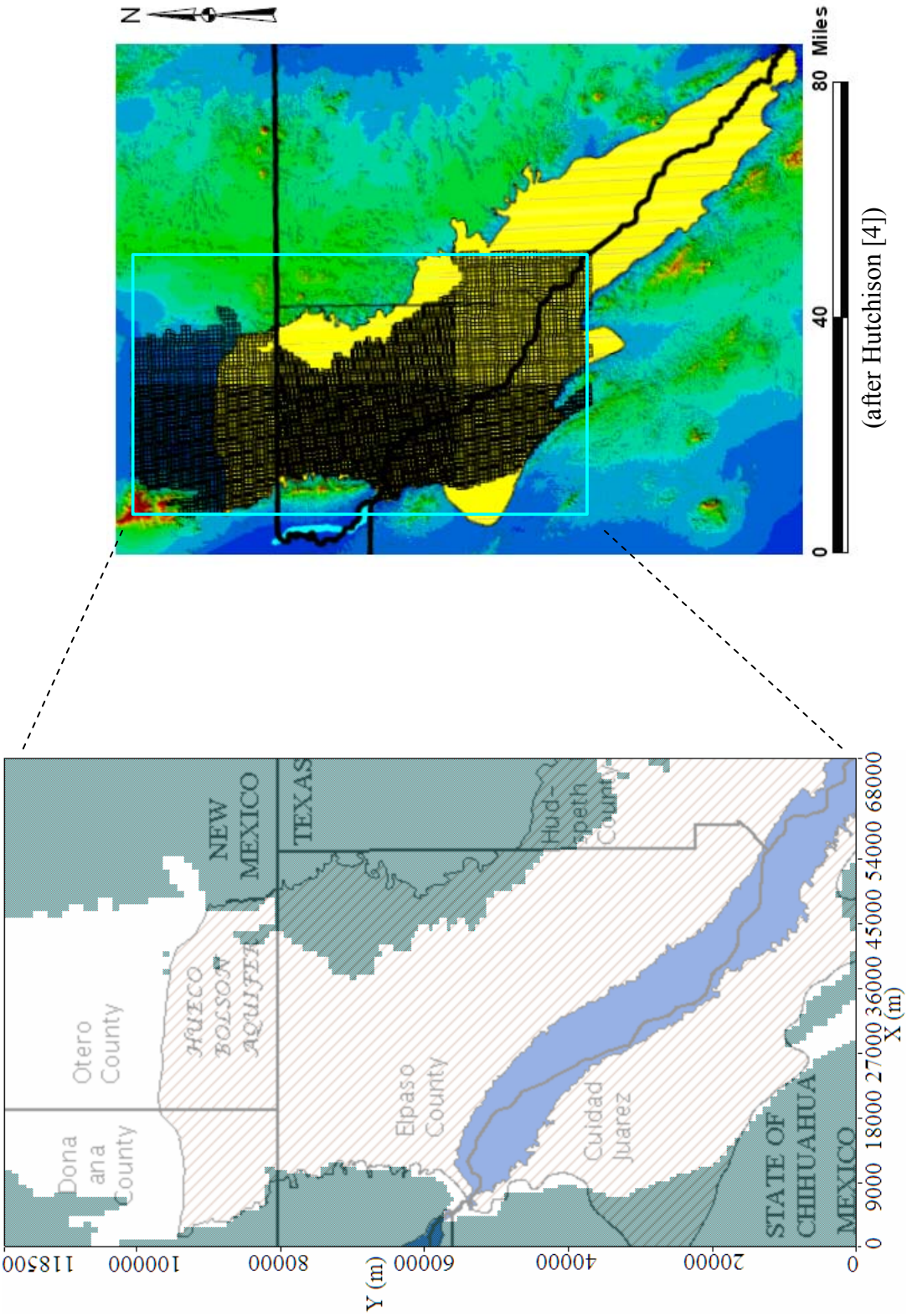

(after Hutchison [4])

Fig. 15. Map showing model area and grid domain in the Hueco Bolson.

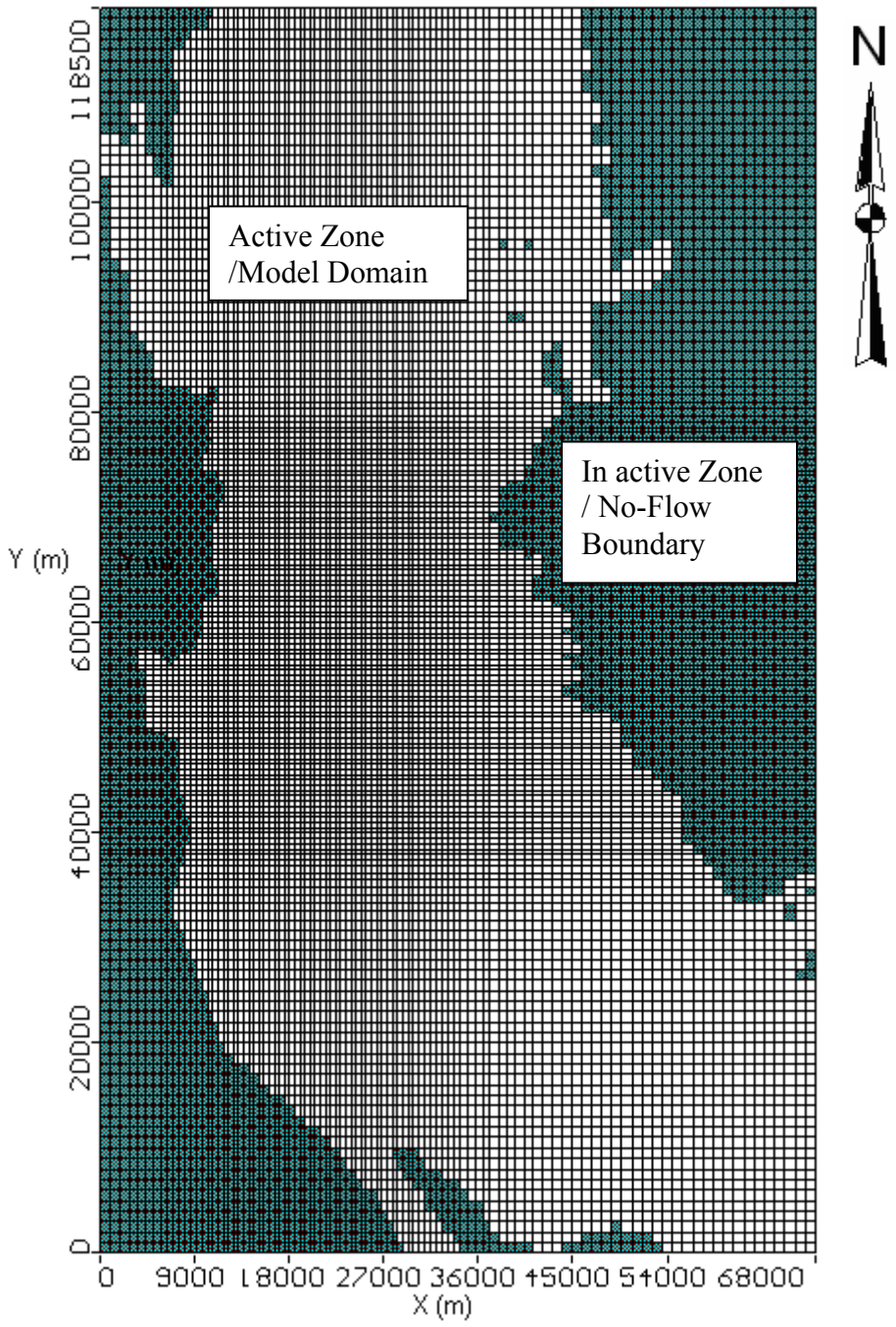

Fig. 16. Model grid, active and inactive zones (no flow boundaries).

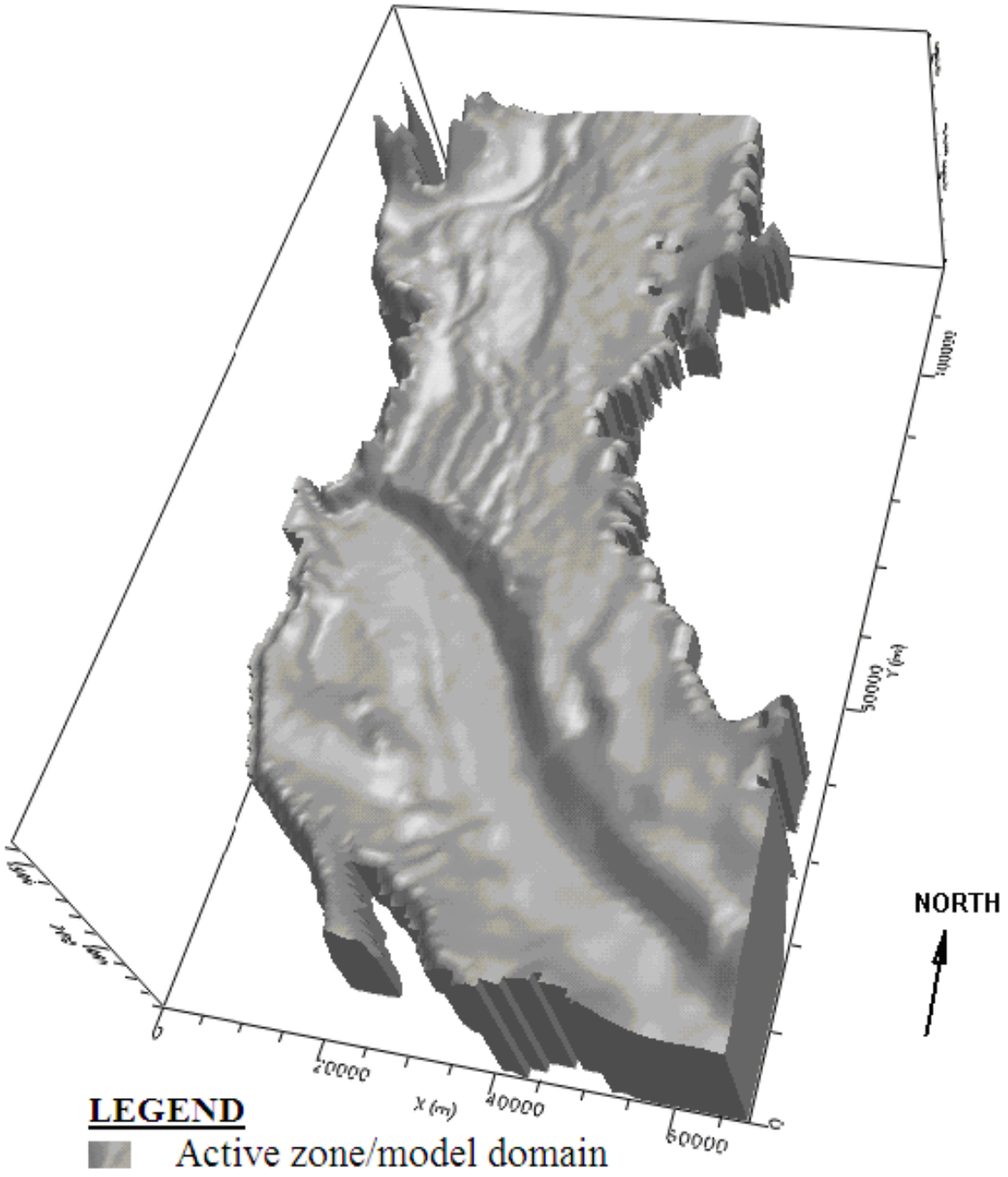

Fig. 17. Model domain (active zone).

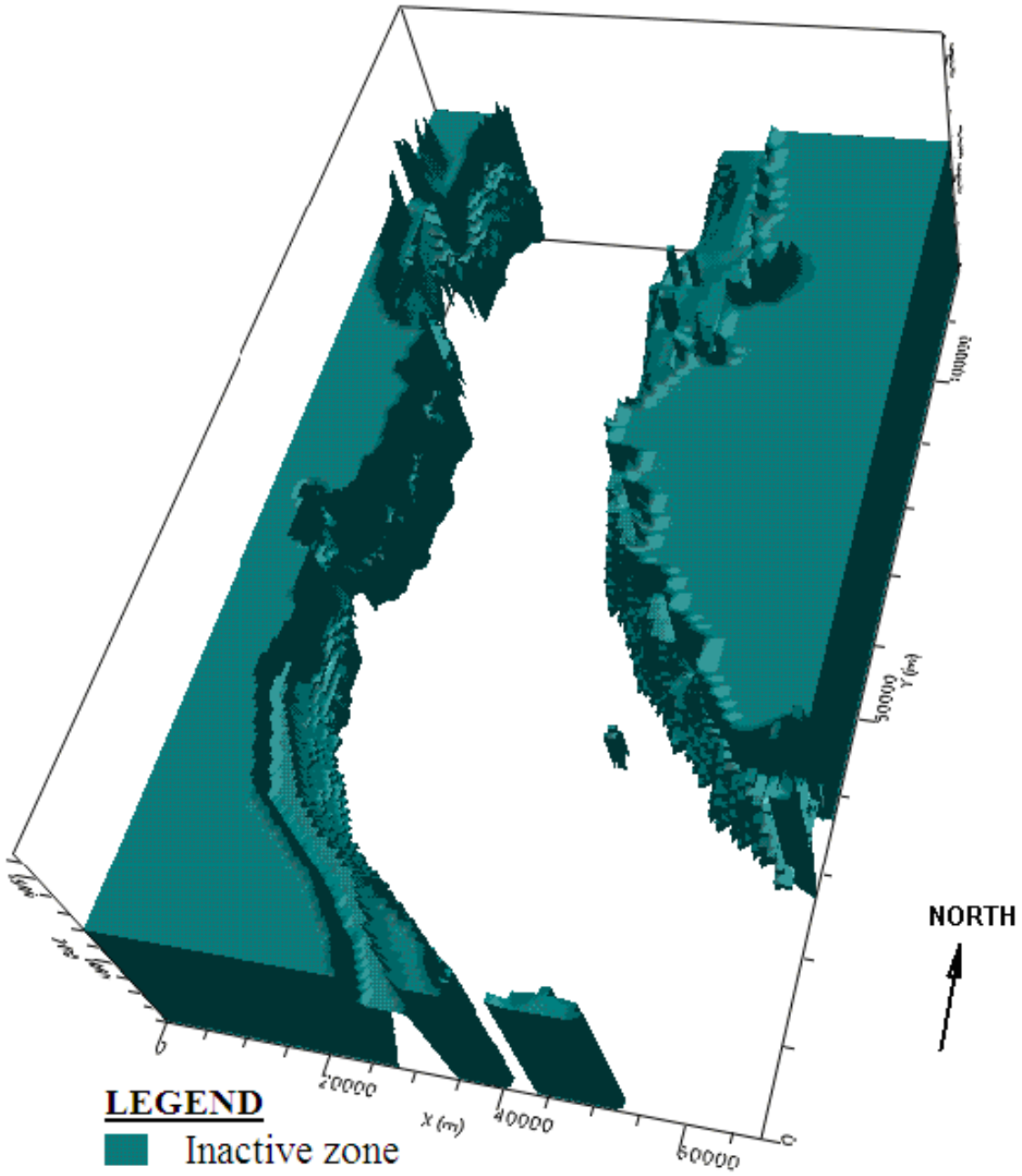

Fig. 18. Inactive zone and no-flow boundaries.

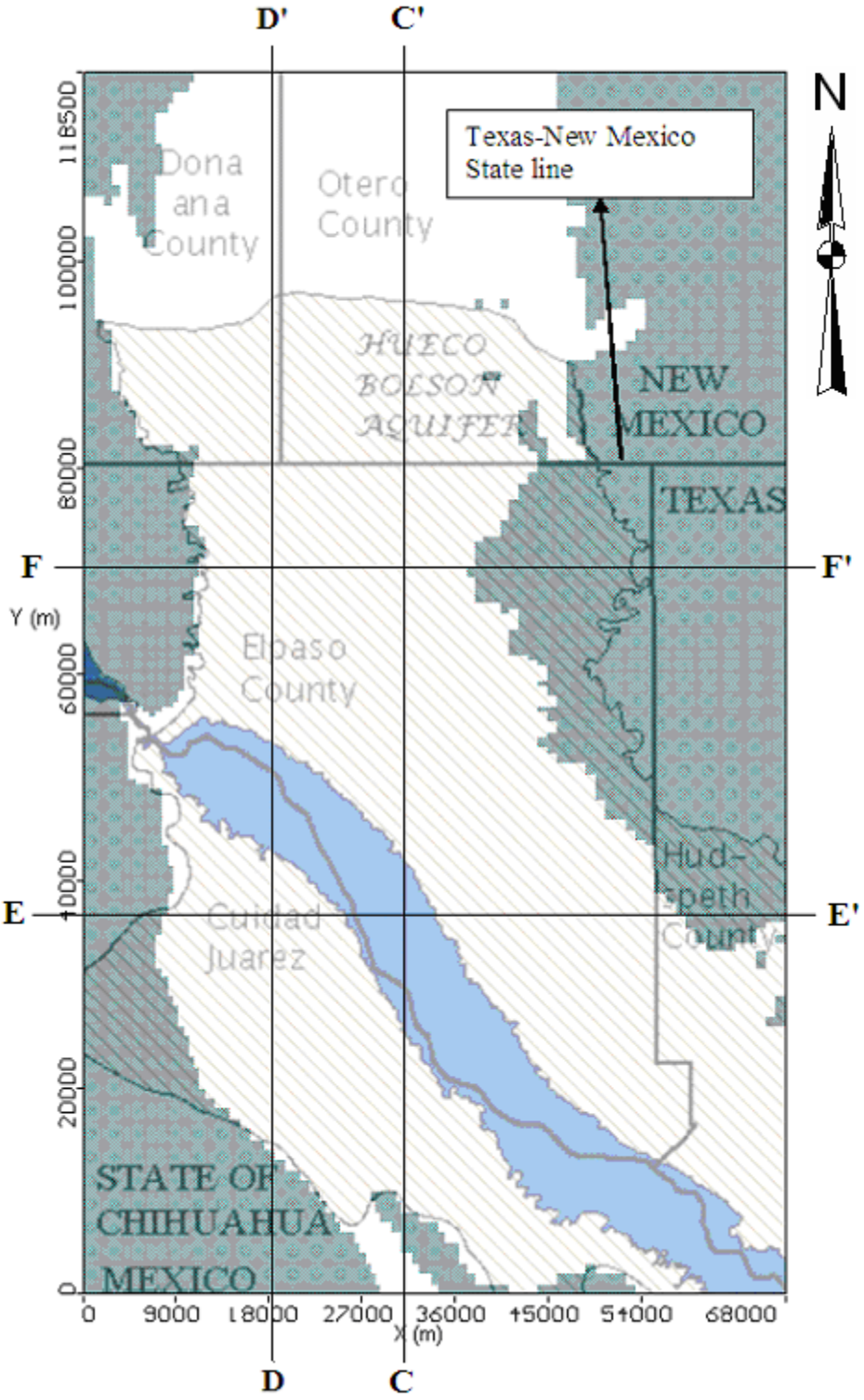

Fig. 19. Modeled area and location of the state line with sections along row 50 (F-F') and 115 (E-E'), and column 34 (D-D') and 49 (C-C').

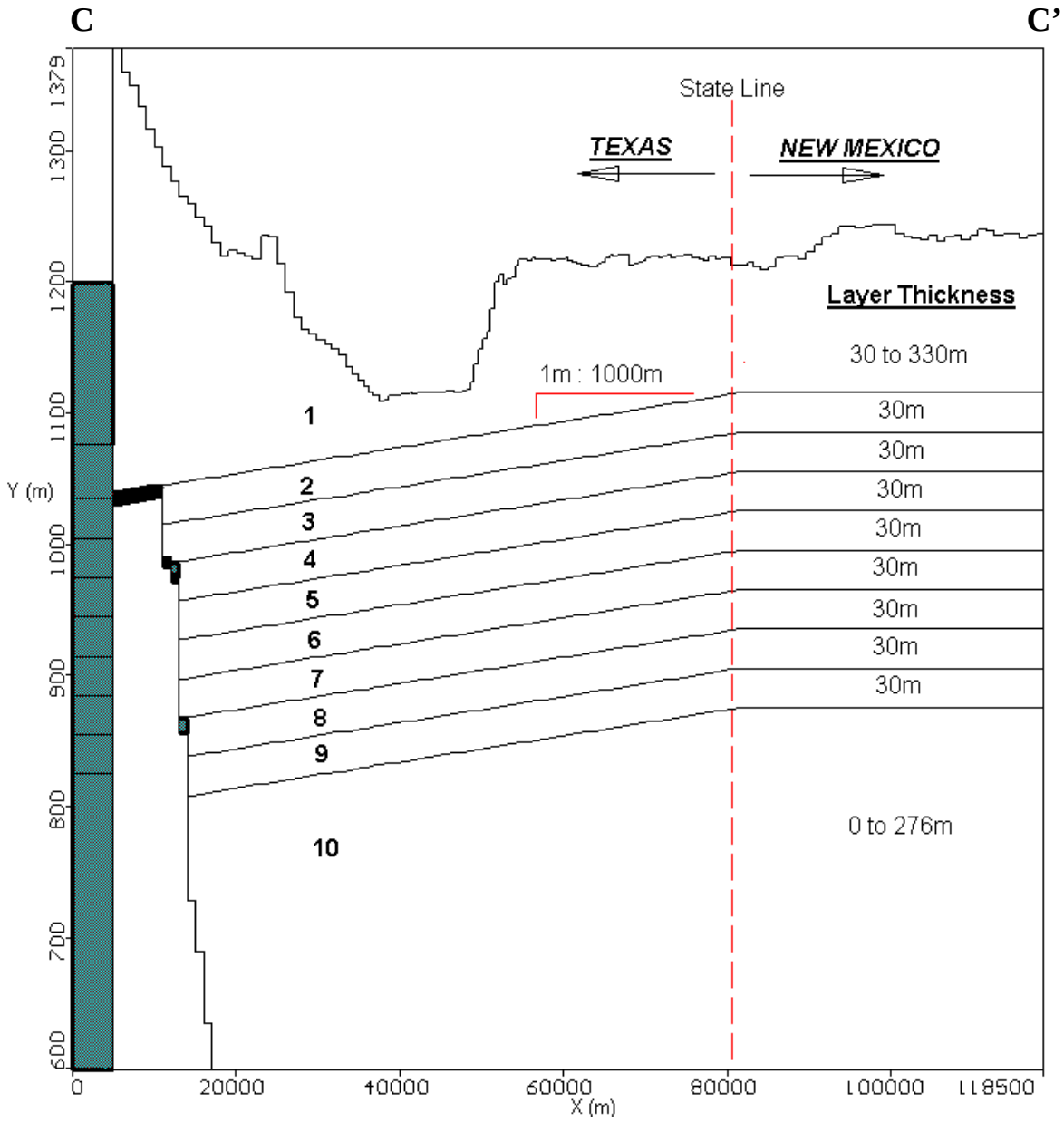

Fig. 20. North to south cross-section (C-C') along column 49 with vertical exaggeration of 160, model layers and thicknesses, grid elevation gradient, and approximate state line location.

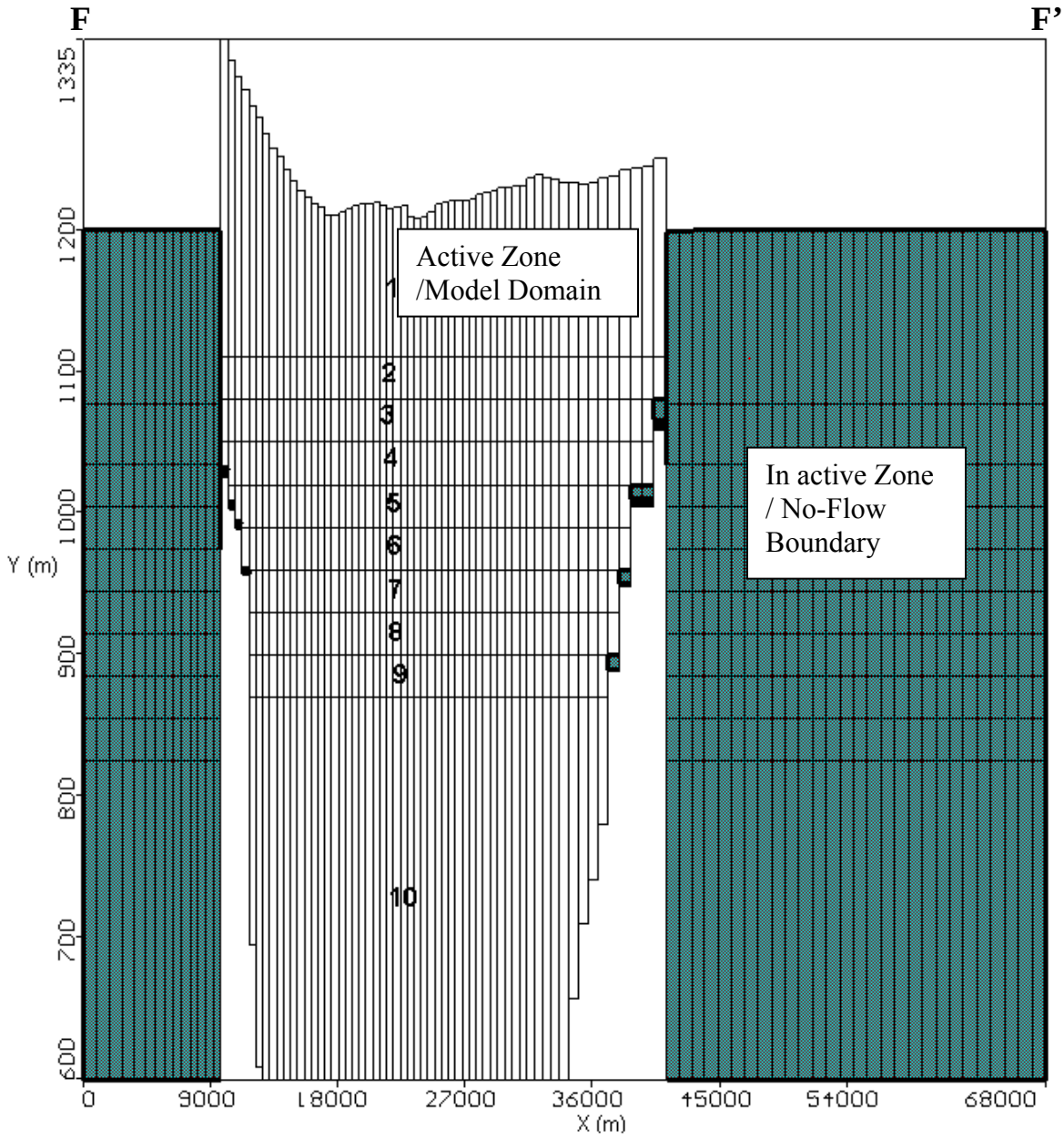

Fig. 21. East to west cross section (D-D') along row 50 with a vertical exaggeration of 100.

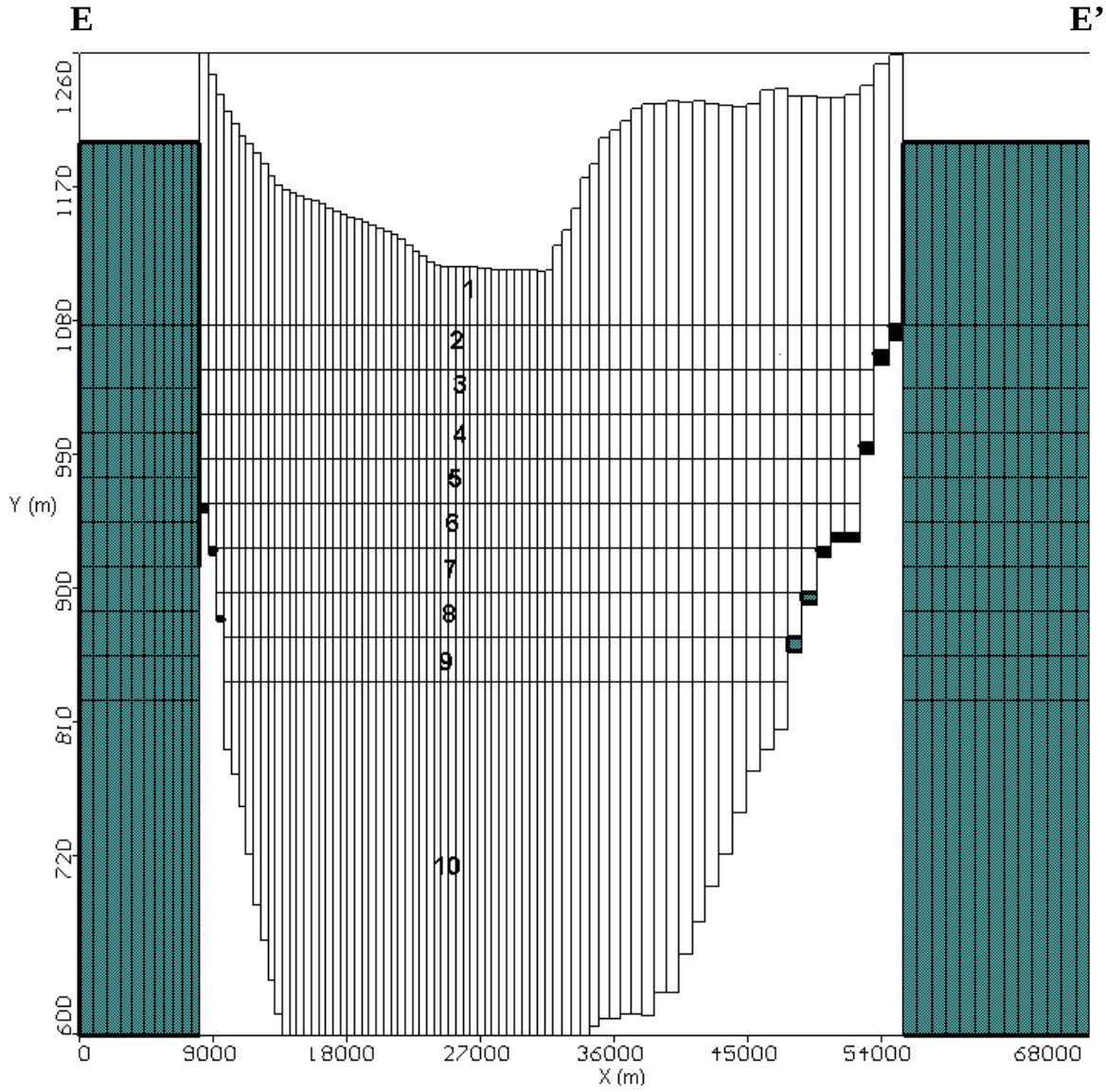

Fig. 22. East to west cross section (E-E') along model row 115 with a vertical exaggeration of 100.

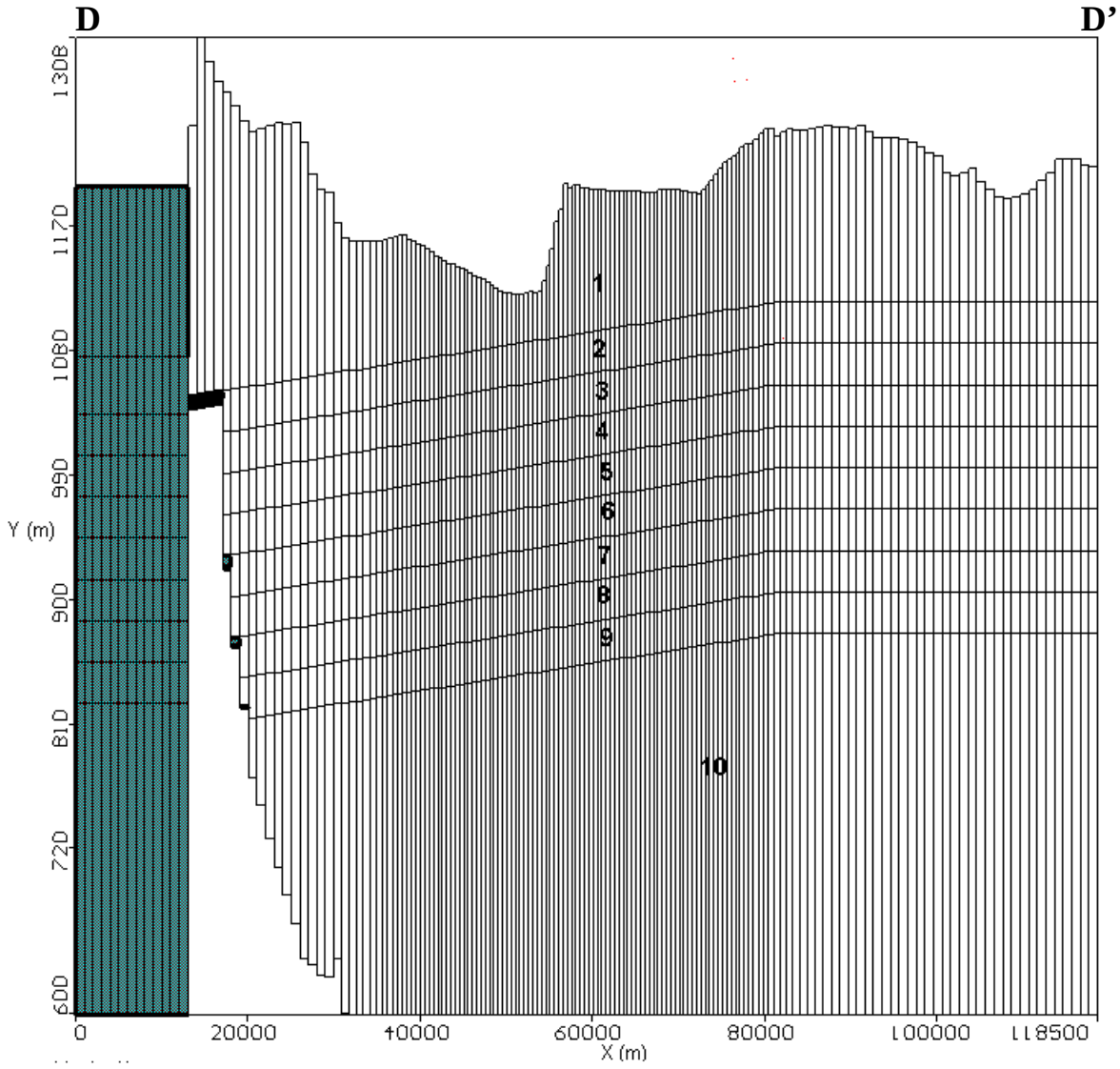

Fig. 23. North to south cross section (F-F') along model column 34 with vertical exaggeration of 160.

Table 4
Transient stress periods and durations from simulation start time in model

Stress Period	Year	Lenght (days)	Duration (days)	Stress Period	Year	Lenght (days)	Duration (days)
1	1903	365	365	48	1950	365	17532
2	1904	366	731	49	1951	365	17897
3	1905	365	1096	50	1952	366	18263
4	1906	365	1461	51	1953	365	18628
5	1907	365	1826	52	1954	365	18993
6	1908	366	2192	53	1955	365	19358
7	1909	365	2557	54	1956	366	19724
8	1910	365	2922	55	1957	365	20089
9	1911	365	3287	56	1958	365	20454
10	1912	366	3653	57	1959	365	20819
11	1913	365	4018	58	1960	366	21185
12	1914	365	4383	59	1961	365	21550
13	1915	365	4748	60	1962	365	21915
14	1916	366	5114	61	1963	365	22280
15	1917	365	5479	62	1964	366	22646
16	1918	365	5844	63	1965	365	23011
17	1919	365	6209	64	1966	365	23376
18	1920	366	6575	65	1967	365	23741
19	1921	365	6940	66	1968	366	24107
20	1922	365	7305	67	1969	365	24472
21	1923	365	7670	68	1970	365	24837
22	1924	366	8036	69	1971	365	25202
23	1925	365	8401	70	1972	366	25568
24	1926	365	8766	71	1973	365	25933
25	1927	365	9131	72	1974	365	26298
26	1928	366	9497	73	1975	365	26663
27	1929	365	9862	74	1976	366	27029
28	1930	365	10227	75	1977	365	27394
29	1931	365	10592	76	1978	365	27759
30	1932	366	10958	77	1979	365	28124
31	1933	365	11323	78	1980	366	28490
32	1934	365	11688	79	1981	365	28855
33	1935	365	12053	80	1982	365	29220
34	1936	366	12419	81	1983	365	29585
35	1937	365	12784	82	1984	366	29951
36	1938	365	13149	83	1985	365	30316
37	1939	365	13514	84	1986	365	30681
38	1940	366	13880	85	1987	365	31046
39	1941	365	14245	86	1988	366	31412
40	1942	365	14610	87	1989	365	31777
41	1943	365	14975	88	1990	365	32142
42	1944	366	15341	89	1991	365	32507
43	1945	365	15706	90	1992	366	32873
44	1946	365	16071	91	1993	365	33238
45	1947	365	16436	92	1994	365	33603
46	1948	366	16802	93	1995	365	33968
47	1949	365	17167	94	1996	366	34334

The model grid and elevations of all the layers increase from the south to the Texas-New Mexico state line (Fig. 19, Fig. 20) at a constant gradient of 1: 1,000. The portions of the layers north of the state line are horizontal. The thickness of the model layers varies throughout the model domain as illustrated (Fig. 20 - Fig. 23). The vertical datum used for the model elevations was that of the National Geodetic Vertical Datum of 1929 (NGVD 29) [5] i.e. the bottom of layer 10 is 600 meters above sea level using NGVD 29.

4.5 TEMPORAL DISCRETIZATION

The transient groundwater flow model created in this study was simulated using 94 annual stress periods representing the time period from 1903 to 1996. To facilitate input of transient data, such as time variant recharge rates, evapotranspiration, stream leakage, and pumping data, into the Visual MODFLOW© pre and post processor the stress periods were converted to durations which assumed time units of days (Table 4). Leap years were accounted for, i.e. the stress period 30, which represents year 1930 (a leap year with 366 days), contains a total duration of 10,958 days from the start of the simulation in the model.

4.6 MODEL INPUT PACKAGES

Groundwater flow in the Hueco Bolson aquifer system in the current model was simulated using 13 file packages, namely, the Basic package (BAS), the Block Centered Flow Package (BCF), the Evapotranspiration package (EVT), the Drain package (DRN), the Discretization package (DIS), the Flow and Head Boundary package (FHB), the

Recharge package (RCH), the Well package (WEL), the Interbed Storage package (IBS), the Horizontal Flow Barrier package (HFB), the Initial Head package (HDS), and the Stream package (STR) [5]. The Algebraic Multi-grid solver (AMG) was used to solve the model for simulations, calibrations, and predictions.

4.6.1 Basic (BAS) package

The Basic package contains input data that defines the model domain. Information pertaining to the active grid cells, which represents the model domain (Fig. 17) and the inactive grid cells (no-flow boundaries) (Fig. 18), were read from the input package file named "HUECOANN2006.BAS."

4.6.2 Discretization (DIS) package

Temporal and spatial discretization data, such stress period lengths, number of layers, rows and columns, horizontal grid spacing, and top / bottom elevations, for the model in MODFLOW 2000 were read from the discretization file named "HUECOANN2006.DIS." The discretization file was created during the MODFLOW 96 to MODFLOW 2000 data conversion process using the USGS MF96TO2K converter.

4.6.3 Flow and Head Boundary (FHB) package

The file "HUECOANN2006.FHB" represents the flow and head boundary package, which contains specified flux data related to the underflows from the Tularosa basin. The FHB package simulates a constant flux of 44.4 m^3/day through cells located in the first row of the model (Fig. 24). This represents a total flux of about 20,424 m^3/day, (approx.7,500,000 m^3/year), which flow through a total of 460 flux cells.

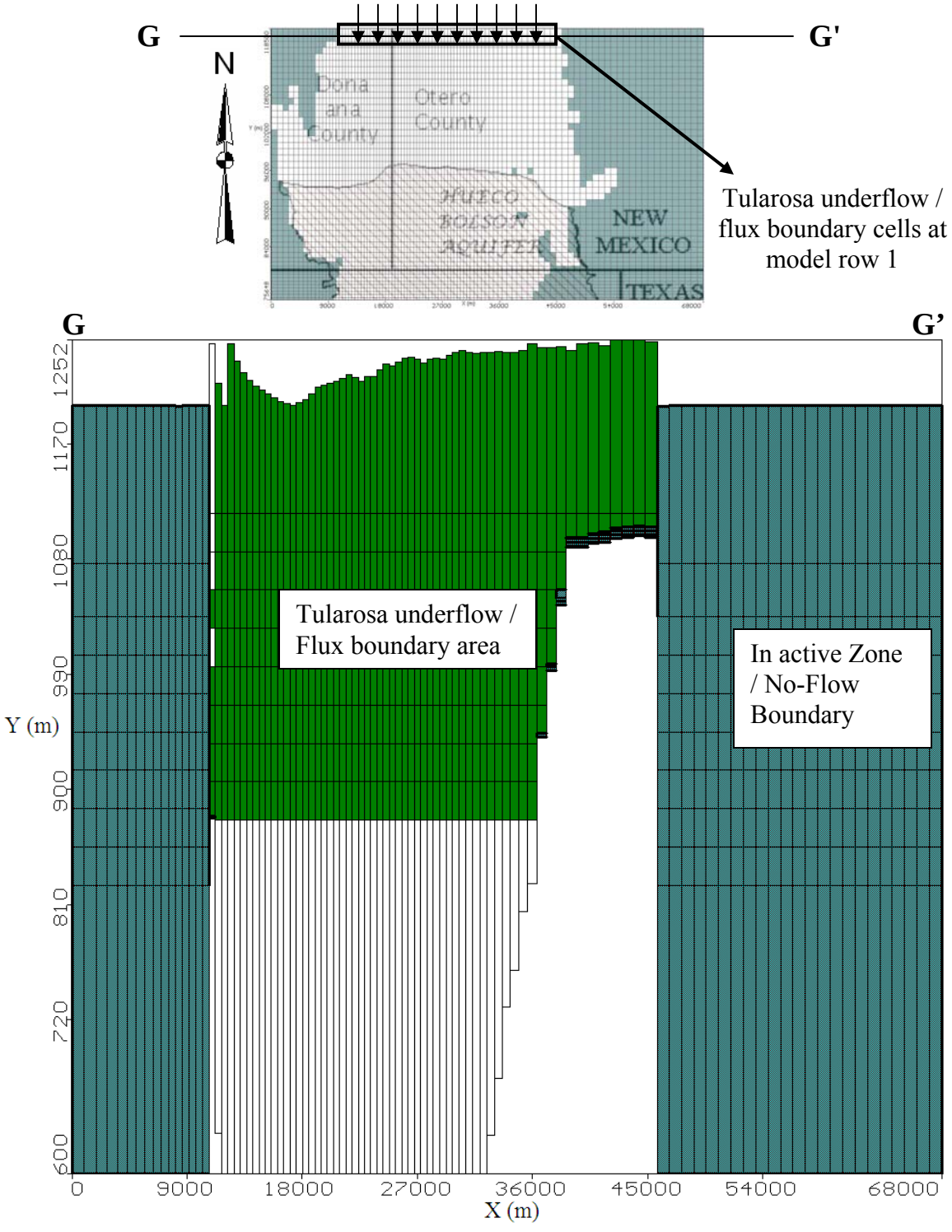

Fig. 24. Tularosa underflow area.

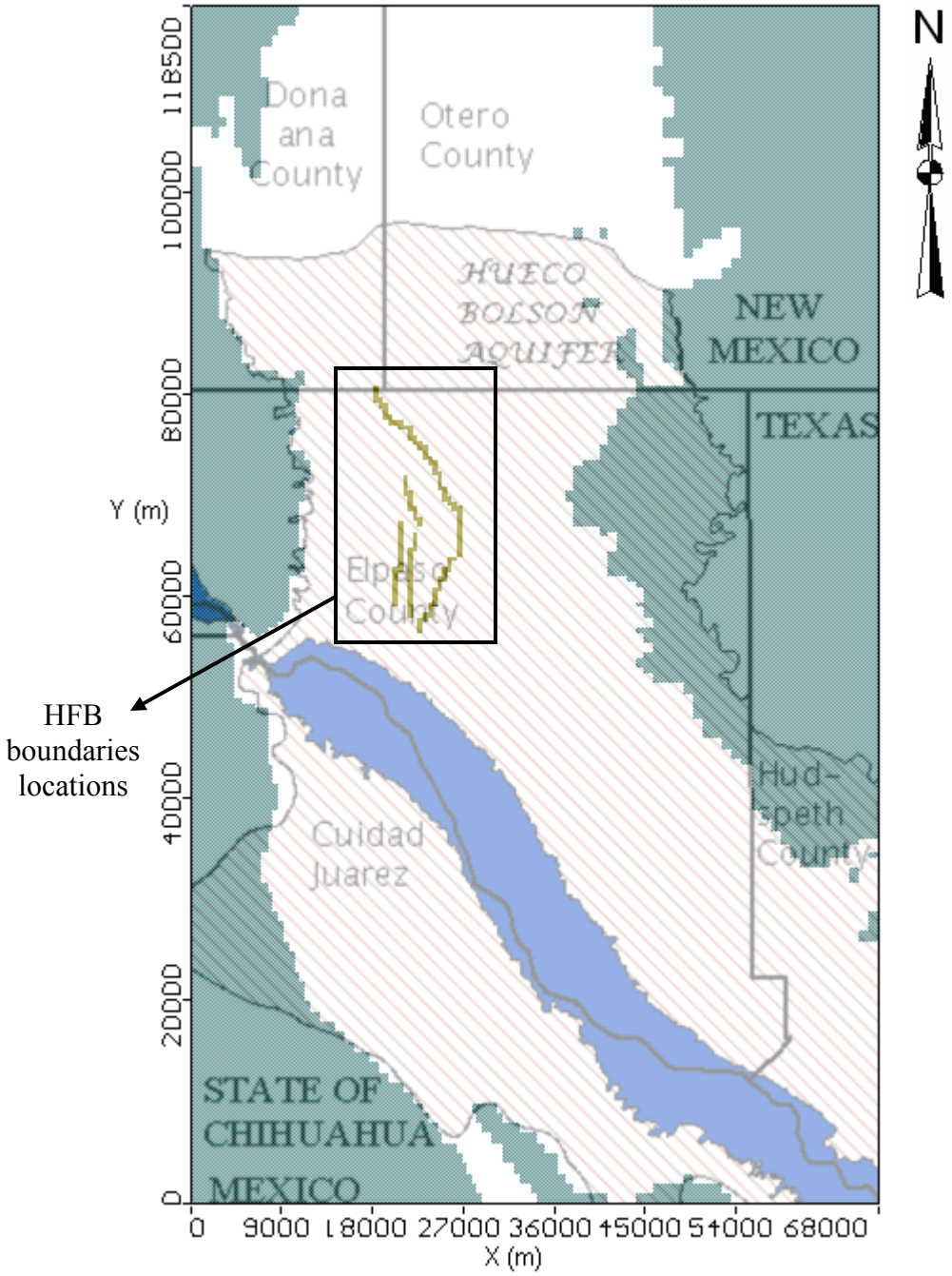

Fig. 25. Location of HFB boundaries.

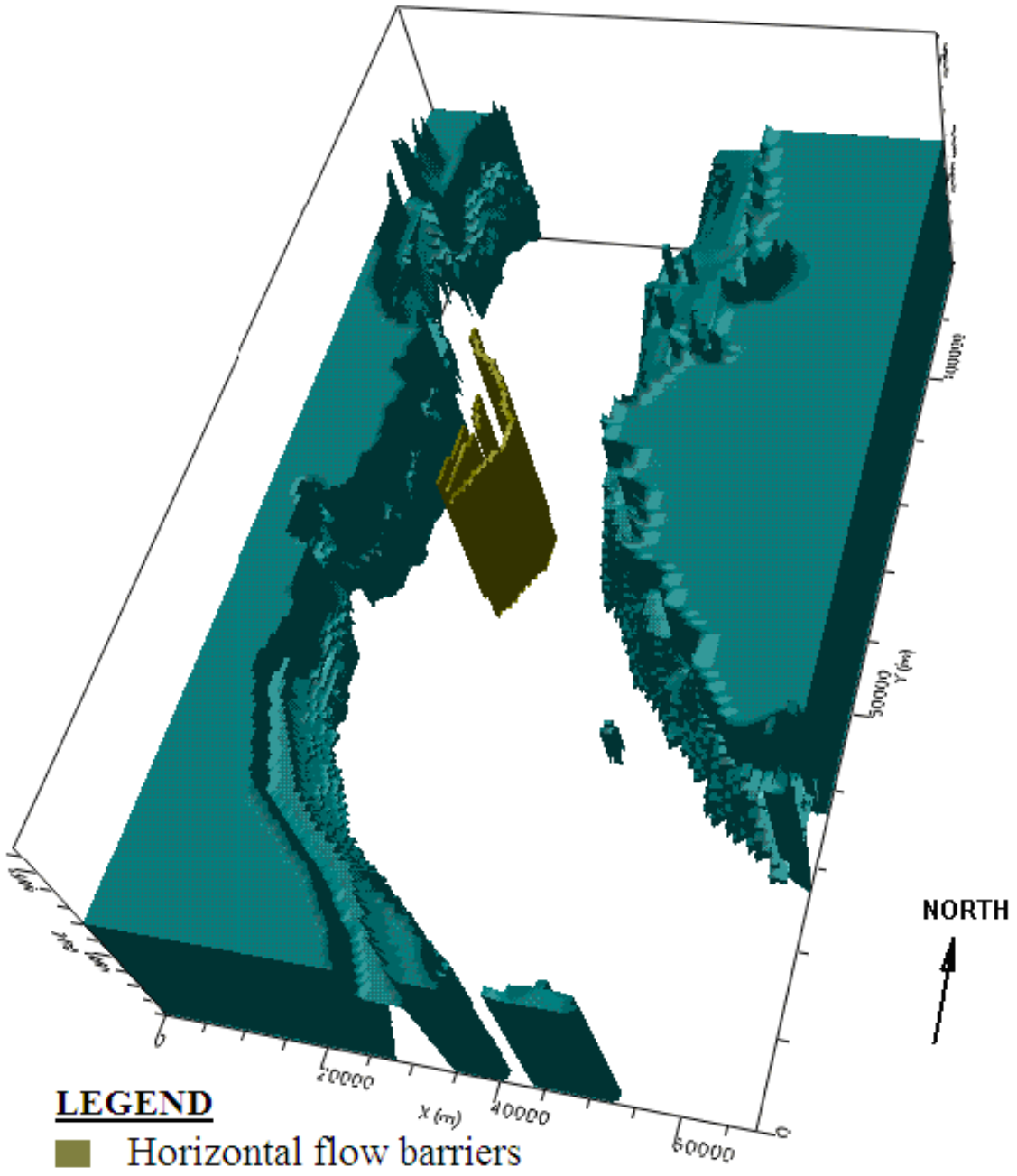

Fig. 26. Location of HFB boundaries in the model domain.

4.6.4 Horizontal Flow Barrier (HFB) package

The faults which impede the groundwater flow were simulated in the model using the horizontal flow barrier (HFB) package. The HFB package was regenerated using the Visual MODFLOW© pre and post processor to facilitate initiation of model runs. The modeled faults, which go through all 10 layers in the model, were located in the El Paso area (Fig. 25 and Fig. 26). The HFB package was read from the file named "HUECOANN2006.HFB" and simulated a total of 1230 HFB cells with 123 fault cells occurring in each model layer. The Hydraulic conductivities of the faults varied from 0.01m/day to 0.001 m/day.

4.6.5 Block Centered Flow (BCF) package

Input data that defines the aquifer layer properties such as, hydraulic conductivity, specific yield, storativity, effective and total porosity total were read in the file named "HUECOANN2006.BCF". Estimates for the different playa facies were determined from the input data from the BCF package and simulation results.

4.6.6 Evapotranspiration (EVT) package

The evapotranspiration processes for the Hueco Bolson in the current model were simulated using the evpotranspiration package. This head dependent boundary data was read from the file named "HUECOANN2006.EVT". The maximum evapotranspiration rate, evapotranspiration surface (land surface), and the extinction depth were specified in the model. The entire model domain is subject to the evapotraspiration calculation when the depth to water is less than the specified extinction depth of 5 meters.

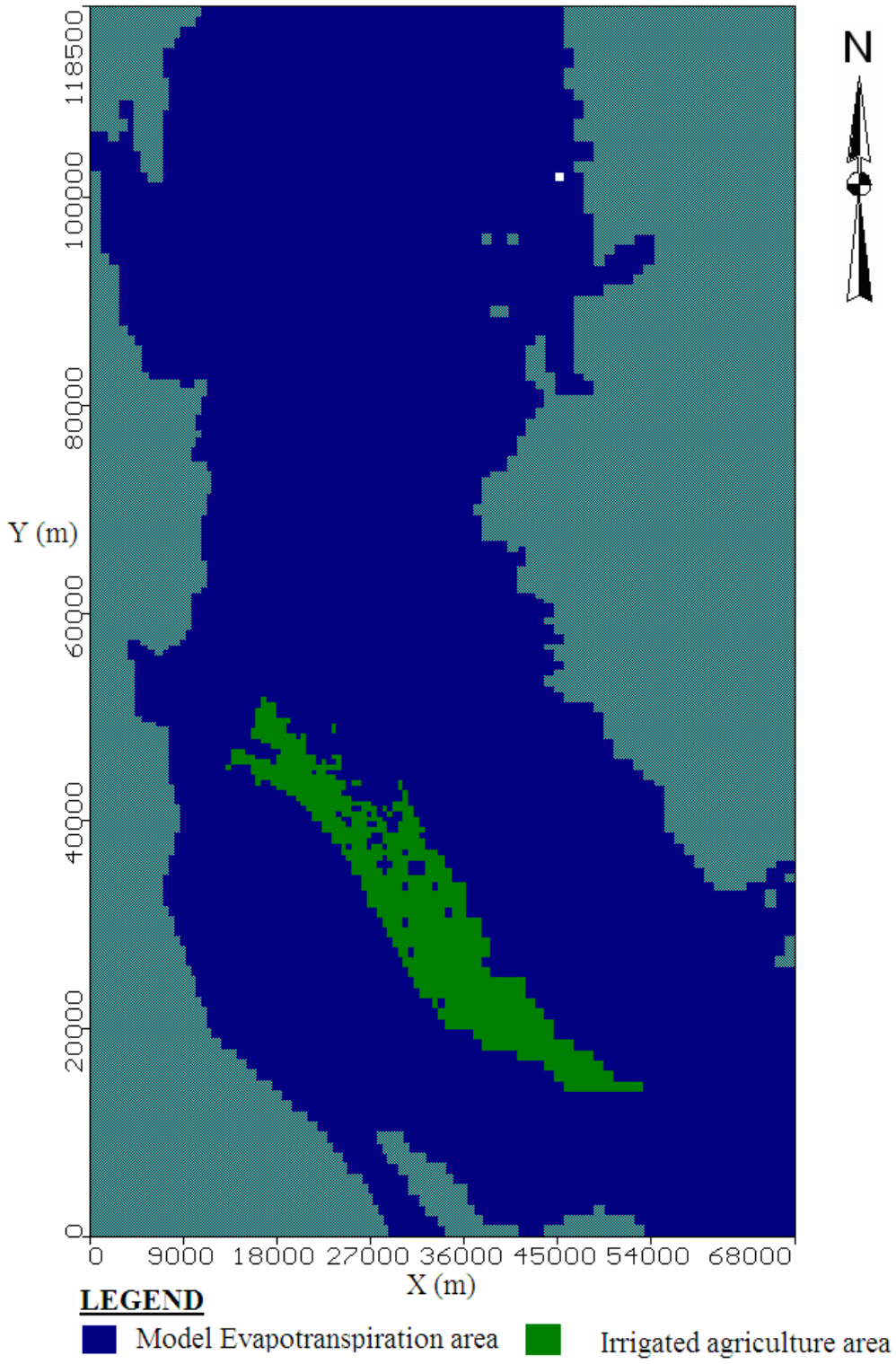

Fig. 27. Evapotranspiration area and excluded irrigated areas.

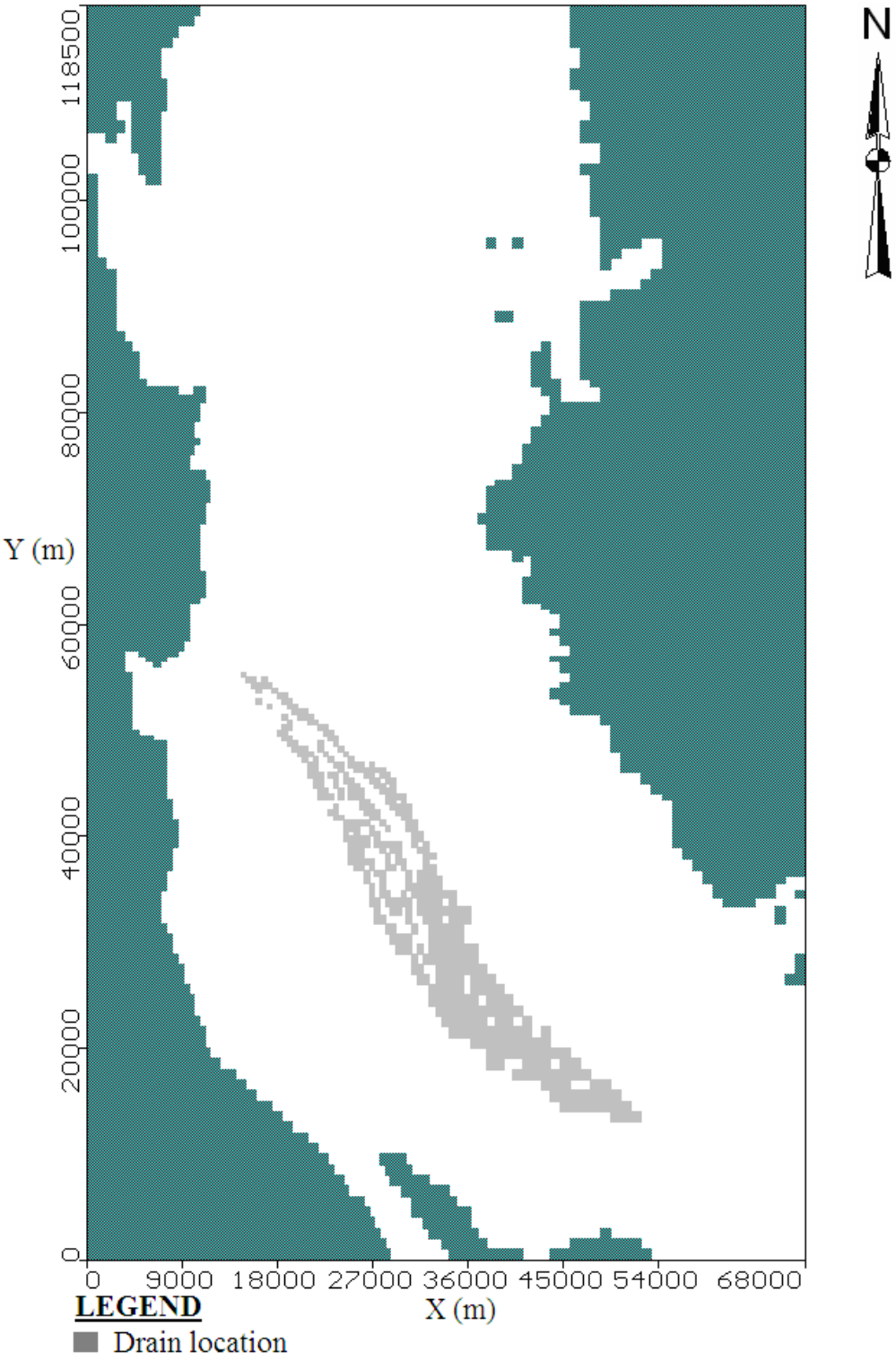

Fig. 28. Drain location.

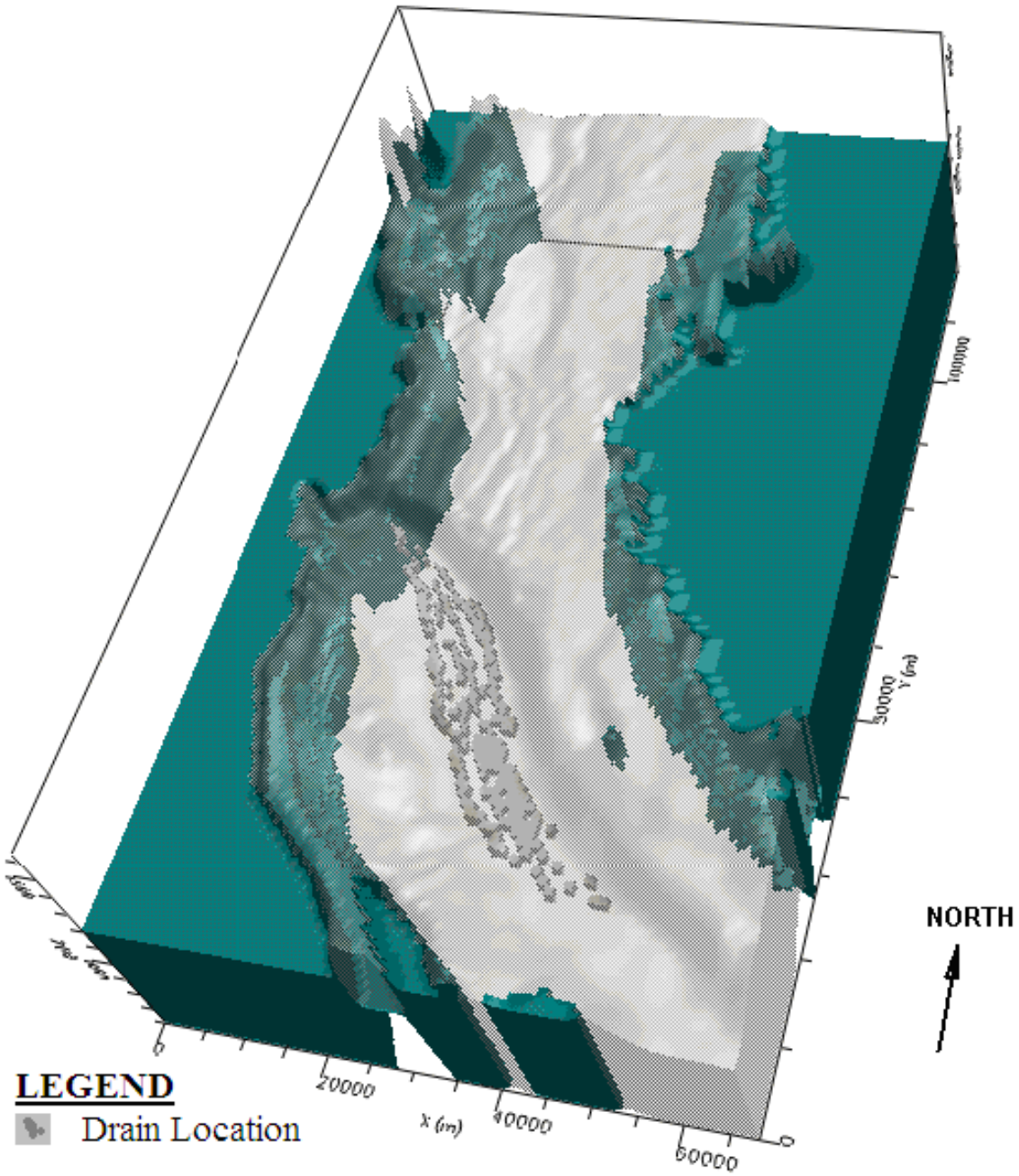

Fig. 29. Drain location in model domain.

A maximum evapotranspiration rate of 1702.06 mm/yr (4.6E-3 m/day) was specified in the model. The irrigated agriculture area located in the Rio Grande Valley is only included as an evapotranspiration area in the start of the simulation from 1903 to 1924 and excluded for the rest of the simulation time. The model evapotranspiration area and the excluded irrigated agriculture area are shown in (Fig. 27).

4.6.7 Drain (DRN) package

The drain package simulated the effects of data related to drains in the model domain. The head dependent boundary data related to the drains was read from the file named "HUECOANN2006.DRN". The drain cells are activated with unchanging boundary elevations and conductance. Using a drain conductance term, movement was simulated which allowed water to discharge from the groundwater system when the head was above the drain boundary head. In the model, the drains, which are also located in the Rio Grande Valley (Fig. 28 and Fig. 29), represent the effects of the change from non irrigated and undrained conditions to the irrigated and drained conditions. In the simulation, the irrigated and drained conditions begin in 1925. Hence, a total of 427 drains cells in the model were only active in the simulation from 1925 to 1996. No drains were active in the start of the simulation from 1903 to 1924.

4.6.8 Stream Routing (STR) package

The interactions related to seepage between the shallow Rio Grande alluvium, the Rio Grande, Franklin Canal, Ascarte wasteway, and the Acequia Marde were simulated using the stream routing package.

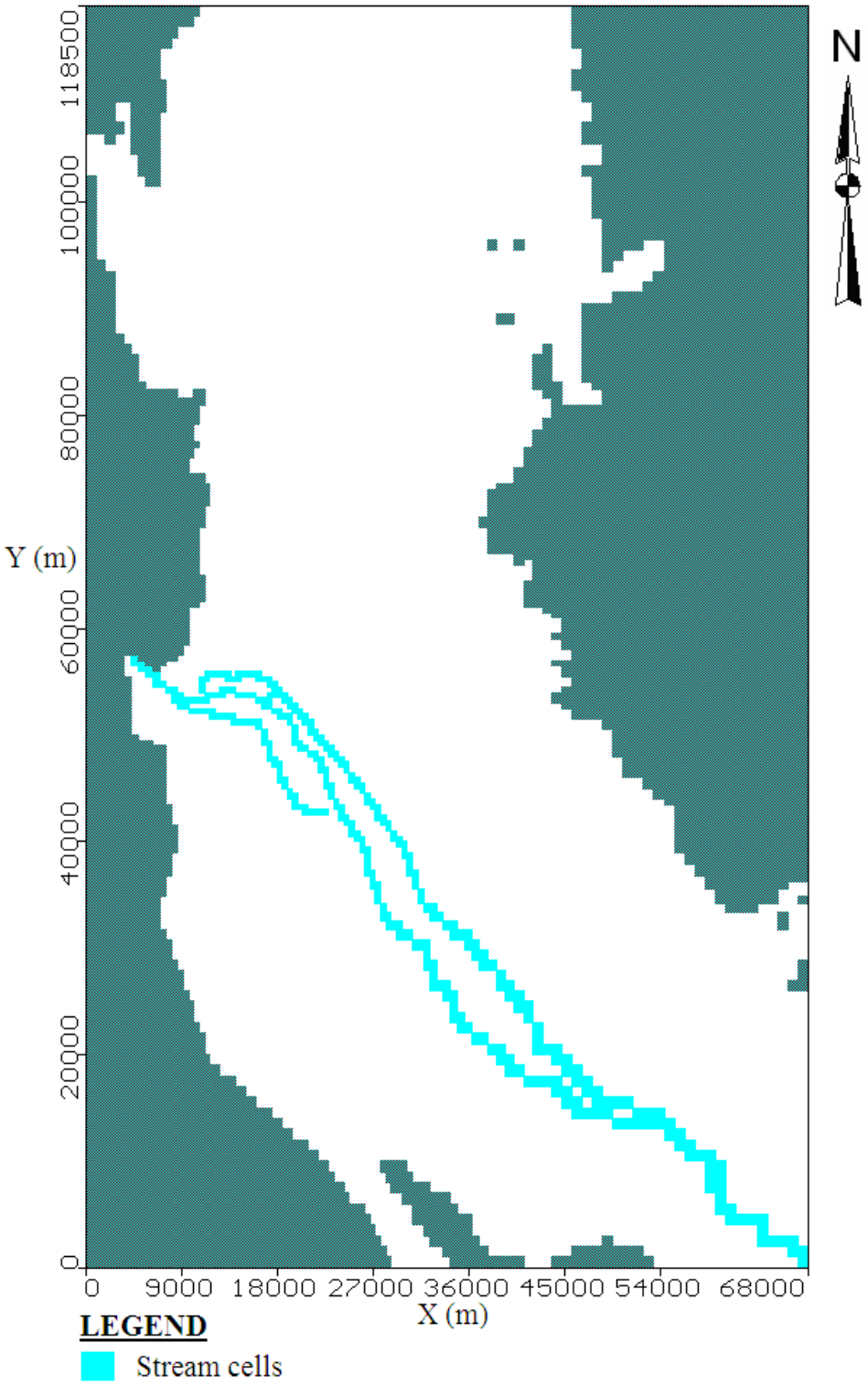

Fig. 30. Stream cells.

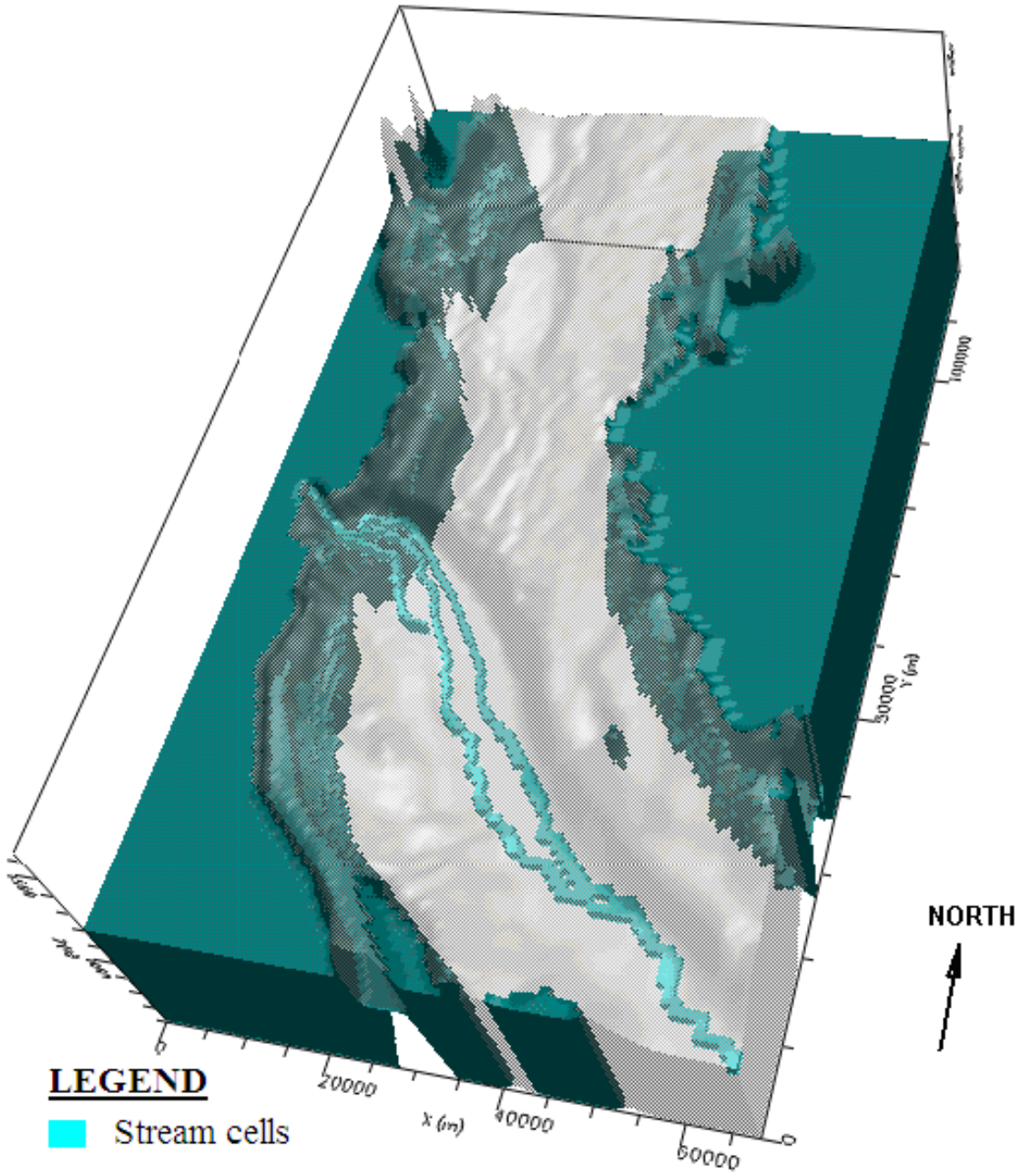

Fig. 31. Stream cells in model domain.

The stream package was also regenerated for MODFLOW 2000 using the Visual MODFLOW© pre and post processor to facilitate initiation of model simulations. The head dependent boundary data related to the stream routing package was read from the file "HUECOANN2006.STR." Specifications for the streambed conductance, surface flow, steam stage elevation, steam top and bottom elevations, channel roughness, and channel slope are contained in the STR package.

Table 5
Stream segments and reaches

Stream segment	# of reaches from start point to end point of segment
1	20
2	5
3	107
4	102
5	30
6	47
7	33

The stream routing package in the model simulated a total of 7 stream segments, which occur in the topmost layer 1 (Fig. 30 and Fig. 31). Specifications for the reaches of each stream segment are shown in Table 5. The streambed conductances for the stream segments ranged from 62 to 7203 m^2/day.

4.6.9 Recharge (RCH) package

The boundary data, which included specified flux data related to mountain front and border irrigation recharge, were read from the file named "HUECOANN2006.RCH."

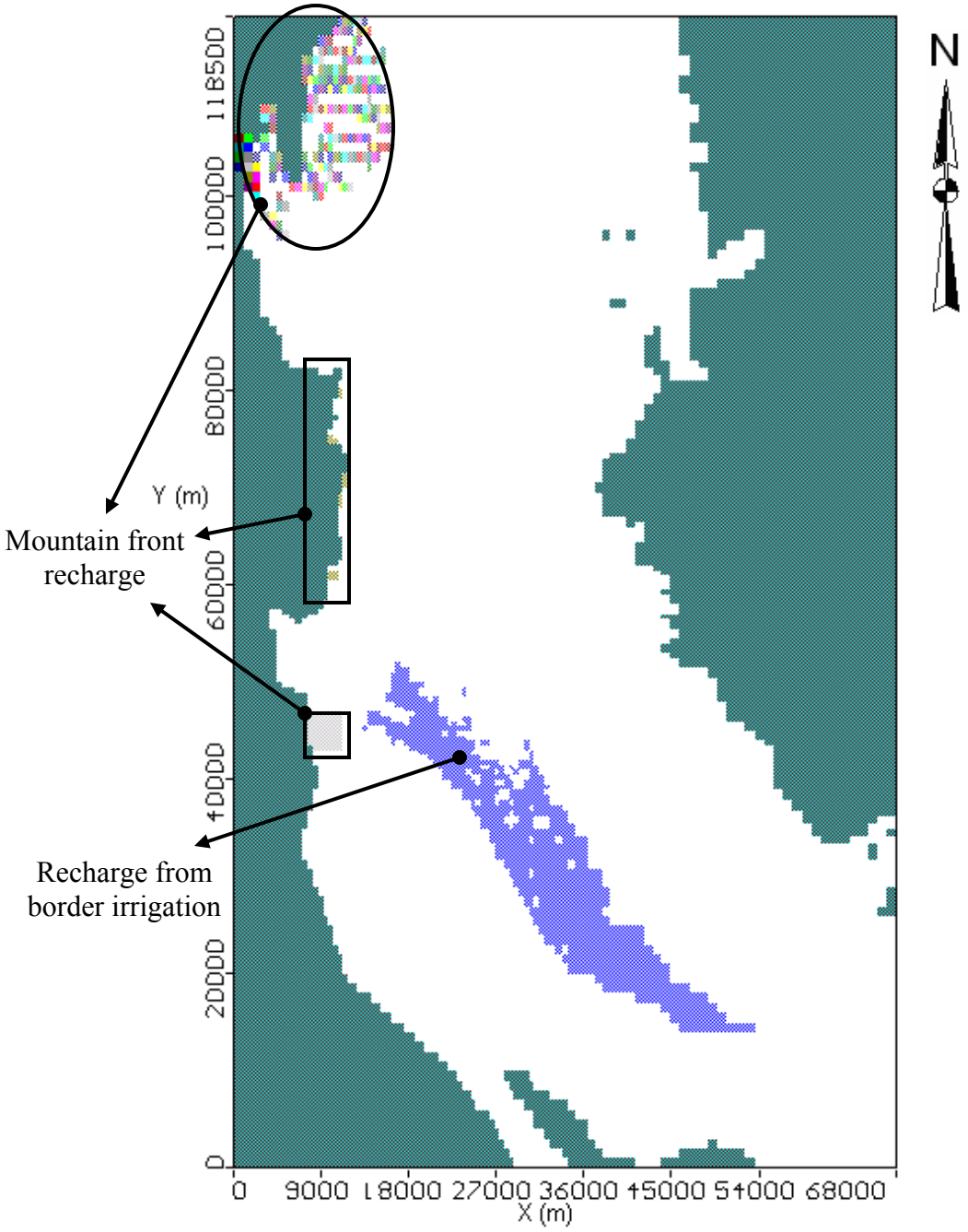

Fig. 32. Model recharge areas.

The recharge package simulated the flux data of recharge from the U.S and Mexican sides, and recharge from irrigation. In the simulations, recharge from border irrigation only occurs on both sides of the border from 1925 to 1996 (Fig. 32). On the U.S. side, mountain front recharge on the eastern side of the aquifer and the base of the Organ and Franklin Mountains were simulated. On the Mexican side, mountain front recharge at an area at the base of the sierra Juarez Mountain was simulated.

4.6.10 Interbed Storage (IBS) package

The interbed storage package simulated the elastic and inelastic compaction that is assumed to occur in all layers. The compaction of the aquifer is a result of the historical pumping which reduced the groundwater elevation. In the current model, interbed storage was read from the file named "HUECOANN2006.IBS." The preconsolidation head arrays for layer 1 were read from the file named "HC1.array." The preconsolidation head arrays for the rest of the layers, 2 through 10 were read from the file named "HC2.array," and the thickness of the interbeds were read from file named "thick10.array." No previous consolidation was assumed. The inelastic storage factor for all the layers is estimated to be 2.0×10^{-3} and the elastic storage factor for all the layers is estimated to be 2.1×10^{-4}.

4.6.11 Initial heads package

Starting heads and initial conditions of the aquifer were obtained from the steady state simulation done by Heywood and Yager (2003).

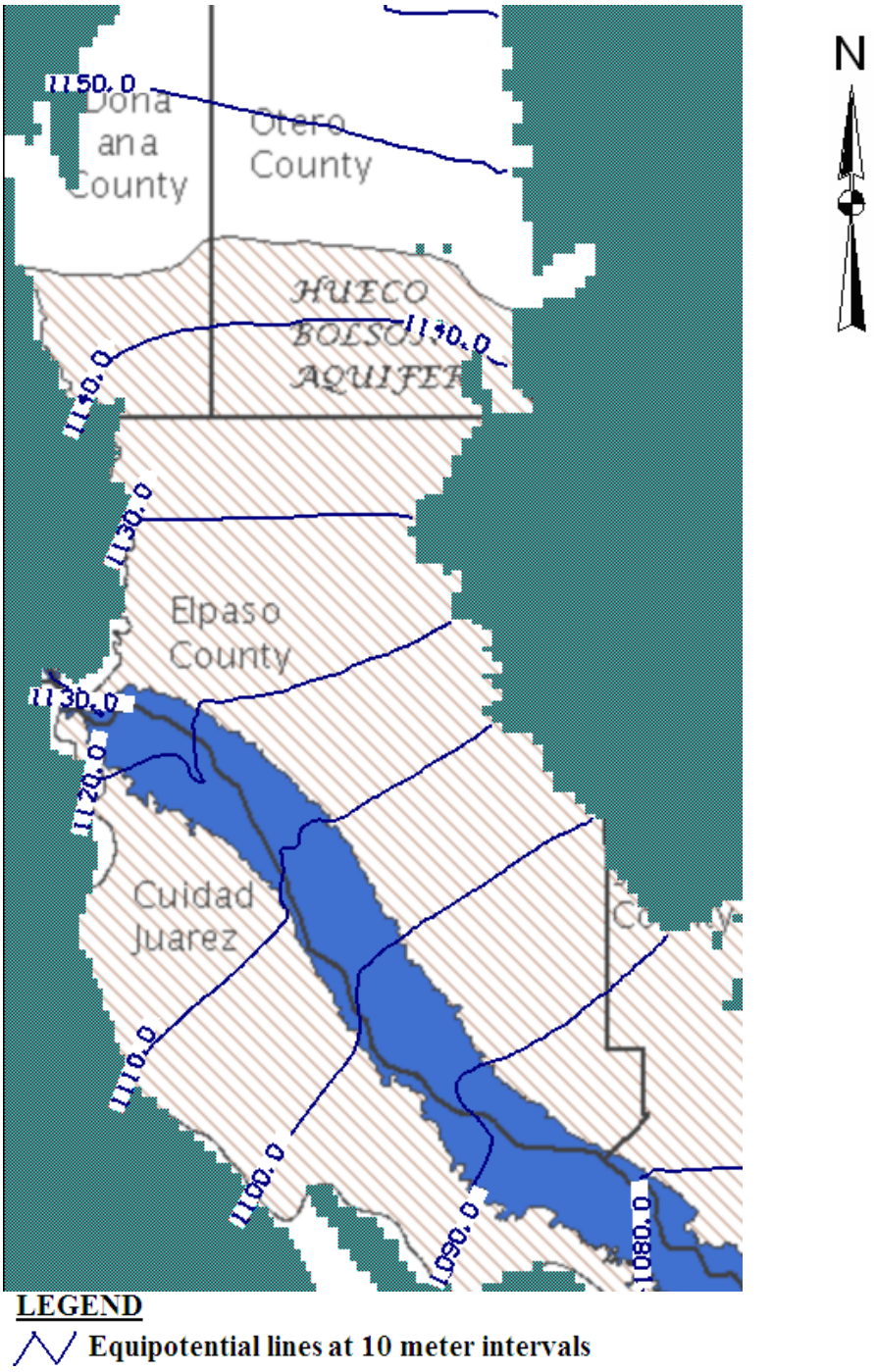

Fig. 33. Initial head equipotential map.

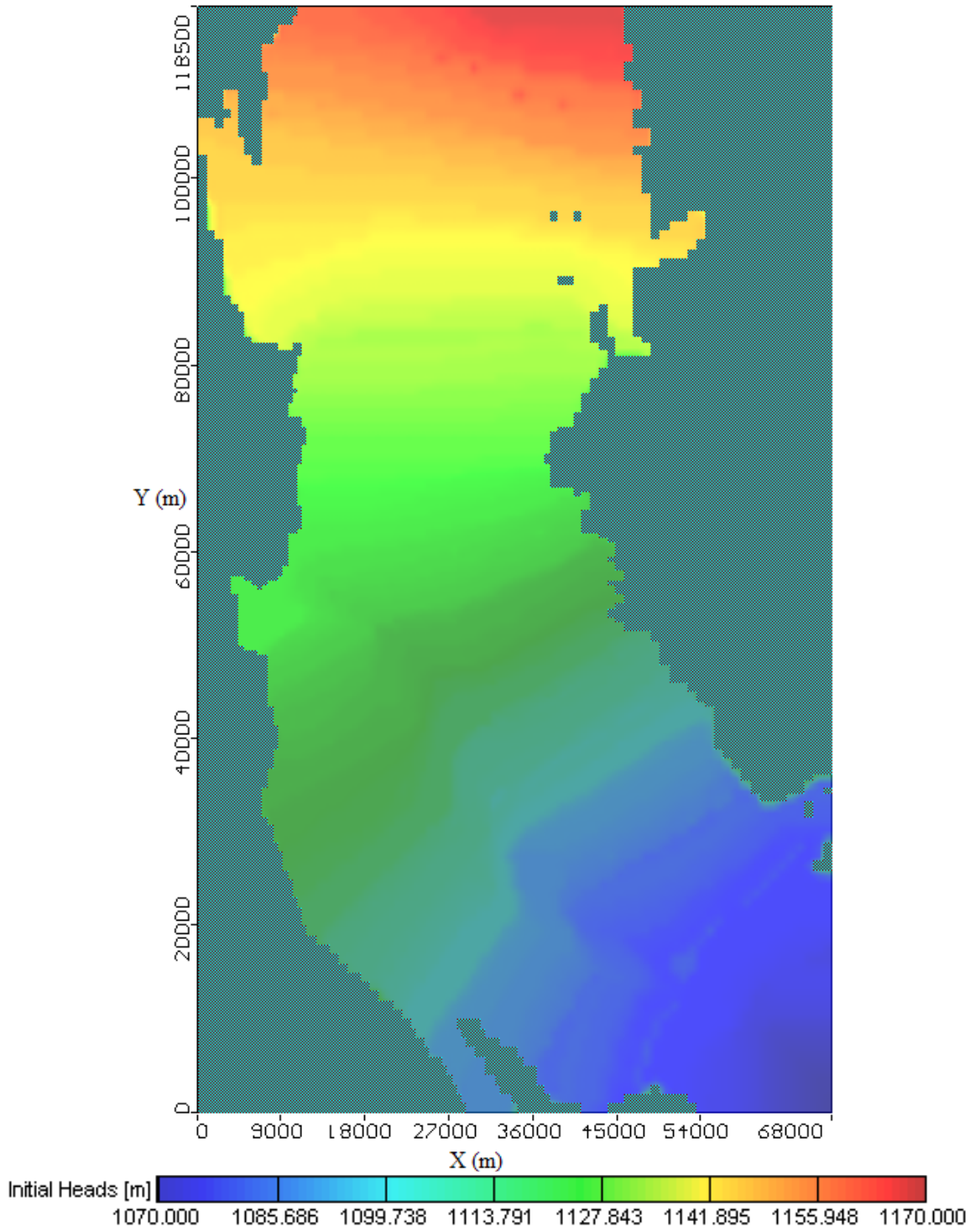

Fig. 34. Initial heads colored map.

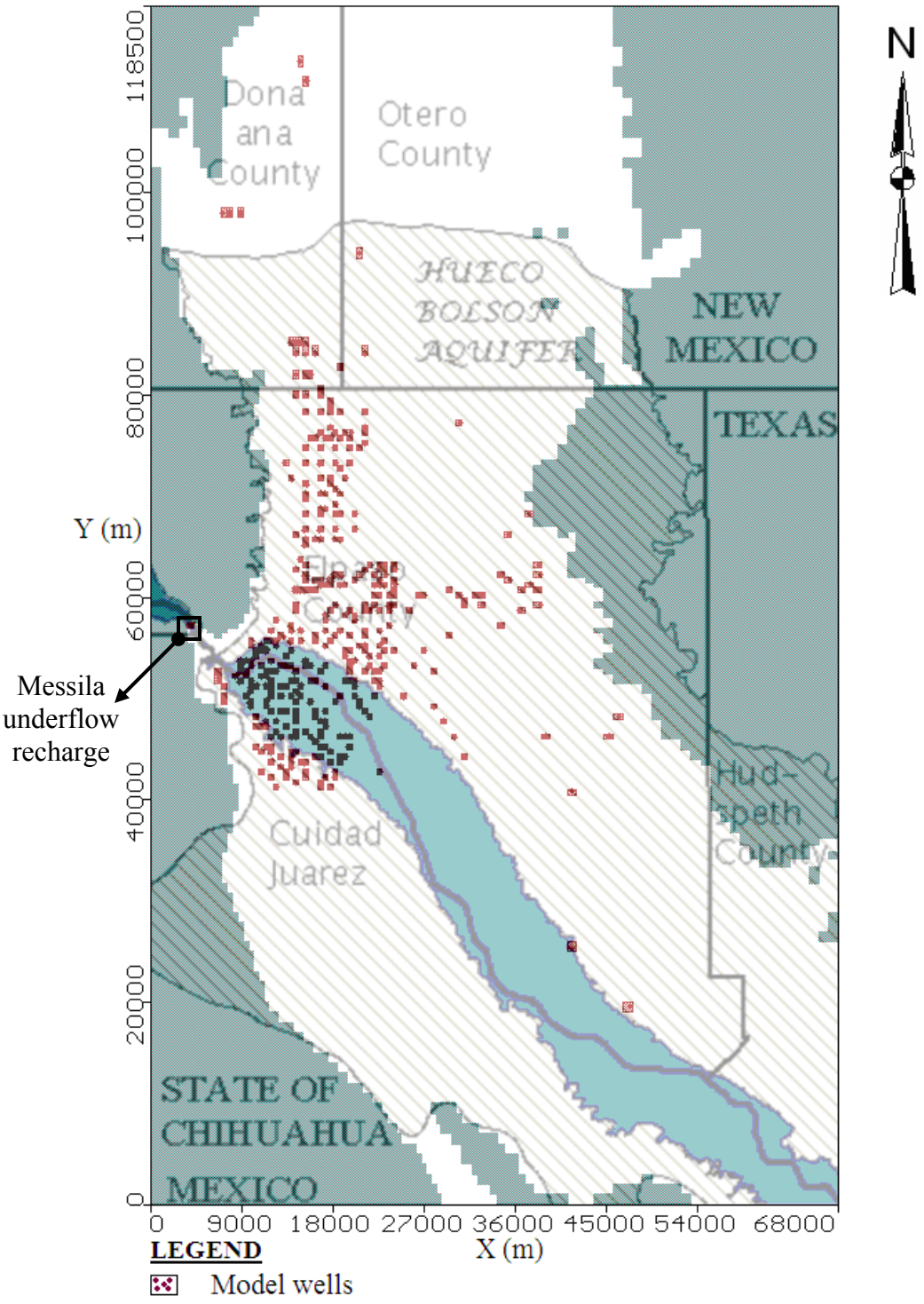

Fig. 35. Pumping and recharge wells.

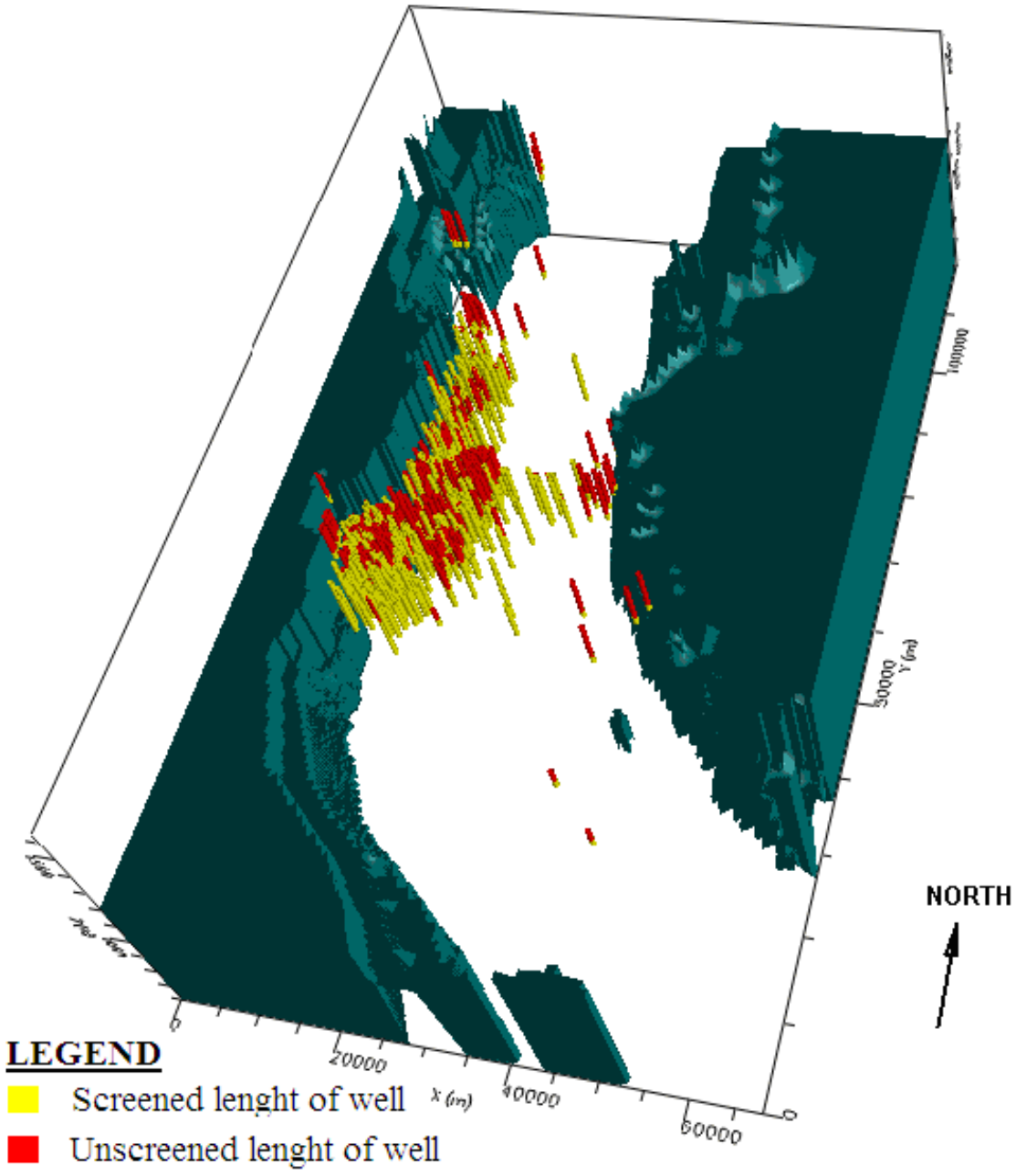

Fig. 36. Pumping and recharge wells in model domain.

The steady state simulation was used to simulate initial parameters representing predevelopment conditions during the creation of the Hueco Bolson GAM [5]. The initial heads of the aquifer range from 1070m to 1160m, decreasing from north to south as shown (Fig. 33 and Fig. 34). In the current model, the data related to the initial heads were read from the file named "HUECOANN2006.VIH," and the resulting head outputs were read from the file named "HUECOANN2006.HDS."

4.6.12 Well package

The well package simulated stresses on the aquifer due to known historical pumping (municipal supply, private wells, military, and industrial), human induced recharge, and the Mesilla underflow. The WEL file in this is model was manually generated by combining well data from the Hueco Bolson GAM MAW package (wells screened in more than one layer) and the WEL package (wells screened in only one layer) into one well file. In the current model, groundwater pumping and human induced recharge were simulated using the regenerated well file named "HUECOANN2006.WEL."

Data for a total of 434 pumping and recharge wells, screened in multiple and single layers (Fig. 35 and Fig. 36) which are located on the U.S. and Mexican sides, were included in the well package. Additionally, an underflow recharge of 338m^3/day from the Mesilla Bolson to the Hueco Bolson was simulated using a well as shown (Fig. 35).

4.6.13 Algebraic Multi-Grid (AMG) solver package

The specifications for the chosen solver package, the AMG solver, were read from the file named "HUECOANN2006.LMG." The AMG solver presents certain advantages and disadvantages over other conventional solvers that were considered, such as the successive over-relaxation (SOR), strongly implicit procedure (SIP), and the preconditioned conjugate-gradient method (PCG) solvers. Some of its advantages include improved coarsening techniques and adaptive damping. A disadvantage of the AMG solver in comparison to other solvers is in high memory usage. However the AMG solver has been proven to solve broader classes of problems related to nonlinear models in shorter times [39].

Solver specifications used for the current model included the convergence criterion, called the budget closure criterion (BCLOSE), which was set at 0.33. The BCLOSE criterion was chosen based on the scale of the problem. Other specifications included a maximum number of iterations (MXITER) of 2000, maximum number of cycles (MXCYC) of 30, and a damping factor (DAMP) of -2. A damping factor of -2 represented the relative residual adaptive damping method. A maximum damping factor (DUP) of 1 and minimum damping factor (DLOW) of 0.1 were used. Fixed values of DAMP can deter the head solution convergence progress in highly nonlinear problems. Adaptive damping methods facilitated convergence by adjusting the amount of damping based on residual fluctuations during the solving process [39].

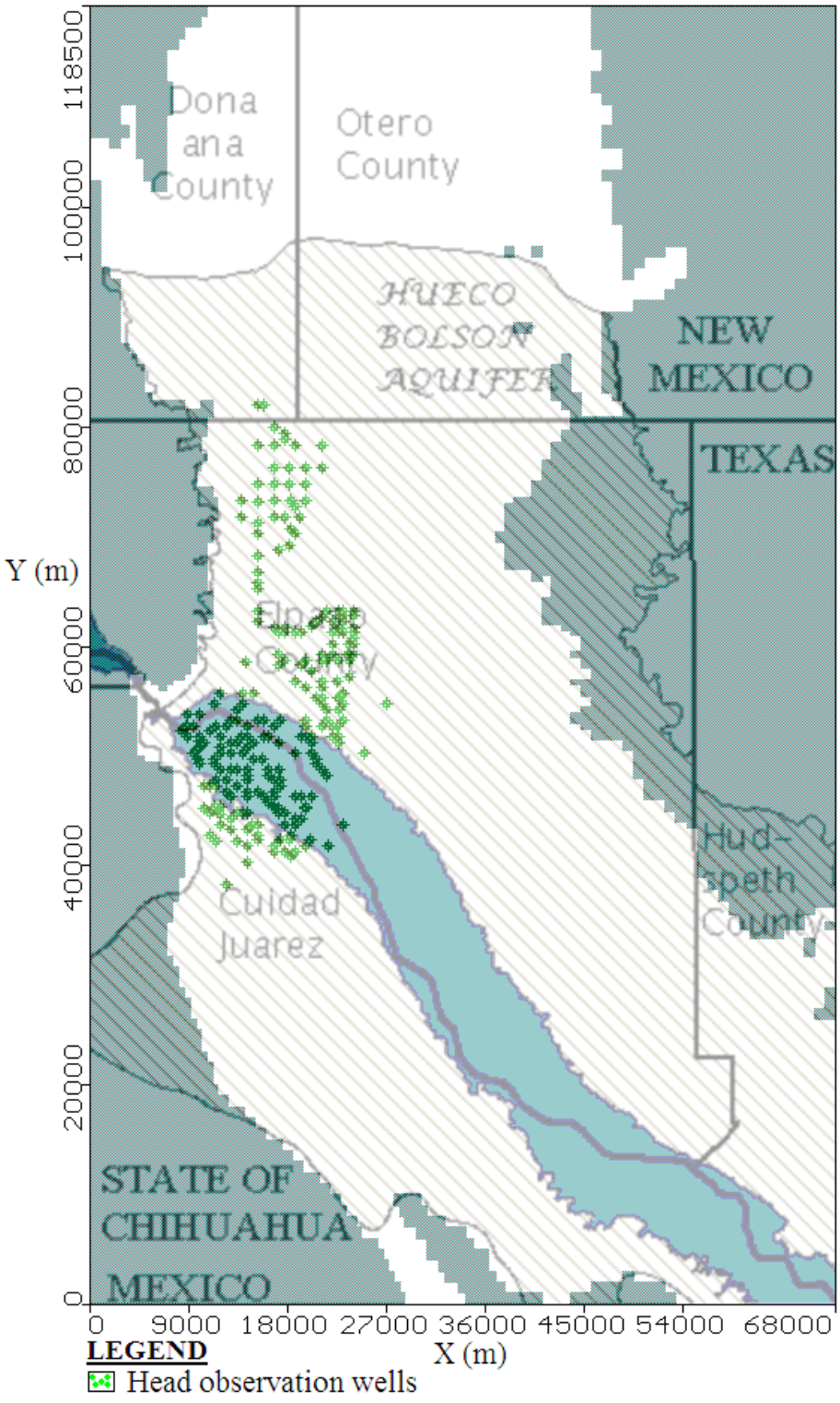

Fig. 37. Calibration dataset head observation wells.

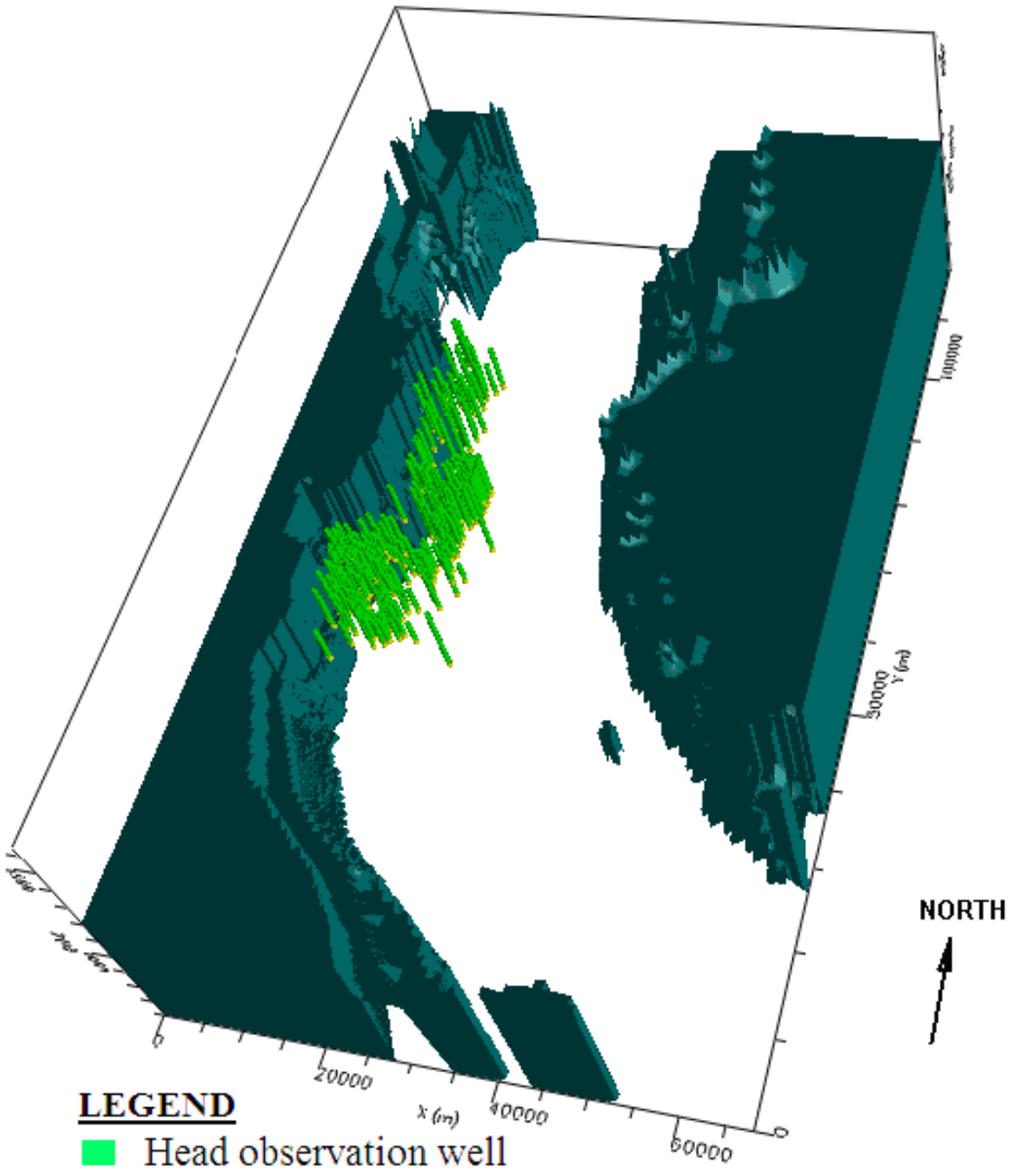

Fig. 38. Head observation wells.

4.7 MODEL CALIBRATION

The simulated heads of the current model were calibrated using Visual PEST© and a data set obtained from the EPWU. The calibration dataset is composed of 2806 head measurements taken in 244 wells from 1935 to 1996. The conductivities and storage parameters were adjusted during the calibration process. The observation well measurements were located throughout the model domain (Fig. 37 and Fig. 38).

The calibration data set consisted of EPWU wells located on the U.S. side and JMAS wells located on the Mexican side of the border. However, due to uncertainty in the reported measurements made on the Mexican side, weights of 67% were applied to the JMAS observation wells and weights of 100% were applied to the EPWU wells. Some specifications for the PEST calibration settings include an initial Marquardt Lambda (RLAMBDA1) of 50, a Lambda adjustment factor (RLAMFAC) of 3, a maximum relative parameter change (RELPARMAX) of 5, and a maximum factor parameter change (FACPARMAX) of 5.

4.8 PREDICTIVE CASE STUDIES

4.8.1 Future water demand and availability

The model developed in this endeavor was employed to perform simulations in a hypothetical scenario. In the hypothetical scenario, the population of the U.S.-Mexico border in the El Paso/Ciudad Juarez area doubles by the year 2050. The water demands also increase accordingly. The development of the prediction model required the determination of the predictive model datasets.

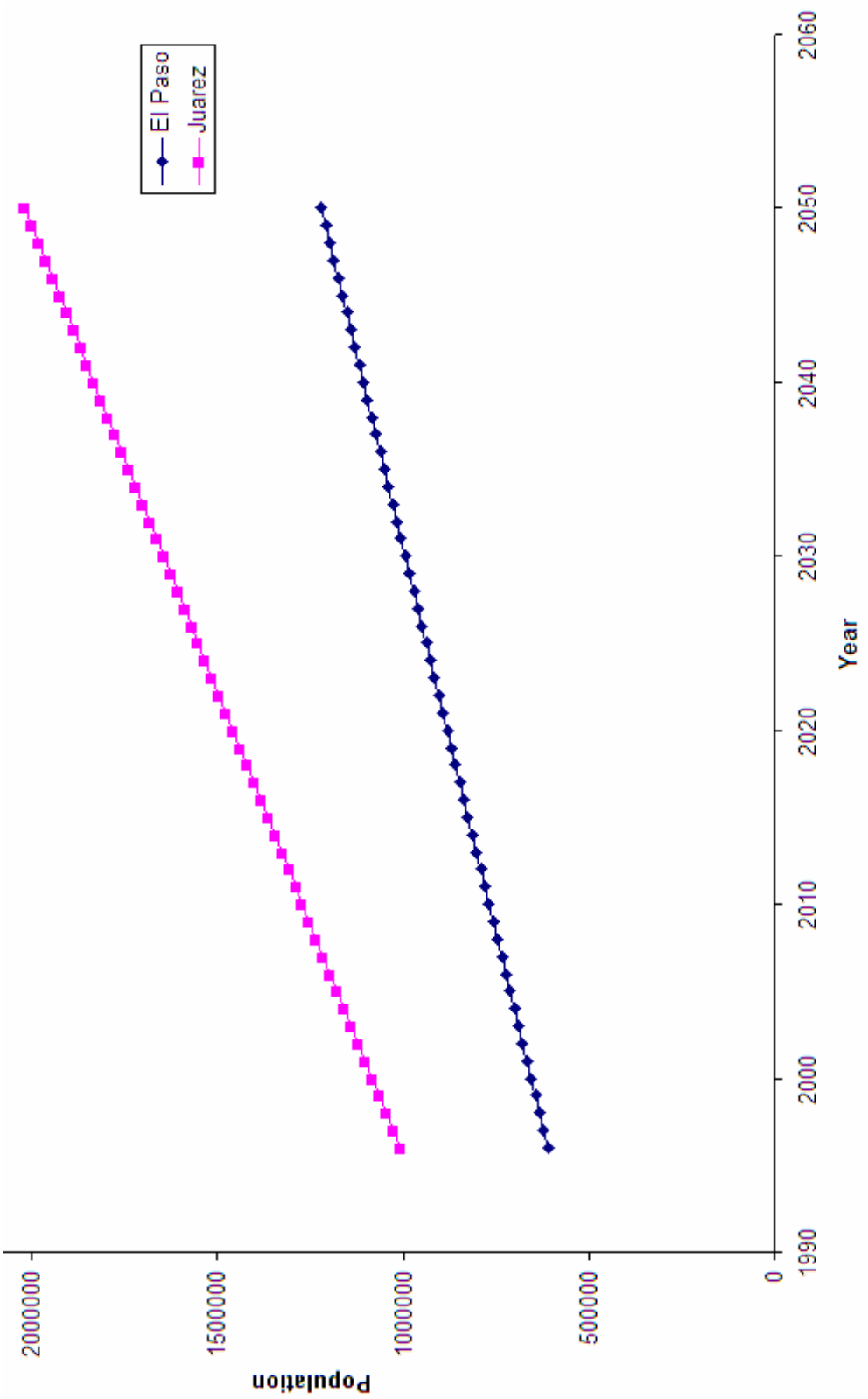

Fig. 39. Predicted population increase for hypothetical scenario.

The only factors that were modified during the predictive simulations were the pumping and human induced recharge. The predictive model datasets were developed by assuming constant mountain front recharge, Tularosa underflow, stream leakage, and evapotranspiration in the stress periods over the prediction period from 1996 through 2050. Data sets for the prediction model, which included pumping demands and human induced recharge, were determined based on linear increase assumptions.

These datasets were determined by doubling the pumping and recharge in the wells in the year 2050 from pumping in the year 1996 following a linear increase during the prediction period. However, the recharge well simulating the Mesilla Bolson underflow was kept constant during the prediction period. The population and water demands from the groundwater supply (groundwater pumping in the aquifer) were increased linearly from the year 1996 (the end of the model simulation) to the year 2050 (Fig. 39). All other aquifer conditions from 1996 were kept constant throughout the predictive scenario. Results pertaining to groundwater availability and supply such as groundwater usage from pumping and storage were obtained and analyzed using ZONEBUDGET.

4.8.2 Border contamination assessment

There are several land-fill and hazardous waste sites located in the U.S.–Mexican border area as identified by the U.S. EPA. Additionally, landfills and other hazardous waste sites are heavily regulated on the U.S side and not as rigorously on the Mexican side. The current model was employed to examine scenarios where the releases of a non reactive conservative contaminant, occurring at an annual rate of 1000 mg/L, unobserved

in the year 1996, and discovered about 50 years later (in the year 2050). These releases occur at 5 solid waste disposal sites. 3 solid waste disposal sites were located on the U.S. side of the border and 2 on the Mexican side of the border.

Fate and transport modeling was performed using MT3DMS©, analyzed, and examined. The sources of potential contamination were modeled as regions within the active model domain, representing the locations of the landfills sites in the border area. In the transport simulations, no initial concentration was assumed and the problem was assumed to be advectively dominated. No physical dispersion was assumed, hence, effects due to dispersivity were not considered in the simulation. Additionally, no chemical reactions of the contaminant were assumed to occur. Solver solution problems, associated with artificial oscillation and numerical dispersion, were mitigated in MT3DMS© by selecting the central finite difference solution method. An effective porosity and total porosity of 0.15 and 0.3 were assumed for the entire model domain.

5. RESULTS AND DISCUSSIONS

Aquifer tests are performed in groundwater modeling to obtain required modeling parameters such as Hydraulic conductivities and storage parameters. Additionally, knowledge of aquifer hydrogeology enables generalizations, which can simplify complicated and highly heterogeneous aquifer geology for modeling purposes. Aquifer tests can not only be expensive, but, additionally, insufficient test results for the required model parameters are obtained from them. Model grid parameters for the entire model domain which are required for simulations are hereby extrapolated from the acquired test results. Therefore, model calibration is required for groundwater models. In this dissertation, data obtained from aquifer field testing were used to establish the numerical limits, by which the model calibration process adjusted the initially determined model parameters. Model calibration is typically employed to produce model results, which corroborate field measured observation data. Measured data, such as aquifer heads, are typically obtained over time. Calibration results are also normally examined at the observation points. It should also be noted that different combinations of model parameter values can result in similar model solutions. In the current model, the vertical and horizontal hydraulic conductivities, and storage parameters (specific storage and specific yield) were adjusted to improve the overall goodness of fit of the model.

5.1 CALIBRATION STATISTICS

Several statistical inferences were employed to provide a good measure of the overall goodness of fit of the model, which include the head residual, the absolute residual mean, the normalized root mean square, and the correlation coefficient.

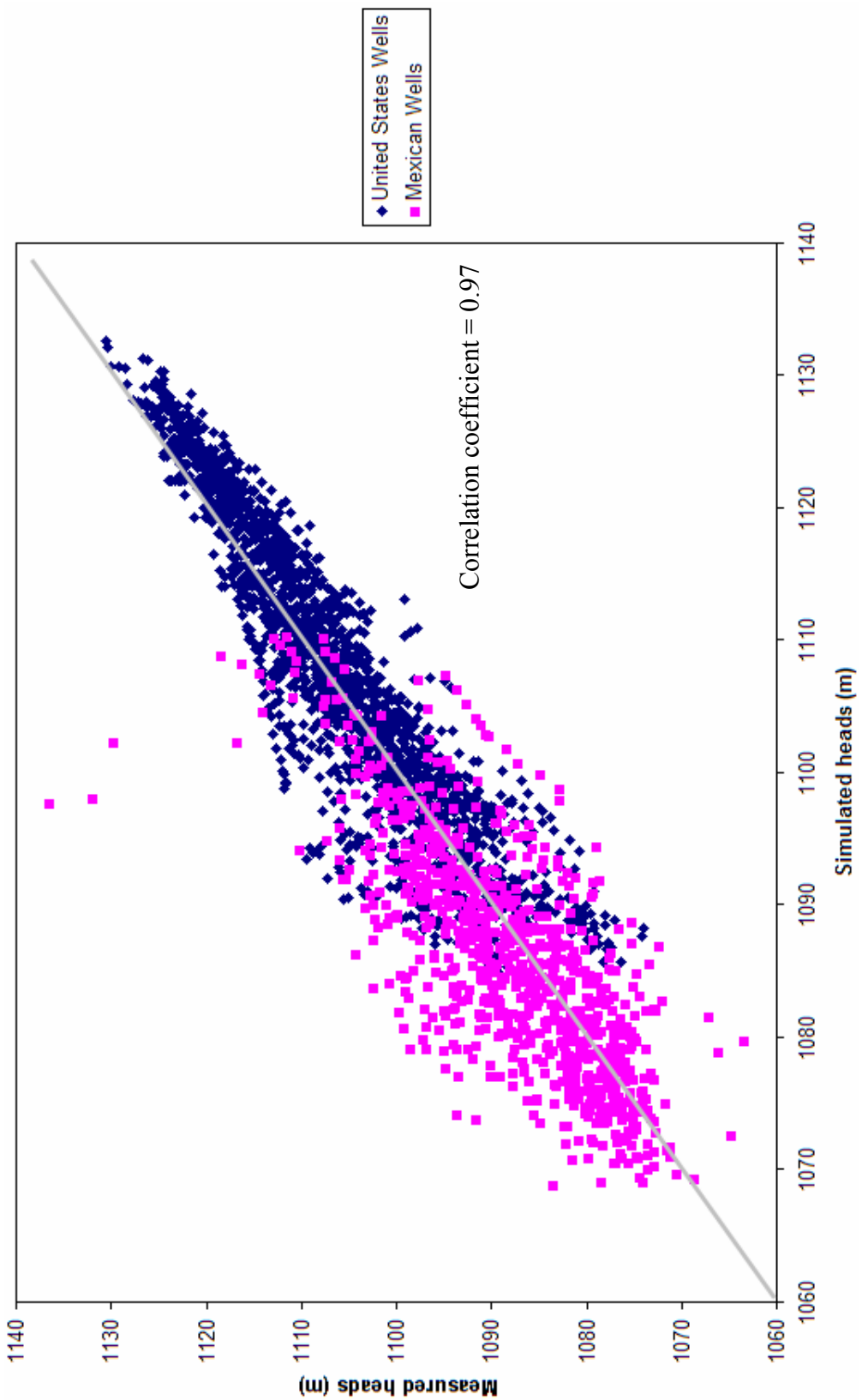

Fig. 40. Observed and measured United States and Mexican wells.

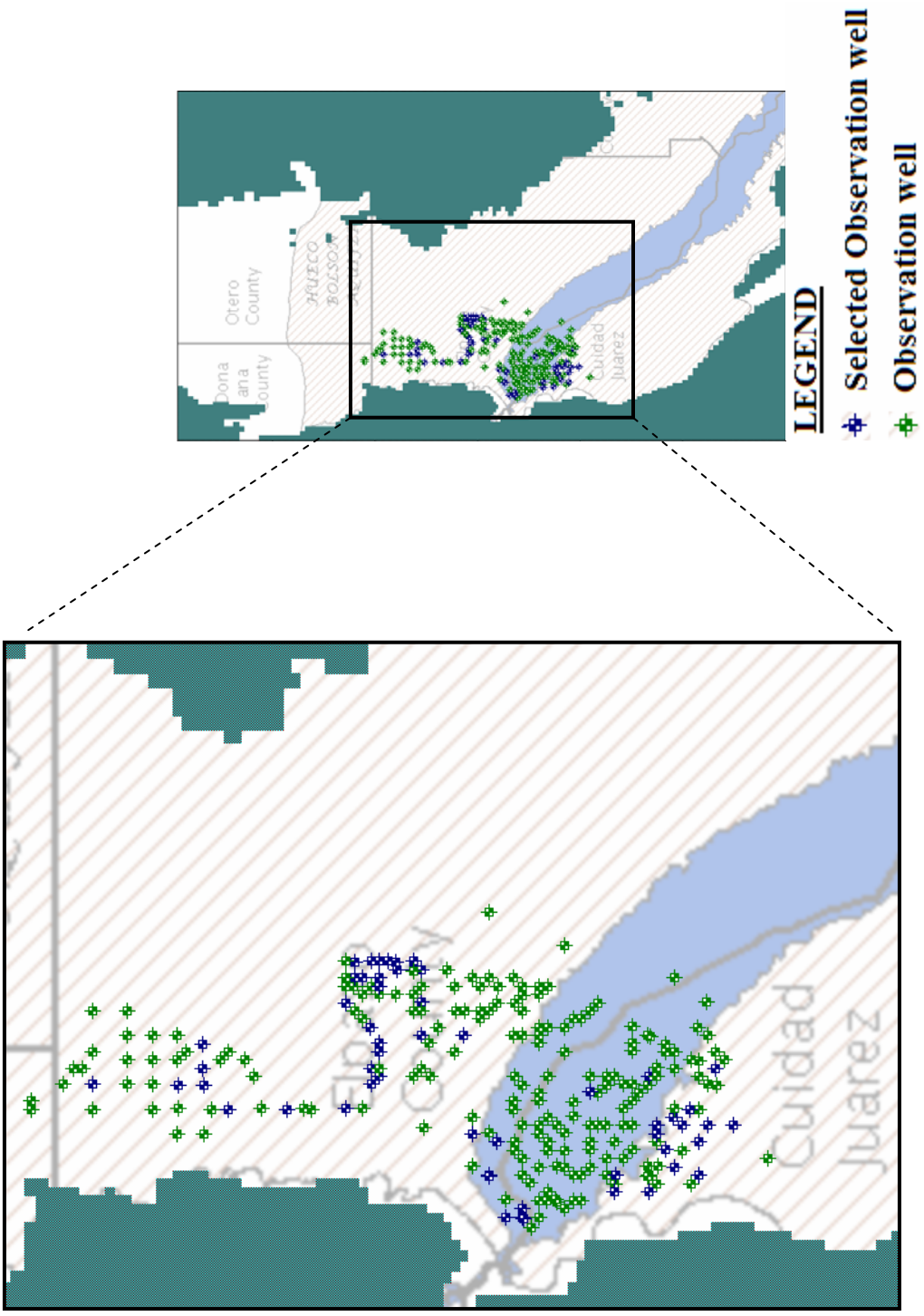

Fig. 41. Selected calibration head wells displayed.

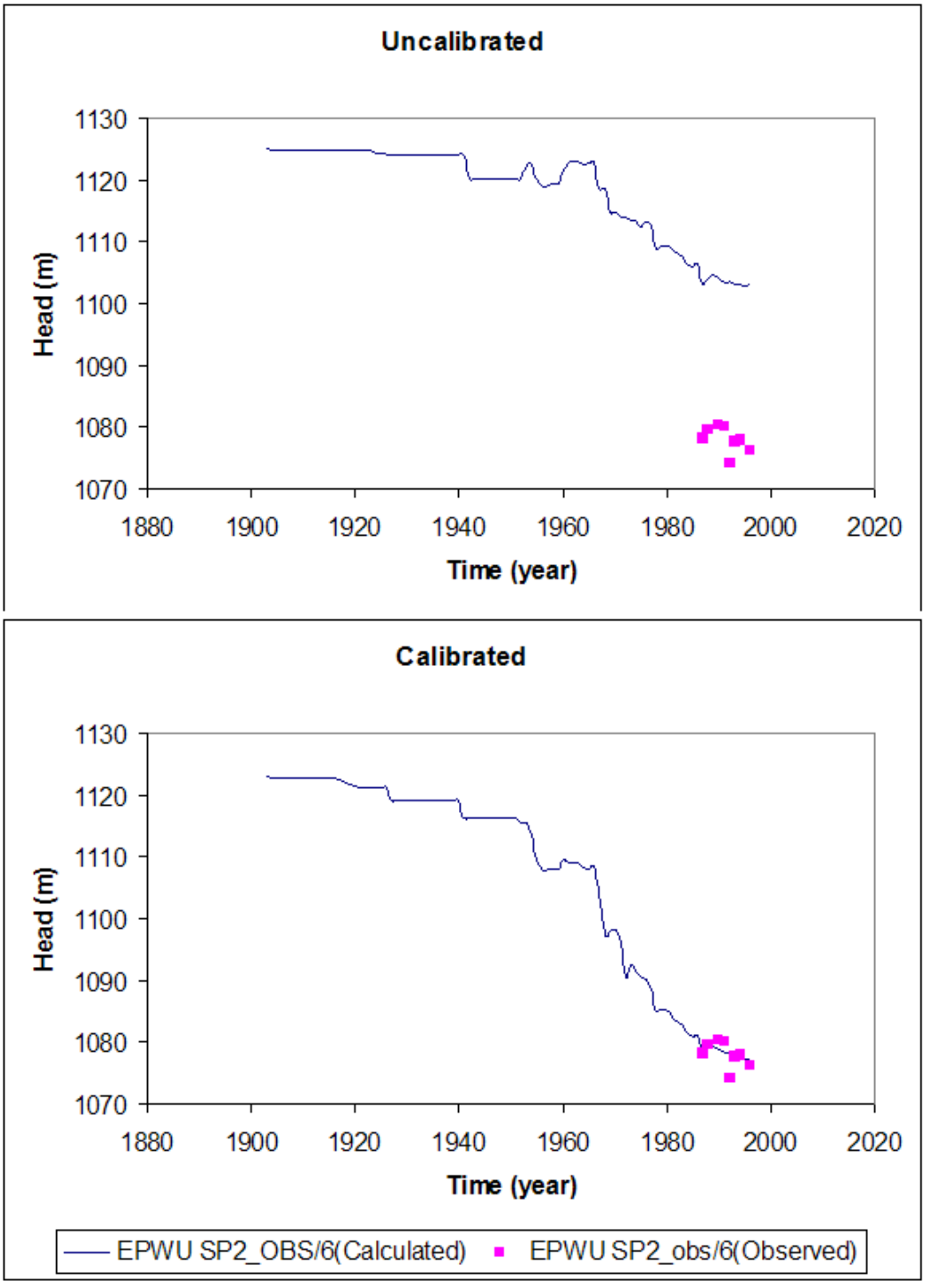

Fig. 42. Time series hydrographs of calibrated and un-calibrated heads at U.S. observation well EPWU SP2.

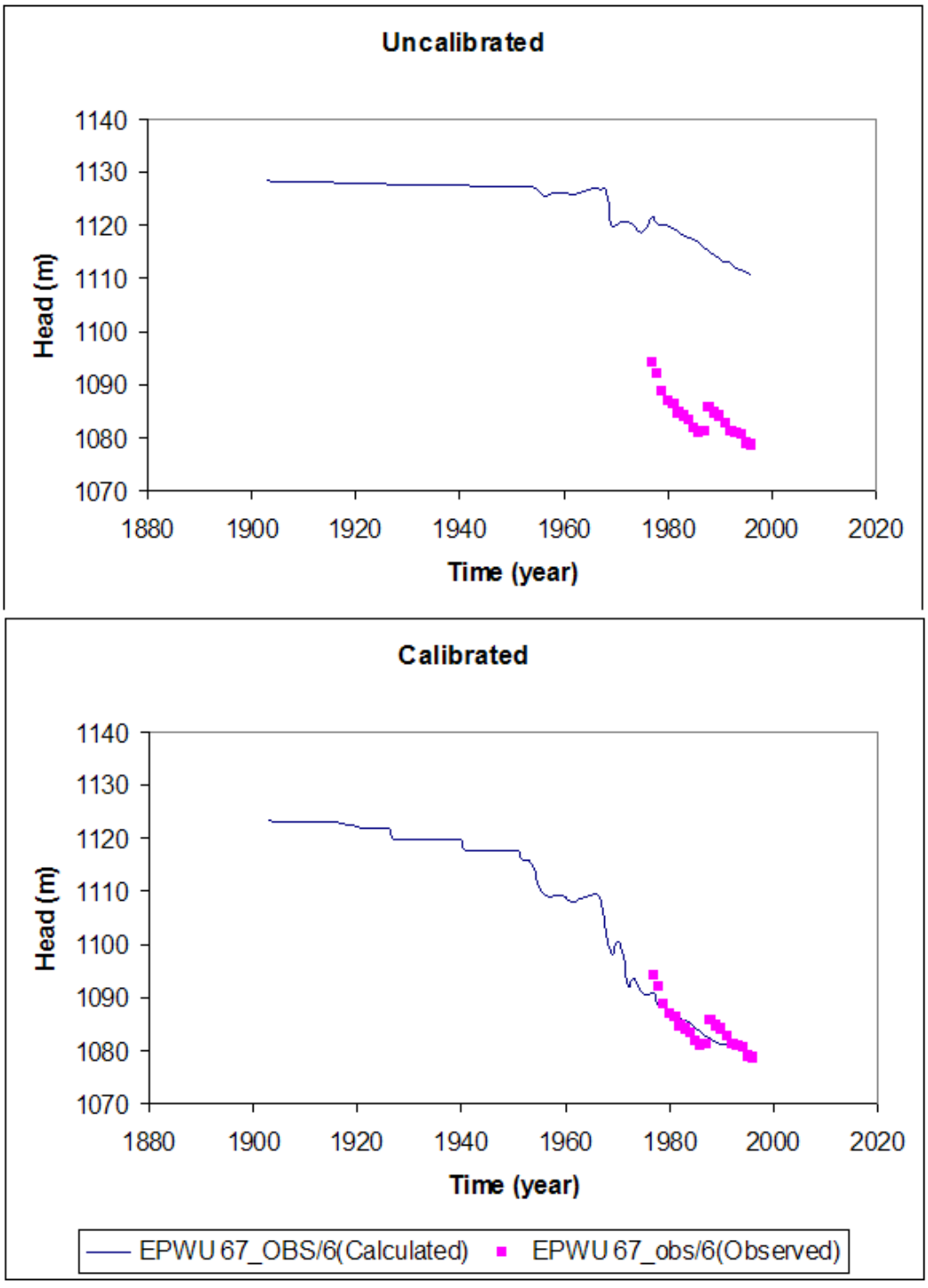

Fig. 43. Time series hydrographs of calibrated and un-calibrated heads at U.S. observation well EPWU 67.

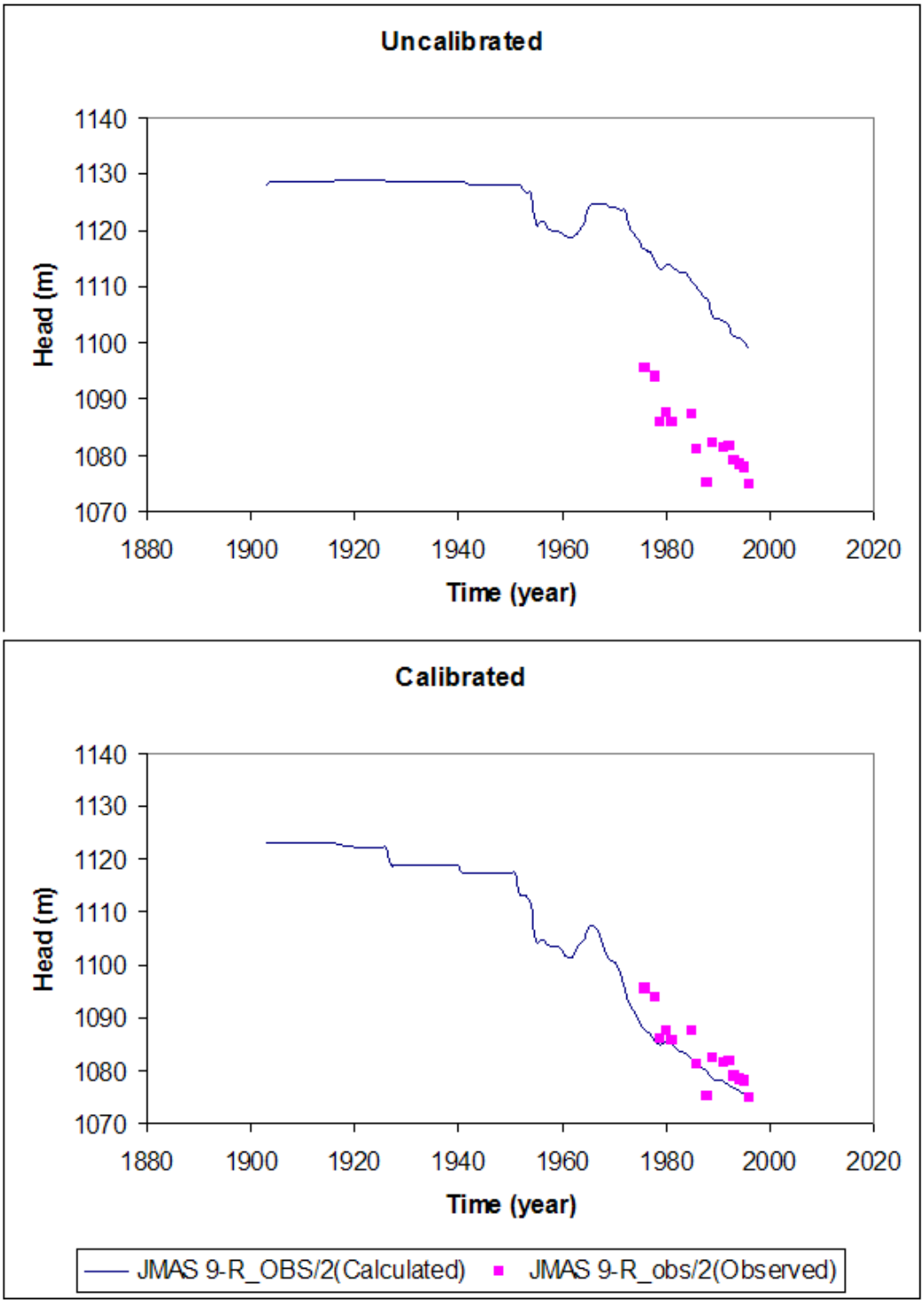

Fig. 44. Time series hydrographs of calibrated and un-calibrated heads at Mexican observation well JMAS 9-R.

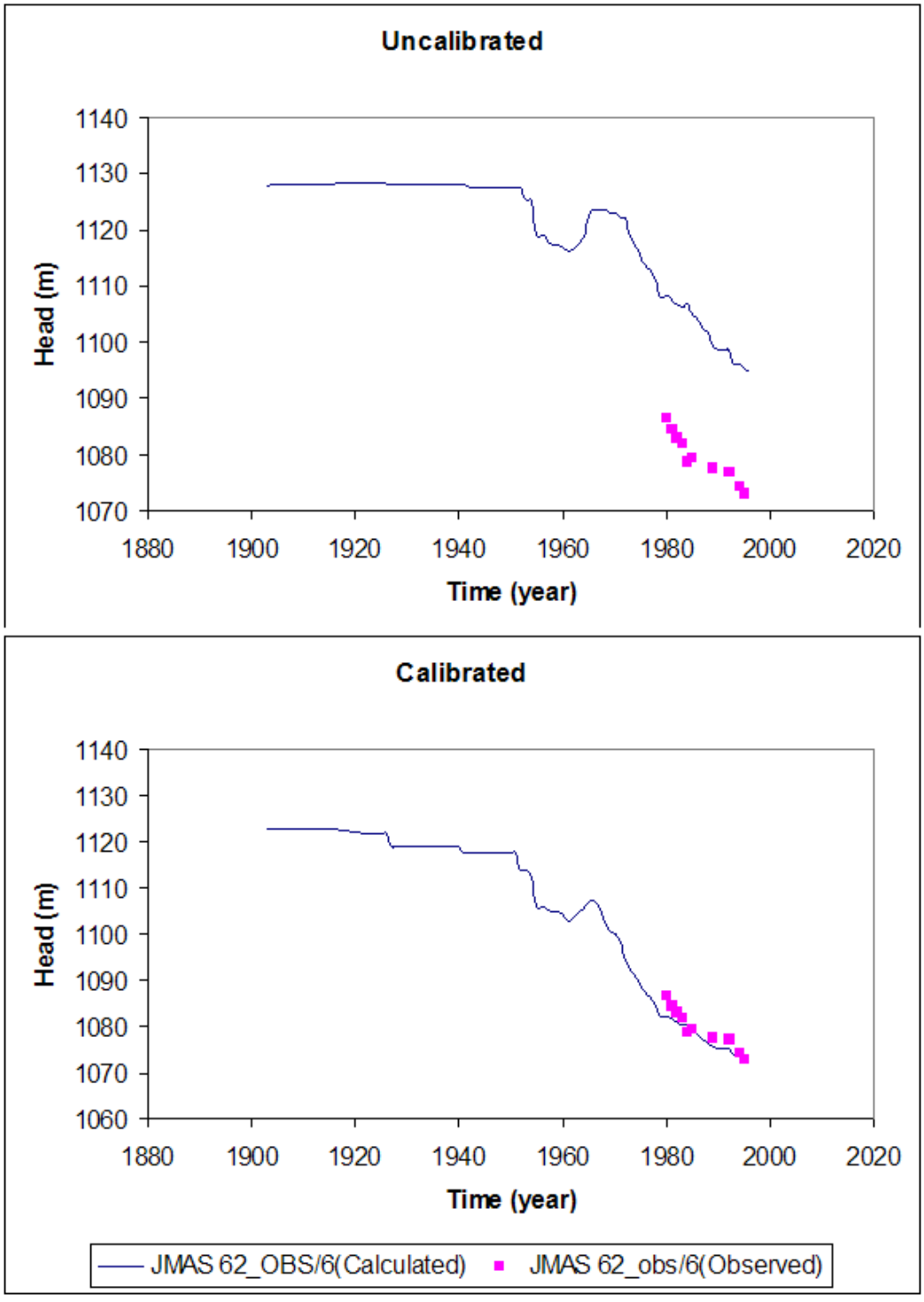

Fig. 45. Time series hydrographs of calibrated and un-calibrated heads at Mexican observation well JMAS 62.

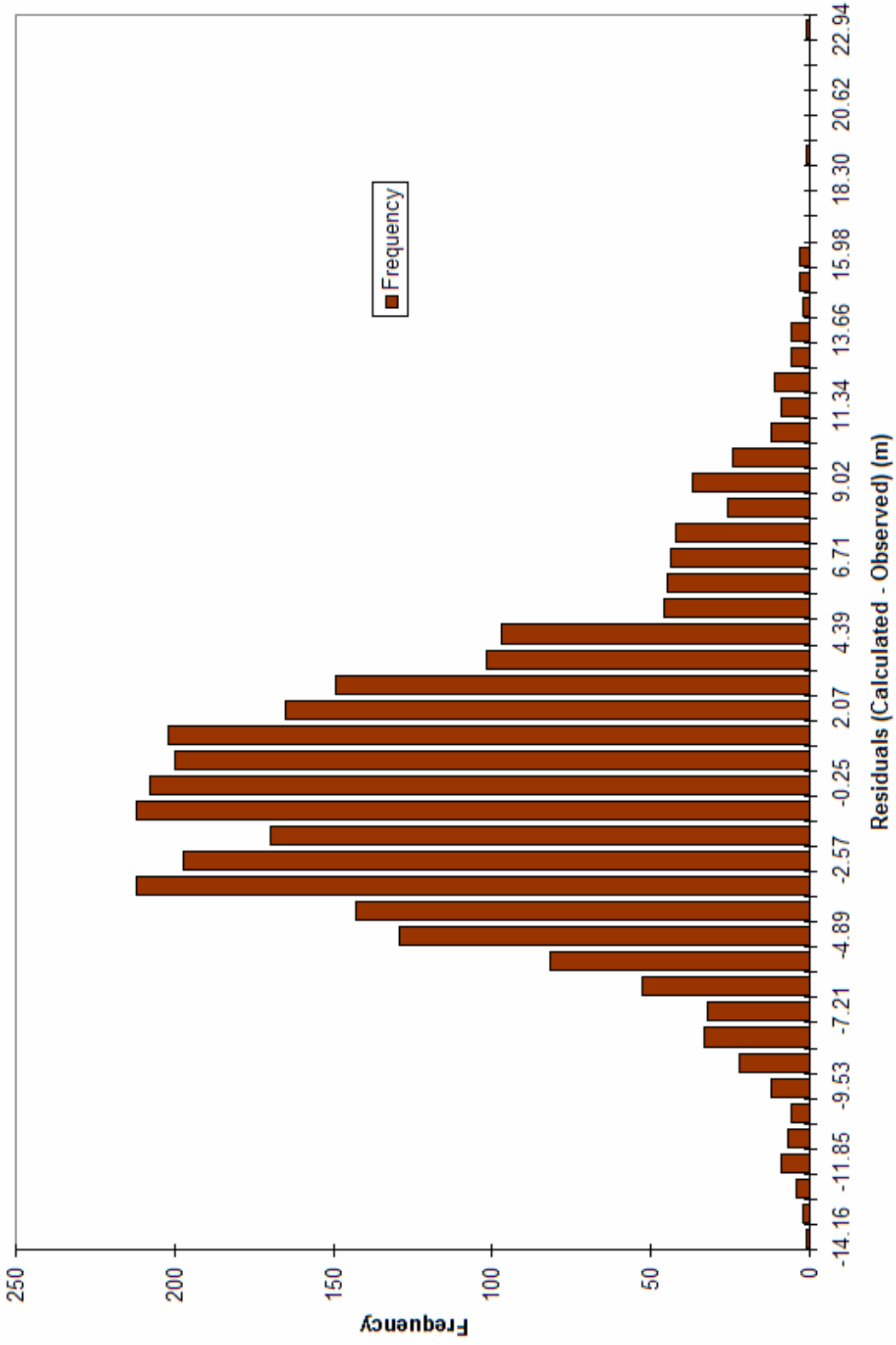

Fig. 46. Weighted calibration residuals histogram at observation wells.

5.1.1 Measured vs. simulated

The model's simulated and observed heads for the U.S and Mexican datasets shown in Fig. 40 produced a correlation coefficient of 0.97. As stated earlier, for calibration procedure, the U.S. measured head data set were given a weight of 1 and the Mexican data set were given a weight of 0.67 (33% less) due to uncertainty. However, the U.S and Mexican measured and simulated heads presented in the graph shown are un-weighted to assist in adequate inspection of the dataset. The scatter of the Mexican data, which is more than the scatter of the U.S dataset, can be a clear indication of the uncertainty in the measurements taken on the Mexican side.

The current model calibrated parameters corroborate field measurements properly. Calibration results presented as hydrographs for selected wells (Fig. 41) are displayed in Appendix A to further illustrate the model goodness of fit. Additionally, 4 measurement wells, EPWU SP2 and EPWU 76 on the U.S. side, and JMAS 9-R and JMAS 62 on the Mexican side, are shown (Fig. 42 - Fig. 45).

5.1.2 Calibration residuals histogram

The calibration residuals, displayed in histogram form (Fig. 46), are the difference between the calculated results and the observed heads at the 244 wells representing all 2802 measurement points temporally and spatially. The calibration residuals were determined using the equation:

$$R_i = H_{cal} - H_{obs} \tag{5}$$

where R_i is the calibration residual at a measurement point, L; H_{cal} is the calculated head

at a measurement point, L; and H_{obs} is the measured head at an observation point, L. Careful inspection of the model residual histogram implies that a majority of simulated heads in the model have residuals of between ±4 meters. The calibration residual histogram is a good visual indicator of how small the discrepancies between the calibrated and measured heads (in the current model) are as a result of the model calibration.

Table 6
Residual statistics

Statistical measure	Value
Standard error of the estimate	0.12 m
Root mean squared error	7.6 m
Normalized root mean squared error	10.4%
Residual Mean	4 m
Abs. Residual Mean	5.8 m

The residual statistics presented in Table 6 provide indications of the overall model goodness of fit.

5.1.3 Absolute residual mean

The average of the residuals at the measurement points is a good indicator of how well the model was calibrated. This inference is typically surmised in the residual mean statistic which is determined by:

$$\overline{R} = \frac{1}{n}\sum_{i=1}^{n} R_i \tag{6}$$

where $\overline{R}$ is the residual mean, L; and n is the number of measurement points, dimensionless. A residual mean of 4 meters was determined for the current model.

However, while the residual mean can be easily determined, a better interpretation of the model residual mean is needed because, in the current model, some negative and positive residual values can either negate each other or produce residual mean values close to zero. A measure of the average of the residuals that depicts a more adequate measure of the model goodness of fit is the absolute residual mean which measures the average magnitudes of the residuals using:

$$\left|\overline{R}\right| = \frac{1}{n}\sum_{i=1}^{n}\left|R_i\right| \tag{7}$$

where $\left|\overline{R}\right|$ is the absolute residual mean, L; and $\left|R_i\right|$ is the absolute value of the calibration residual at a measurement point, L. The absolute residual mean is a better interpretation of the model goodness of fit. The absolute residual mean of the current model illustrates that on an average, the discrepancy between measured and simulated heads is about 5.8 meters. This residual mean, which is approximately 0.5% of the model simulated heads, is an indicator of good model calibration.

5.1.4 Standard error of the estimate

A measure of the variability of the model residuals around the expected residual value is the standard error of the estimate which is determined by:

$$\sigma_{est} = \sqrt{\frac{\frac{1}{n-1}\sum_{i=1}^{n}(R_i - \overline{R})^2}{n}} \tag{8}$$

where σ_{est} is the standard error of the estimate, L. In the current model, a low standard error of the estimate of 0.12 meters was obtained, signifying minimal model result errors.

5.1.5 Normalized root mean squared error

The root mean squared error is the average of the squared differences in measured and simulated heads or the residuals. The root mean squared error is typically calculated in groundwater flow models and used as a measure of the model's goodness of fit. It is determined using the equation:

$$RMSE = \sqrt{\frac{1}{n}\sum_{i=1}^{n} R_i^2} \tag{9}$$

where *RMSE* is the root mean squared error, L. However, the RMSE doesn't incorporate the scale of the potential range in simulated data values adequately enough. A normalized RMSE which is expressed as a percentage has been determined to be a more representative measure of fit. The normalized RMSE is determined using;

$$NormRMSE = \frac{RMSE}{(H_{obs})_{\max} - (H_{obs})_{\min}} \tag{10}$$

where *NormRMSE* is the normalized root mean squared error, L; $(H_{obs})_{\max}$ is the maximum measured head value, L; and $(H_{obs})_{\min}$ is the minimum measured head value, L. Relatively low values of normalized RMSE in comparison to head values are preferred. In the current model, an RMSE of 7.6 meters was determined which is approximately 0.7% of the simulated heads in the model. Additionally, a normalized RMSE of 10% was determined which also signifies a good model fit.

5.2 PARAMETERS AND PROPERTIES

Model calibration and simulations produce optimum values for model components in the entire model domain.

Table 7
Comparisons of calibrated model parameters and properties

Parameter	Current Model	Heywood and Yager
Horizontal hydraulic conductivity		
Alluvial fan facies	3.5 - 7.0 m/d	6.0 - 7.7 m/d
Recent fluvial sediments	1.2 - 7.3 m/d	2.8 - 7.2 m/d
Fluvial and alluvial facies	6.2 - 9.2 m/d	6.4 - 7.2 m/d
Lacustrine playa facies	0.1 - 3.5 m/d	0.5 - 1.4 m/d
Faults	1×10^{-3} - 1×10^{-2} m/d	1×10^{-3} - 1×10^{-2} m/d
Vertical hydraulic conductivity		
Alluvial fan facies	5.1×10^{-4} - 2.0×10^{-1} m/d	6×10^{-4} - 2×10^{-3} m/d
Recent fluvial sediments	2×10^{-2} - 2×10^{-1} m/d	6×10^{-2} - 6×10^{-1} m/d
Fluvial and alluvial facies	1.0×10^{-3} - 1.3×10^{-1} m/d	1×10^{-2} - 1.5×10^{-2} m/d
Lacustrine playa facies	7.2×10^{-4} - 8.8×10^{-2} m/d	6×10^{-3} - 1×10^{-1} m/d
Specific yeild	0.177	0.177
Specific storage (elastic)	8.3×10^{-7} - 1×10^{-5} m-1	2×10^{-6} - 1×10^{-5} m-1
Specific storage (inelastic)	7.0×10^{-5} m^{-1}	7×10^{-5} m^{-1}
Conductance per unit length		
Rio Grande	1.6 - 2.0 m/d	1.6 - 2.0 m/d
Agricultural drains	2 - 1.6×10^{1} m/d	2 - 1.6×10^{1} m/d
irrigation canals	3.0 m/d	3.0 m/d
Evapotranspiration extinction depth	5 m	5 m
Maximum evapotranspiration rate	4.6×10^{-3} m/d	4.6×10^{-3} m/d
Manning's n:		
Rio Grande	0.03	0.03
Franklin Canal, Acequia Madre	0.03	0.03

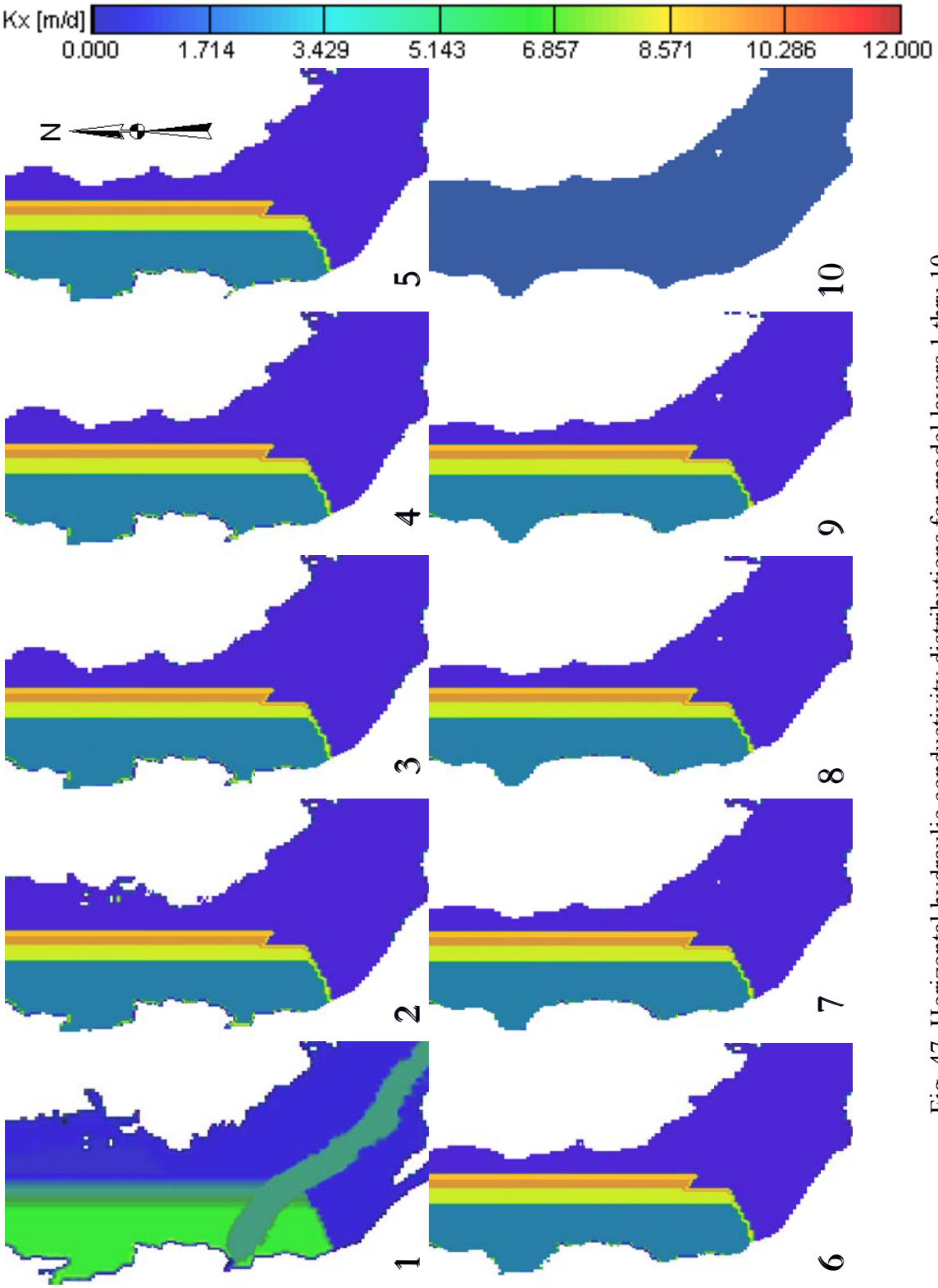

Fig. 47. Horizontal hydraulic conductivity distributions for model layers 1 thru 10.

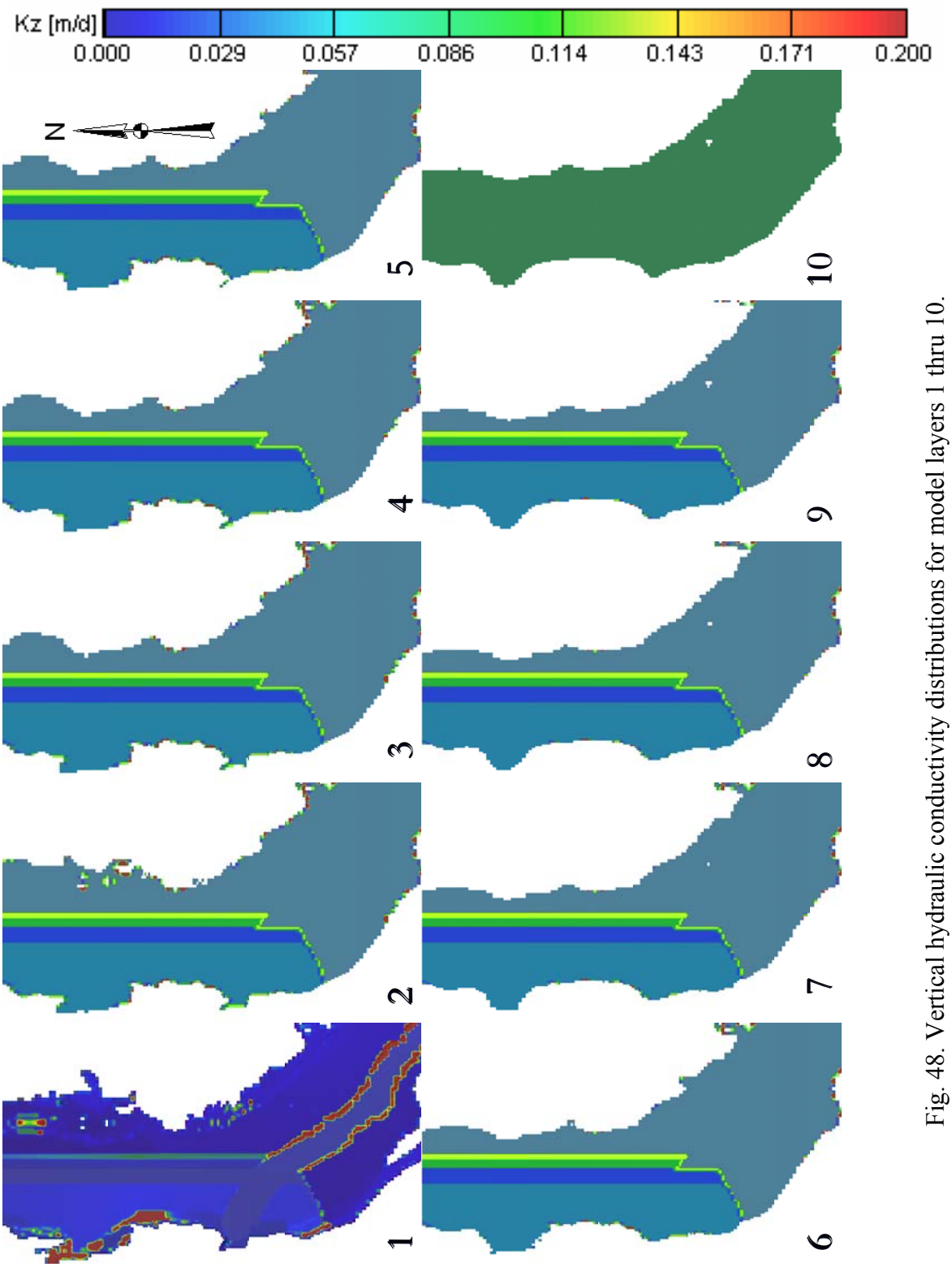

Fig. 48. Vertical hydraulic conductivity distributions for model layers 1 thru 10.

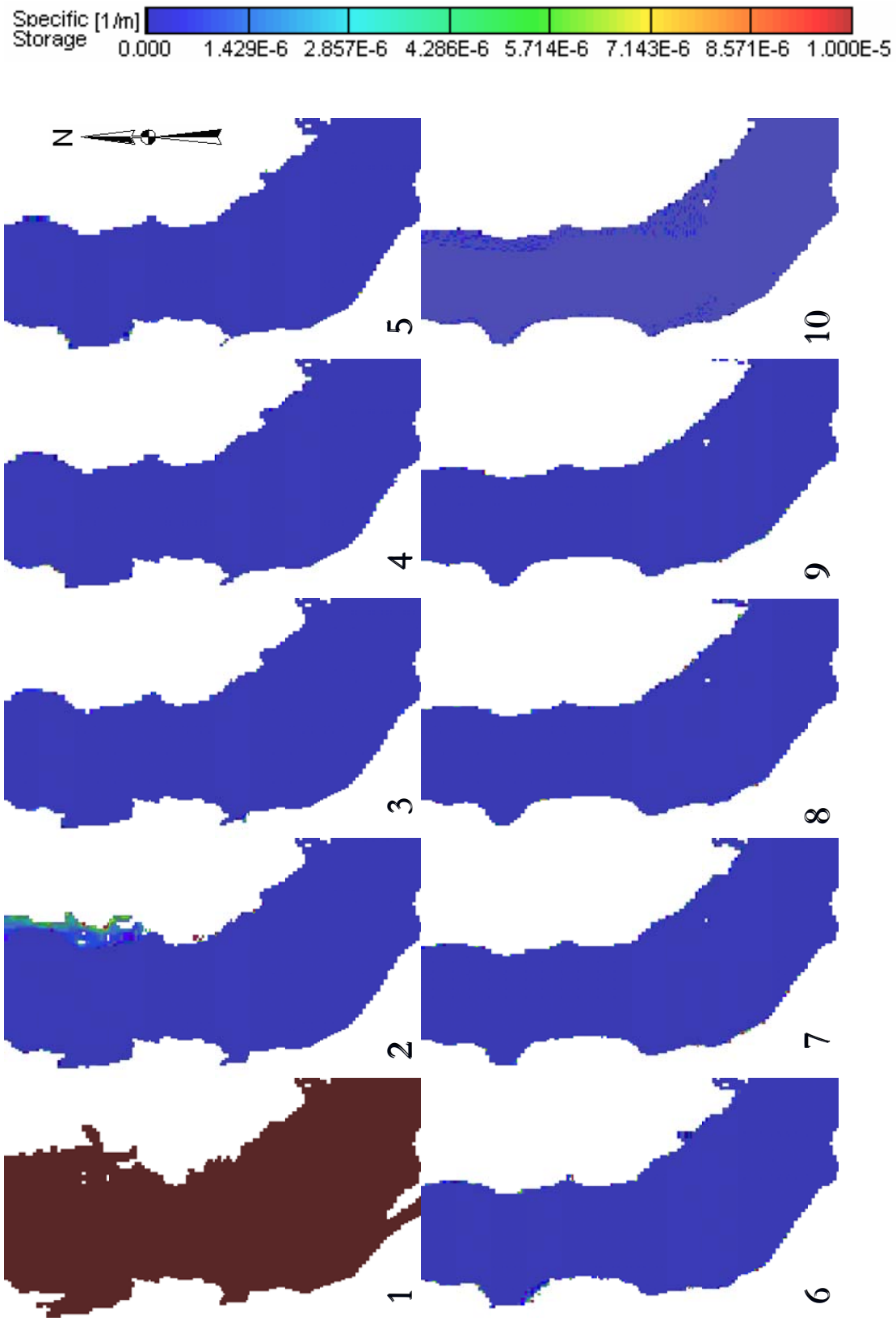

Fig. 49. Specific storage distributions for model layers 1 thru 10.

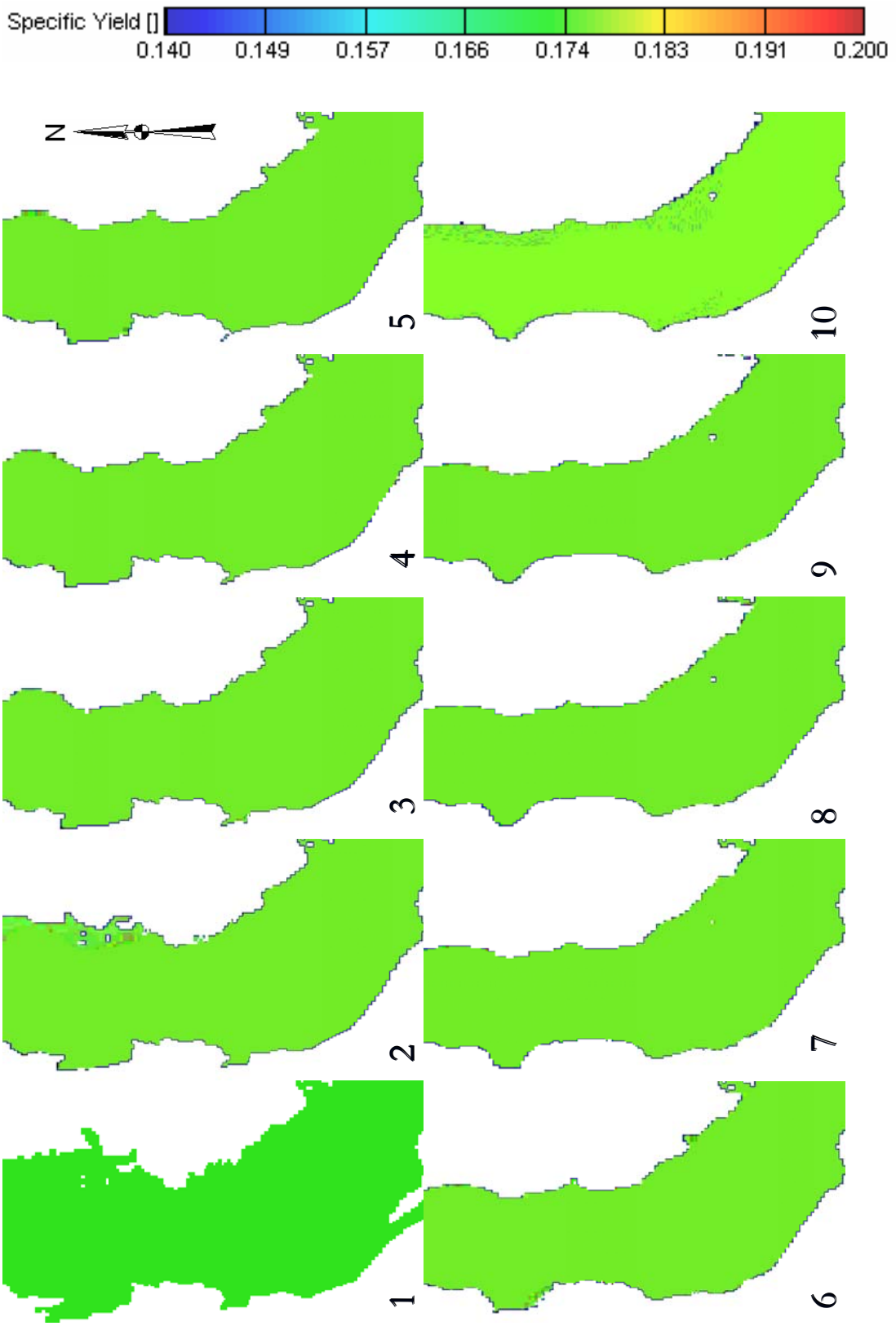

Fig. 50. Specific yield distributions for model layers 1 thru 10.

Model components include model parameters such as recharge, and model properties such as hydraulic conductivity and storage. Model parameters and property values from the current model and comparisons to the Heywood and Yager [5] model are shown in Table 7.

5.2.1 Horizontal and vertical hydraulic conductivities

The horizontal and vertical hydraulic conductivities were initially assigned to different zones in the current model based on the generalized geological facies. In the current model, these generalized geological facies are the fluvial facies, alluvial-fan facies, lacustrine-playa facies, and recent alluvial facies. Horizontal hydraulic conductivities of between 0.1 and 9.2 m/day and vertical hydraulic conductivities of between 5.1×10^{-4} and 2.0×10^{-1} m/day were observed in the model. Distributions of the vertical and horizontal hydraulic conductivities for all ten layers (Fig. 47 and Fig. 48) show that the alluvial fan and fluvial facies represent the highest hydraulic conductivities.

Significant pumping due to wells occur predominantly within the areas characterized as the alluvial fan and fluvial facies. The horizontal and vertical hydraulic conductivities in the current model may differ from horizontal and vertical conductivities determined from tests. These differences can be attributed to a variety of factors. The main reason for these differences lie in the fact that pumping tests will only examine relatively small portions of the aquifer, which usually only constitute the portions of the aquifers around the test wells. Additionally, there are usually small numbers of test wells relative to the sizes of the aquifers (due to cost constraints), which are usually largely spaced in proximity from one another. High levels of heterogeneity, which are typically

not incorporated into large regional scale models, are lost. The horizontal and vertical conductivities, which are usually more representative of regional conditions, enable inferences and general understandings of the heterogeneity of the aquifer.

5.2.2 Storage

The specific storage and the specific yield are two parameters in the model that define the storage characteristics of the aquifer. These two properties influence water level fluctuation over time and were adjusted during the calibration process. The specific yield, which is typically related to the unconfined part of the aquifer, is the volume of water that the unconfined part of the aquifer releases from storage as the water level in a unit surface area of the aquifer declines due to pumping. Likewise, the specific storage applies only to the confined parts of the aquifer, as does the volume of water that enters or is released from storage in response to changes in water level. Distributions of the specific storage and specific yield for all 10 model layers are shown in Fig. 49 and Fig. 50 respectively. A specific yield for the aquifer of 0.177 was determined. A specific storage of 1×10^{-5} was determined for the first model layer, which represented the unconfined parts of the Hueco Bolson. A specific storage of about 1.1×10^{-6} on average was determined for all the other 9 model layers. Storage properties in the current model which were also initially extrapolated from pumping tests are sufficient for modeling and simulation purposes. These calibrated storage properties are highly simplified and may not be representative of properties on a local scale. A general understanding of the storage potential of the Hueco Bolson can be understood on a regional scale. Based on the water budget results, the aquifer exhibits relatively high water storage capabilities.

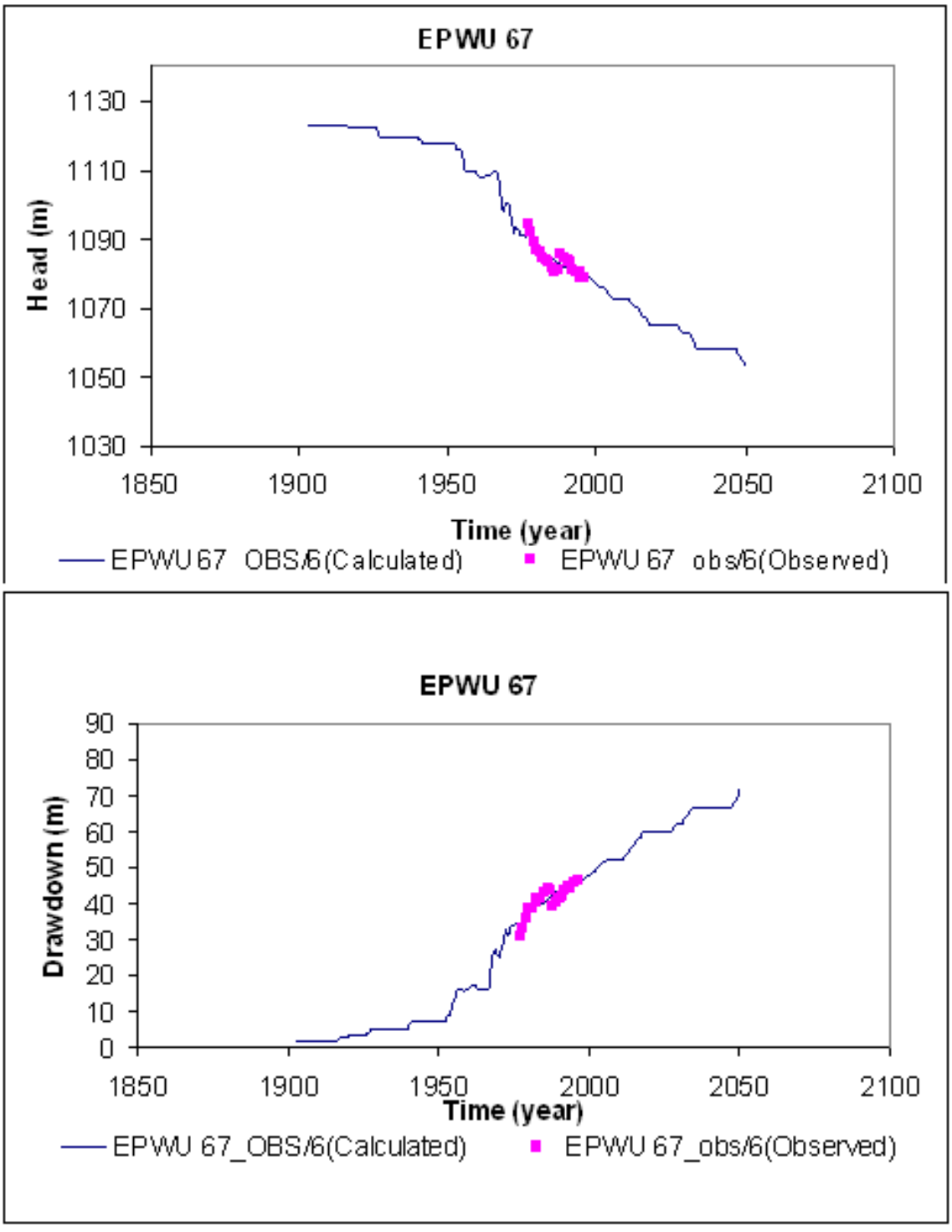

Fig. 51. Head and drawdown hydrographs for EPWU 67.

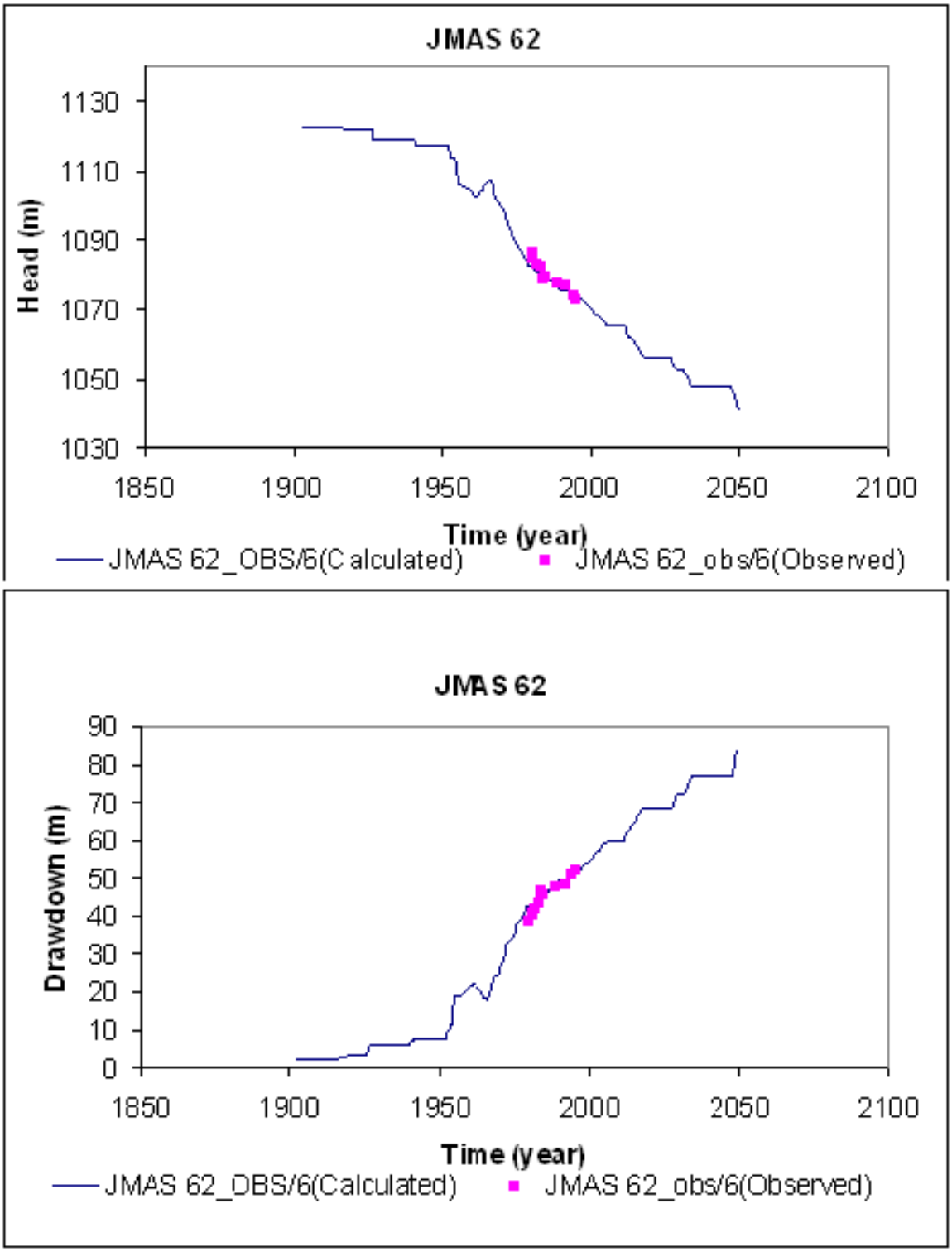

Fig. 52. Head and drawdown hydrographs for JMS 62.

5.3 HEADS AND DRAWDOWNS

5.3.1 Simulated hydraulic heads

Fig. 51 and Fig. 52 both illustrate the simulated hydraulic heads and drawdowns in JMAS 62 and EPWU 67. Additionally, heads and drawdowns for other JMAS and EPWU wells (Fig. 41) for either side of the border are presented in Appendix A. Head declines are largest in the El Paso/Ciudad Juarez area, where a majority of the pumping wells are located. In 1977, heads of about 1105 and 1100 meters on average were observed for the U.S. and Mexican sides (a drop of about 18 meters from the initial heads). In 1996, heads of about 1093 and 1077 meters on average were observed for the U.S. and Mexican sides (a 35 meter drop from the initial heads).

In 2035, heads of about 1083 and 1059 meters on average are observed for the U.S. and Mexican sides (a 47 meter drop from initial heads). In 2050, heads of about 1076 and 1056 meters on average are observed for the U.S. and Mexican sides (a 58 meter drop from the initial heads). These head declines are due to historical pumping when large amounts of water are released from storage in response to the pumping needs. More declines are to be expected within the prediction period. Additionally, heads are consistently lesser on the Mexican side than the U.S. side as a result of the differences in populations and pumping needs on either side of the Border.

5.3.2 Drawdowns

Significant drawdowns are also observed in the El Paso/Ciudad Juarez area. Hydrographs presented in Fig. 51, Fig. 52, and Appendix A also illustrates simulated

drawdowns in the El Paso/Ciudad Juarez area. Drawdowns in 1977 were 20 meters on average on the Mexican side and 18 meters on the U.S. side. In later years such as 1996, drawdowns increased to 41 meters on average on the Mexican side and 31 meters on the U.S side. Drawdowns are also predicted in years 2032 and 2050 to increase to 59 meters and 62 meters on average on the Mexican side. On the U.S side, drawdowns predicted for years 2032 an 2050 are 43 meters and 47 meters.

In general, results indicate that the model drawdown in response to pumping on the Mexican side is more pronounced than the model drawdown response on the U.S. side. The drawdowns on the Mexican sides are larger, due to the fact that the Ciudad Juarez population is significantly larger than the El Paso population. Additionally, Ciudad Juarez relies on the Hueco Bolson for almost 100% of its water supply and El Paso, which has historically relied significantly on the Hueco Bolson, has increased its surface water usage to supplement its groundwater supplies.

Table 8
1965 model water budget inflow and outflow components compared to prior results

	1965 OUTFLOW (m^3/day)		1965 INFLOW (m^3/day)	
COMPONENT	Model	Heywood and Yager	Model	Heywood and Yager
STORAGE	8148	14839	226515	211952
WELLS	248102	285195	338	18797
DRAIN	13542	80238	0	0
EVAPOTRANSPIRATION	50551	155032	0	0
STREAM	0	301	64073	276010
INTERBED STORAGE	173	149	5146	4626
RECHARGE	0	0	3852	3944
TULAROSA UNDERFLOW	0	0	20424	20425
TOTAL	320517	535755	320347	535755
In - Out =	-169 m^3/day			
1965: Percent error =	-0.02%			

Table 9
1978 model water budget inflow and outflow components compared to prior results

	1978 OUTFLOW (m^3/day)		1978 INFLOW (m^3/day)	
COMPONENT	Model	Heywood and Yager	Model	Heywood and Yager
STORAGE	3622	5275	383269	347370
WELLS	427721	481335	338	29019
DRAIN	17695	193754	0	0
EVAPOTRANSPIRATION	46844	182497	0	0
STREAM	0	34	86489	431384
INTERBED STORAGE	15	54	17007	12251
RECHARGE	0	0	21973	22497
TULAROSA UNDERFLOW	0	0	20424	20425
TOTAL	495897	862950	529498	862946
In - Out =	-33602 m^3/day			
1965: Percent error =	6.55%			

Table 10
1996 model water budget inflow and outflow components compared to prior results

	1996 OUTFLOW (m^3/day)		1996 INFLOW (m^3/day)	
COMPONENT	Model	Heywood and Yager	Model	Heywood and Yager
STORAGE	17342	11723	358618	331910
WELLS	457967	606696	3683	42848
DRAIN	16077	226160	0	0
EVAPOTRANSPIRATION	38473	190963	0	0
STREAM	0	0	107693	581509
INTERBED STORAGE	168	189	15269	19645
RECHARGE	0	0	38521	39442
TULAROSA UNDERFLOW	0	0	20424	20425
TOTAL	530027	1035778	544208	1035778
In - Out =	-14180 m^3/day			
1965: Percent error =	2.64%			

Table 11
2032 model water budget inflow and outflow component predictions

	Model	
COMPONENT	2032 OUTFLOW (m^3/day)	2032 INFLOW (m^3/day)
STORAGE	11461	503362
WELLS	630071	5914
DRAIN	12574	0
EVAPOTRANSPIRATION	35664	0
STREAM	0	107022
INTERBED STORAGE	15	42889
RECHARGE	0	38521
TULAROSA UNDERFLOW	0	20424
TOTAL	689784	718132
In - Out =	28348 m^3/day	
1965: Percent error =	3.94%	

Table 12
2050 model water budget inflow and outflow component predictions

	Model	
COMPONENT	2050 OUTFLOW (m^3/day)	2050 INFLOW (m^3/day)
STORAGE	16750	593623
WELLS	706250	7028
DRAIN	11727	0
EVAPOTRANSPIRATION	36296	0
STREAM	0	104748
INTERBED STORAGE	20	53691
RECHARGE	0	38521
TULAROSA UNDERFLOW	0	20424
TOTAL	771044	818034
In - Out =	46991 m^3/day	
1965: Percent error =	5.74%	

5.4 WATER BUDGETS AND PREDICTIONS

5.4.1 Water budgets

Table 8 through Table 10 shows the current model water budget in m^3/day for years 1965, 1978, and 1996 in comparison to the Heywood and Yager [5] results. Model inflows and out flows for days in years 1965, 1978, and 1996 are also illustrated in

Appendix D. The greatest influx of water consistently occurs from the water released from storage and stream leakage. The interbed storage water release, human induced recharge wells, mountain-front recharge, and the Tularosa underflow are also other important, but lesser, sources of water influx. The induced pumping for water needs, evapotranspiration, and agricultural drains remain consistently the most significant forms of outflow. Other sources of outflow, such as water entering the aquifer storage and the interbed storage, exist but to a much lesser degree. Water budget predictions for years 2032 and 2050 are shown in Fig. D- 4 and Fig. D- 5.

The water budget results show that the aquifer responded to increased pumping to supply the needs of the growing border area population by releasing more water from storage. However, as the aquifer releases more water from storage, significant stresses on the aquifer occur as demonstrated by significant drawdowns in the El Paso/Ciudad Juarez area.

Table 13
Predicted water demands and availability for 2032 and 2050

	El Paso	Ciudad Juarez
1996		
Population	610,000	1,009,770
Water demand	136,000,000 m^3/year	225,000,000 m^3/year
Groundwater recoverable from pumping	167,000,000 m^3/year	
2032		
Population	1,016,667	1,682,950
Water demand	227,000,000 m^3/year	376,000,000 m^3/year
Groundwater recoverable from pumping	230,000,000 m^3/year	
2050		
Population	1,220,000	2,019,540
Water demand	272,000,000 m^3/year	450,000,000 m^3/year
Groundwater recoverable from pumping	258,000,000 m^3/year	

5.4.2 Predictions

The model's predictive capability is reasonably demonstrated by the fit of the model's simulated water levels to the measured water-levels described earlier. The model was employed to predict drawdowns, fluxes, and water availability which are directly related to the water budget. The predicted water budget results illustrating inflows and outflows for 2032 and 2050 are shown in Table 11 and Table 12. Data in Table 13, displays the predicted population in 2032 and 2050 determined following the linear increase in the prediction period (Fig. 39). Additionally, the water demand for Ciudad Juarez in Table 13 was determined by multiplying the El Paso water demand by a factor of 1.7, incorporating the difference in magnitudes of the El Paso area and the Ciudad Juarez area populations into the water demands. The predicted populations and water demands for 2032 and 2050 were also determined following the linear increase in the prediction period.

According to results, in the year 2032, the water demand in the El Paso/Ciudad Juarez area is predicted to be about 600,000,000 m^3/year. The groundwater availability is only about 230,000,000 m^3/year in the area. Additionally, in the year 2050, the water demand increases to about 722,000,000 m^3/year, when the groundwater availability is only 258,000,000 m^3/year. Prediction results reveal that current groundwater resources will not be sufficient enough to solely sustain the water demands of the population. Additionally, if the groundwater is pumped as the sole source of water to the population, aquifer depletion can be anticipated by year 2032.

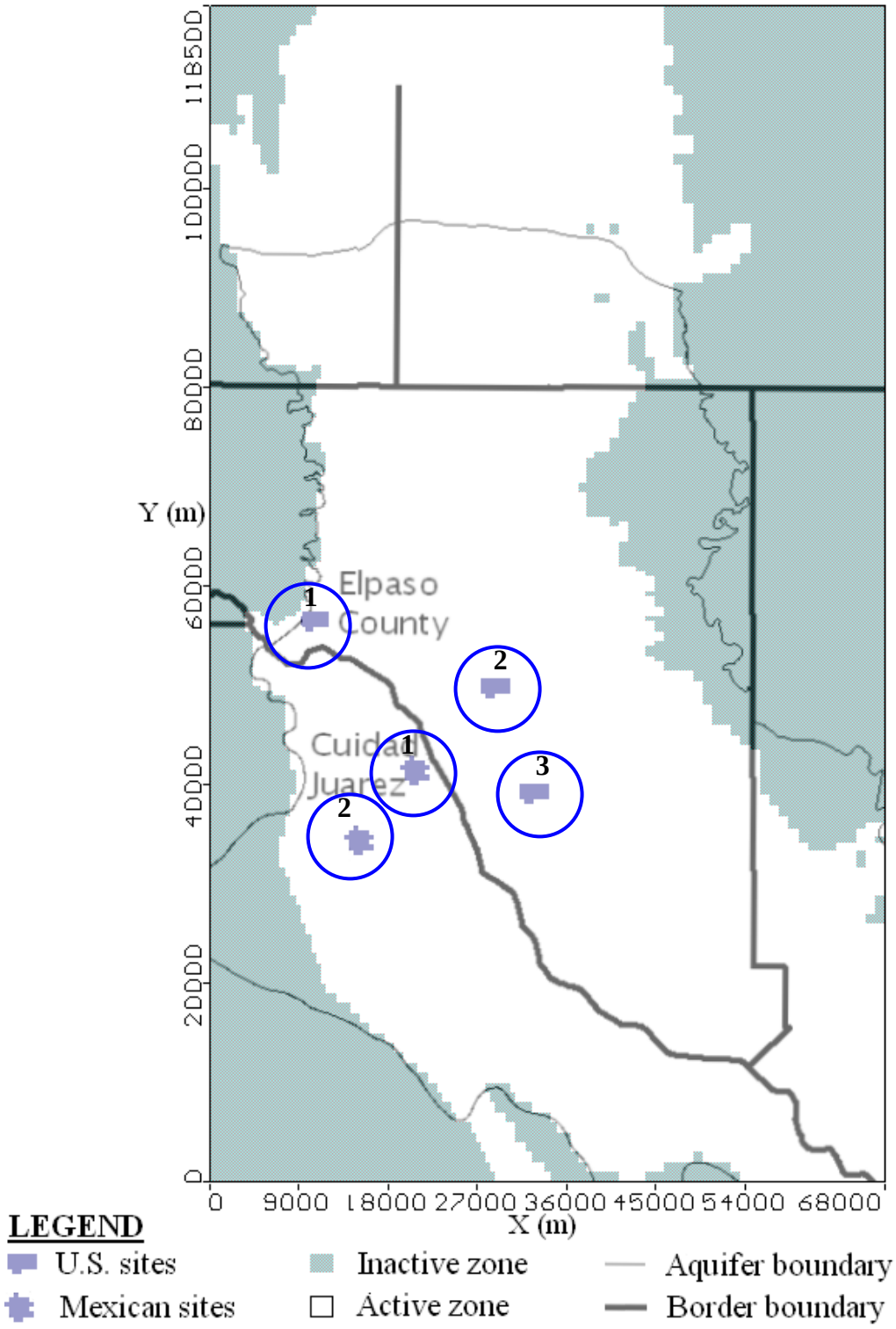

Fig. 53. 5 solid waste disposal site locations in the El Paso/Ciudad Juarez border area.

To reduce groundwater dependence on the Hueco Bolson, El Paso is supplementing it water needs by usage of Rio Grande water and employing other strategies such as water pricing, recycling of treated water, and use of grey water [40]. Ciudad Juarez is currently capping Hueco Bolson water pumping to 2001 water withdrawal plans to meet growing water demands by withdrawal from the Mesilla Bolson and other aquifers in Chihuahua [40].

5.5 ASSESSMENT OF POTENTIAL CONTAMINANT TRANSPORT IN THE EL PASO/CIUDAD JUAREZ BORDER AREA

To assess the potential of cross border contamination from areas located on both sides of the border, a fate and transport assessment was performed. To access fate and transport potential of contamination occurring on the border from year 1996 to 2050, 5 sites were located within the El Paso/Ciudad Juarez border region as shown (Fig. 53), 3 on the El Paso side of the border, and 2 on the Ciudad Juarez side of the Border.

El Paso site 1 and Juarez site 1, which where both located approximately 2 miles and 1.5 miles from the border, were both located close to the border in the El Paso Valley area, overlying the Rio Grande Alluvial aquifer. El Paso site 2 and El Paso site 3 were located approximately 5 and 4 miles off the border line on the U.S. side. Juarez site 2 was also located approximately 5 miles off the border line on the Mexican side of the border. Results from transport simulations for all 5 sites are presented Appendix B. Transport Results include 3-D isosurface concentration perspective views, cross-section, and plan views of contaminant plumes for years 1997, 2020, 2035, and 2050. Minimal downward and lateral spreading of the contamination was observed from El Paso site 2 (Fig. B- 6 to

Fig. B- 9), El Paso site 3 (Fig. B- 11 to Fig. B- 14), and Juarez site 2 (Fig. B- 21 to Fig. B- 24). However significant downward and lateral spreading was observed from El Paso site 1 (Fig. B- 1 to Fig. B- 4) and Juarez site 1 (Fig. B- 16 to Fig. B- 19).

El Paso site 1 and Juarez site 1 were found to be the locations with the highest potentials for groundwater and cross-border contamination. El Paso site 1 and Juarez site 1 were located within the El Paso Valley area which overlies the Rio Grande alluvial aquifer. The site geologies at El Paso site 3 exhibited relatively low values of hydraulic conductivities. However, the site geologies at El Paso site 1, El Paso site 2, Juarez site 1, and Juarez site 2 indicate relatively high values of horizontal and vertical hydraulic conductivities. Additionally, the contamination transport was significantly influenced by the groundwater flow directions and head differences at the sites. Quantitative summaries of head differences across the sites for years 1997, 2025, and 2050 are displayed in Table 14 and Table 15. Additionally, qualitative summaries of hydraulic conductivities and head differences at the sites are displayed in Table 16. Flow direction profiles displayed in Appendix C include the velocity directions for the first 3 model layers for years 1997, 2025, and 2050.

Table 14
Site horizontal head differences in years 1997, 2025, and 2050

Site	1997 (m)	2025 (m)	2050 (m)
El Paso site 1	6.5	3.0	1.5
El Paso site 2	1.5	3.0	1.5
El Paso site 3	0.0	0.0	1.5
Juarez site 1	10.0	9.0	2.5
Juarez site 2	0.0	1.5	0.5

Table 15
Site vertical head differences in years 1997, 2025, and 2050 between model layers

Site	1997 (m)	2025 (m)	2050 (m)
El Paso site 1	6.0	7.0	7.0
El Paso site 2	3.0	3.0	3.0
El Paso site 3	0.0	0.0	0.0
Juarez site 1	7.0	7.0	7.0
Juarez site 2	0.0	0.0	0.0

Table 16
Qualitative summaries and levels of contamination at sites

Site	Head Gradients	Geology	Level of contamination
El Paso site 1	High	Permeable	High
El Paso site 2	Low	Permeable	Low
El Paso site 3	Low	Not too Permeable	Low
Juarez site 1	High	Permeable	High
Juarez site 2	Low	Permeable	Low

At El Paso site 1, the groundwater flow is towards Ciudad Juarez in year 2050. The groundwater flow at El Paso site 1 is also relatively high, due to significant head differences and the relatively high permeability of the geology (Fig. B- 5). Therefore, significant lateral spreading and cross border contamination occurs at El Paso site 1 in year 2050. At Juarez site 1, the groundwater flow is towards the well field in Ciudad Juarez. The groundwater flow at Juarez site 1 is also high due to significant head differences and high permeability of the geology (Fig. B- 20). As a result, significant lateral spreading and cross border contamination also occur at Juarez site 1 in year 2050.

At El Paso site 2, head differences are very small and the geology is considerably permeable (Fig. B- 10). The groundwater flows at El Paso site 2 are minimal due to very small head difference, which causes low groundwater flows at the site. Consequently, cross-border contamination doesn't occur at El Paso site 2 in year 2050. At El Paso site 3,

head differences are also very small. Additionally, the groundwater flows are very minimal due to low permeability of the geology around the site (Fig. B- 15). Head differences at El Paso site 3 are very small as well. Consequently, cross-border contamination doesn't occur at this site in year 2050. At Juarez site 2, the groundwater flow was also observed to be insignificant due to small head differences at the site.

The groundwater flow at Juarez site 2 is towards the well field in Ciudad Juarez. However, while the geology at Juarez site 2 was considerably permeable, cross-border contamination didn't occur at this site because of low flow. The greatest potentials for contamination were found to be from El Paso site 1 and Juarez site 1, which were both located within certain portions of the El Paso Valley area overlying the Rio Grande Alluvial aquifer. Transport results suggest that portions of the aquifer, where head differences are high (6 meters or more) and permeability of the geologies are high, have the highest potentials of contaminant migration.

Transport results also suggest that the complex geologic makeup and high permeability of the Rio Grande alluvial aquifer, in the subsurface system of the El Paso/Ciudad Juarez border area, tends to be sensitive to significant lateral and downward contaminant movement. Additional stream leakage occurring in this area of the aquifer increases head differences and flow velocities around the site areas overlying the Rio Grande alluvial aquifer, causing significant lateral spread of contamination. Results suggest that contamination occurring in portions of the El Paso Valley could spread very rapidly. A more detailed and focused study of the underlying aquifer system is required to better assess this issue.

5.6 MODEL LIMITATIONS AND IMPROVEMENT SUGGESTIONS

5.6.1 Limitations of parameters, properties and transport assessment

Limitations are to be anticipated in groundwater models. Groundwater models attempt to represent reality by mimicking natural in-situ processes. However, the overall complexity of natural systems are usually not able to be incorporated in groundwater models, as is the case of the Hueco Bolson, which is a highly complex and heterogeneous system. While prior studies have acquired data on the aquifer, lack of more accurate data still remains a major limitation of the ground water flow and transport model. The model assumptions also limit its applicability. The aquifer media complexities within the flow system in the study area were simplified into four hydrogelogic facies, located in all 10 layers for modeling purposes. In reality each of the hydrologic characterizations may consist of large numbers of different zones of varying characteristics which are hydraulically connected in varying degrees. Additionally, results from aquifer tests used to determine initial distributions of aquifer properties prior to calibration were very limited. Test results are not available for many areas of the model domain. Therefore, high degrees of local heterogeneities are not captured in the model.

The field measured hydraulic heads were used as the principal calibration targets in the current model. In the major areas of concern, which include portions of the aquifer located in the El Paso/Ciudad Juarez area that have historically been studied, sufficient head targets were available for model calibration. However, the El Paso/Ciudad Juarez area of concern (the location for the majority of the calibration head measurements) only constituted approximately 20% of the entire model domain. In the remainder of the

aquifer, there is a lack of available measured hydraulic head data for calibration. The model calibration could be repeated and improved with more measured head data in the remainder of the aquifer domain.

The input data for the model evapotranspiration rates were obtained from measured pan-evaporation. This method is useful for obtaining potential estimates of evapotranspiration where the water table is near the ground surface. However, in portions of the aquifer, the proximity of the water table to the land surface may be substantial. Therefore, actual maximum evapotranspiration rates may be much higher or much lower. Input maximum evapotranspiration rates, extinction depths, and recharge distributions could be improved by the employment of newly developed tools such as the Soil and Water Assessment Tool (SWAT) and applicable data [41].

The current transport model developed to assess the potential cross-border contamination was developed on the basis of the fore mentioned assumptions. These assumptions were made to analyze a worst case scenario of contaminant releases. However, in reality, aquifer media transport properties such as variable porosity and dispersivity distributions could exist in the model domain. In addition, initial concentrations of solutes could exist in certain areas in the model domain. Other transport process such as inflow and outflows of solutes at different boundary conditions, chemical reactions of solutes, and radioactive decay could also occur.

5.6.2 Limitations for model applicability

The model is suitable for tasks which include, but are not limited to, studies related to regional conditions in the aquifer and assessment of regional impact of

proposed management strategies. However, the model may not be capable of being employed in its current state for undertakings which entail simulations of individual well dynamics and predictions of aquifer responses and contaminant transport at specific points (such as small municipalities). This model may not accurately predict water level declines in a single well because site-specific aquifer hydrologic properties are not incorporated into the model. These limitations are largely due to the fact that the model grids cells, on an average, are a square mile large. Refined models with smaller grid sizes will be best suited for dealing with more localized conditions. Most pre and post processors support localized grid refinement features, which enable more focused and localized assessments.

While the current model maintains stress periods lengths of a year, shorter stress periods will enable better incorporation of the effects of seasonal climate change into the model. Seasonal and climate changes have been found to affect the flows of the Rio Grande [8]. The incorporation of the effect of seasonal and climate changes, which directly affect stream discharge into the aquifer, will be important to the surface and groundwater interactions.

6. SUMMARY AND CONCLUSIONS

An improved three-dimensional numerical groundwater flow and transport model was developed for the Hueco Bolson alluvial aquifer system in the El Paso/Ciudad Juarez area. The model consists of 10 layers, 100 rows and 165 columns. Layer thicknesses vary throughout the model domain. Grid sizes also vary from 500 x 500 meters to 1000 x 1000 meters. The model simulates 94 stress periods which begins in 1903 and ends in 1996. The model was developed to assess potential cross border ground water contamination from solid waste disposal sites located in the border area. The current GAM for the Hueco Bolson was used as the basis for the development of the model in this research. The model in this research was developed by employing the updated MODFLOW 2000 code, the Visual MODFLOW pre and post processors, and data from input file packages from Hueco Bolson GAM.

There are 13 file packages used to model natural processes such as recharge, evapotranspiration, geologic faults, pumping wells, and surface/groundwater interactions in the current model. The file packages are, the Basic package (BAS), the Block Centered Flow Package (BCF), the Evapotranspiration package (EVT), the Drain package (DRN), the Discretization package (DIS), the Flow and Head Boundary package (FHB), the Recharge package (RCH), the Well package (WEL), the Interbed Storage package (IBS), the Horizontal Flow Barrier package (HFB), the Initial Head package (HDS), and the Stream package (STR) [5]. The Algebraic Multi-grid solver (AMG) was used to solve the model for simulations, calibrations, and predictions. The MF96TO2K was used to convert the basic model files from the MODFLOW 96 format to the MODFLOW 2000

format. The MAW package and the WEL file in the Hueco Bolson GAM were combined into one well file. There are currently 434 wells screened in multiple and single layers in the model.

Model calibration was performed using Visual PEST© and a data set obtained from the EPWU composed of 2806 head measurements. The head measurements were taken in 244 wells from 1935 to 1996. Conductivities and storage parameters were adjusted during the calibration process. ZONEBUDGET was used calculate the water budget from all model inflows and outflows. MT3DMS© was used to perform transport simulations for all 5 solid waste disposal sites located within the model domain in the border area.

The calibrated model parameters produced results which corroborated field measured observation data well. The border area population is expected to double by the year 2050. Hence, the calibrated model was employed to perform predictions. A prediction of groundwater availability in response to the water demands of the increasing population over the next 53 years, from 1997 to 2050, was performed. The aquifer also exhibited high storage potential. Additionally, high levels of drawdown were observed in the El Paso/Ciudad Juarez area. Drawdowns on the Mexican side were higher than drawdowns on the U.S. side due to the higher populations and groundwater usage in Ciudad Juarez. Future water demands far exceeded the groundwater availability.

A fate and transport component was also incorporated in the flow model. Fate and transport results were most sensitive to hydraulic conductivities and flow directions at the sites. The transport assessment revealed that the areas where vertical and horizontal

hydraulic conductivities were relatively high exhibited the highest potentials for cross-border contamination. The sites that were located within the vicinity of the El Paso Valley (were the geology is highly complex and permeable) exhibited the most lateral and downward contaminant movement. Transport results also suggest that areas in the model domain where head differences are significant and permeability is high, particularly areas within the El Paso Valley where stream leakage occur, possessed the highest potentials for contaminant migration.

In conclusion, significant improvements have been made to the simulation and modeling capabilities for the El Paso/Ciudad Juarez border area. The groundwater flow and transport model developed in this research addresses water resources issues pertaining to the El Paso/Ciudad Juarez border area. The model results illustrate that the Hueco Bolson will respond to excessive pumping by releasing more water from storage than the aquifer is being recharged with. Results have also shown that drawdowns will significantly increase and heads will decrease in the future, which could ultimately lead to aquifer depletion. Results also indicate that if pumping in the Hueco Bolson continues as it is currently, it will cease to be a viable source of water supply by year 2032.

Additionally, contamination occurring on the U.S. side can affect groundwater resources on the Mexican side and vice versa, depending on the following factors: groundwater flow direction, permeability of the geology, and regional groundwater flow velocities (which are directly related to the head differences). Additionally, an agreement between US and Mexico can be considered where, in the future, the aquifer will be retained for usage by El Paso and Ciudad Juarez only during water shortages, in order to

aid in preserving the diminishing natural water resources. Finally, the current study presents a new direction pertaining to groundwater modeling in the Hueco Bolson that can be utilized for future assessments of water availability and water quality in the aquifer.

REFERENCES

[1] City of El Paso. El Paso - Juarez regional historic population summary. City of El Paso Development Services Department, Planning Division; 2007.

[2] Texas Water Development Board. GIS data for the major and minor aquifers of Texas. TWDB website: http://www.twdb.state.tx.us/mapping/gisdata.asp. Accessed November 15, 2006.

[3] U.S. EPA, Summary of selected environmental indicators. The U.S.-Mexico Border XXI Program: Progress Report 1996-2000. EPA 909-R-00-002; 2000.

[4] Hutchison WR. Hueco Bolson groundwater conditions and management in the El Paso Area. El Paso, TX: El Paso Water Utilities (EPWU); 2004.

[5] Heywood CE, Yager RM. Simulated groundwater flow in the Hueco Bolson, an alluvial-basin aquifer system near El Paso, TX. US Geological Survey Water-Resources Investigations Report 02-4108, 73 p; 2003.

[6] New Mexico Water Resources Research Institute (NMWRRI). GIS data for the U.S.-Mexican Border area. NMWRRI Data and Information System: http://wrri.nmsu.edu/wrdis/ftp.html. Accessed February 25, 2006.

[7] Chavez OE. Mining of internationally shared aquifers: The El Paso/Juarez Case. Natural Resources 2000;40(2):237-60.

[8] Liverman DM, Varady RG, Chávez O, Sánchez R. Environmental issues along the United States-Mexico border: Drivers of change and responses of citizens and institutions. Annual Review of Energy and the Environment 1999;24:607-43.

[9] Hebard EM. A Focus on a binational watershed with a view toward fostering a cross-border dialogue. Natural Resources 2000;40(2):282-340.

[10] Blackman A, Palma A. Scrap tires in Ciudad Juarez and El Paso: Ranking the risks. Journal of Environment and Development 2002;11(3):247-66.

[11] Groschen GE. Simulation of groundwater flow and the movement of saline water in the Hueco Bolson Aquifer, El Paso, Texas, and adjacent areas. US Geological Survey Open-File Report 92-171, 87 p; 1994.

[12] Hibbs BJ, Boghici R. On the Rio Grande Aquifer: Flow relationships, salinization, and environmental problems from El Paso to Fort Quitman, TX. Environmental and Engineering Geoscience 1999;5:51-9.

[13] Hutchison WR. Groundwater Management in El Paso, Texas. Ph.D dissertation. EL Paso, TX: University of Texas at El Paso; 2006.

[14] Ashworth JB, Hopkins J. Aquifers of Texas. Report 345. Austin, TX: Texas Water Development Board; 1995.

[15] LBG-Guyton. Brackish groundwater manual for Texas regional water planning groups. Texas Water Development Board; 2003.

[16] Sheng Z, Devere J. Understanding and managing the stressed Mexico-USA transboundary Hueco Bolson aquifer in the El Paso del Norte region as a complex system. Hydrogeology Journal 2005;13:813-25.

[17] Langford RP. Segmentation of the Rio Grande alluvial surface and evolution of the Rio Grande rift. Proceedings of the 53rd annual meeting (April 29 to May 2, 2001) of the Rocky Mountain Section, Geological Society of America, Boulder, CO; 2001.

[18] Paso del Norte Water Task Force. Water planning in the Paso del Norte: Towards regional coordination. Paso del Norte Water Task Force: http://www.sharedwater.org. Accessed January 12, 2001.

[19] Hume B. Water in the United States-Mexico border Area. Natural Resources 2000;40(2):189-97.

[20] Texas Water Development Board. Water for Texas. State Water Plan, Vol. 1; 2002.

[21] Mace R, Ridgeway C. Major goal achieved with major Groundwater Availability Models (GAMs). A quarterly publication of the Texas Water Development Board, Austin, TX, Vol 14(4); 2004.

[22] Leggat ER, Davis ME. Analog model study of the Hueco Bolson near El Paso, Texas. Texas Water Development Board Report 28, 26 p; 1966.

[23] Meyer WR. Digital model for simulated effects of ground-water pumping in the Hueco Bolson, El Paso area, Texas, New Mexico, and Mexico U.S. Geological Survey Water-Resources Investigations 58-75, 31 p; 1976.

[24] Lee Wilson and Associates, Report 3- Hydrogeology of the Hueco Bolson: Prepared for the public services board, city of El Paso, TX; 1985a.

[25] Lee Wilson and Associates, Report 4- Technical framework for evaluation of proposed Hueco Basin appropriations: Prepared for the public services board, city of El Paso, TX; 1985b.

[26] Lee Wilson and Associates, Research Memoranda 3- Solute transport model for the Hueco Bolson Recharge project: Prepared for the public services board, city of El Paso, TX; 1991.

[27] Kernodle JM. Results of simulations by a preliminary numerical model of land subsidence in the El Paso, Texas, area. U.S. Geological Survey Water Resources Investigations Report 92-4037, 35 p; 1992.

[28] Bredehoeft JD, Pinder GF. Digital analysis of areal flow in multiaquifer groundwater systems- a quasi three-dimensional model. Water Resources Research 1970;6(3):883-8.

[29] McDonald MG, Harbaugh AW. A modular three-dimensional finite-difference groundwater flow model. Reston, VA: US Geological Survey Open-File Report 83-875; 1988.

[30] McDonald MG, Harbaugh AW. User's documentation for MODFLOW-96, and update to the US Geological Survey modular finite difference ground-water flow model. Reston, VA: US Geological Survey Open-File Report 96-485; 1996.

[31] Mays WL. Water resources engineering (first edition): John Wiley & Sons, Inc, New York, NY; 2001.

[32] Harbaugh AW, Banta ER, Hill MC, McDonald MG. MODFLOW-2000, the US Geological Survey modular groundwater model; user guide to modularization concepts and the groundwater flow process. US Geological Survey Open-File Report 00-92 ; 2000.

[33] Zheng C. MT3D: A modular three-dimensional transport model for simulation of advection, dispersion and chemical reactions of contaminants in groundwater systems: documentation. US Army Engineer Research and Development Center; 1990.

[34] Zheng C, Wang PP. MT3DMS: A modular three-dimensional multi-species model for simulation of advection, dispersion and chemical reactions of contaminants in groundwater systems: documentation and user's guide. Vicksburg, MS: SERDP-99-1, US Army Engineer Research and Development Center; 1999.

[35] Doherty J. PEST: Model-Independent Parameter Estimation. Watermark Numerical Computing, Brisbane, Australia; 2004.

[36] Harbaugh AW. ZONEBUDGET: A computer program for calculating subregional water budgets using results from the US Geological Survey modular three-

dimensional finite-difference ground-water flow model. US Geological Survey Open-File Report 90-392 ; 1990.

[37] Wurbs RA, James WP. Water resources engineering: Prentice Hall, Upper Saddle River, NJ; 2002.

[38] Waterloo Hydrogeologic Inc. Visual MODFLOW v. 4.1. Premium Edition, user's manual,Waterloo, Ontario, Canada; 2005.

[39] Mehl SW, Hill MC. MODFLOW-2000, the US Geological Survey modular groundwater model; user guide to the LINK-AMG (LMG) package for solving matrix equation using an algebraic multigrid solver. US Geological Survey Open-File Report 01-177 ; 2001.

[40] Marty F. Managing international rivers: problems, politics, and institutions, Peter Lang Publishing, Bern: 2001.

[41] Arnold JG, Srinivasan R, Muttiah RS, Williams JR. Large area hydrologic modeling and assessment, part 1: Model development. Journal of the American Water Resources Association 1998;34(1):73-89.

APPENDIX A

MODEL HEAD AND

DRAWDOWN HYDROGRAPHS

JMAS (MEXICAN) WELLS

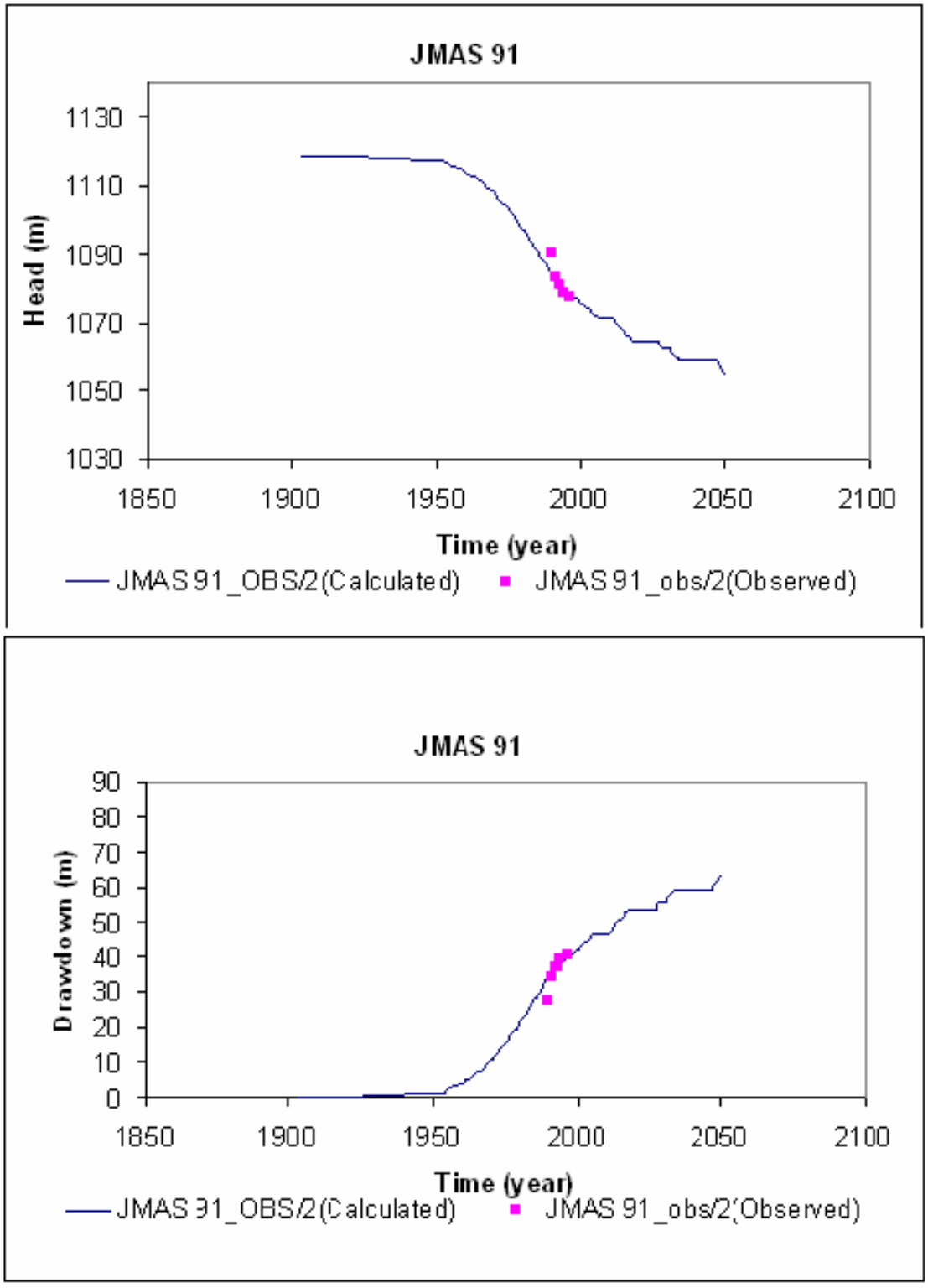

Fig. A- 1. Head and drawdown hydrographs for JMAS 91

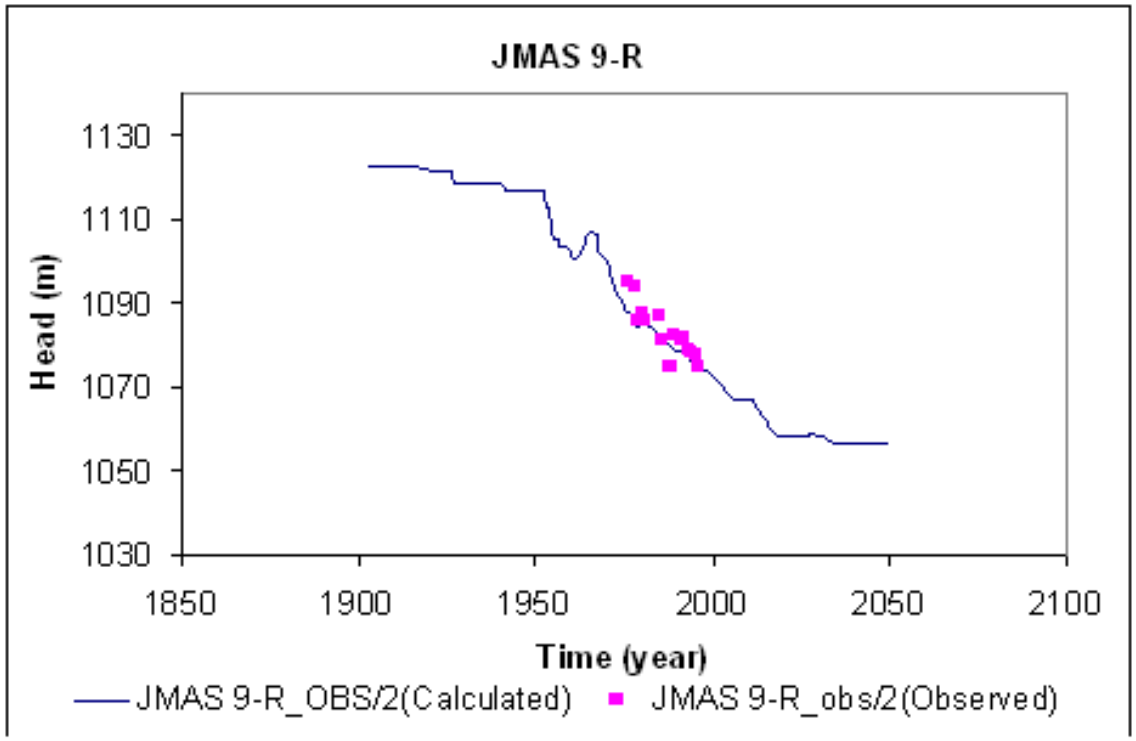

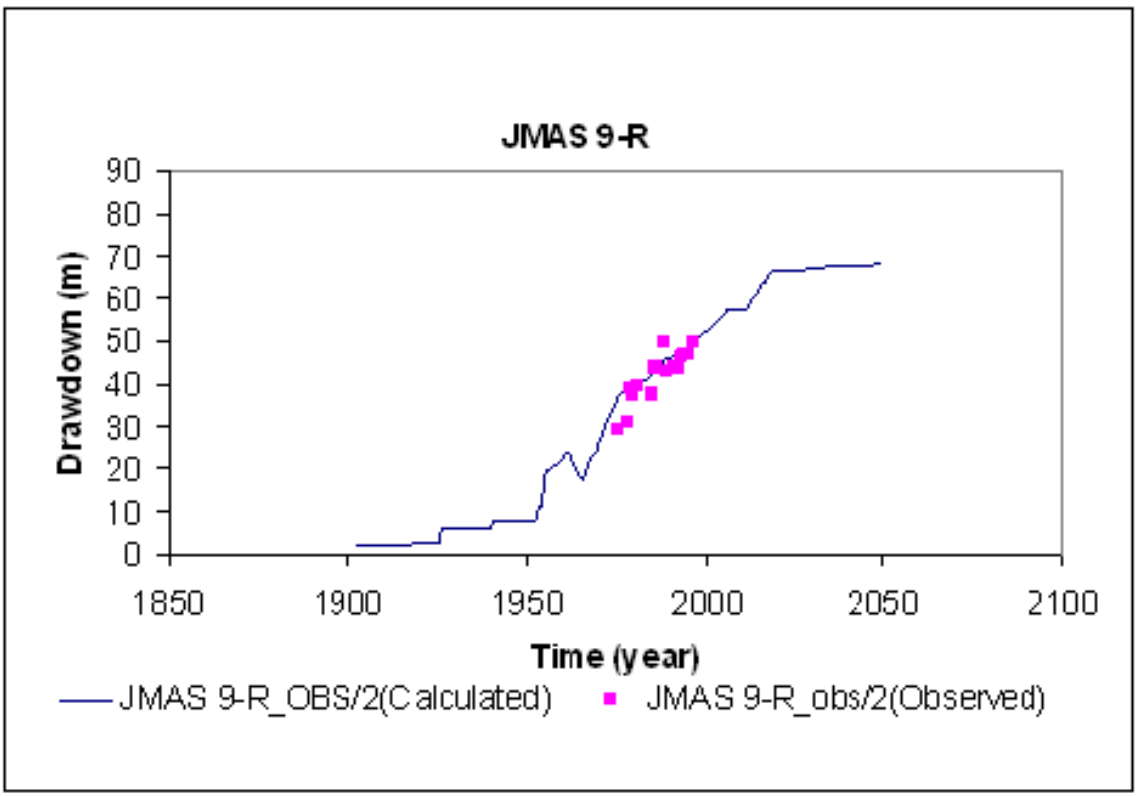

Fig. A- 2. Head and drawdown hydrographs for JMAS 9-R

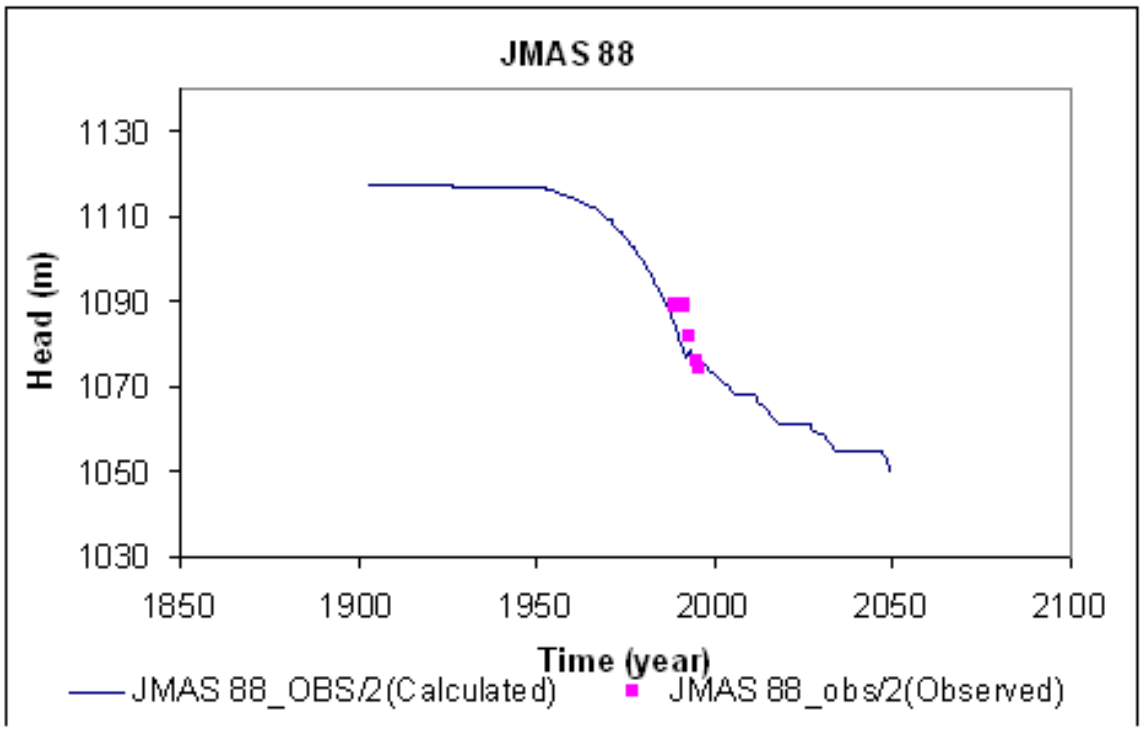

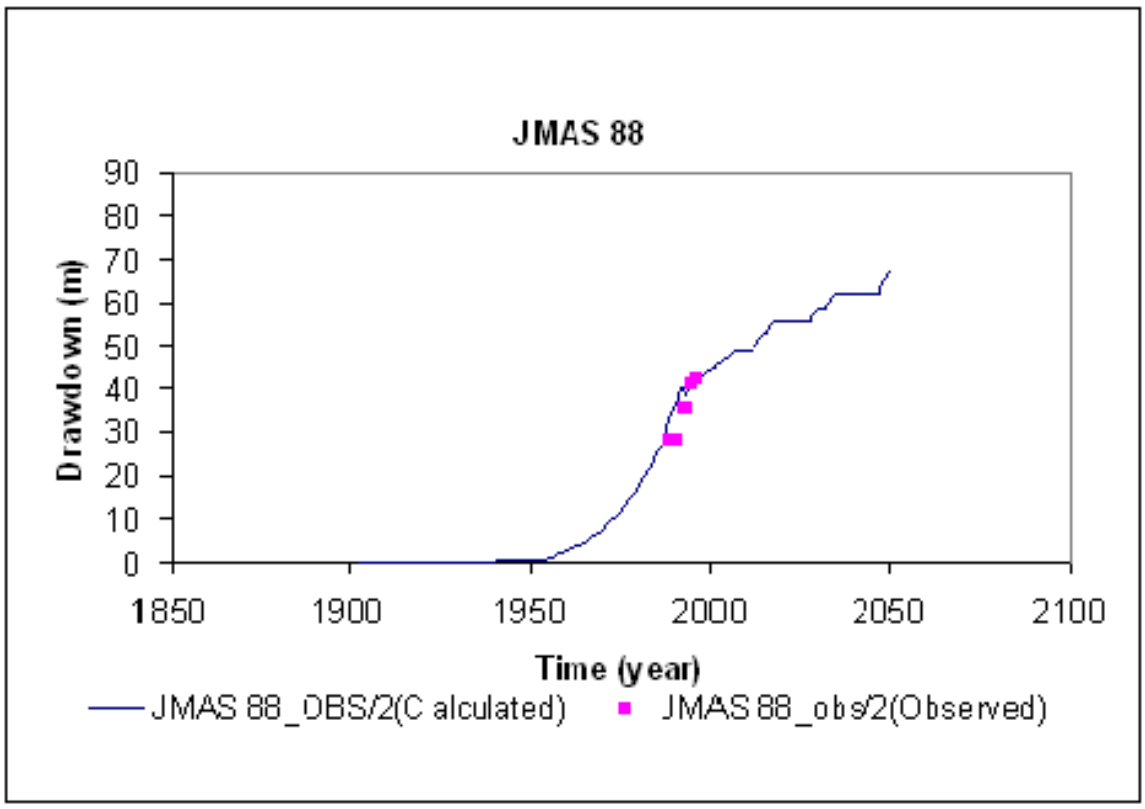

Fig. A- 3. Head and drawdown hydrographs for JMAS 88

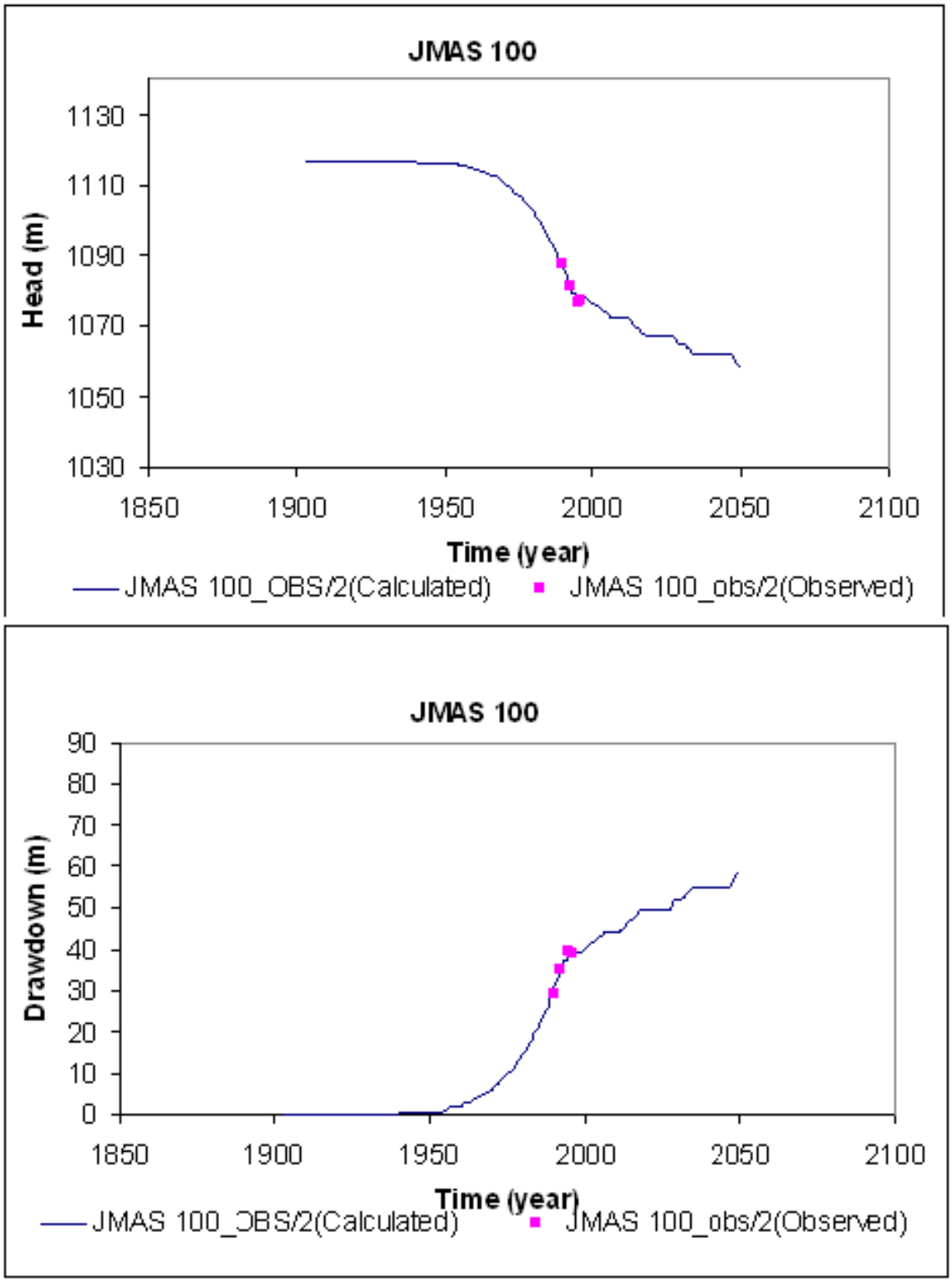

Fig. A- 4. Head and drawdown hydrographs for JMAS 100

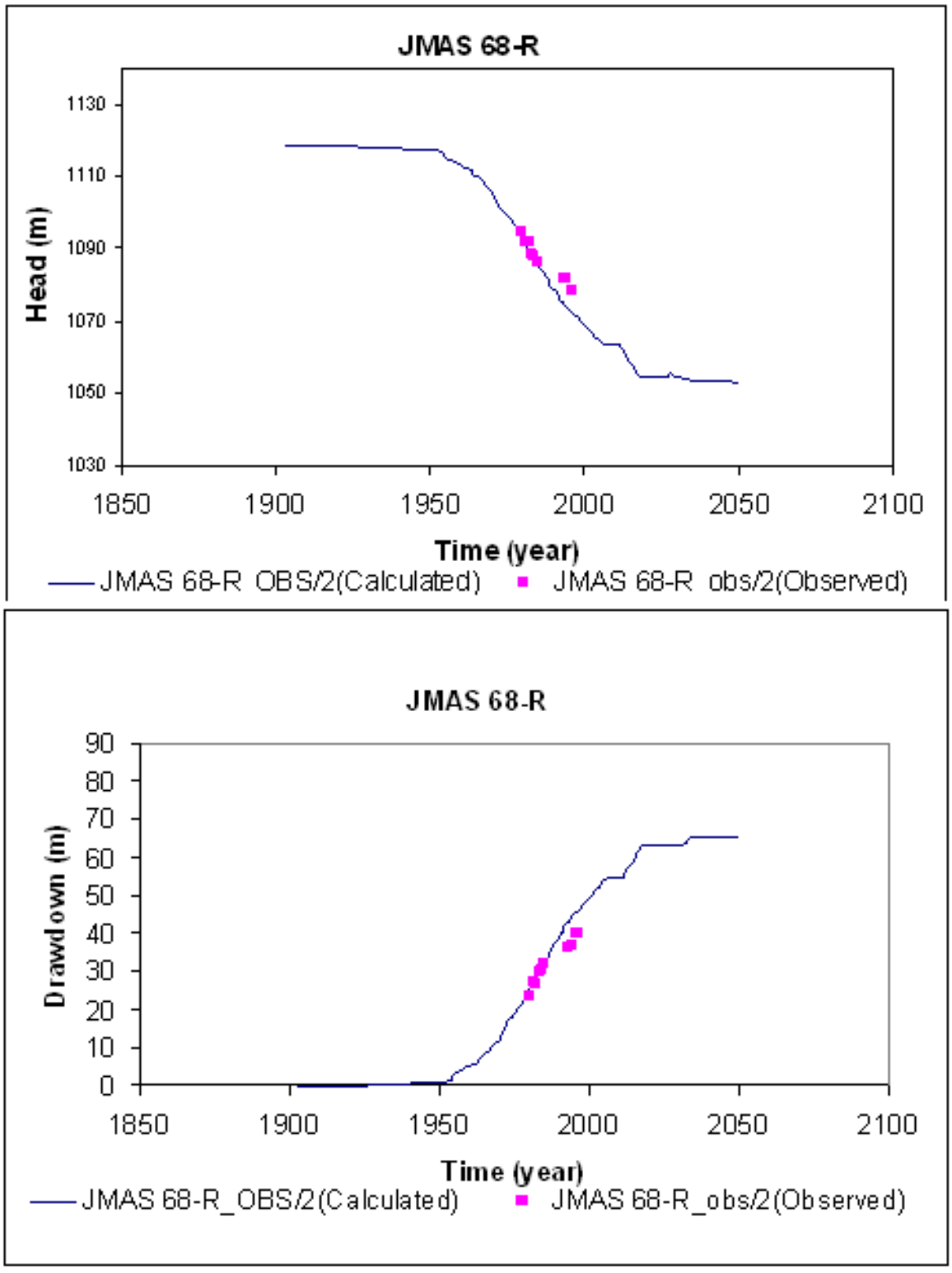

Fig. A- 5. Head and drawdown hydrographs for JMAS 68-R

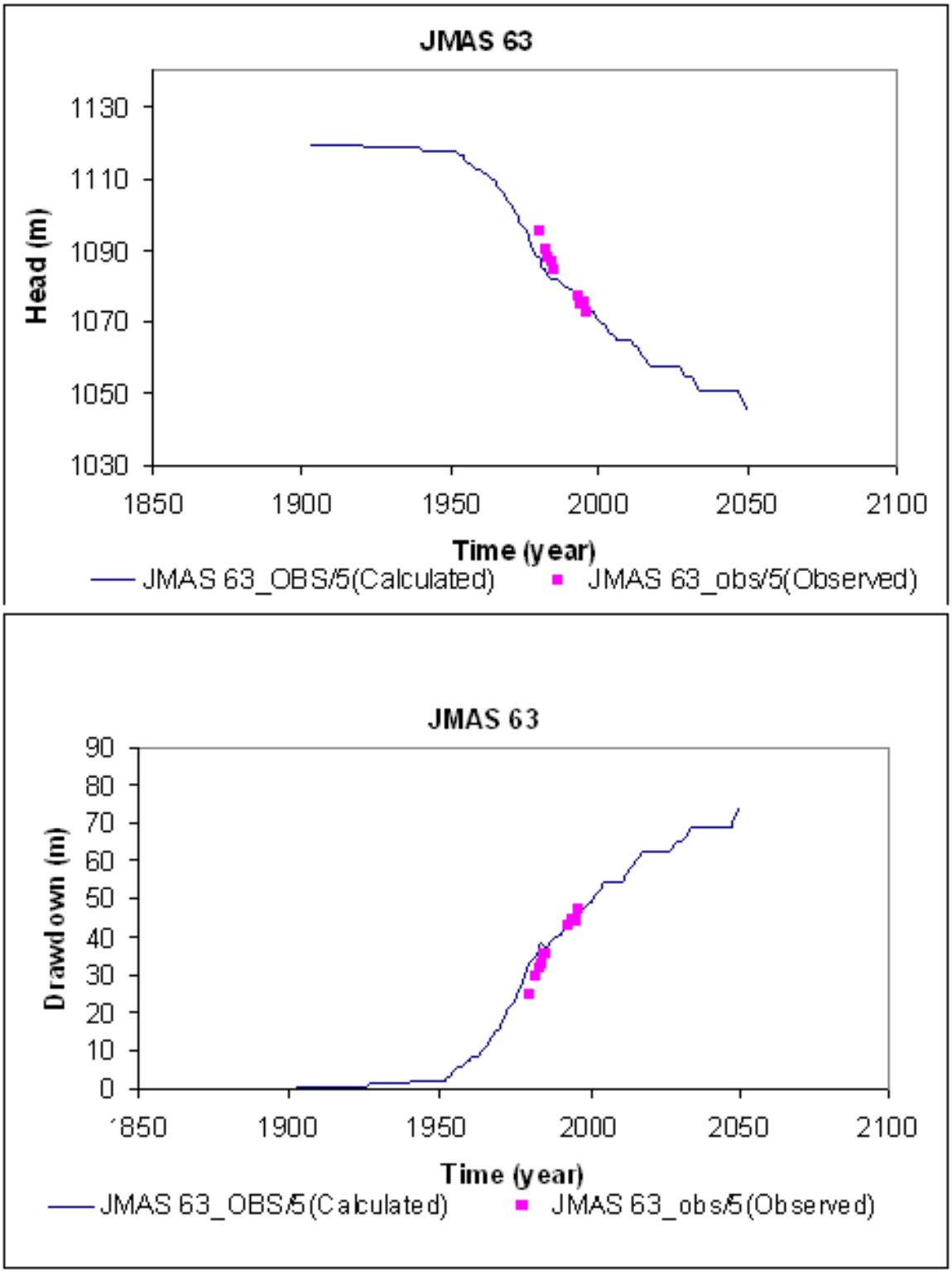

Fig. A- 6. Head and drawdown hydrographs for JMAS 63

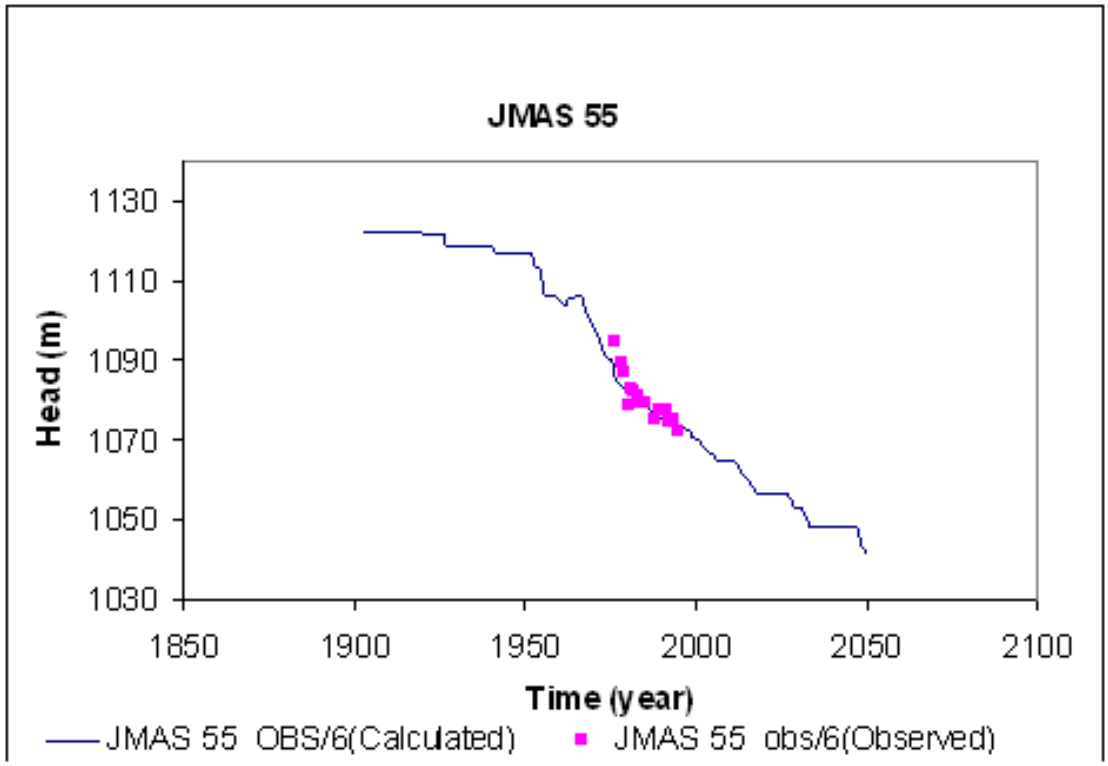

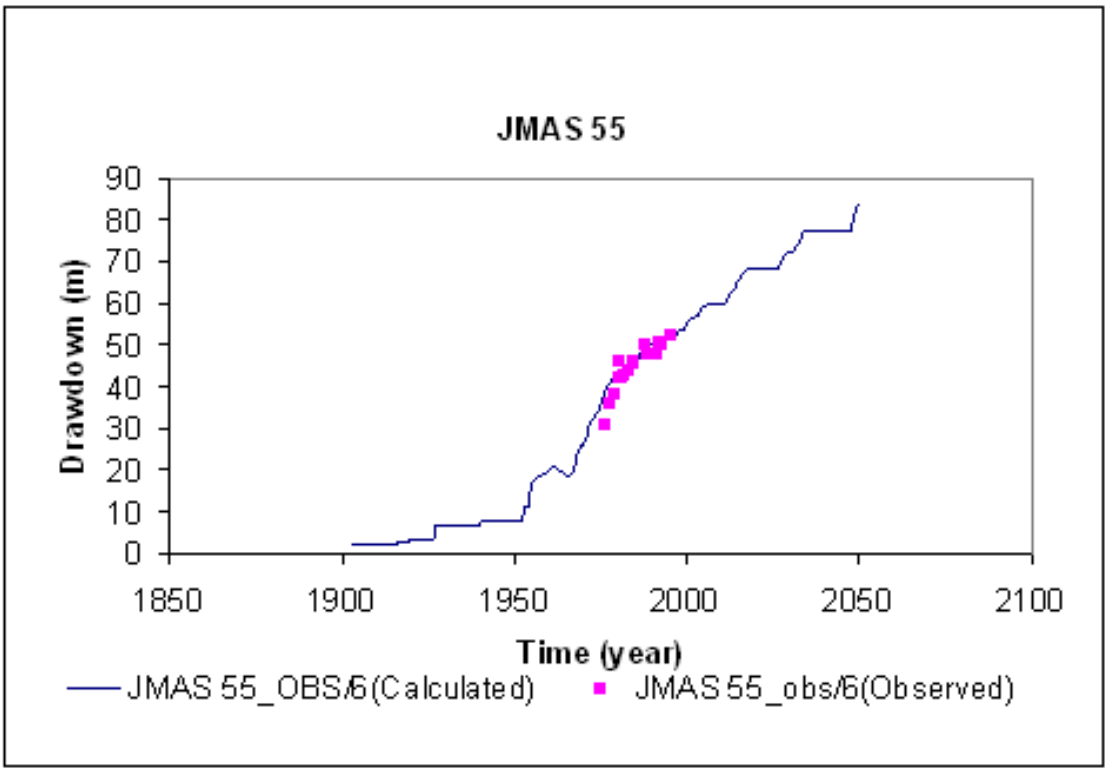

Fig. A- 7. Head and drawdown hydrographs for JMAS 55

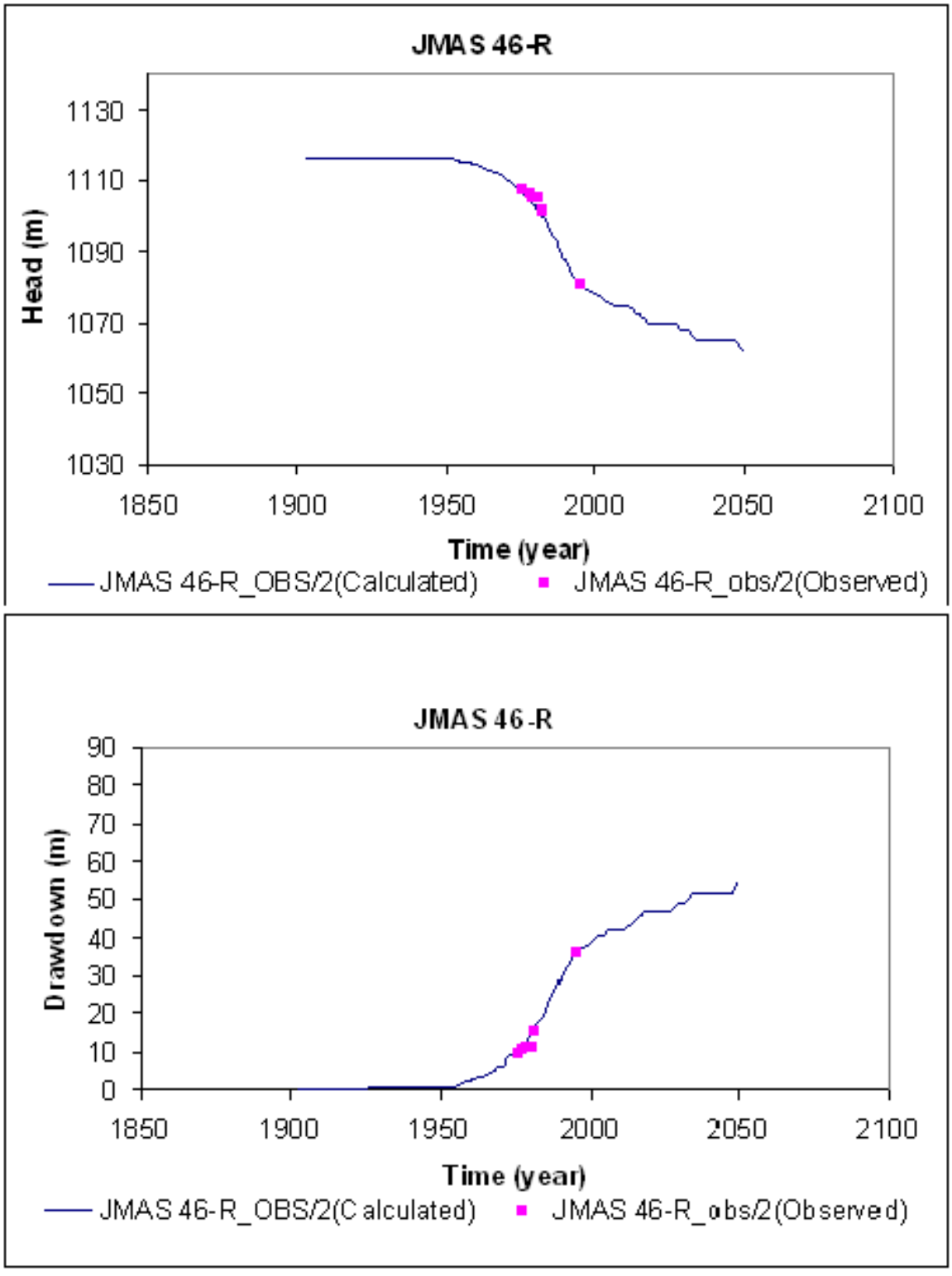

Fig. A- 8. Head and drawdown hydrographs for JMAS 46-R

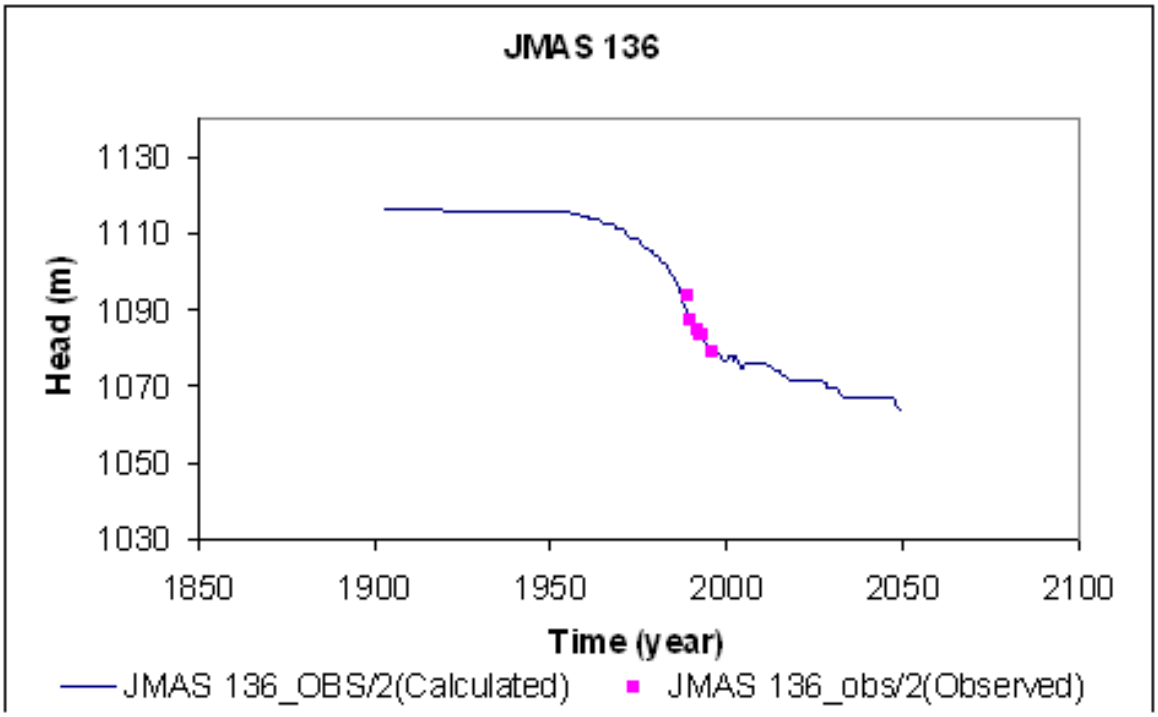

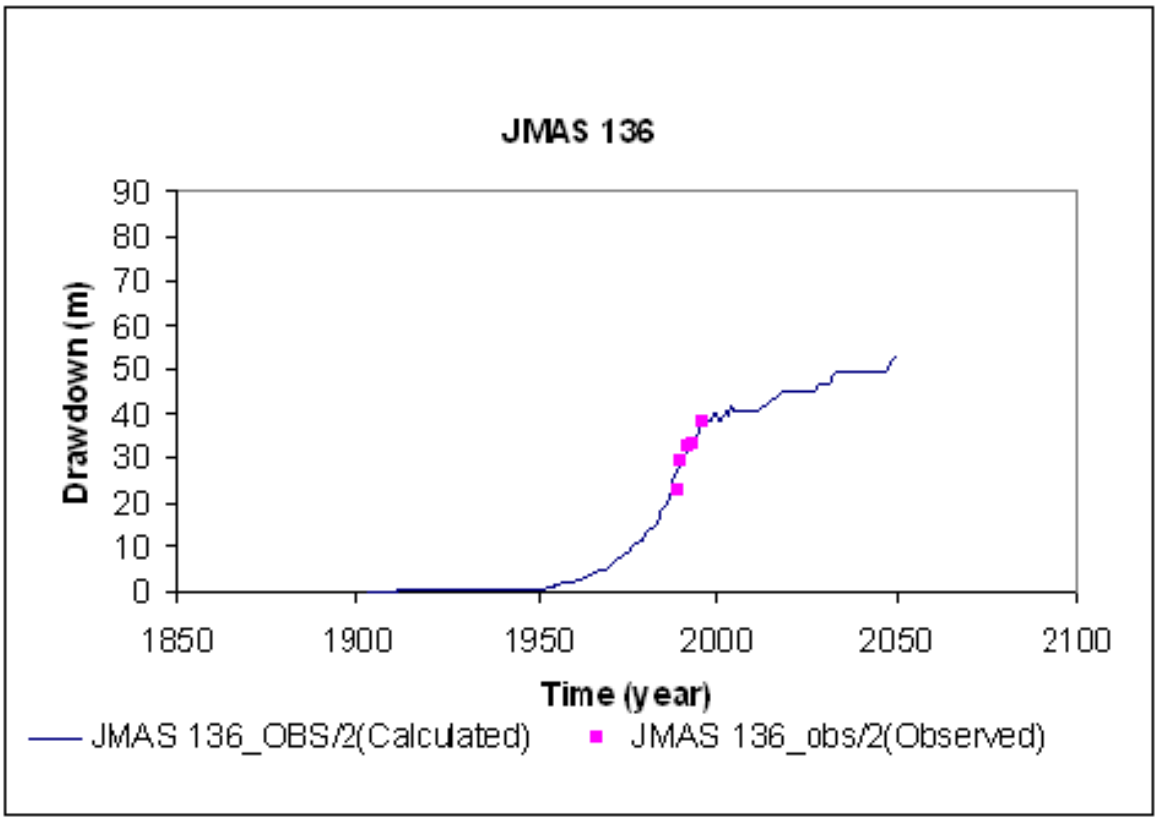

Fig. A- 9. Head and drawdown hydrographs for JMAS 136

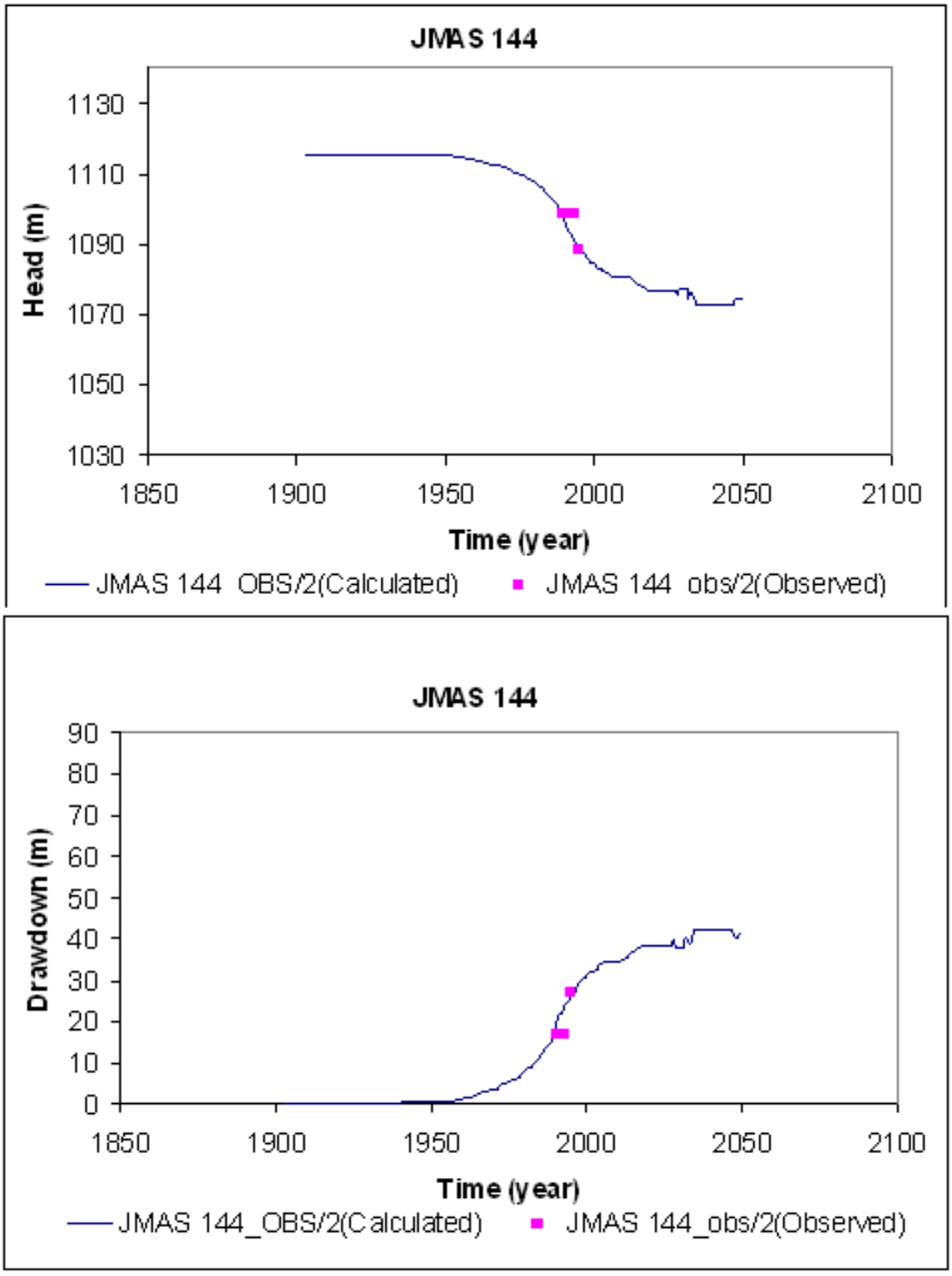

Fig. A- 10. Head and drawdown hydrographs for JMAS 144

EPWU (U.S.) WELLS

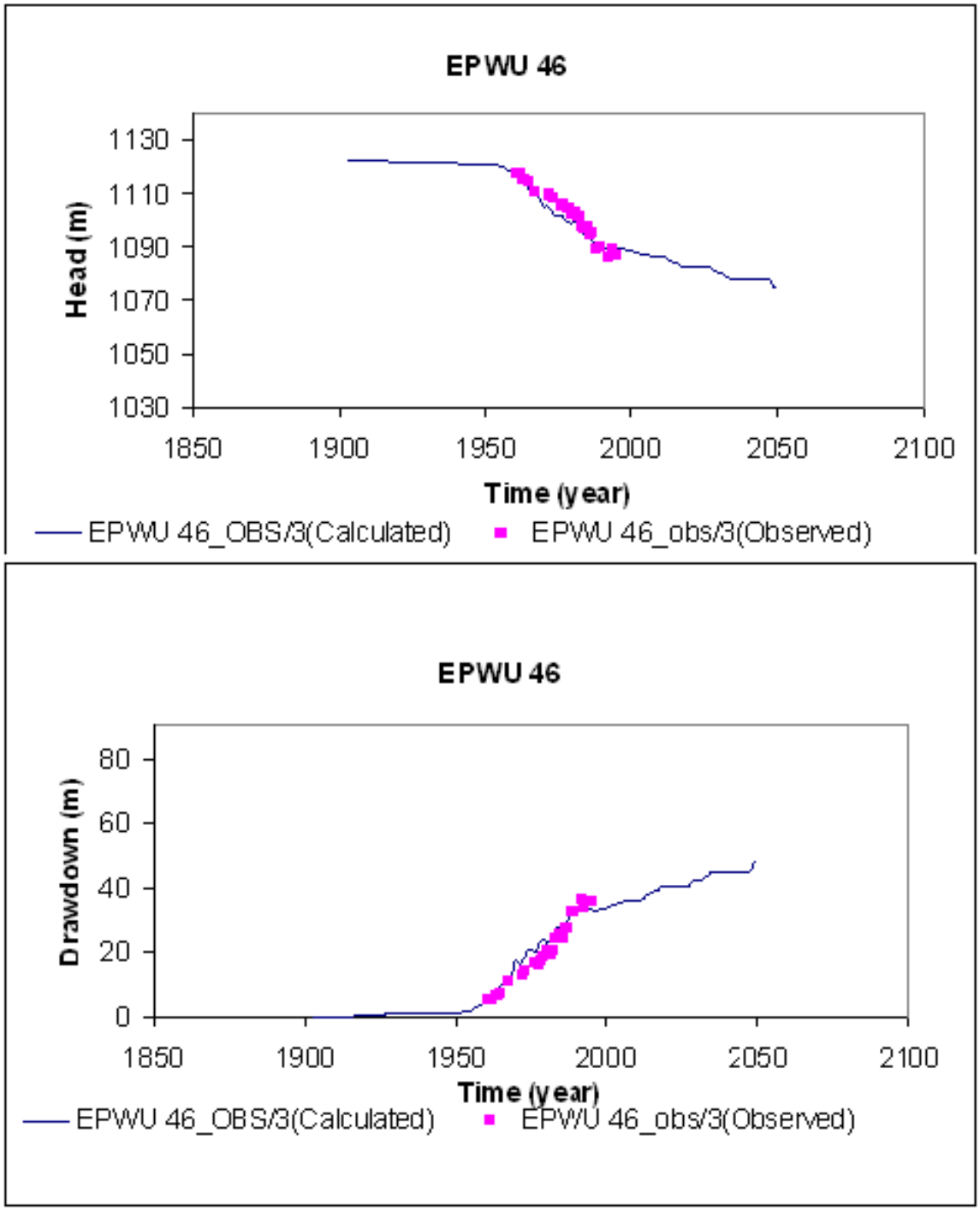

Fig. A- 11. Head and drawdown hydrographs for EPWU 46

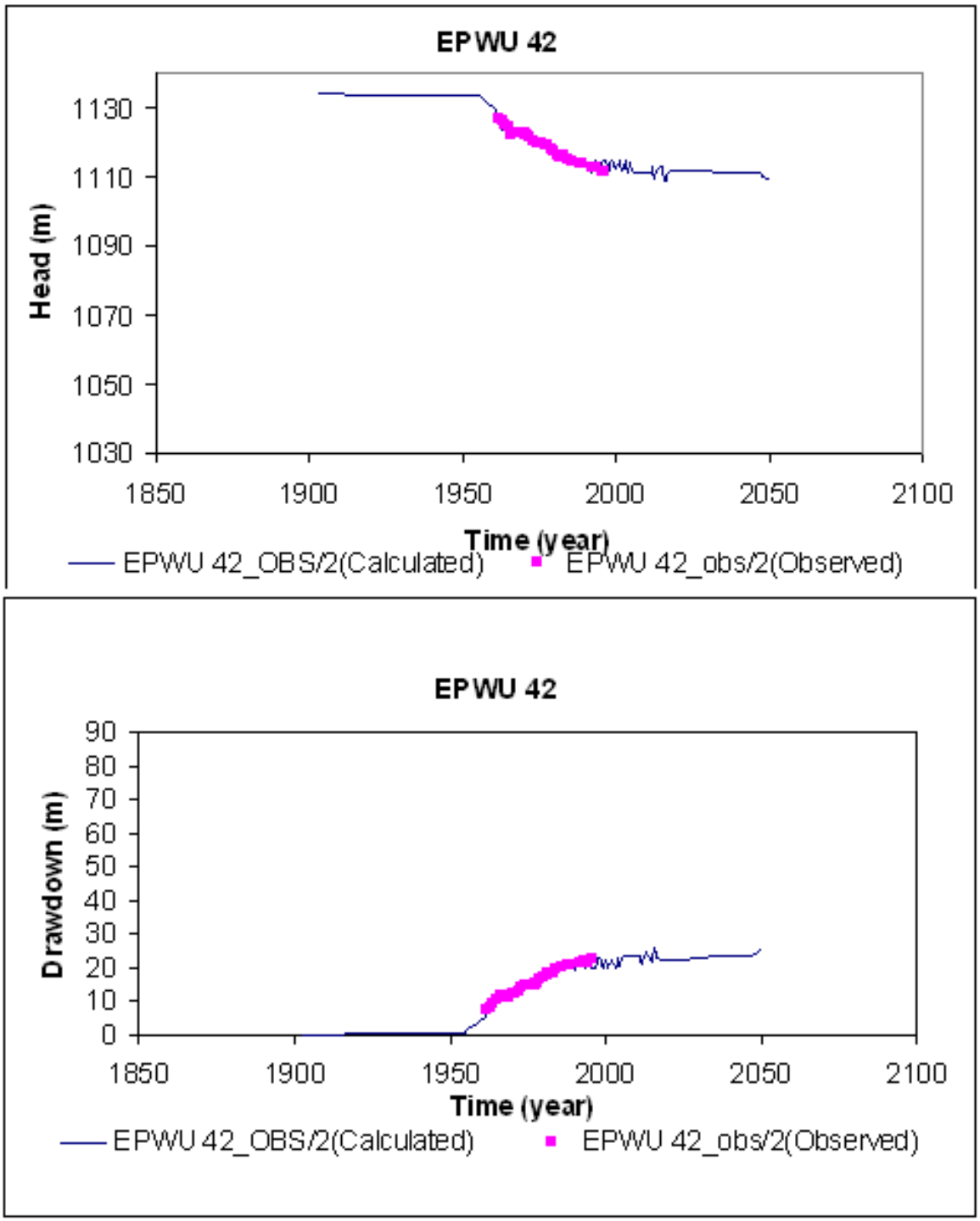

Fig. A- 12. Head and drawdown hydrographs for EPWU 42

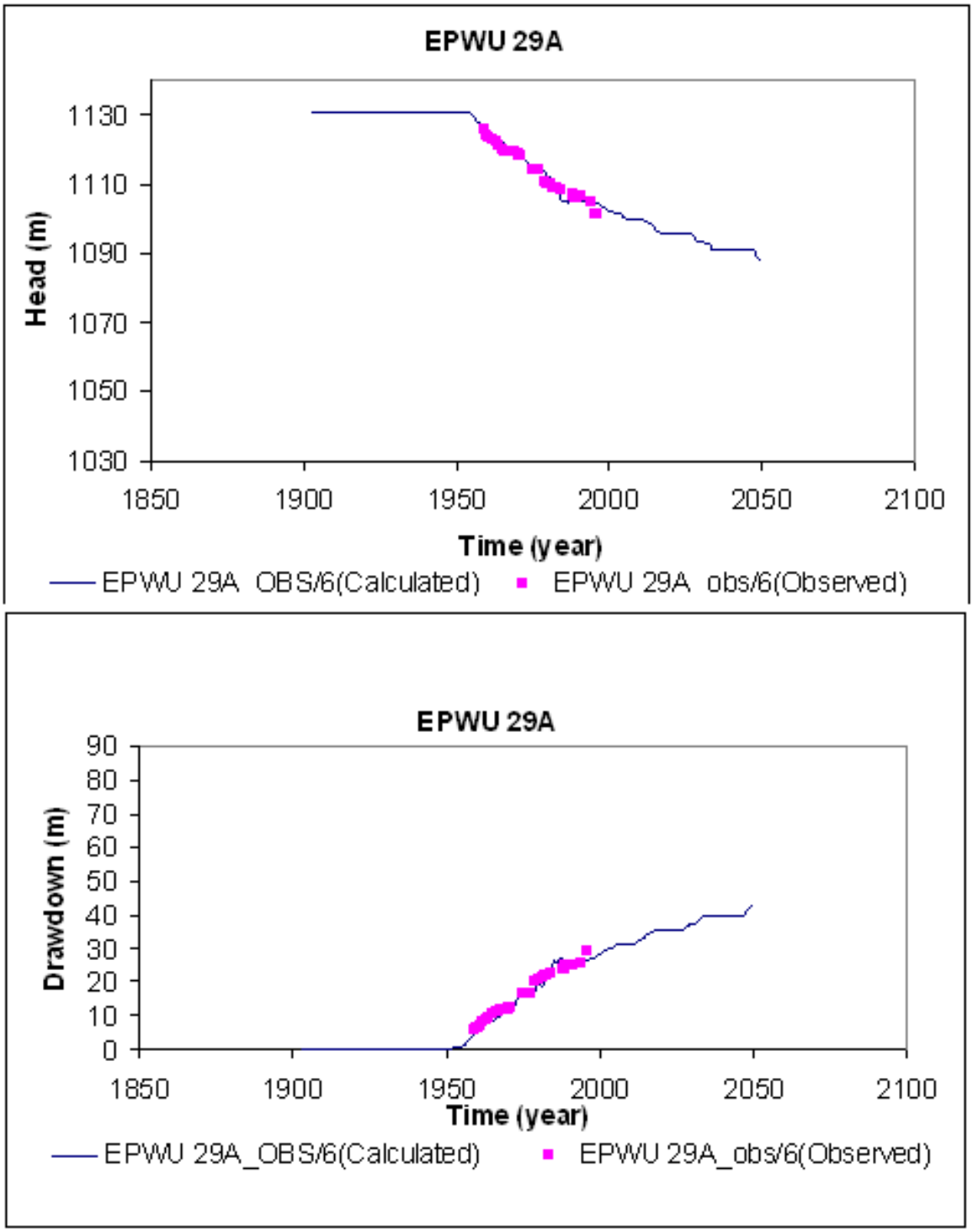

Fig. A- 13. Head and drawdown hydrographs for EPWU 29A

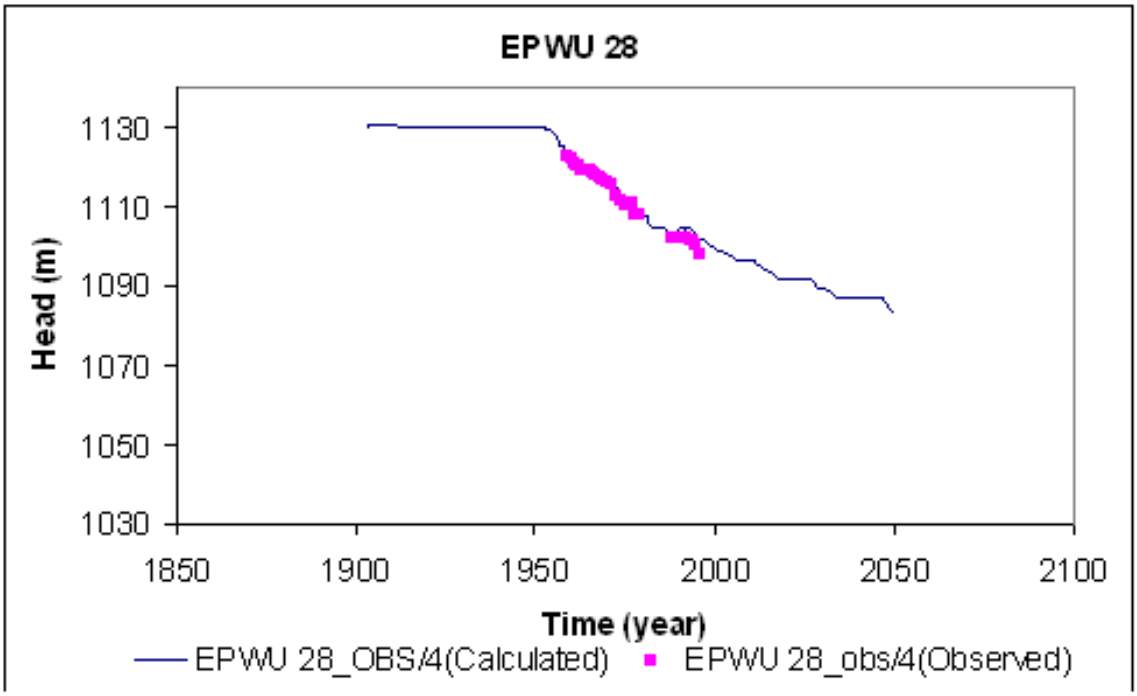

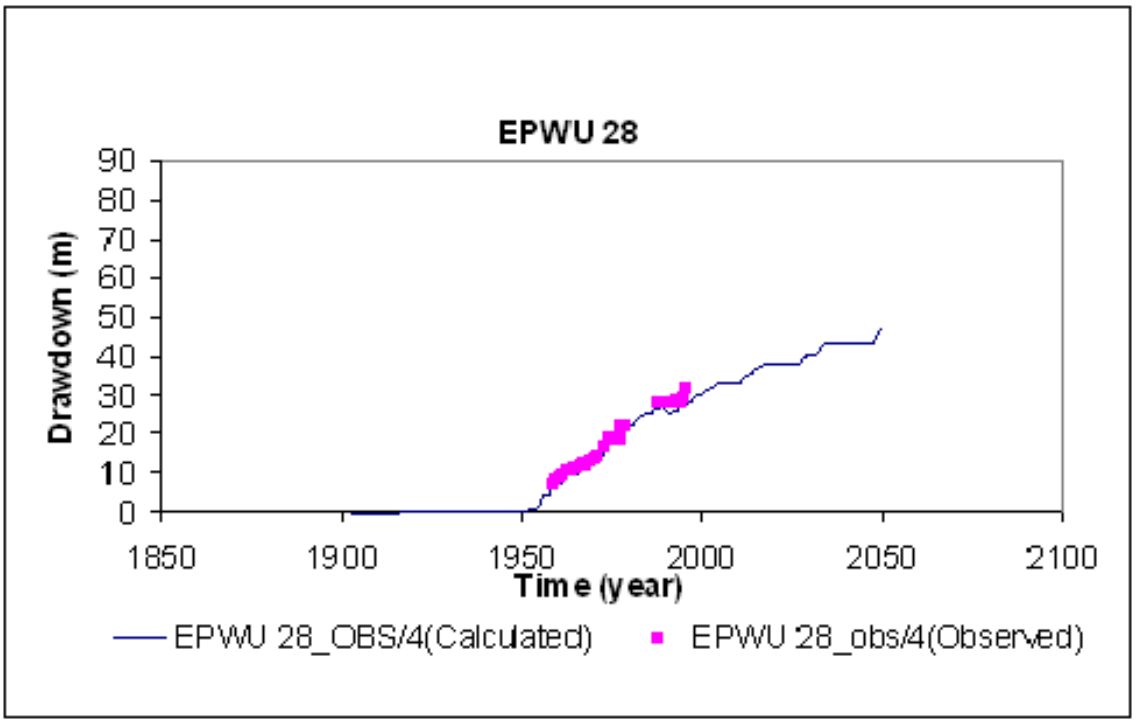

Fig. A- 14. Head and drawdown hydrographs for EPWU 28

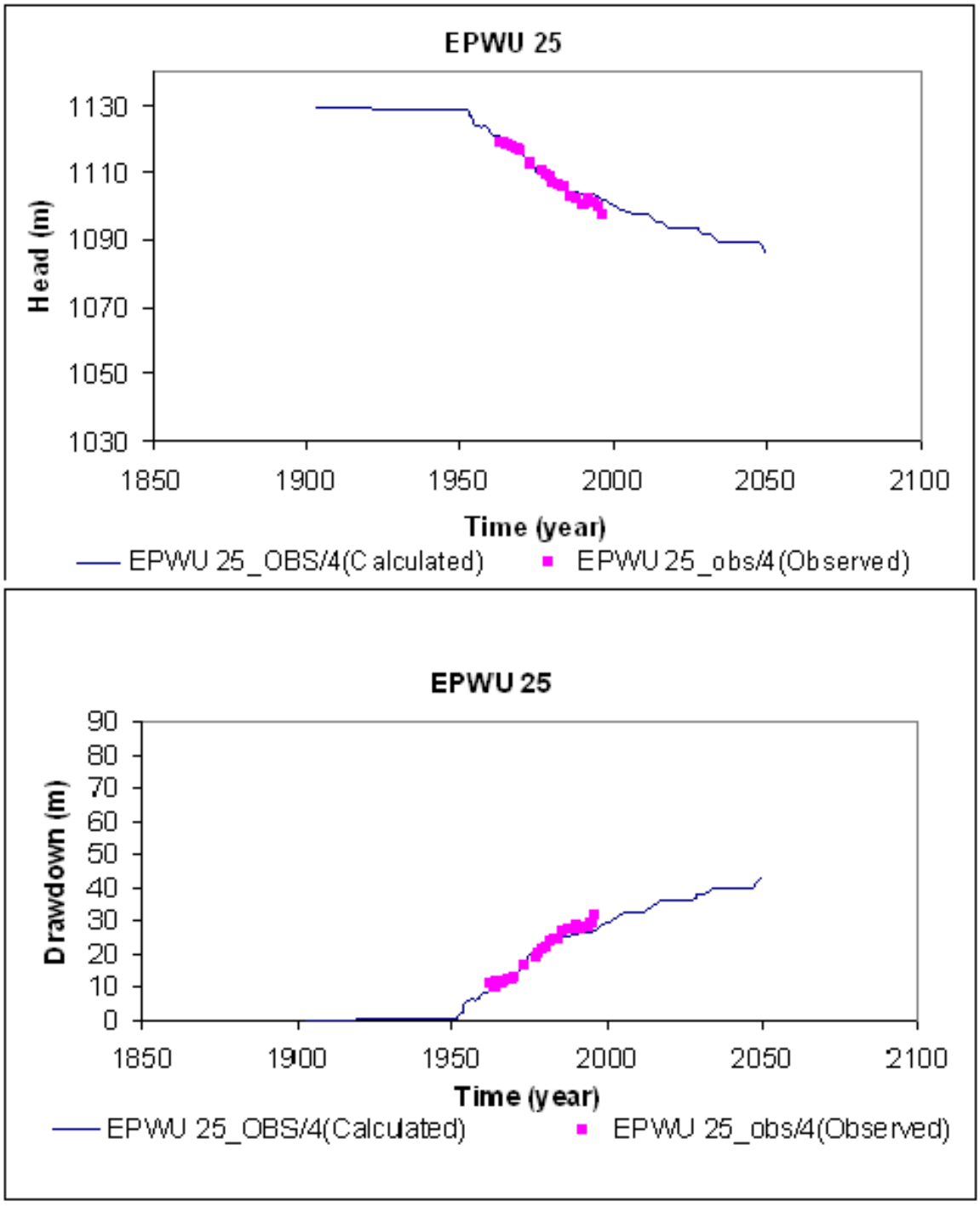

Fig. A- 15. Head and drawdown hydrographs for EPWU 25

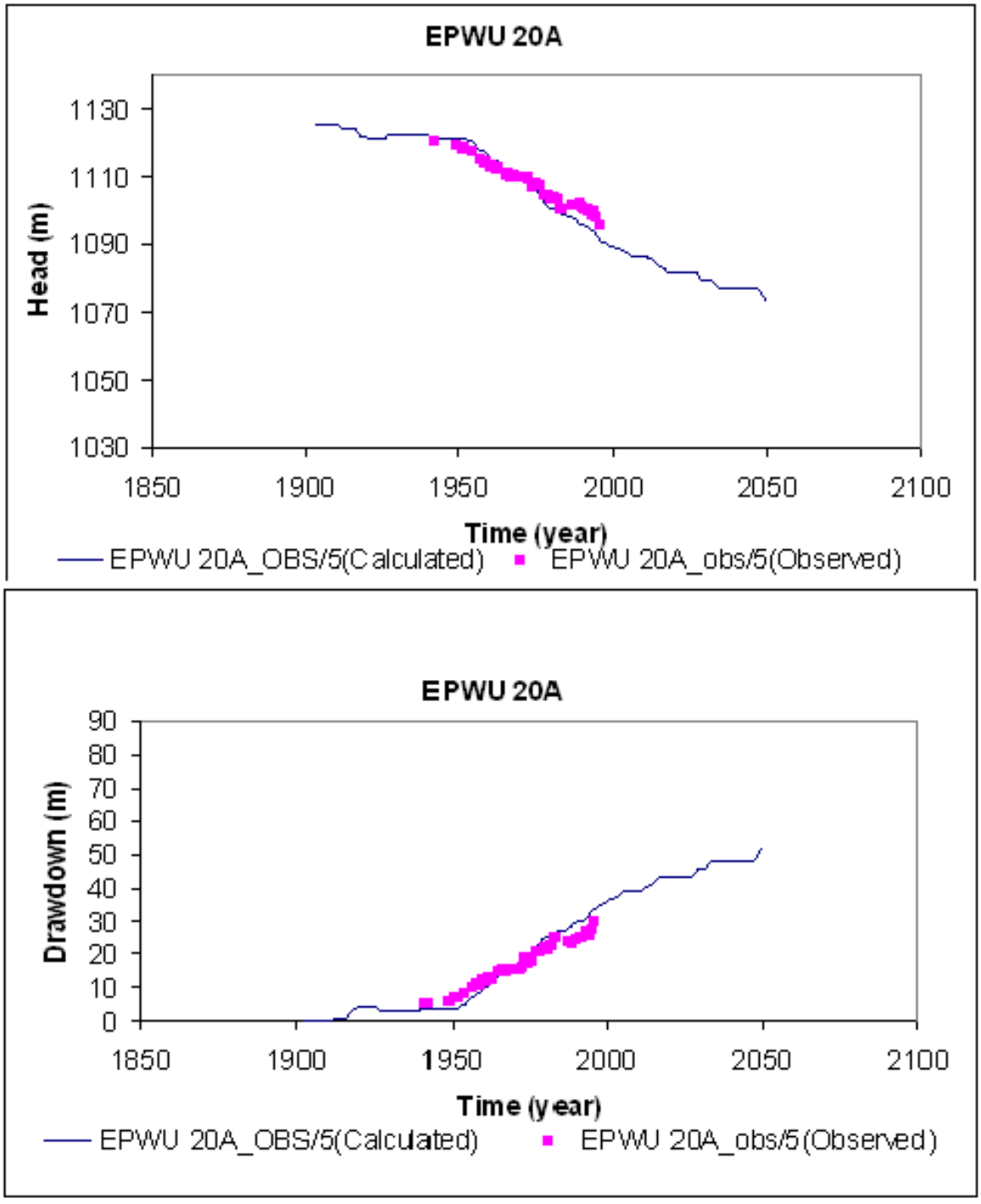

Fig. A- 16. Head and drawdown hydrographs for EPWU 20A

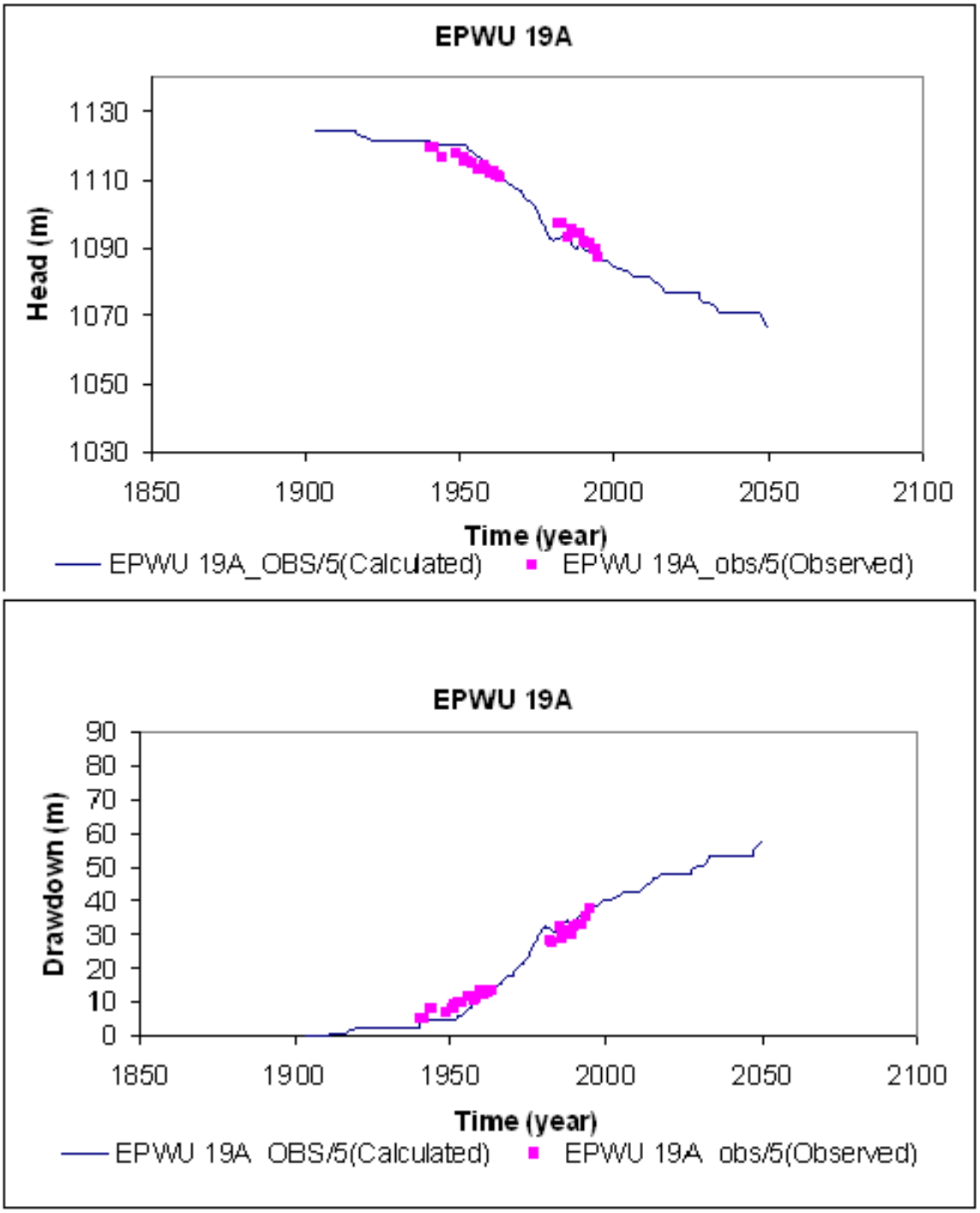

Fig. A- 17. Head and drawdown hydrographs for EPWU 19A

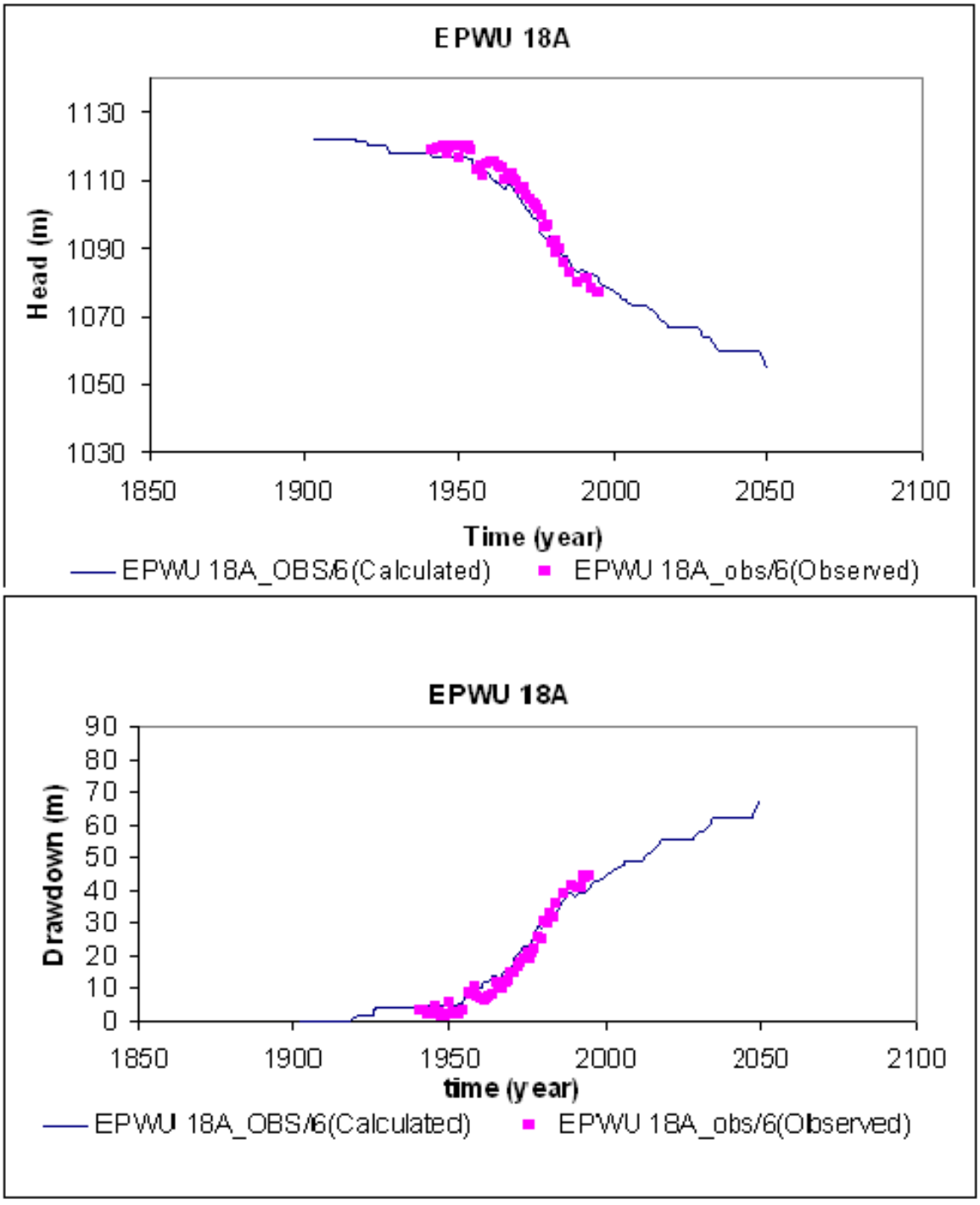

Fig. A- 18. Head and drawdown hydrographs for EPWU 18A

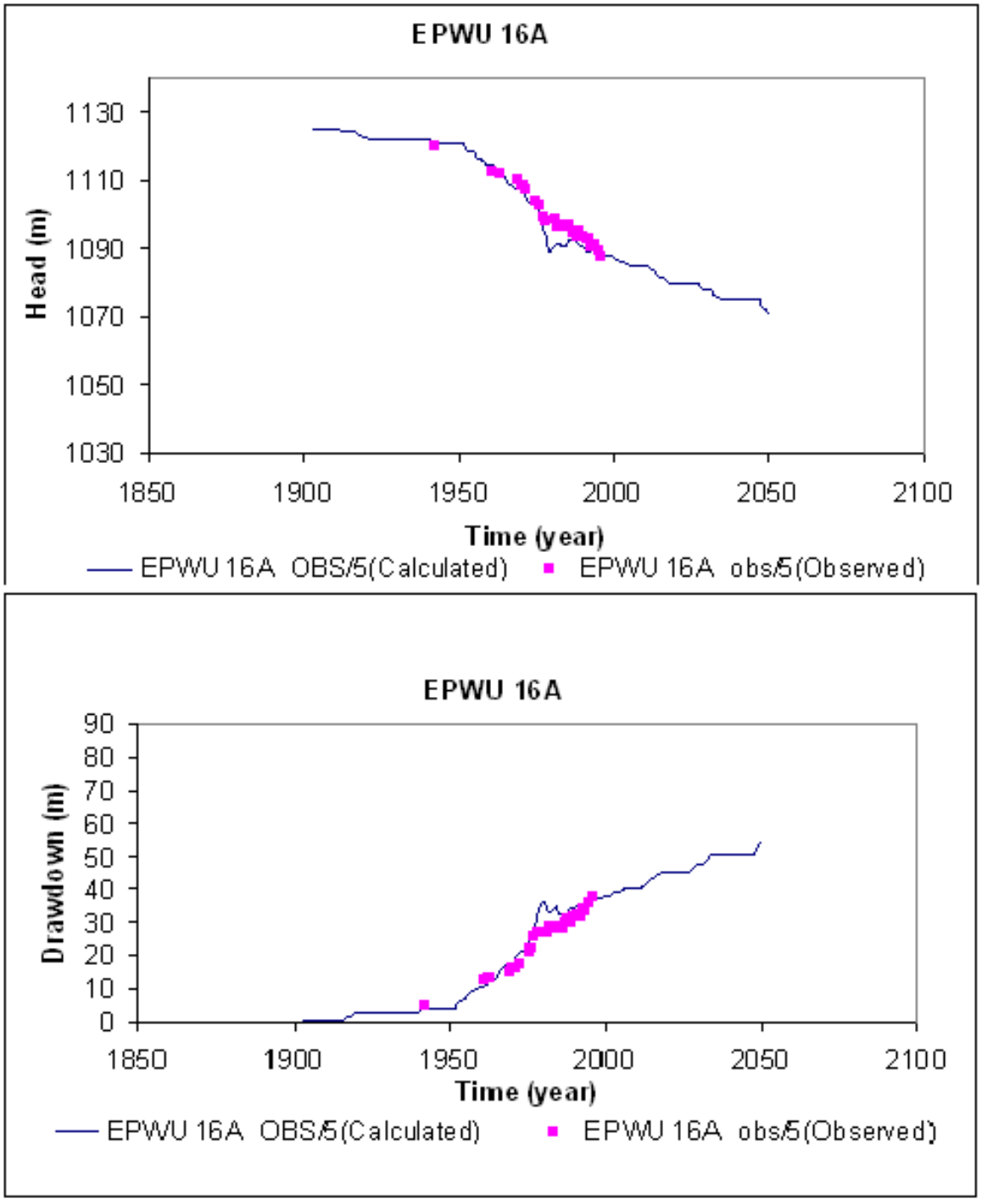

Fig. A- 19. Head and drawdown hydrographs for EPWU 16A

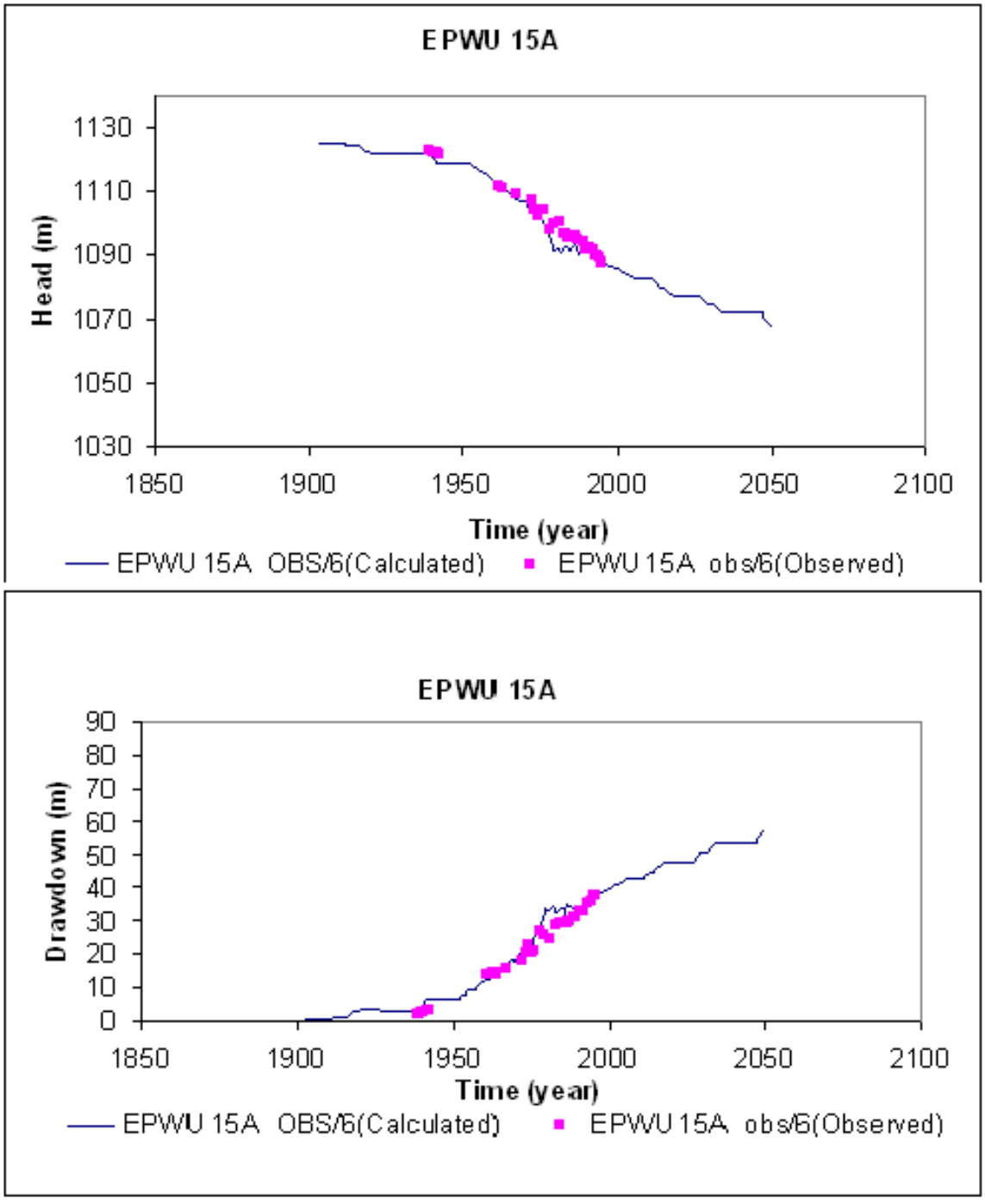

Fig. A- 20. Head and drawdown hydrographs for EPWU 15A

APPENDIX B

CONTAMINANT FATE AND

TRANSPORT SIMULATION RESULTS AT SITES

EL PASO SITE 1

- **1997, 2020, 2035, and 2050 contaminant plume color maps**
- **East to west vertical hydraulic conductivity (K_z) cross-section at site**
- **East to west horizontal hydraulic conductivity (K_x) cross-section a at site**

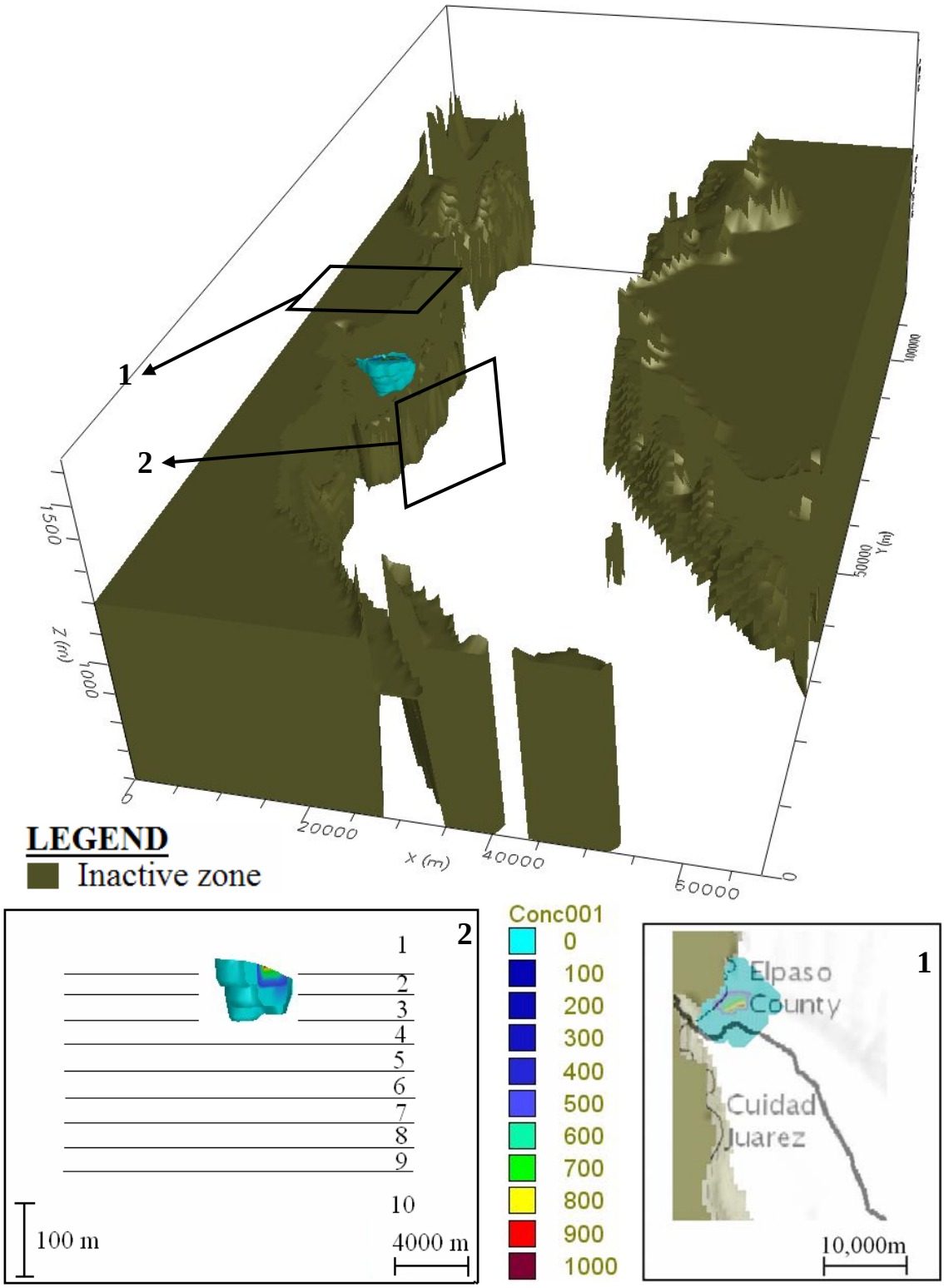

Fig. B- 1. El Paso site 1 concentration (mg/L) plume color map for year 1997

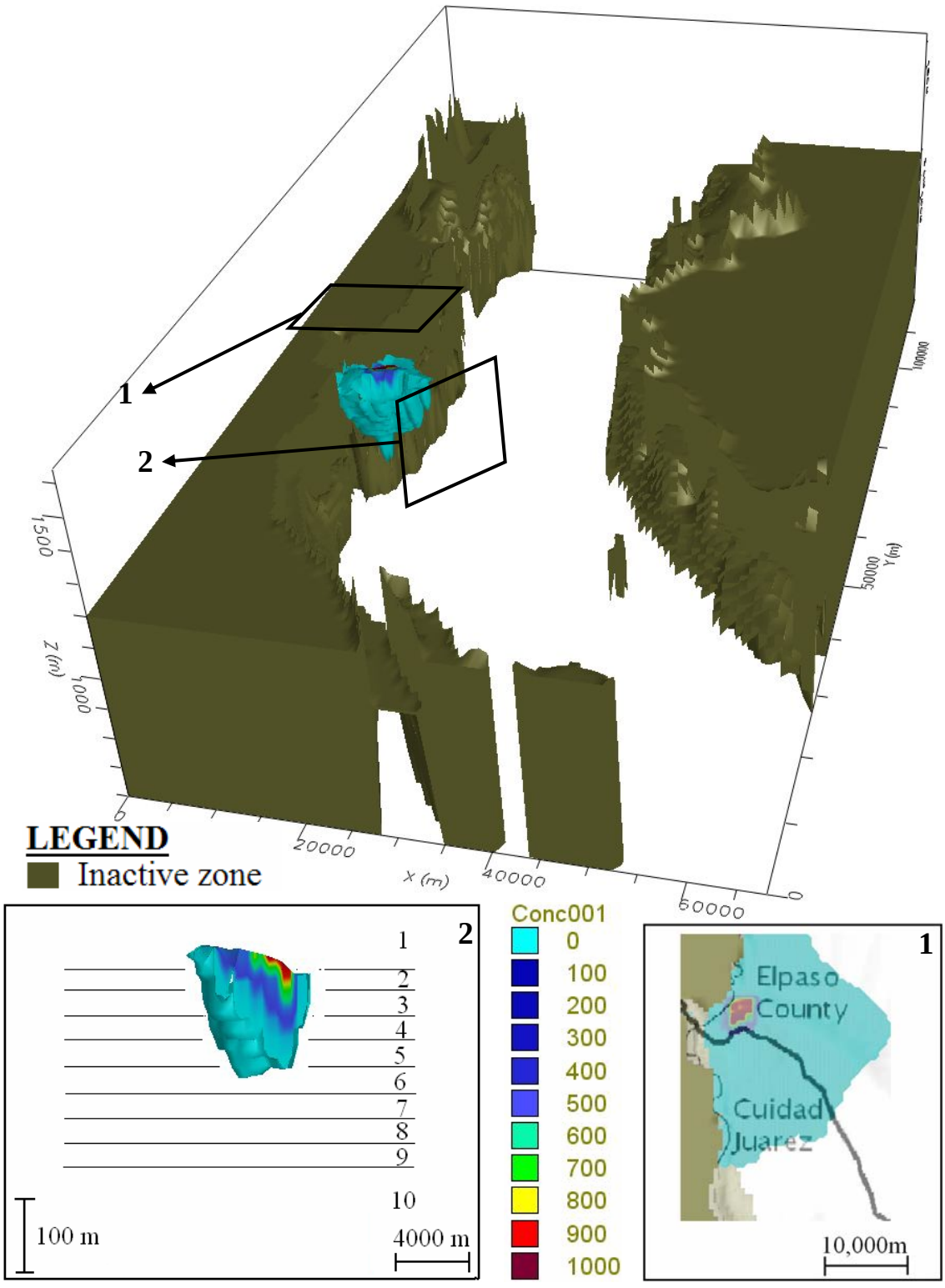

Fig. B- 2. El Paso site 1 concentration (mg/L) plume color map for year 2020

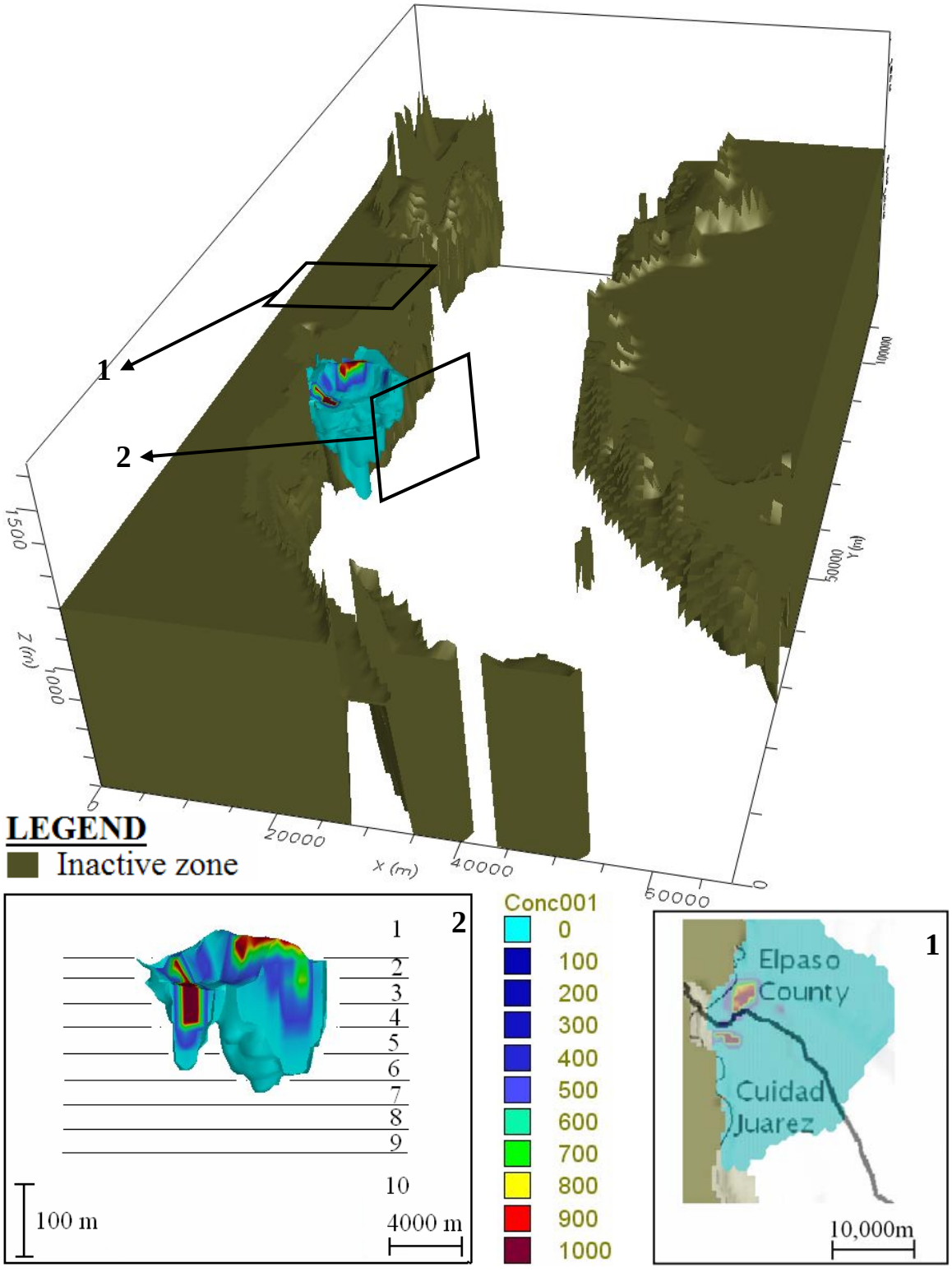

Fig. B- 3. El Paso site 1 concentration (mg/L) plume color map for year 2035

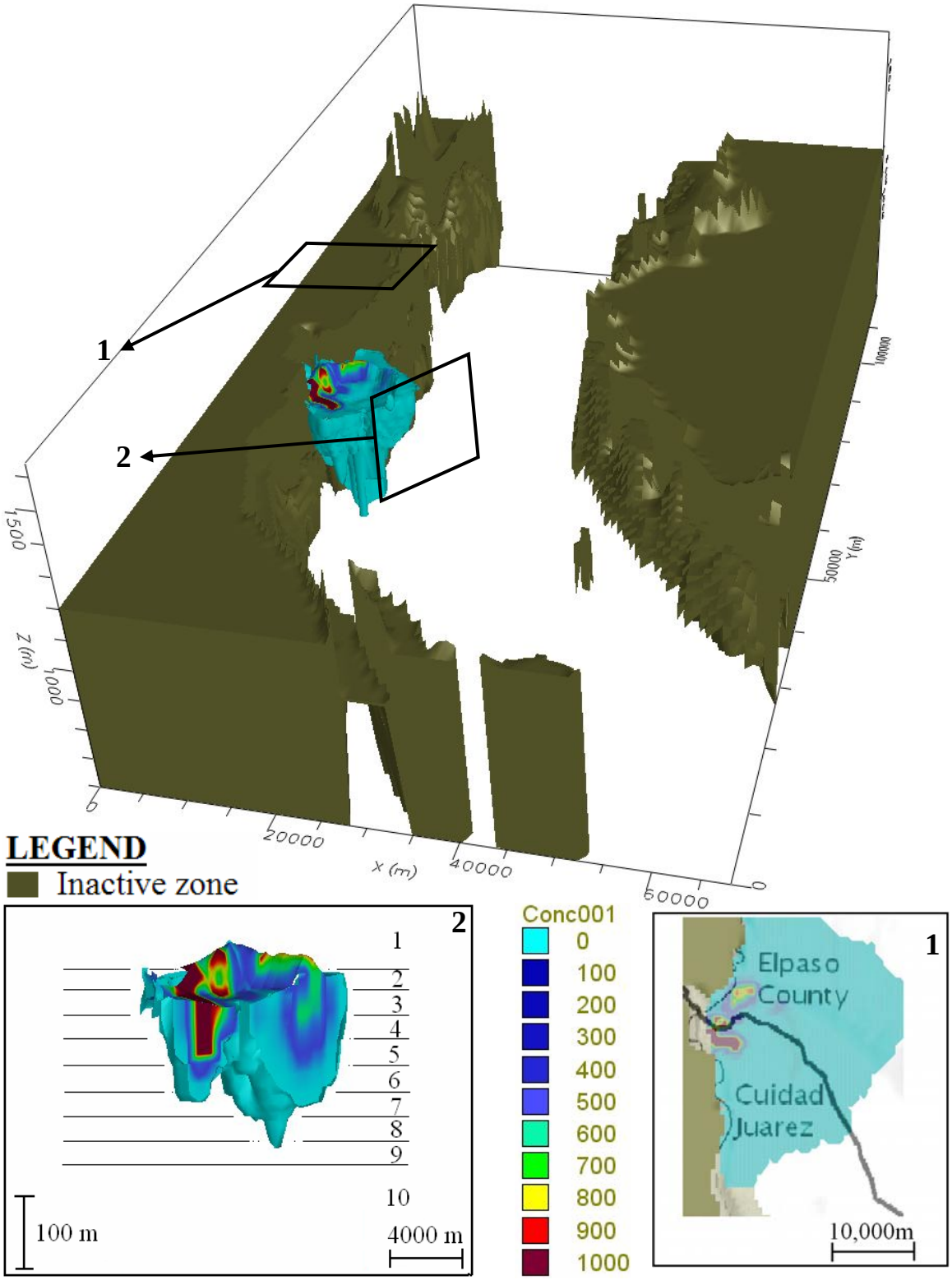

Fig. B- 4. El Paso site 1 concentration (mg/L) plume color map for year 2050

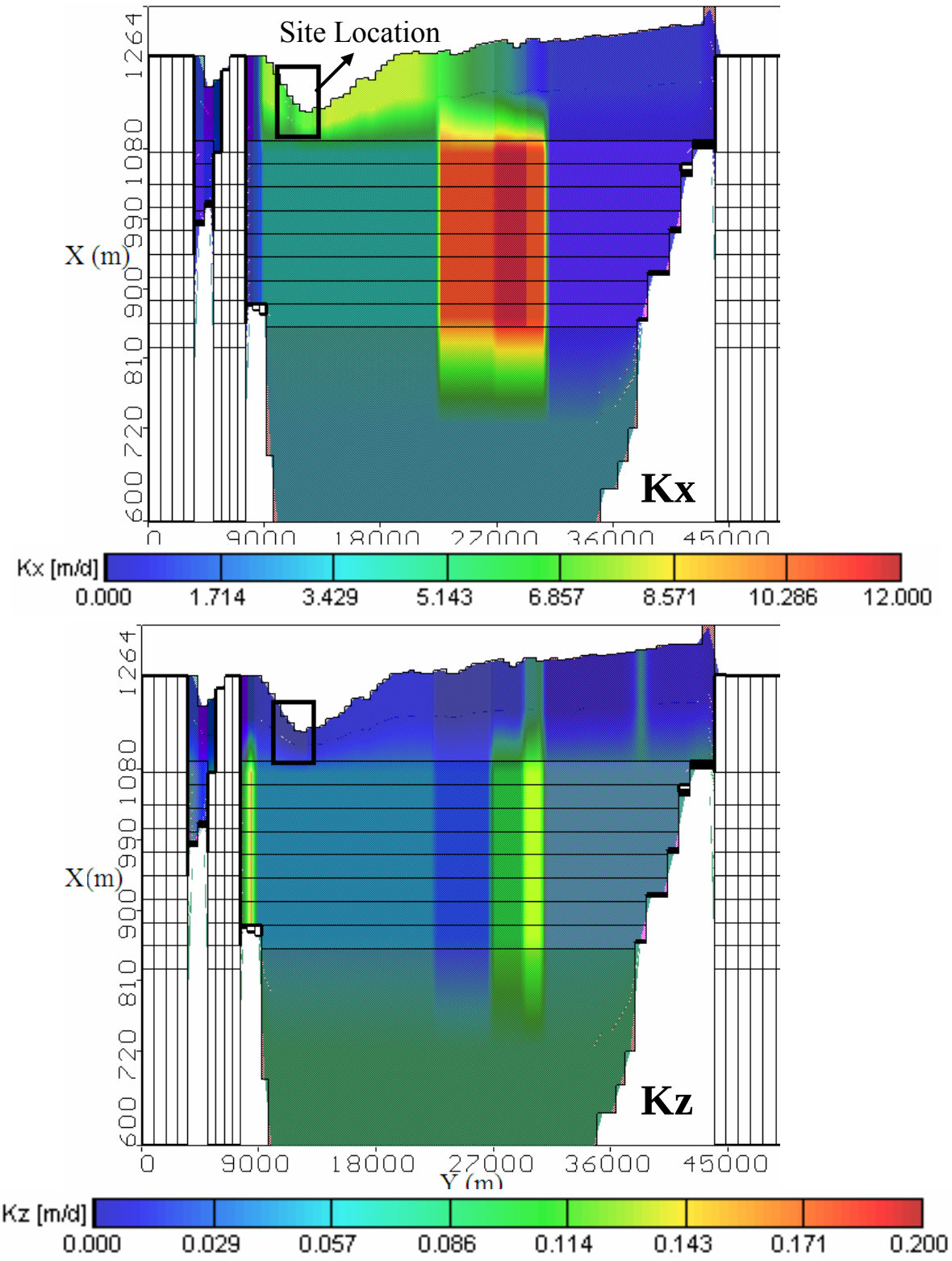

Fig. B- 5. Cross-section at El Paso site 1 showing vertical (K_z) and horizontal (K_x) hydraulic conductivities

EL PASO SITE 2: B-6 to B-10

- **1997, 2020, 2035, and 2050 contaminant plume color maps**
- **East to west vertical hydraulic conductivity (K_z) cross-section at site**
- **East to west horizontal hydraulic conductivity (K_x) cross-section a at site**

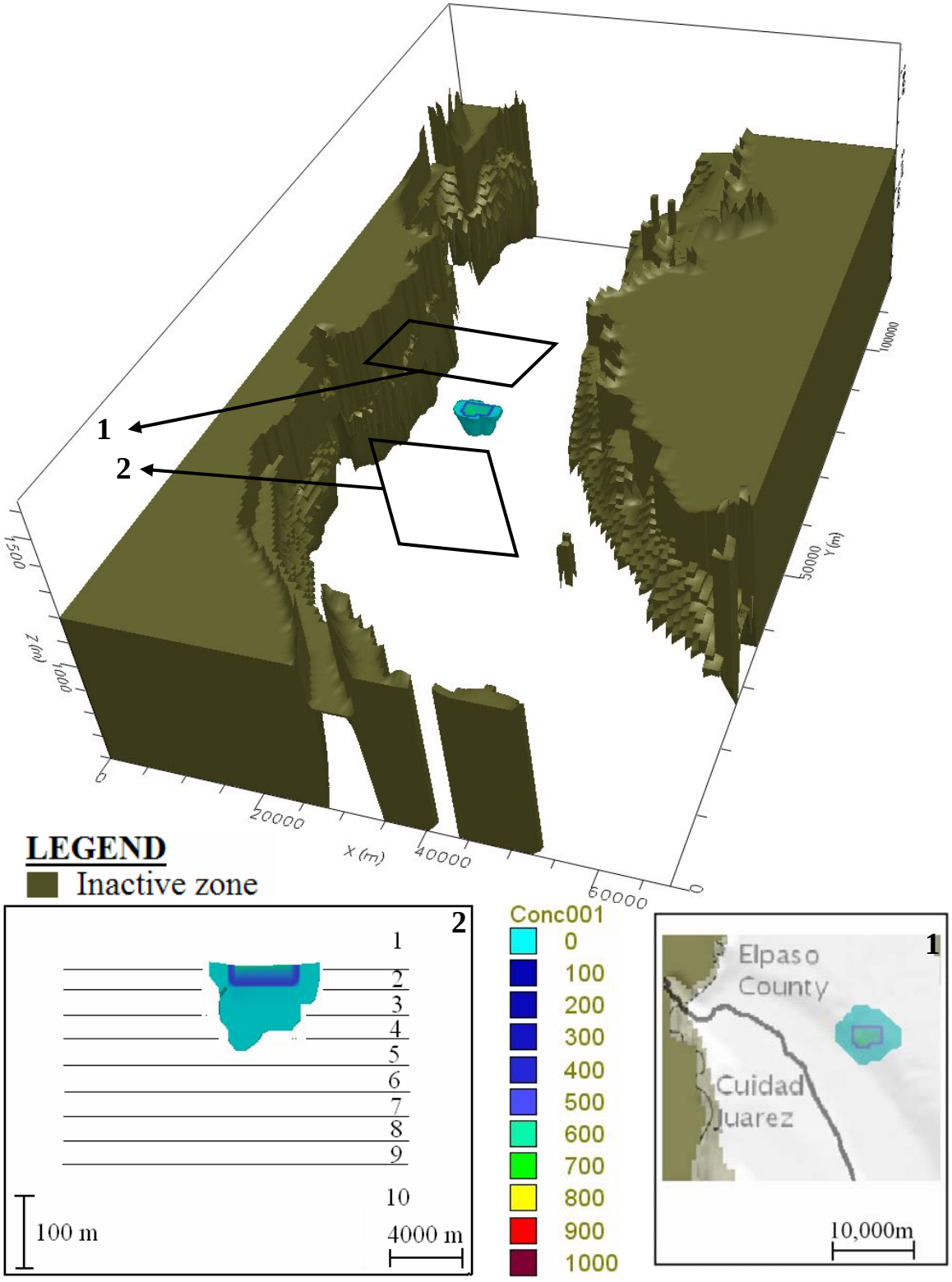

Fig. B- 6. El Paso site 2 concentration (mg/L) plume color map for year 1997

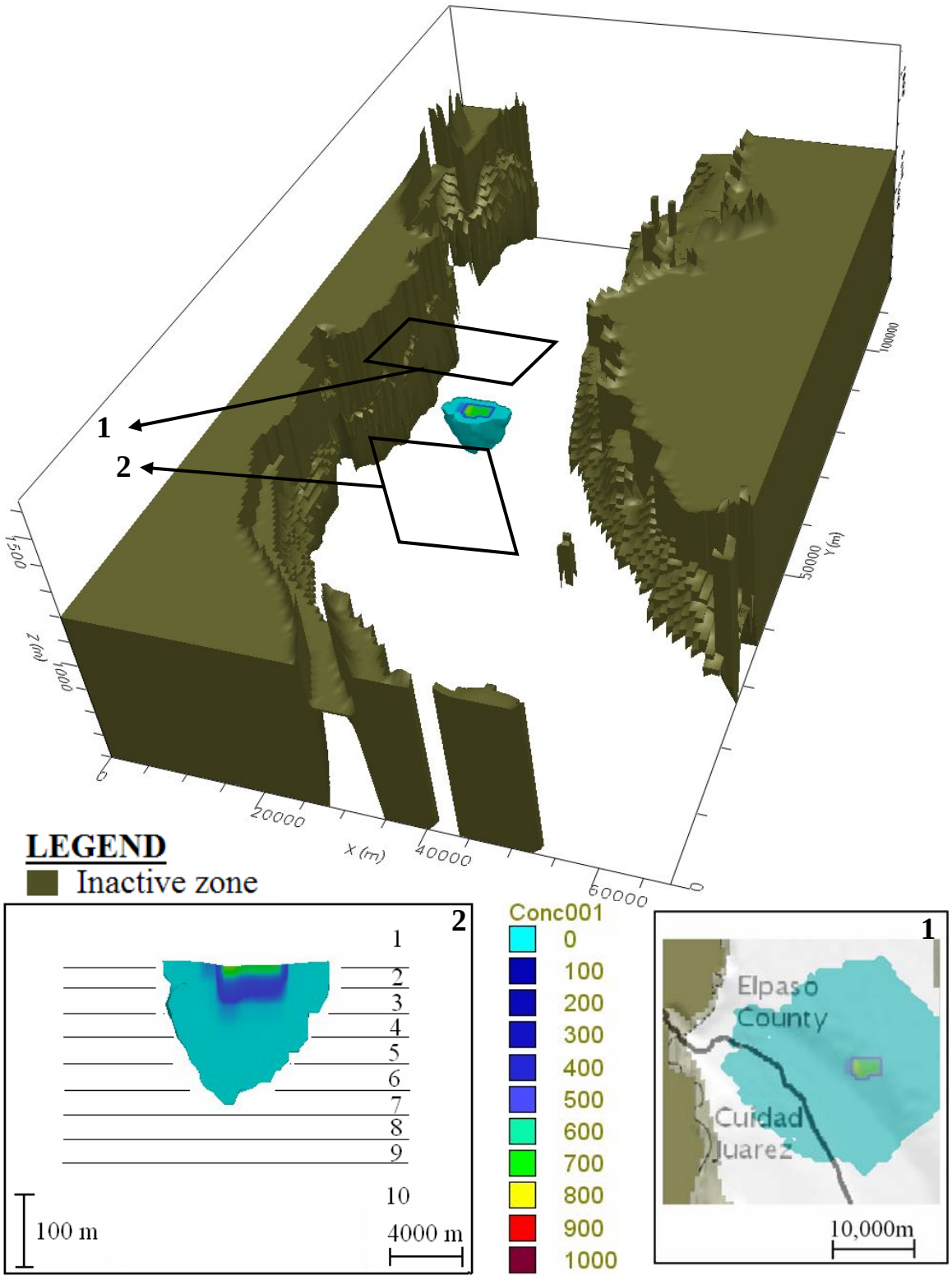

Fig. B- 7. El Paso site 2 concentration (mg/L) plume color map for year 2020

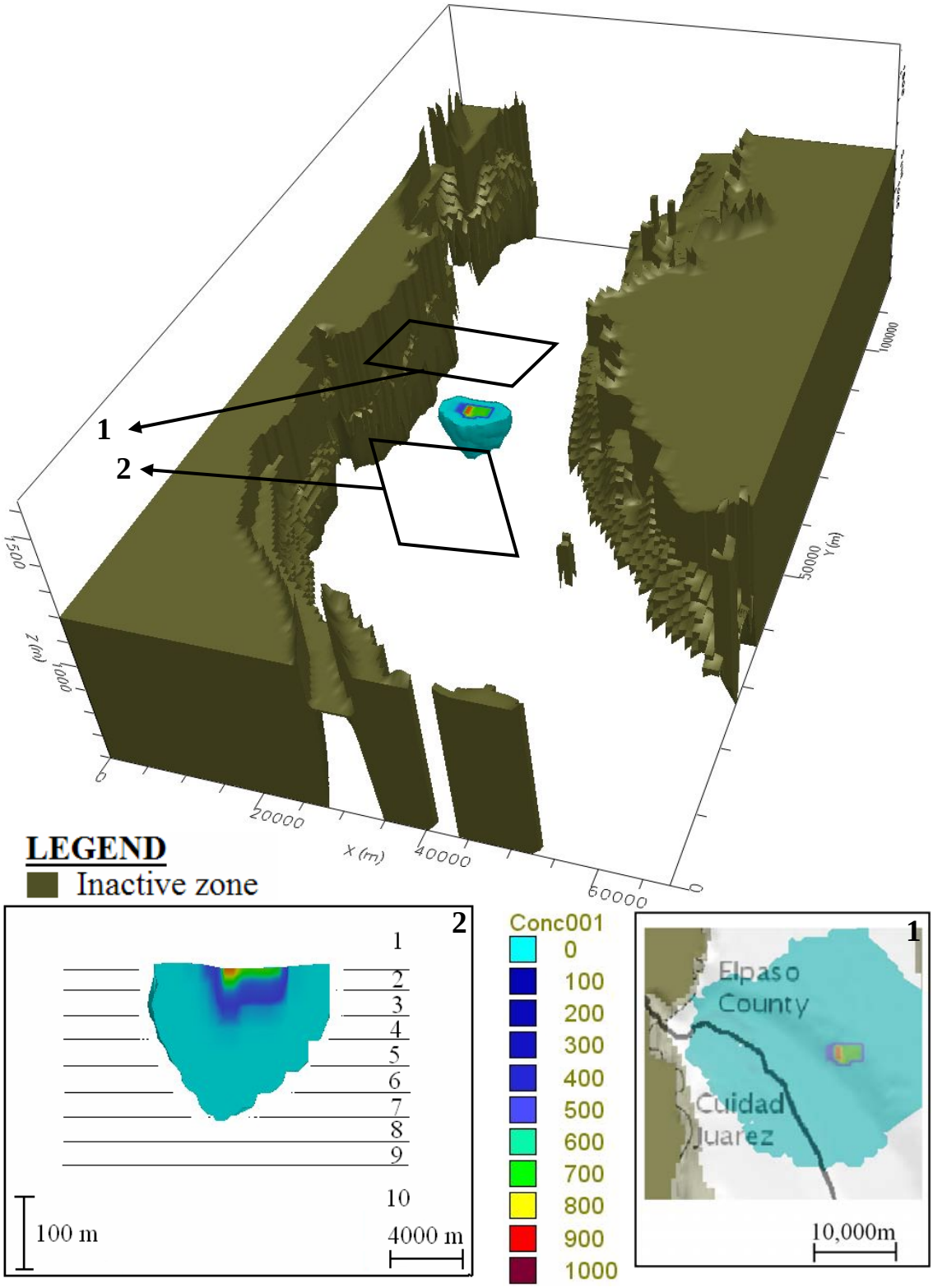

Fig. B- 8. El Paso site 2 concentration (mg/L) plume color map for year 2035

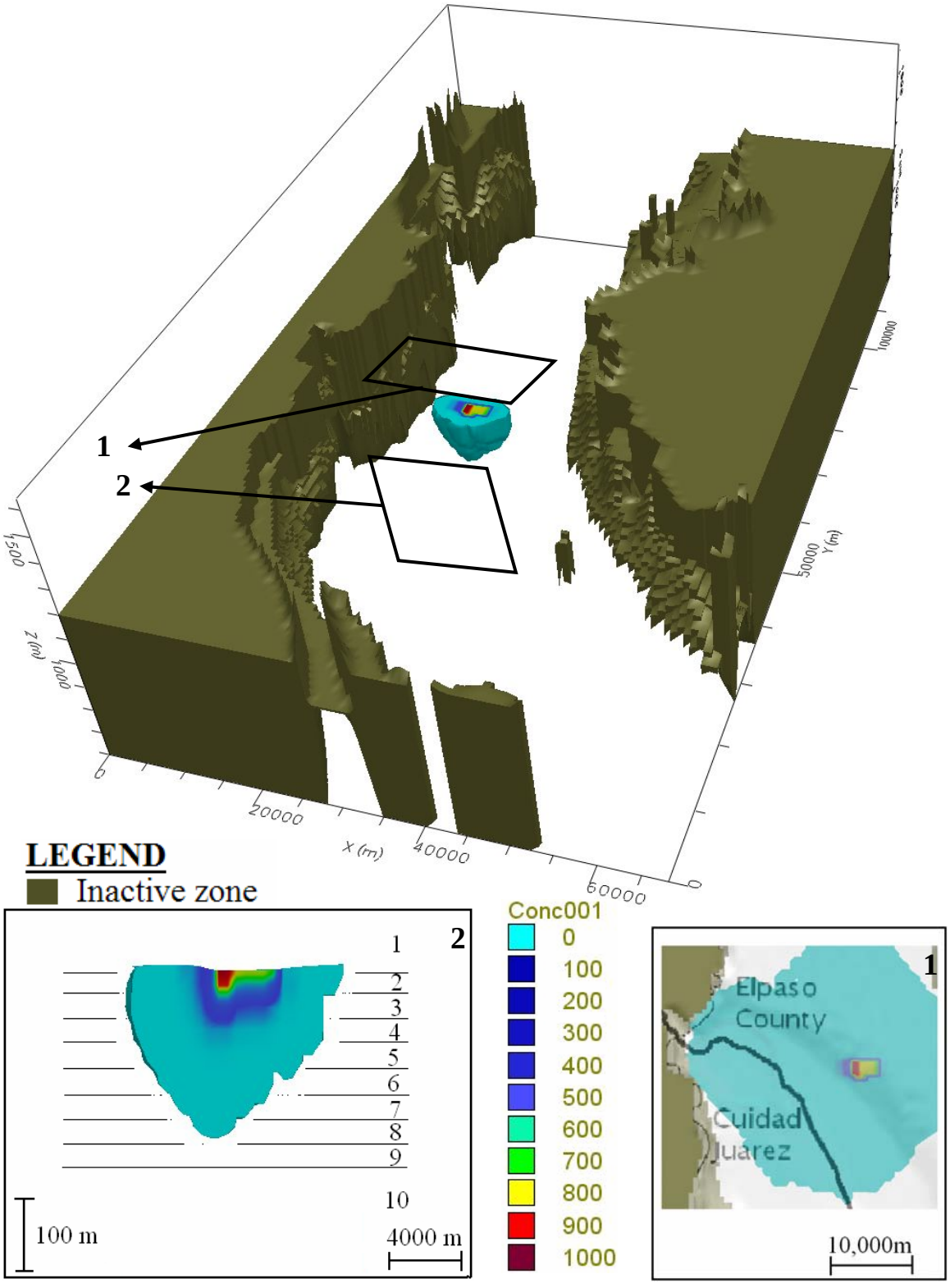

Fig. B- 9. El Paso site 2 concentration (mg/L) plume color map for year 2050

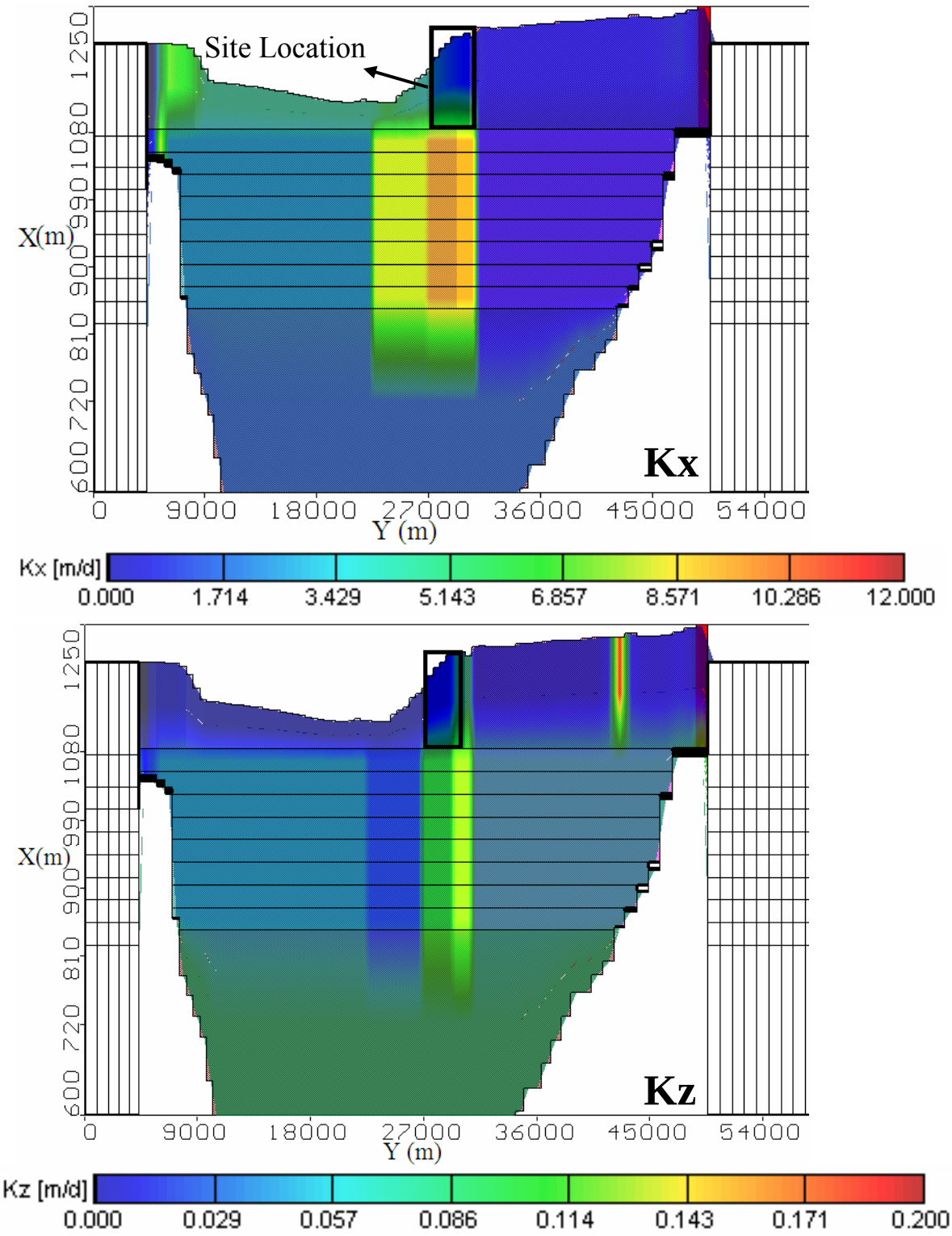

Fig. B- 10. Cross-section at El Paso site 2 showing vertical (K_z) and horizontal (K_x) hydraulic conductivities

EL PASO SITE 3

- **1997, 2020, 2035, and 2050 contaminant plume color maps**
- **East to west vertical hydraulic conductivity (K_z) cross-section at site**
- **East to west horizontal hydraulic conductivity (K_x) cross-section a at site**

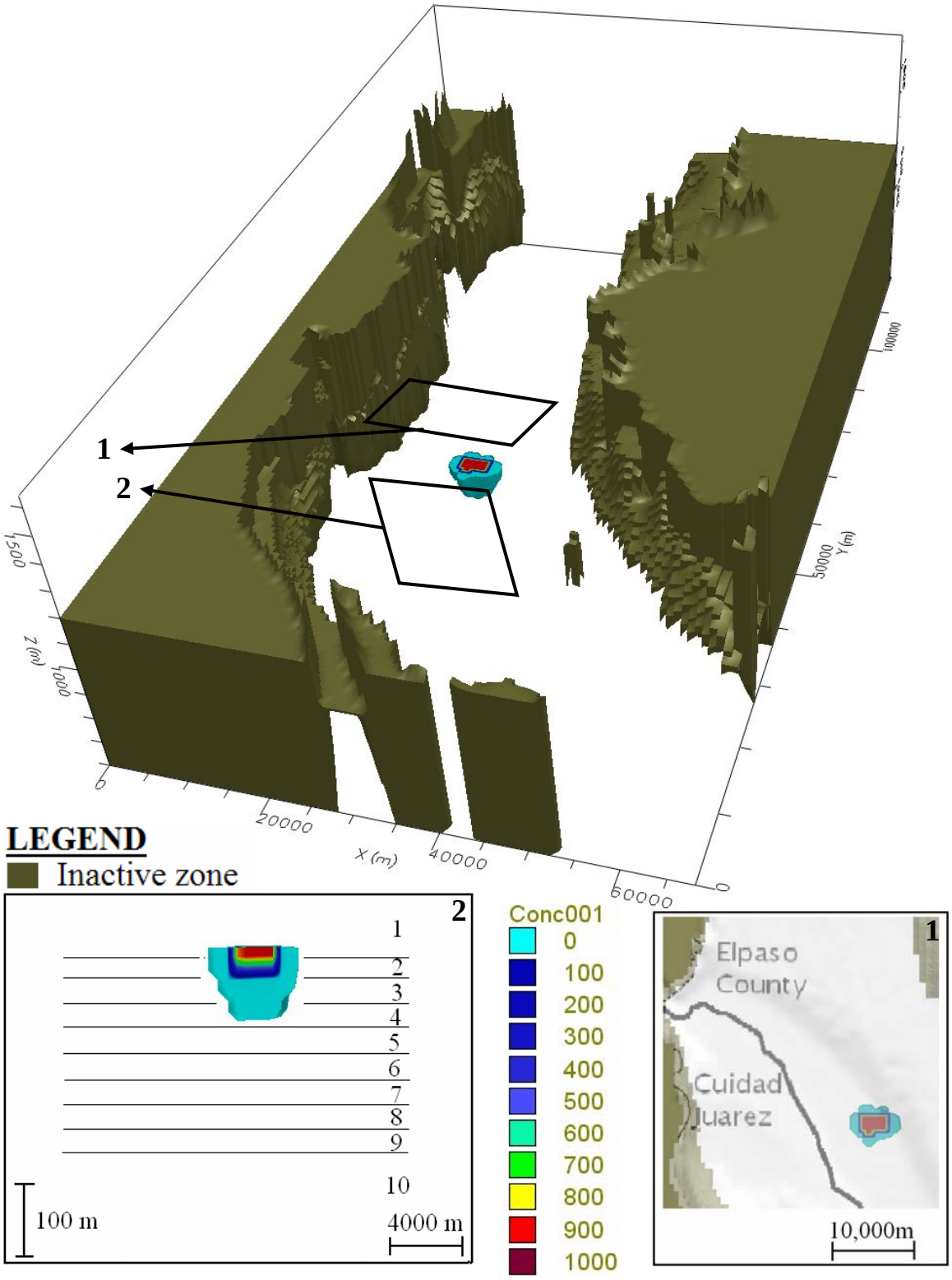

Fig. B- 11. El Paso site 3 concentration (mg/L) plume color map for year 1997

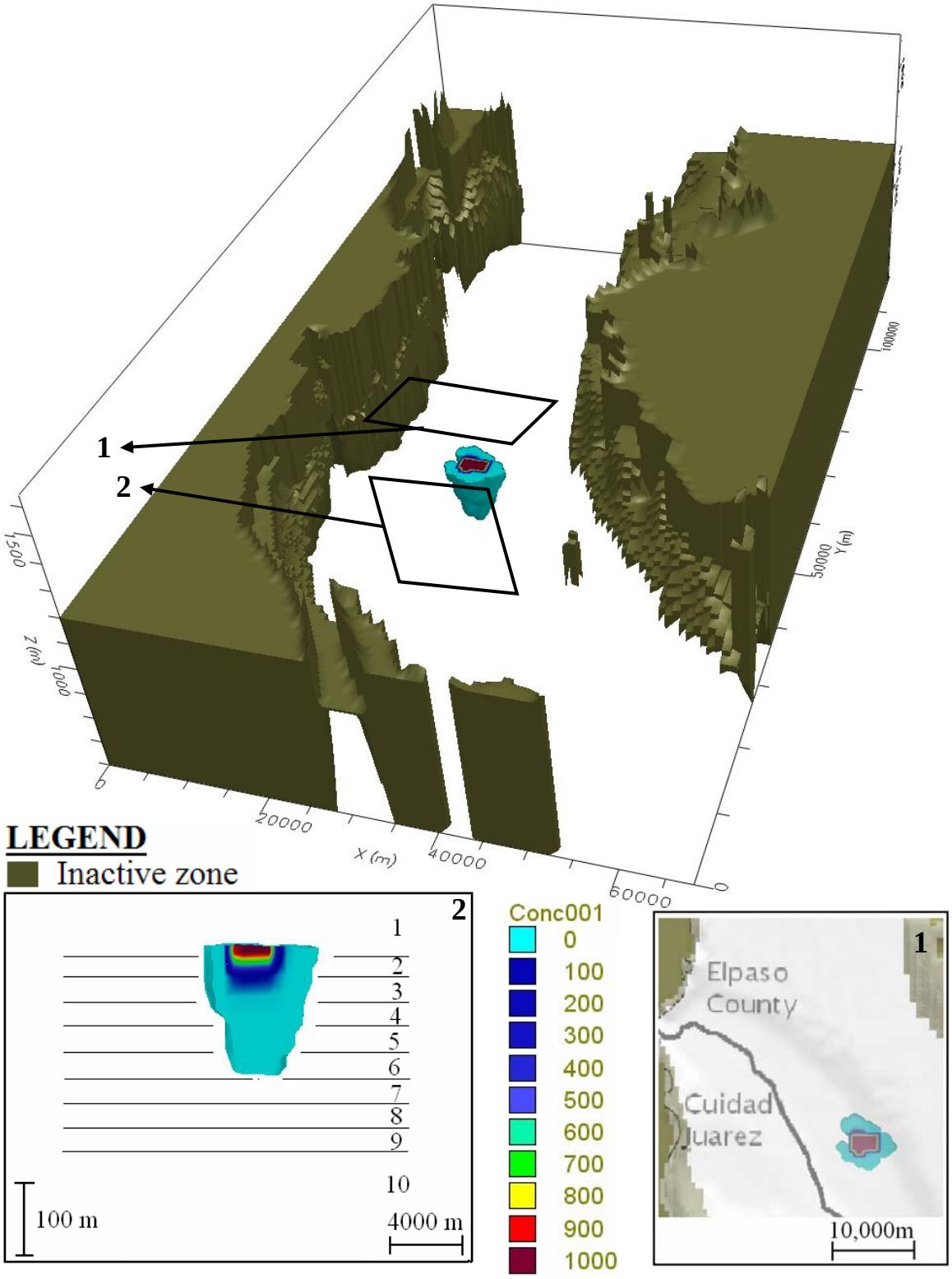

Fig. B- 12. El Paso site 3 concentration (mg/L) plume color map for year 2020

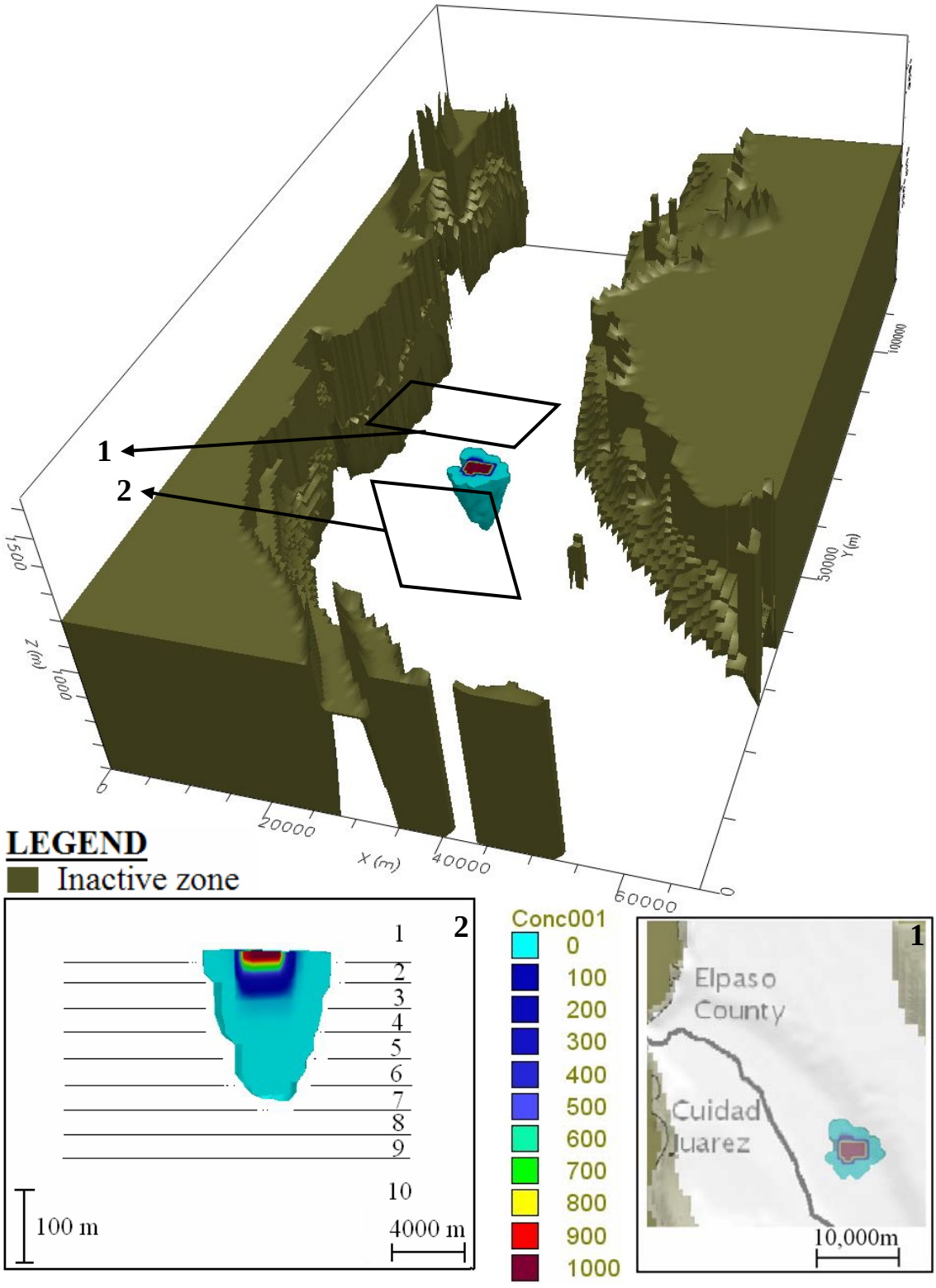

Fig. B- 13. El Paso site 3 concentration (mg/L) plume color map for year 2035

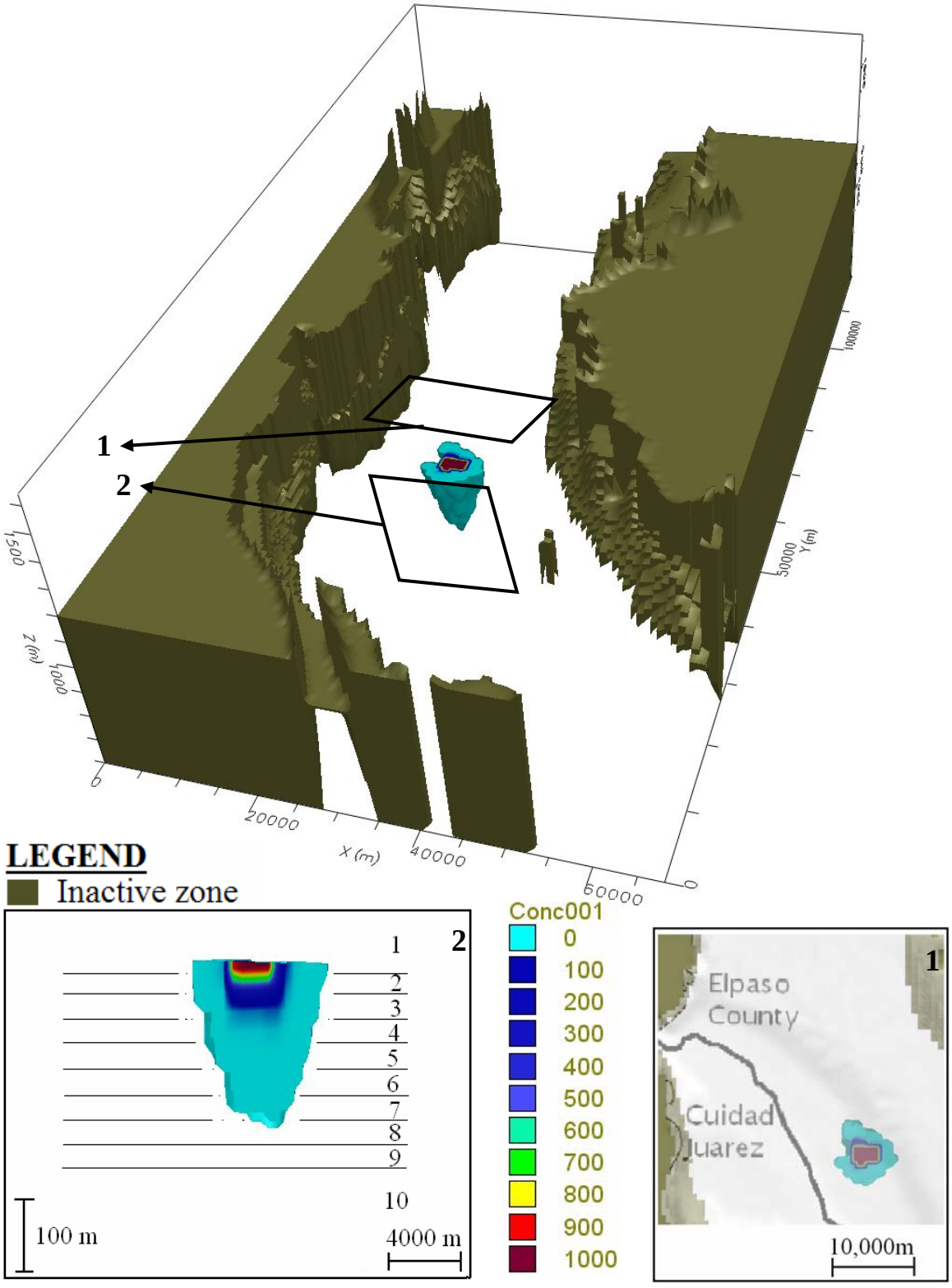

Fig. B- 14. El Paso site 3 concentration (mg/L) plume color map for year 2050

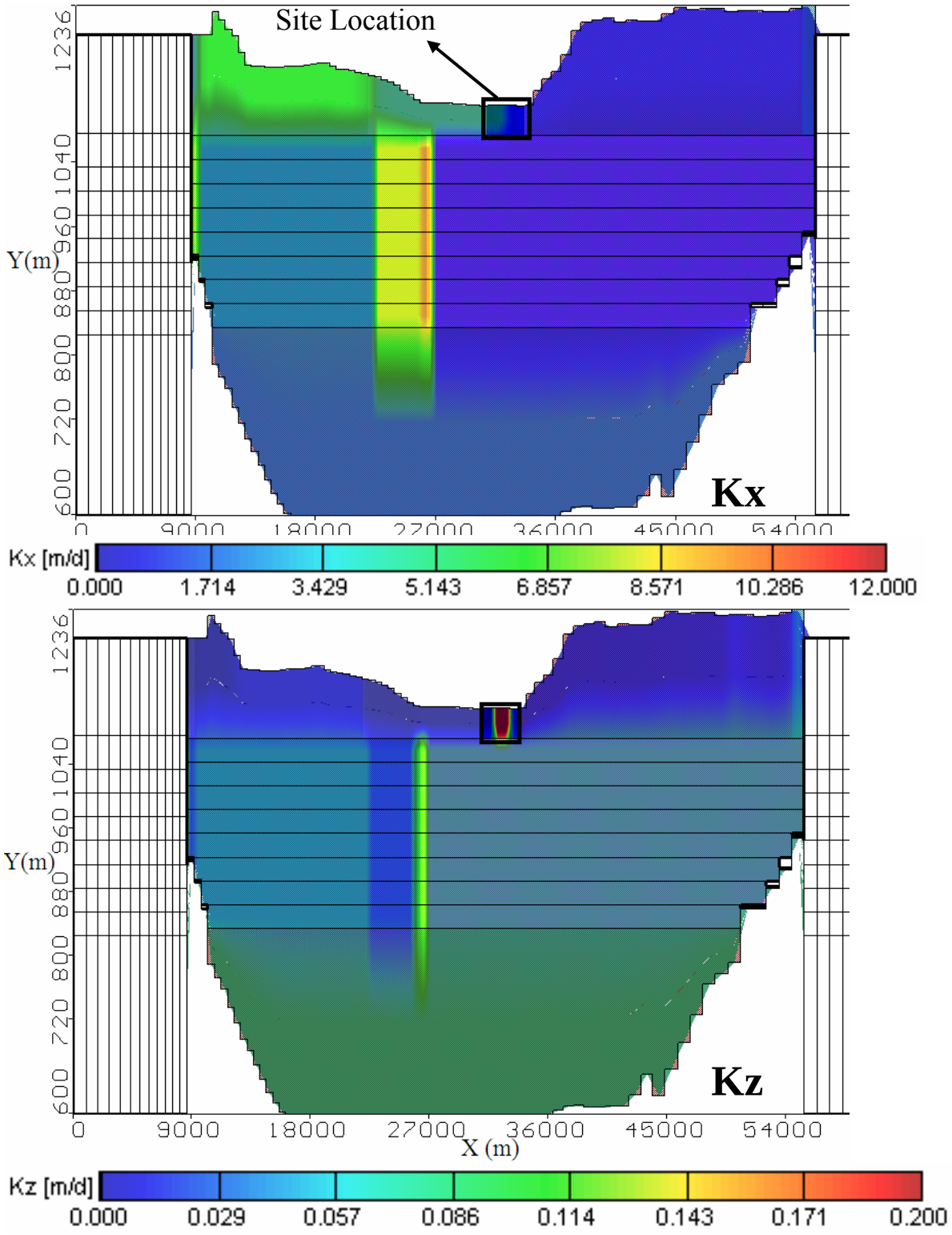

Fig. B- 15. Cross-section at El Paso site 3 showing vertical (K_z) and horizontal (K_x) hydraulic conductivities

JUAREZ SITE 1

- **1997, 2020, 2035, and 2050 contaminant plume color maps**
- **East to west vertical hydraulic conductivity (K_z) cross-section at site**
- **East to west horizontal hydraulic conductivity (K_x) cross-section a at site**

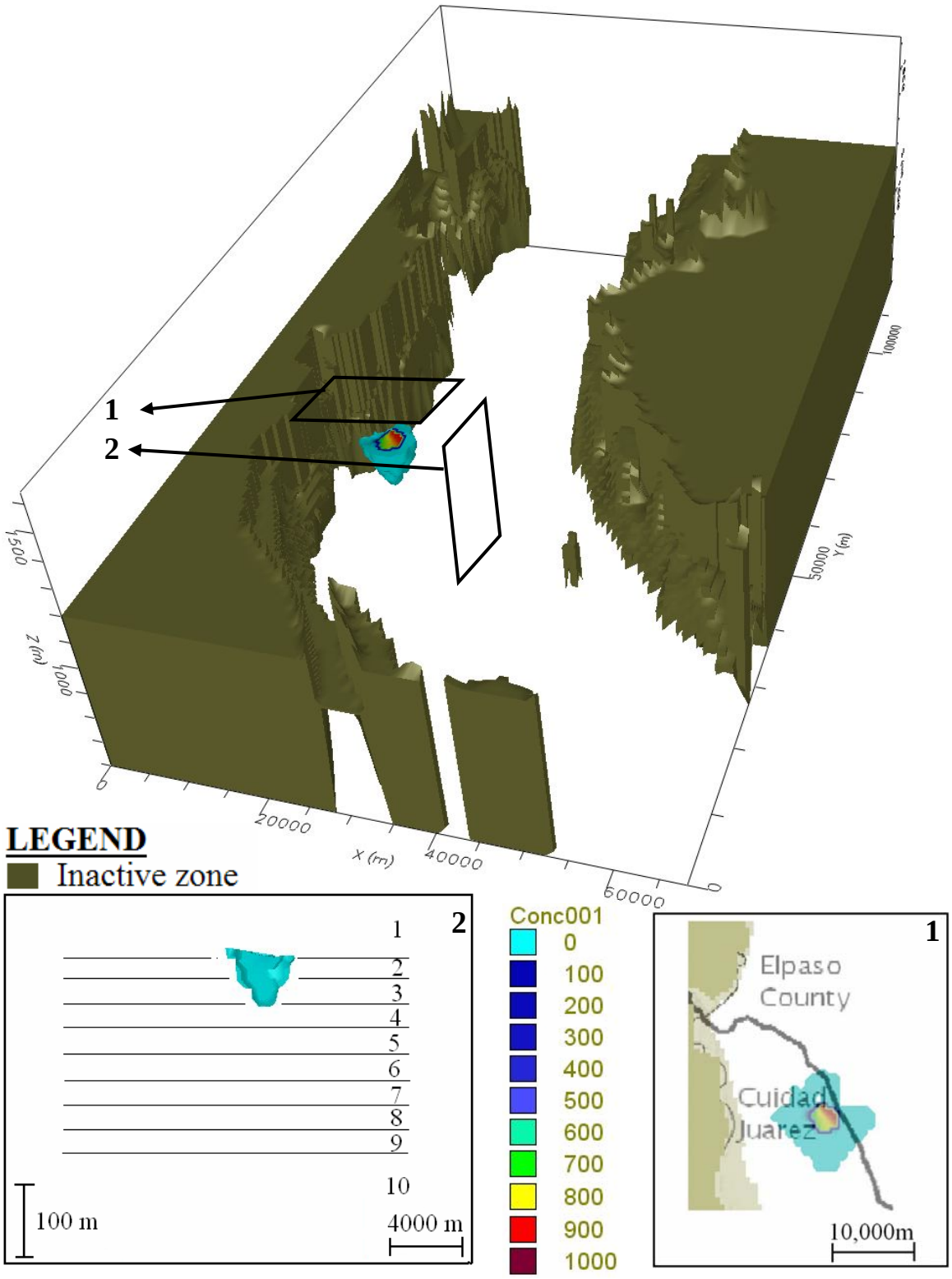

Fig. B- 16. Juarez site 1 concentration (mg/L) plume color map for year 1997

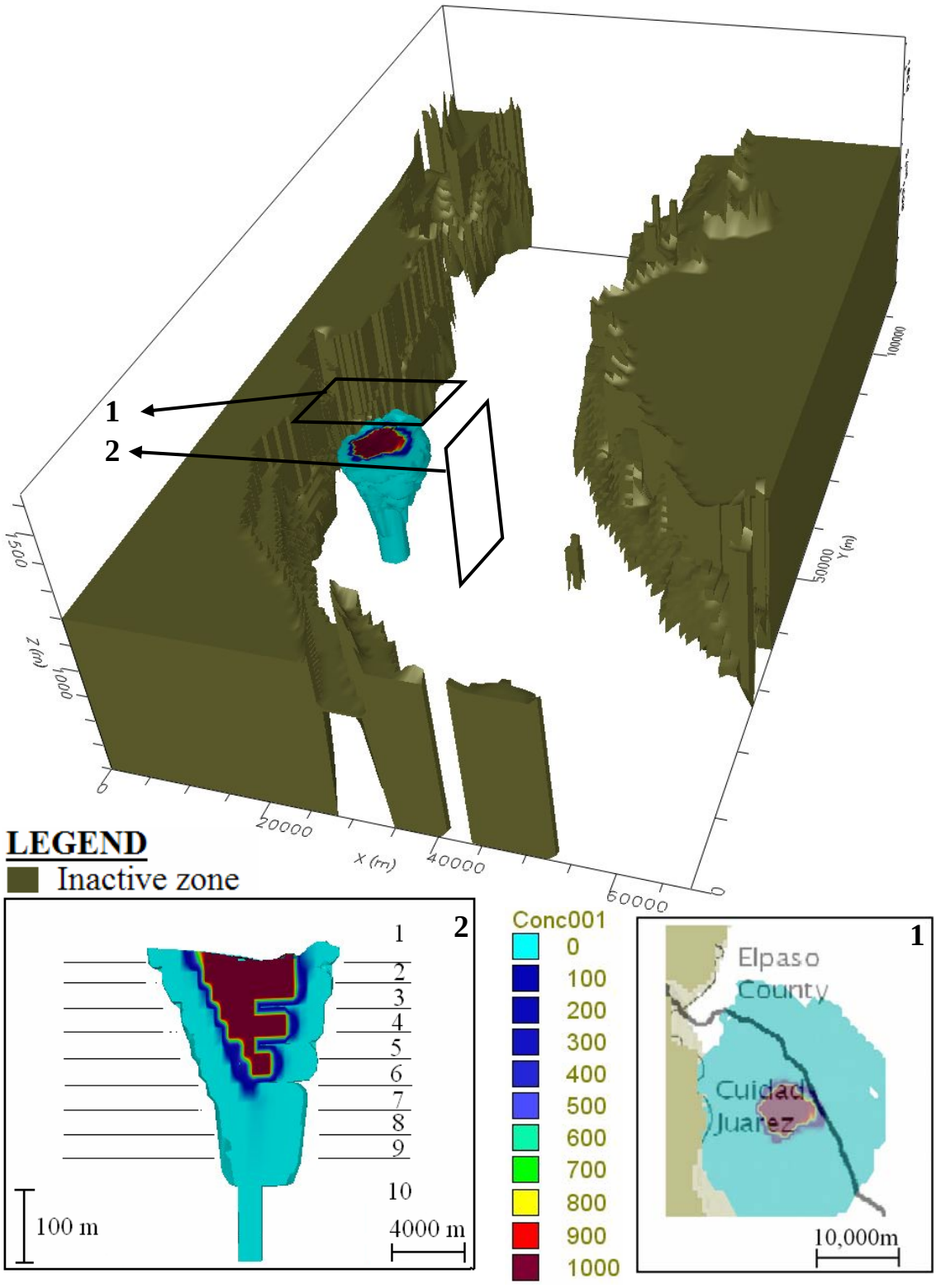

Fig. B- 17. Juarez site 1 concentration (mg/L) plume color map for year 2020

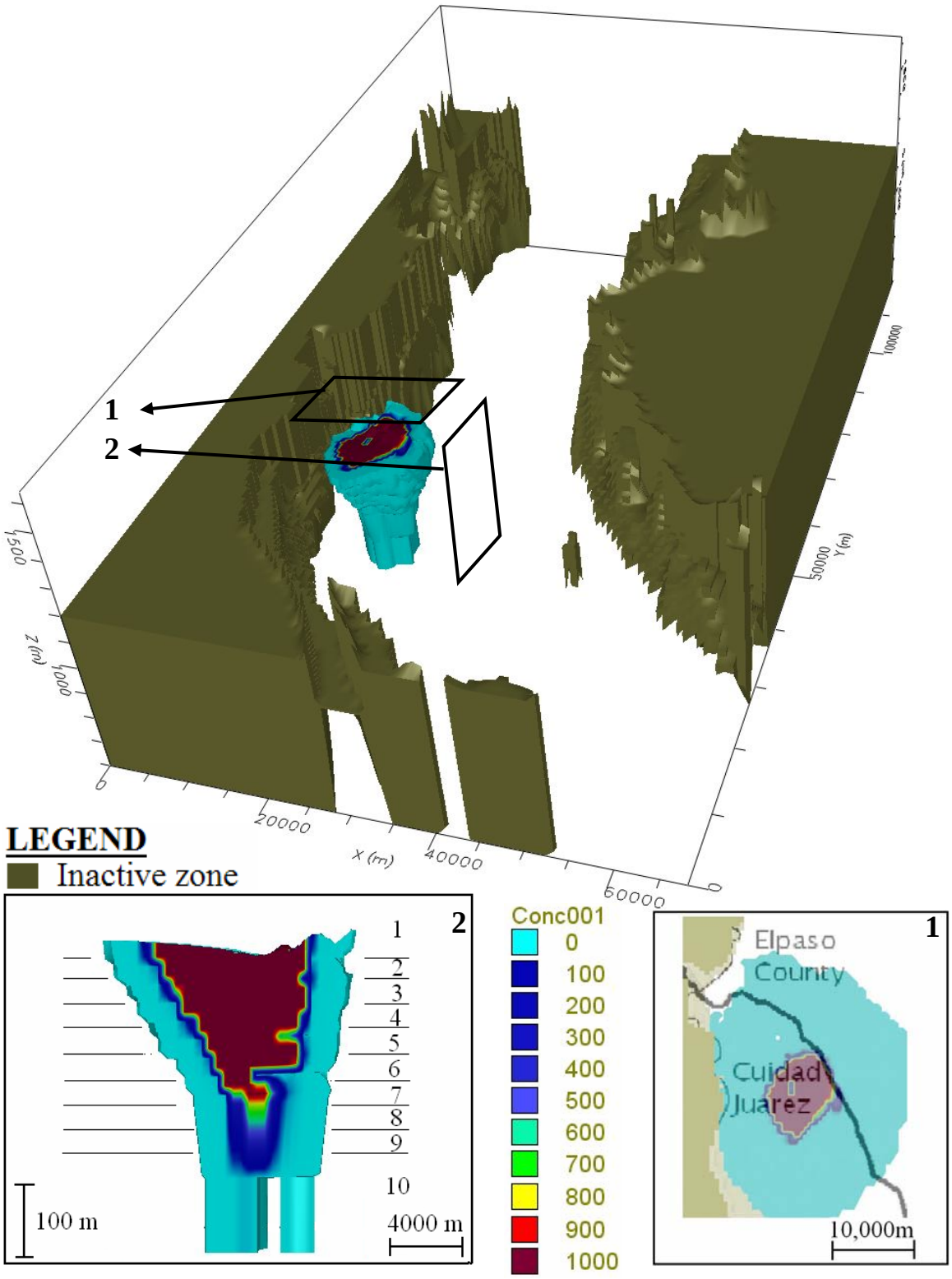

Fig. B- 18. Juarez site 1 concentration (mg/L) plume color map for year 2035

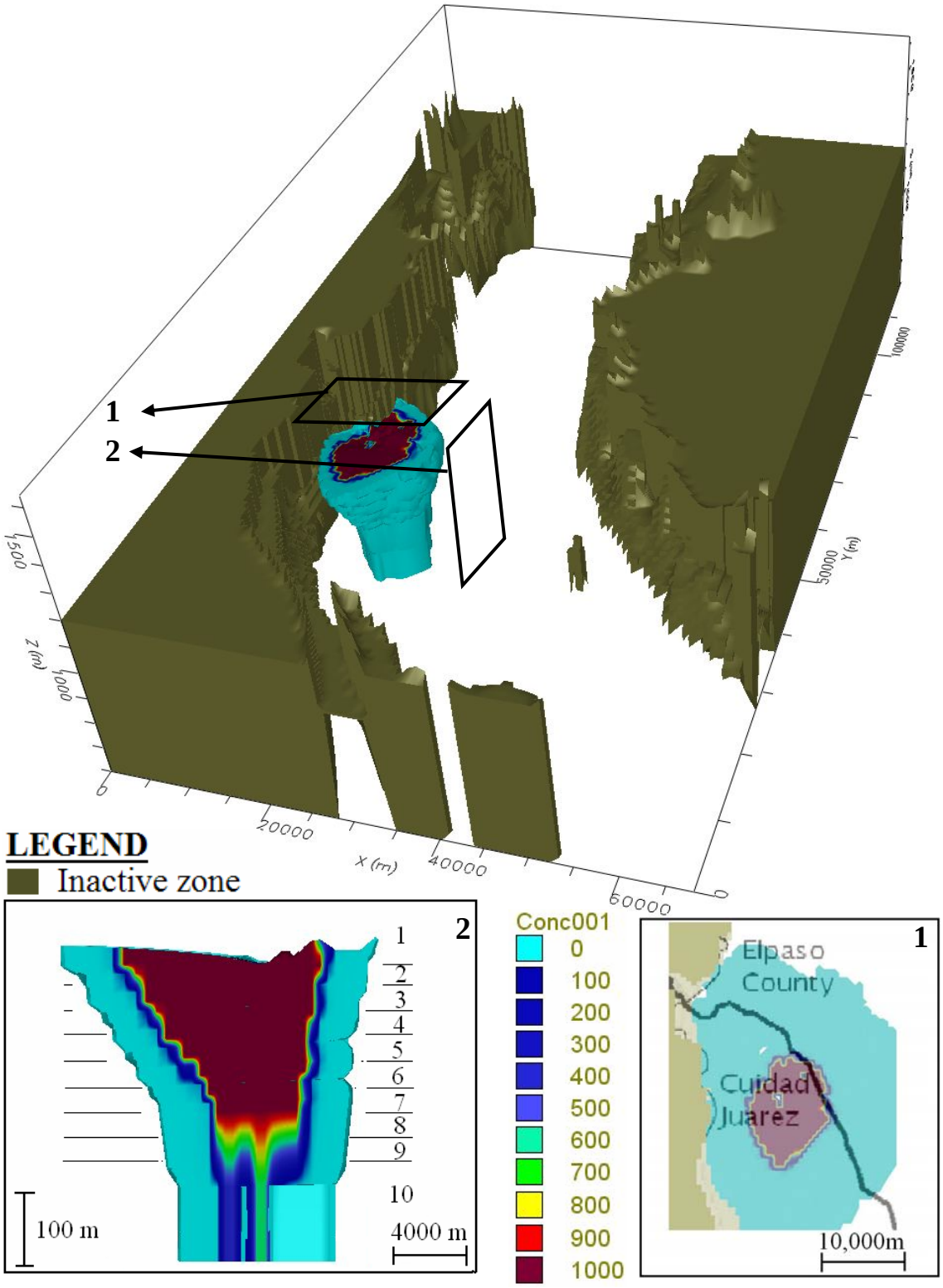

Fig. B- 19. Juarez site 1 concentration (mg/L) plume color map for year 2050

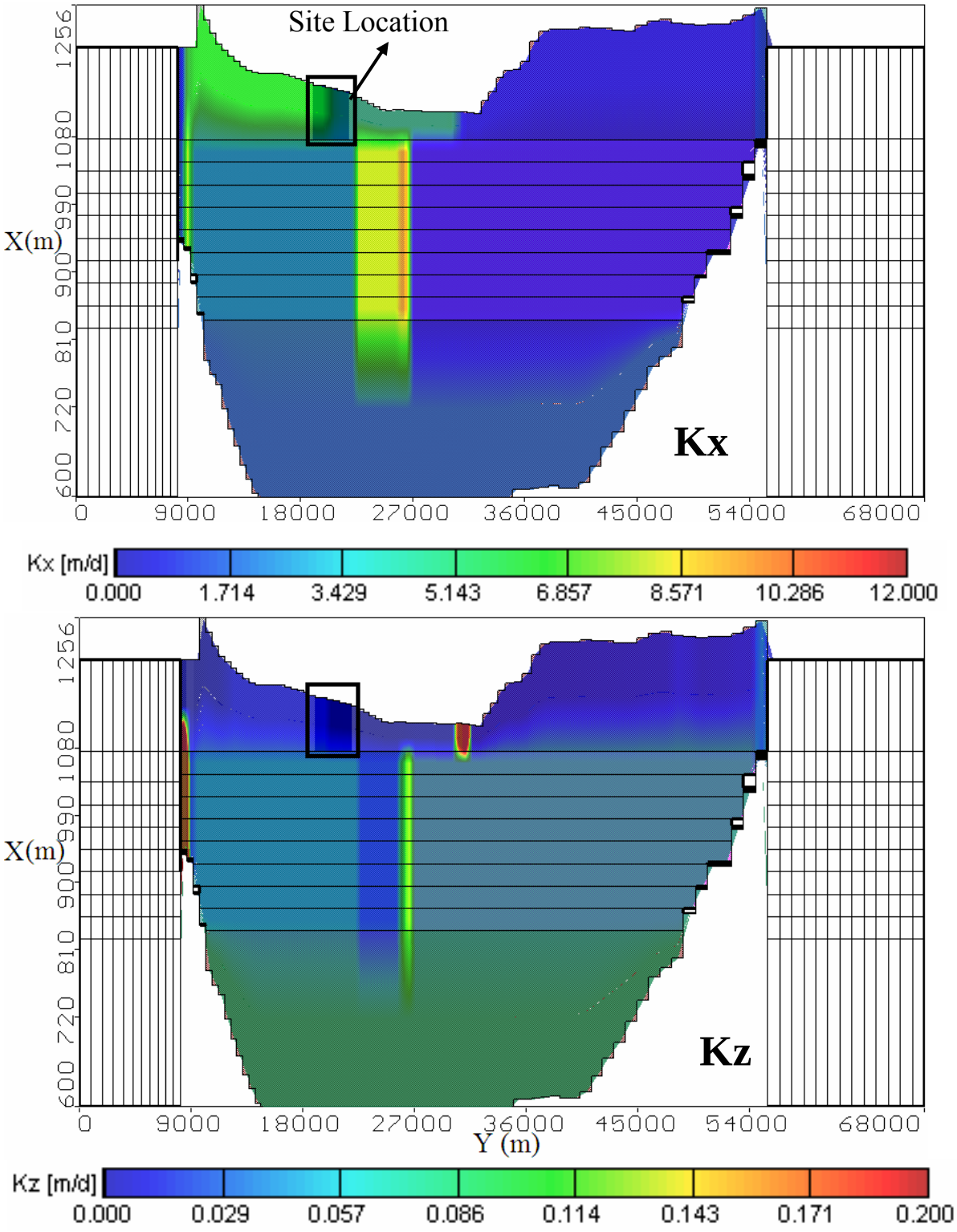

Fig. B- 20. Cross-section at Juarez site 1 showing vertical (K_z) and horizontal (K_x) hydraulic conductivities

JUAREZ SITE 2

- **1997, 2020, 2035, and 2050 contaminant plume color maps**
- **East to west vertical hydraulic conductivity (K_z) cross-section at site**
- **East to west horizontal hydraulic conductivity (K_x) cross-section a at site**

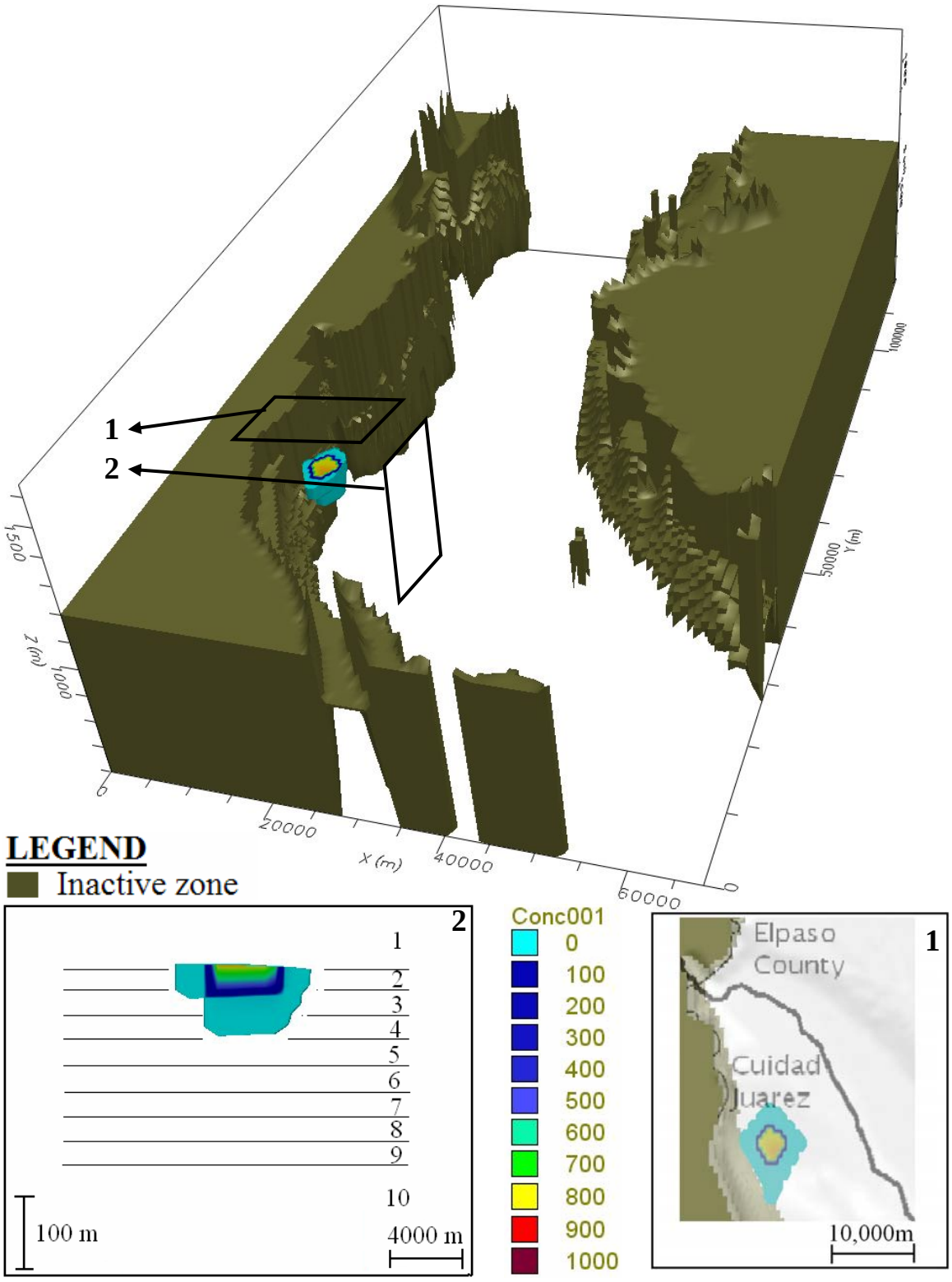

Fig. B- 21. Juarez site 2 concentration (mg/L) plume color map for year 1997

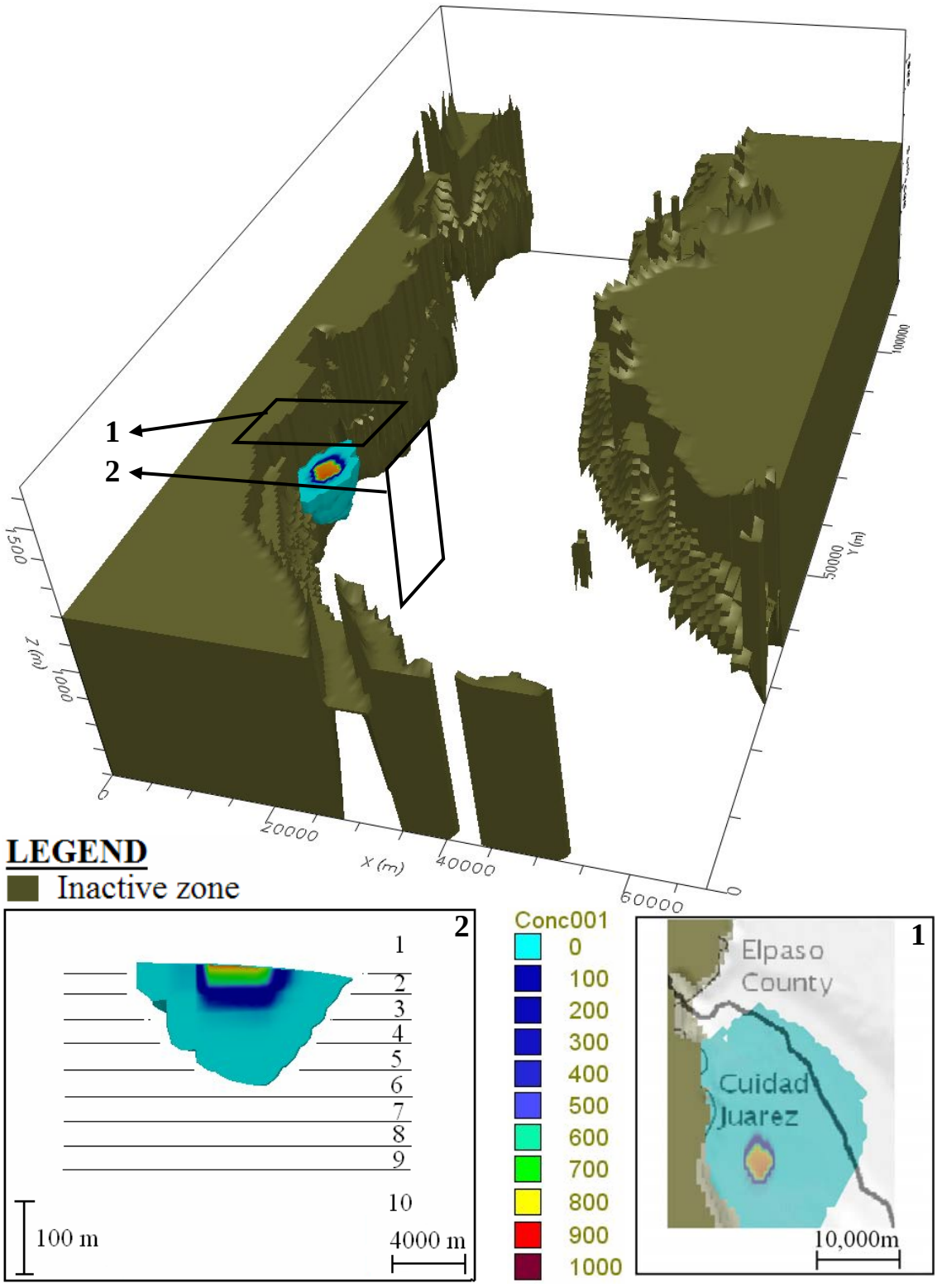

Fig. B- 22. Juarez site 2 concentration (mg/L) plume color map for year 2020

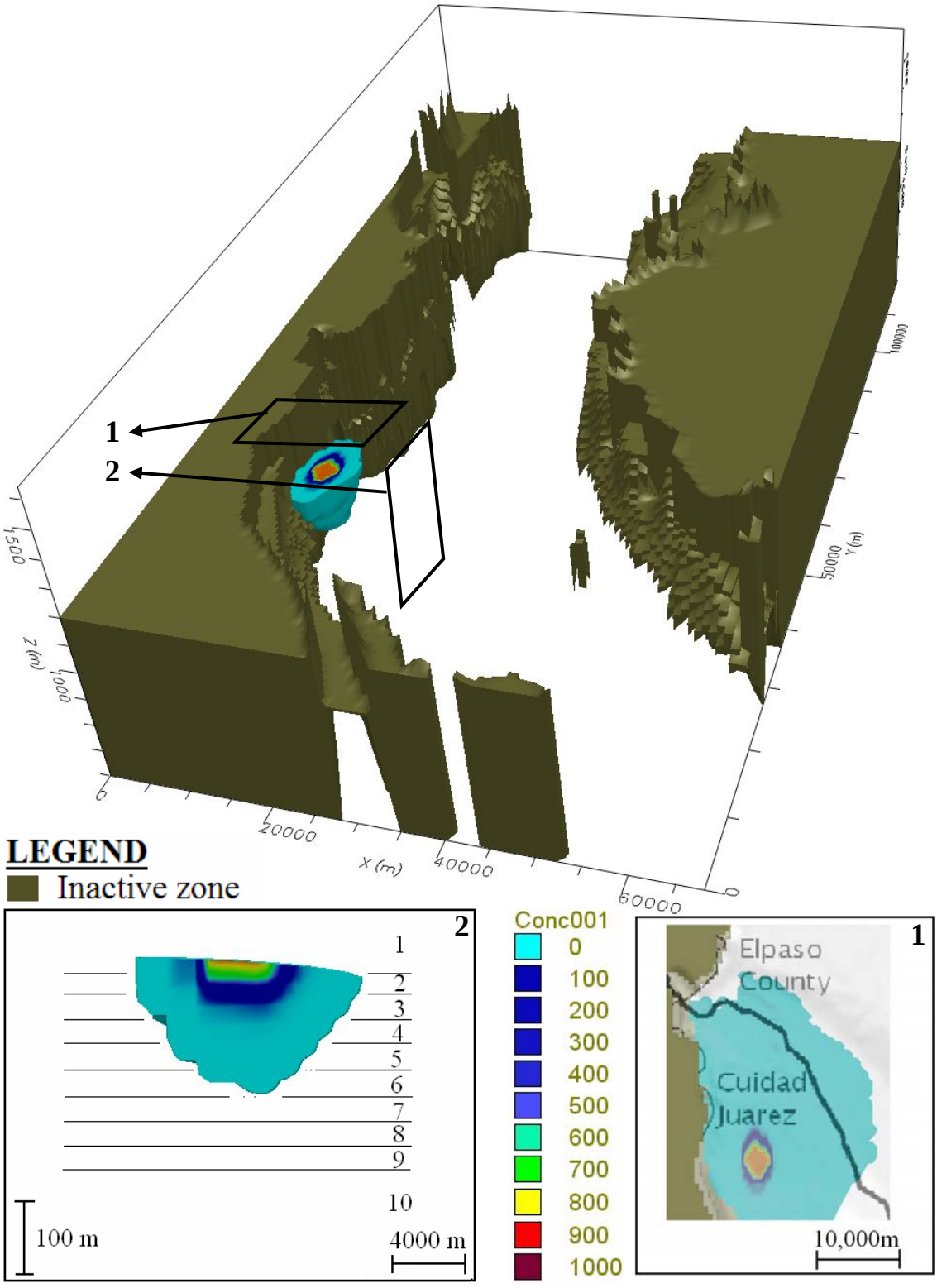

Fig. B- 23. Juarez site 2 concentration (mg/L) plume color map for year 2035

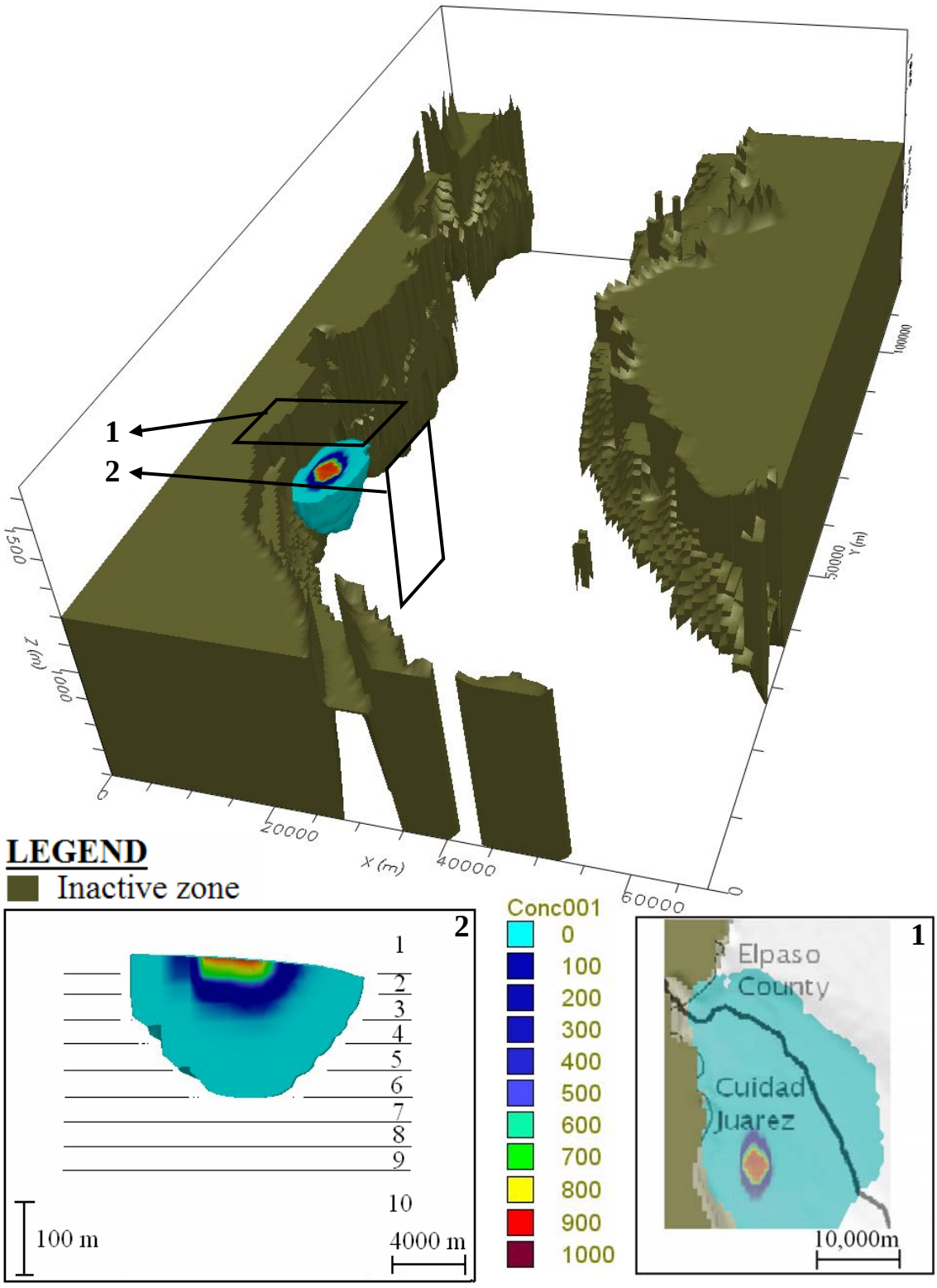

Fig. B- 24. Juarez site 2 concentration (mg/L) plume color map for year 2050

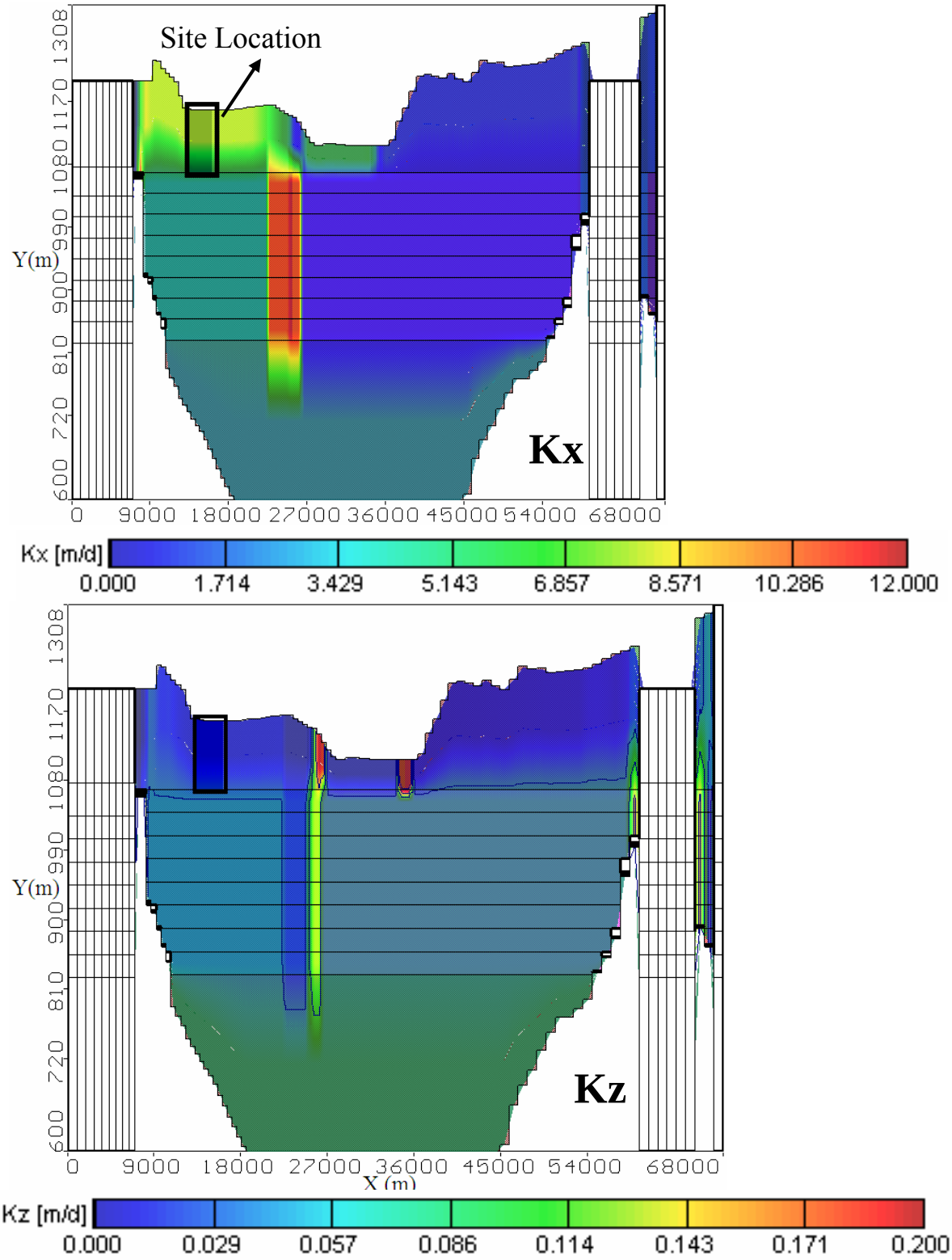

Fig. B- 25. Cross-section at Juarez site 2 showing vertical (K_z) and horizontal (K_x) hydraulic conductivities

APPENDIX C

VELOCITY DIRECTION PROFILES

1997 VELOCITY DIRECTION PROFILES: LAYER 1, 2 AND 3

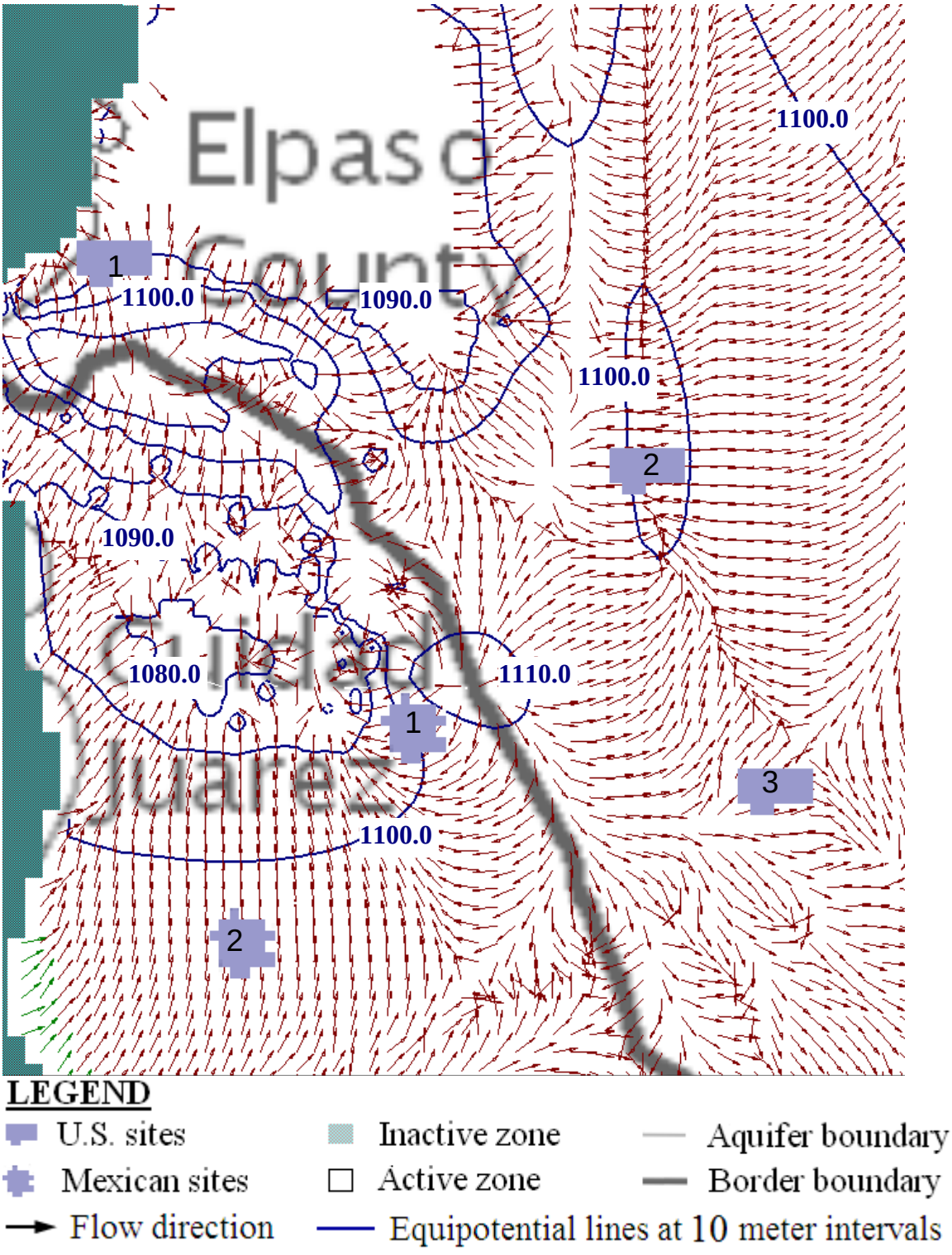

Fig. C- 1. Year 1997 heads and flow velocity direction for model layer 1

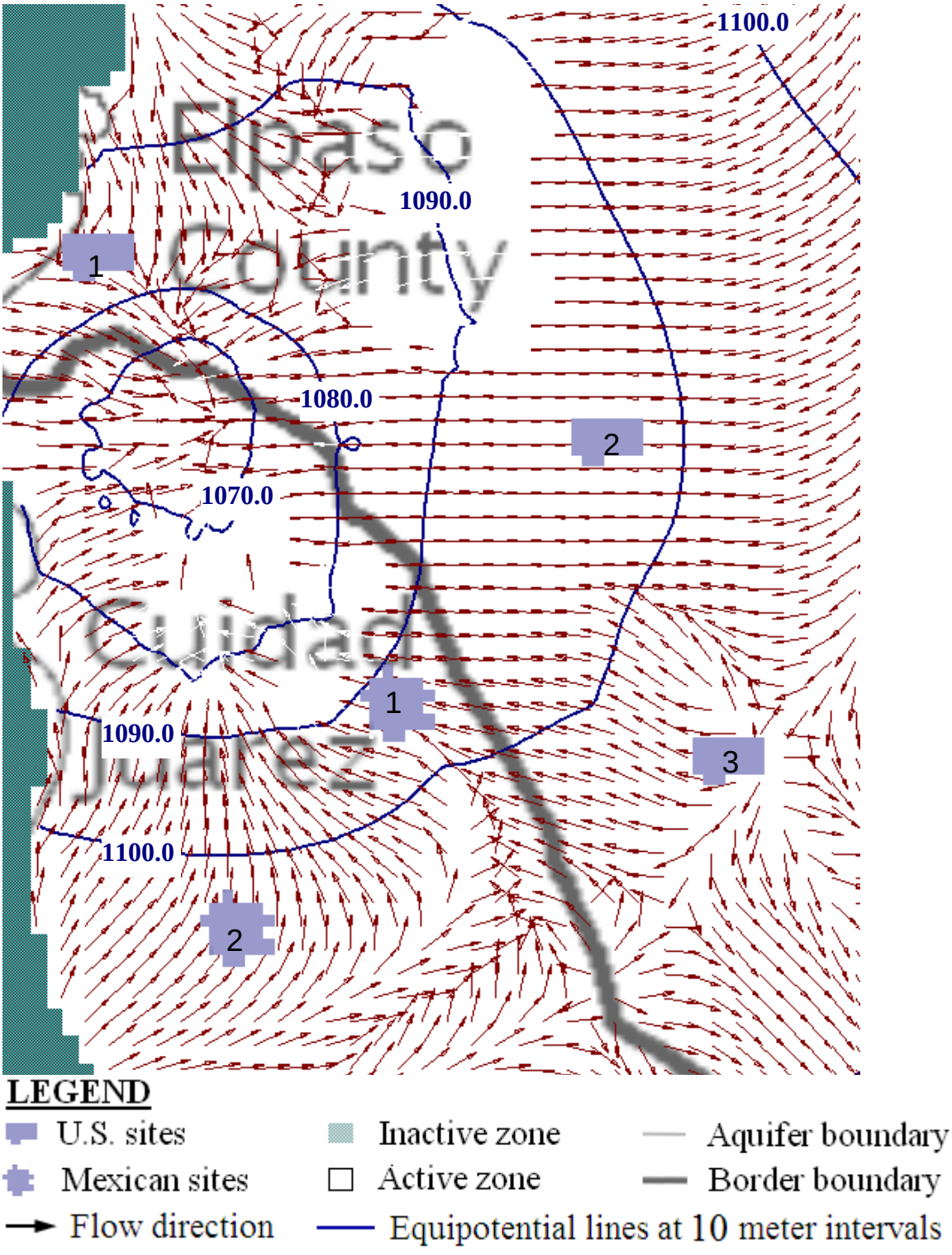

Fig. C- 2. Year 1997 heads and flow velocity direction for model layer 2

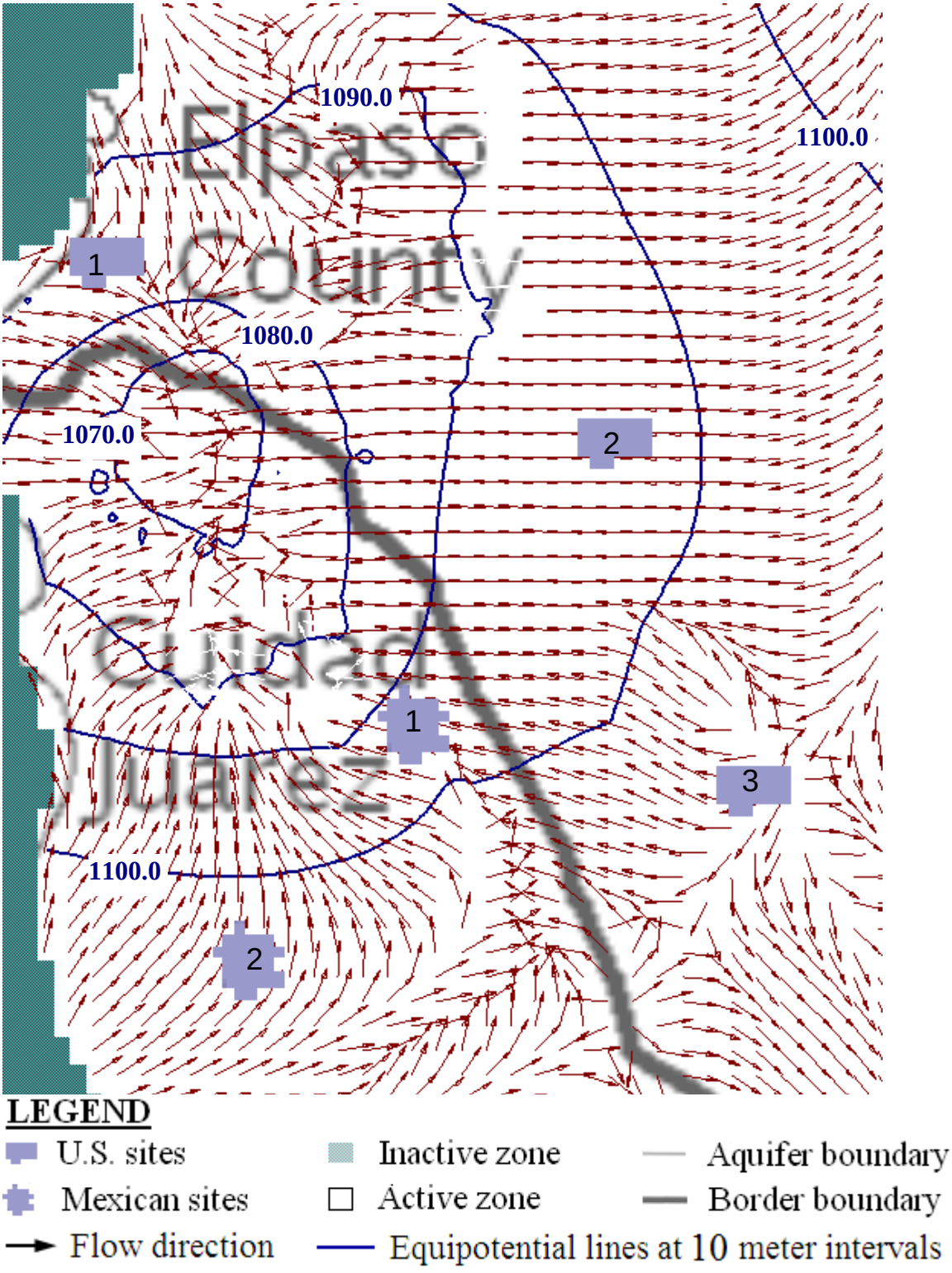

Fig. C- 3. Year 1997 heads and flow velocity direction for model layer 3

2025 VELOCITY DIRECTION PROFILES: LAYER 1, 2 AND 3

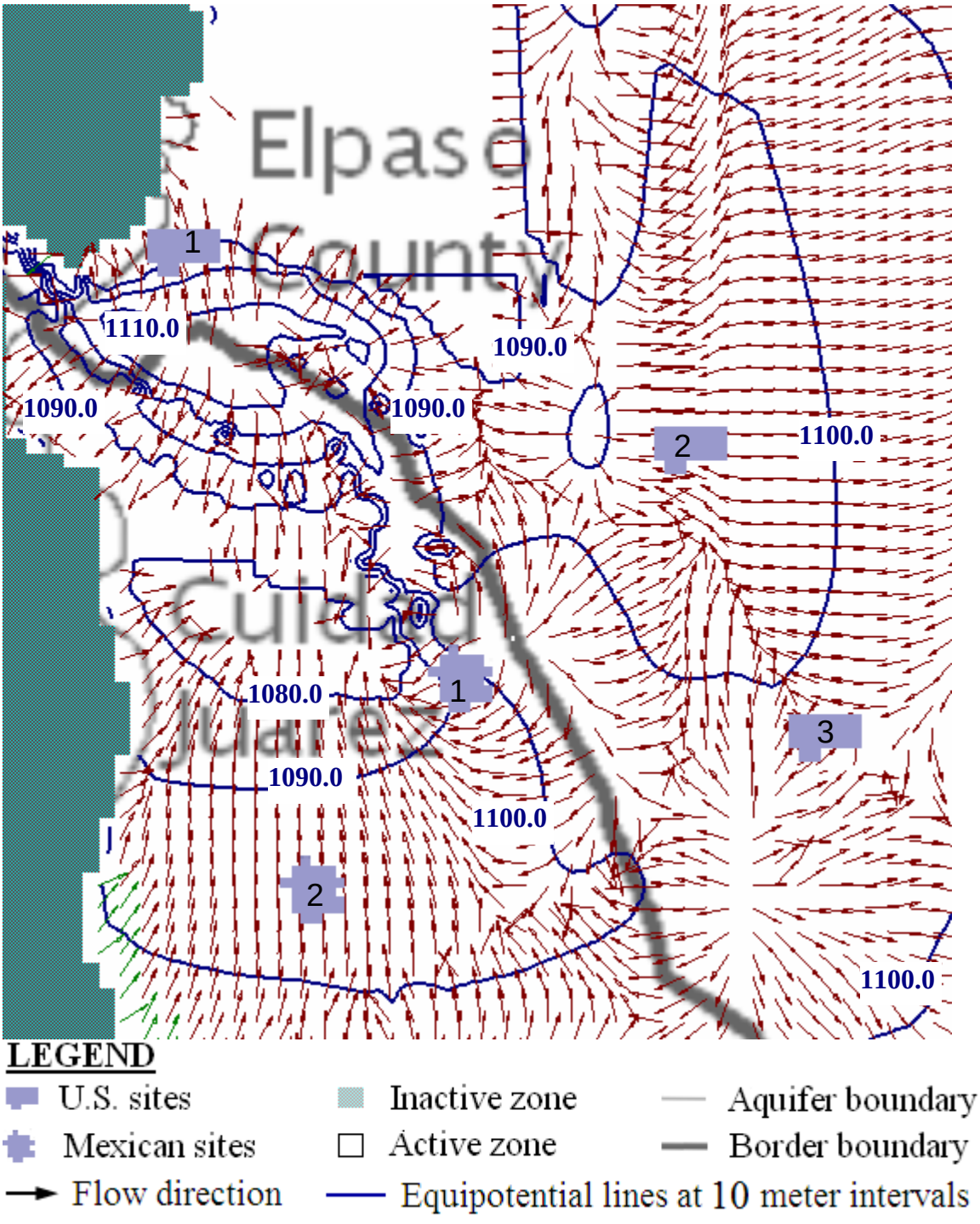

Fig. C- 4. Year 2025 heads and flow velocity direction for model layer 1

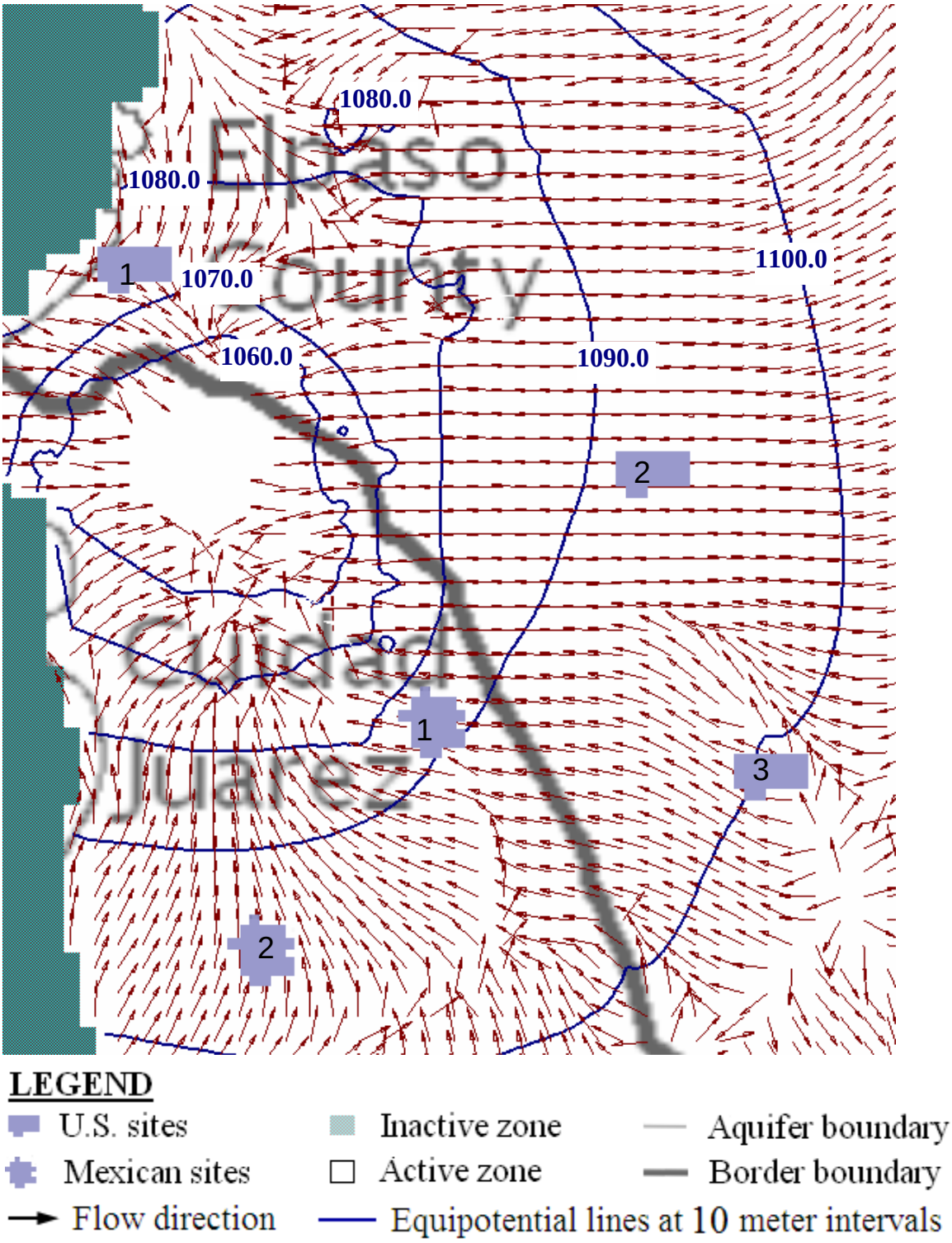

Fig. C- 5. Year 2025 heads and flow velocity direction for model layer 2

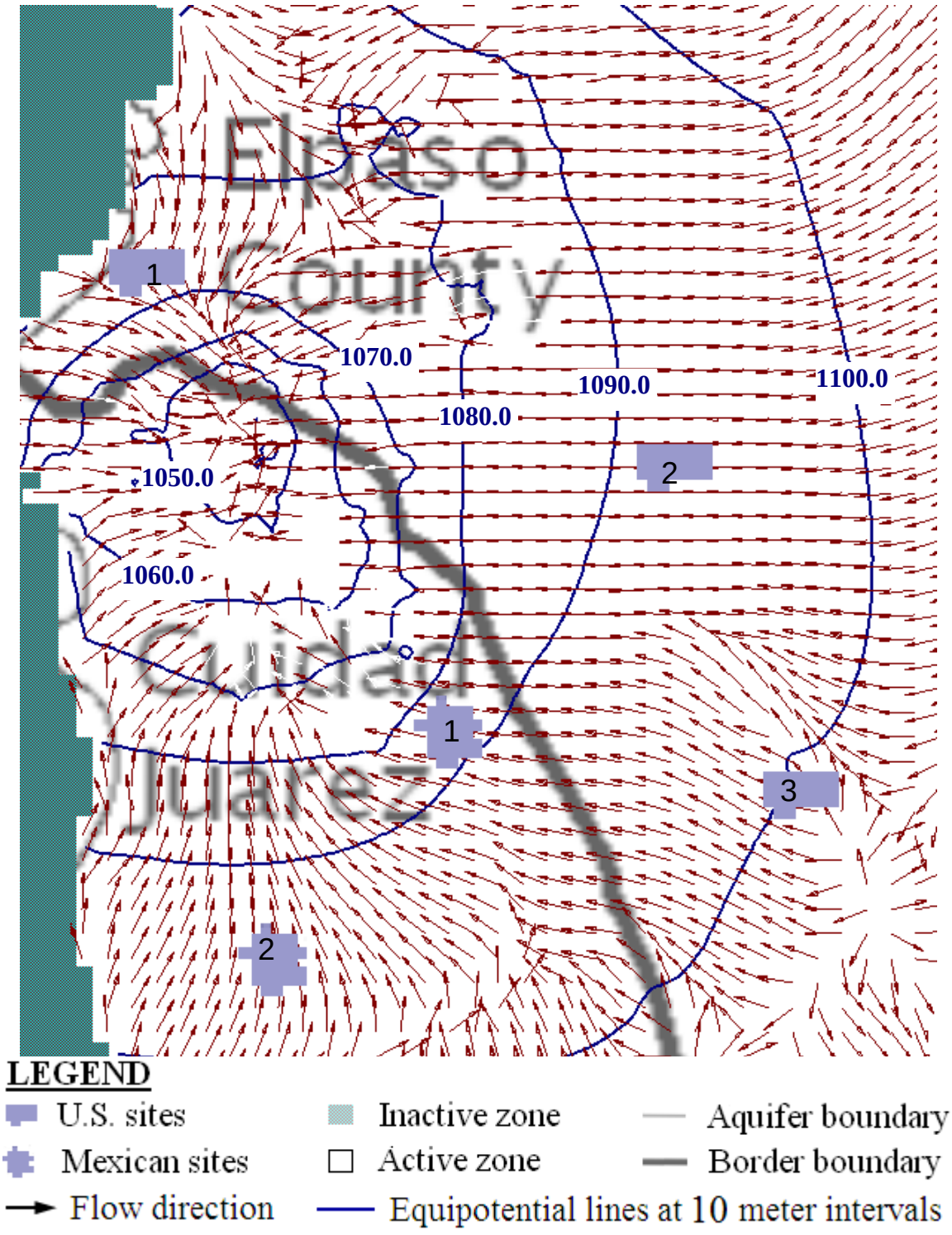

Fig. C- 6. Year 2025 heads and flow velocity direction for model layer 3

2050 VELOCITY DIRECTION PROFILES: LAYER 1, 2 AND 3

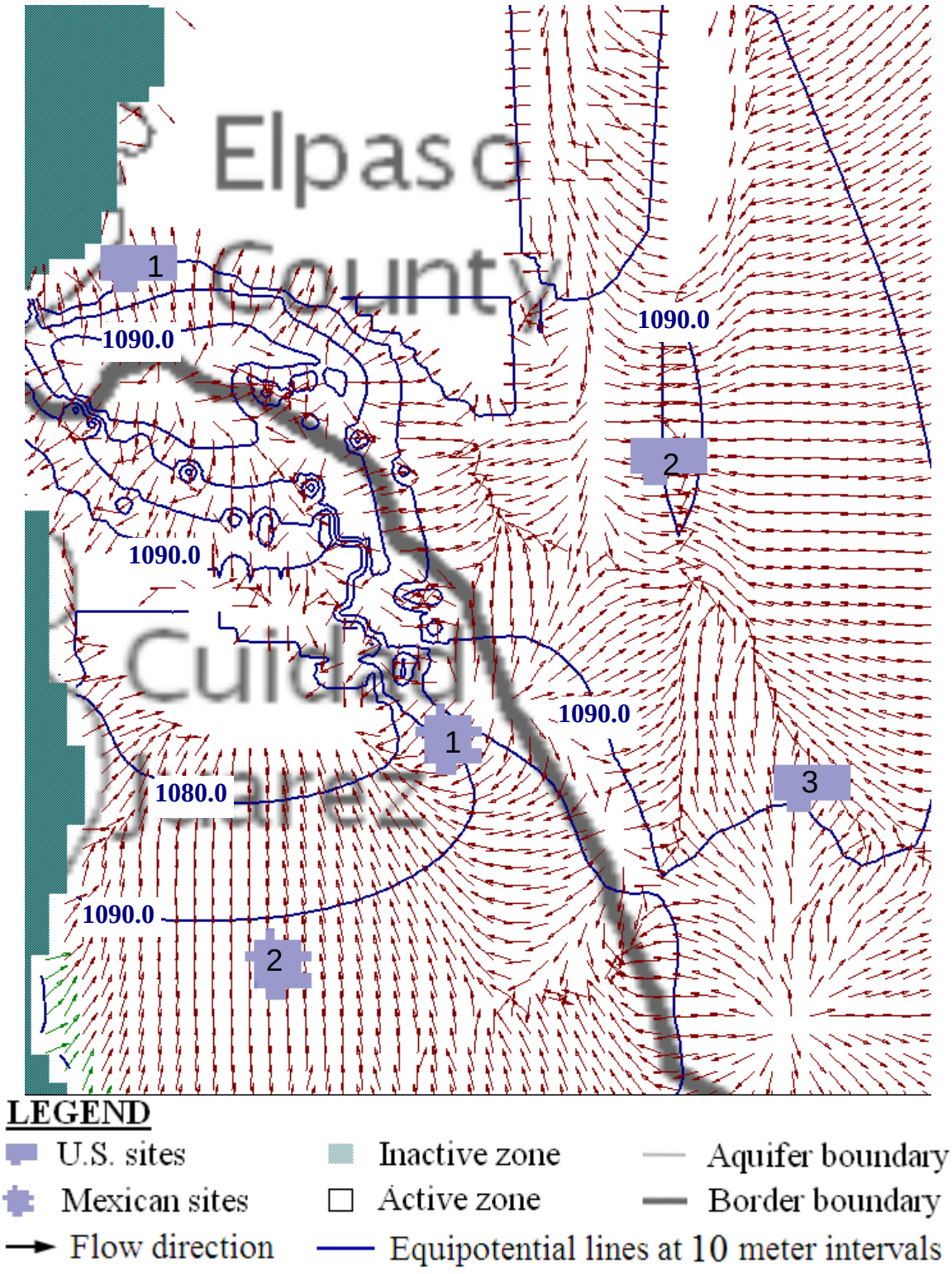

Fig. C- 7. Year 2050 flow velocity direction for model layer 1

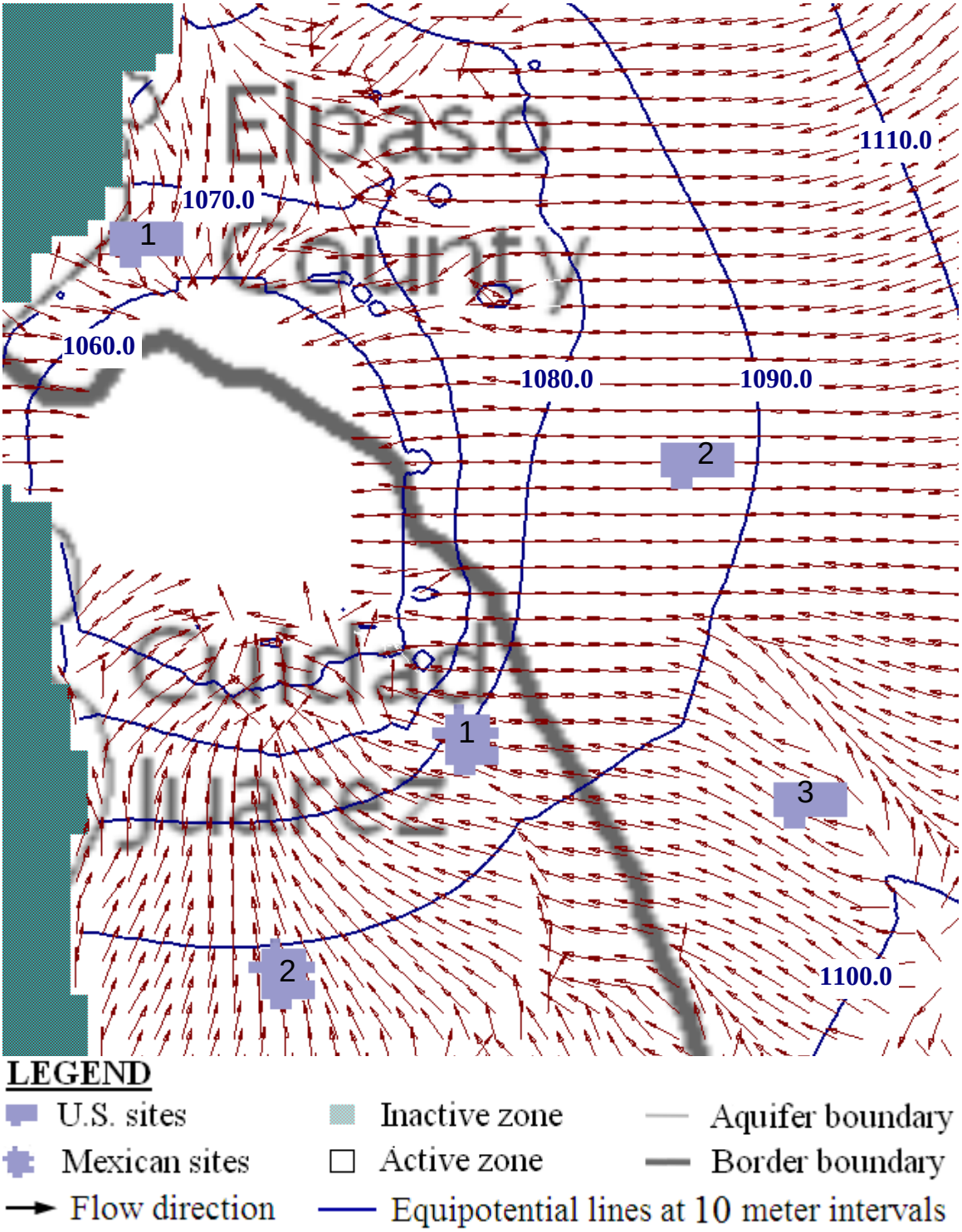

Fig. C- 8. Year 2050 flow velocity direction for model layer 2

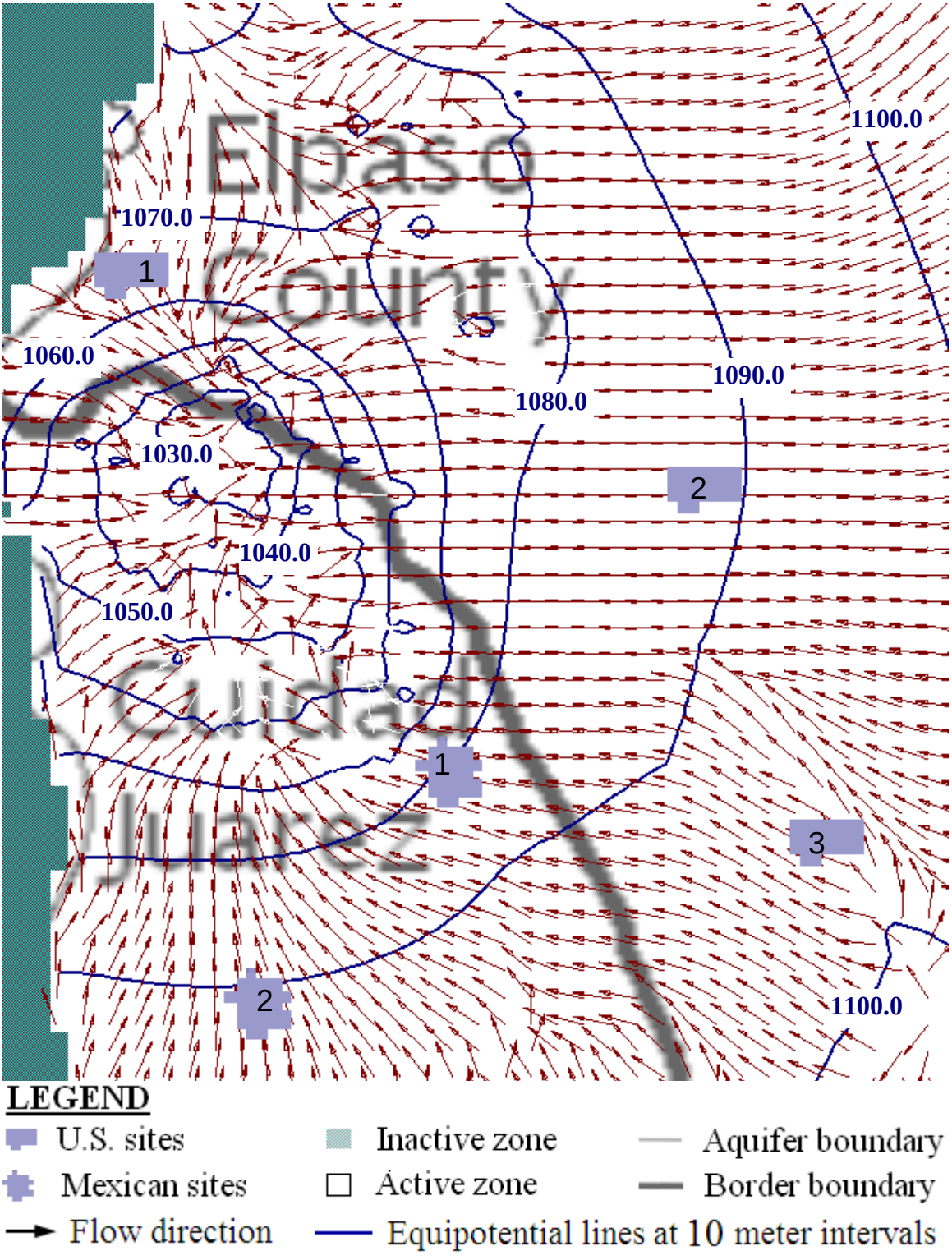

Fig. C- 9. Year 2050 flow velocity direction for model layer 3

APPENDIX D

WATER BUDGET RESULTS

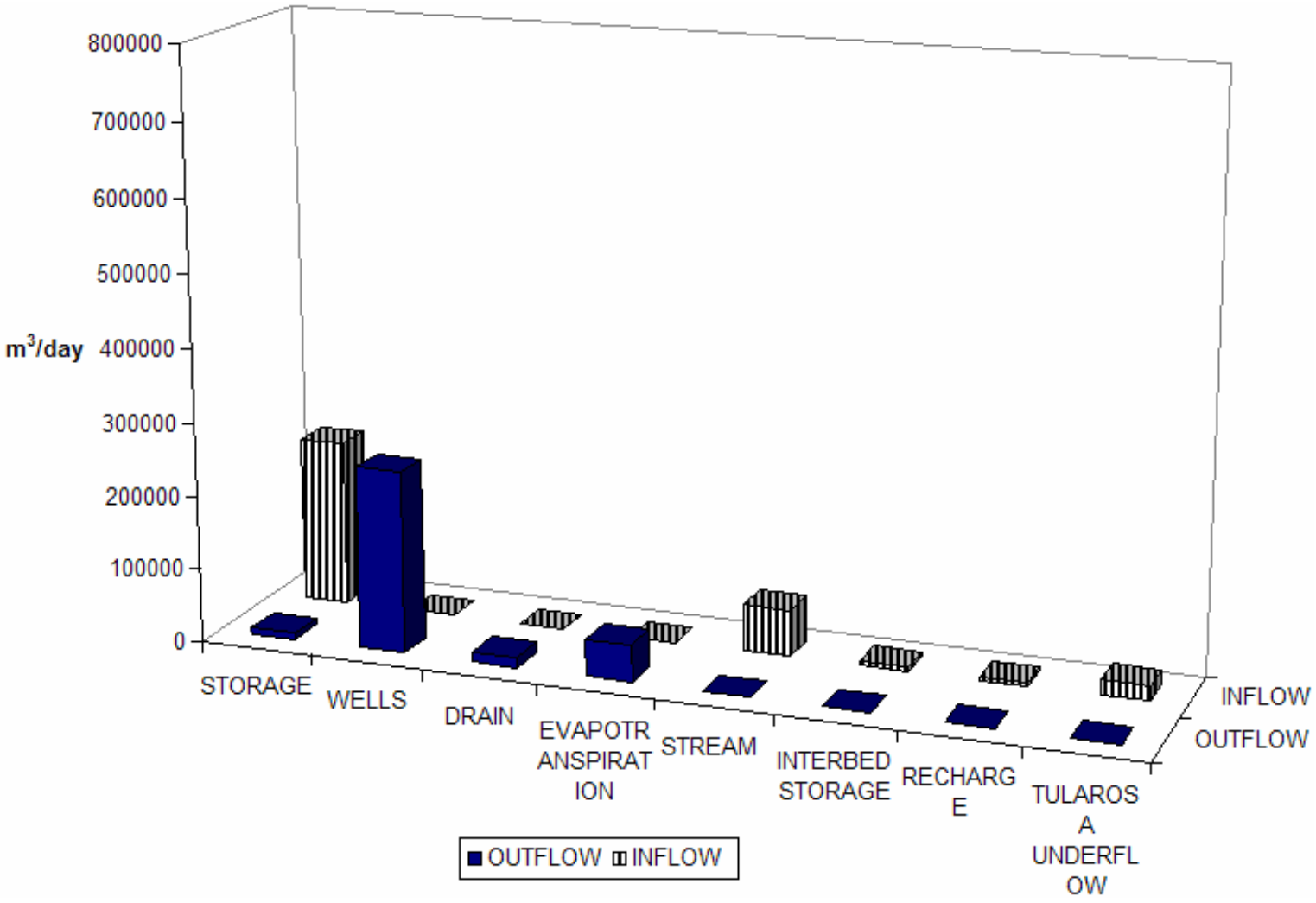

Fig. D- 1. Water budget inflow and outflow components for 1965.

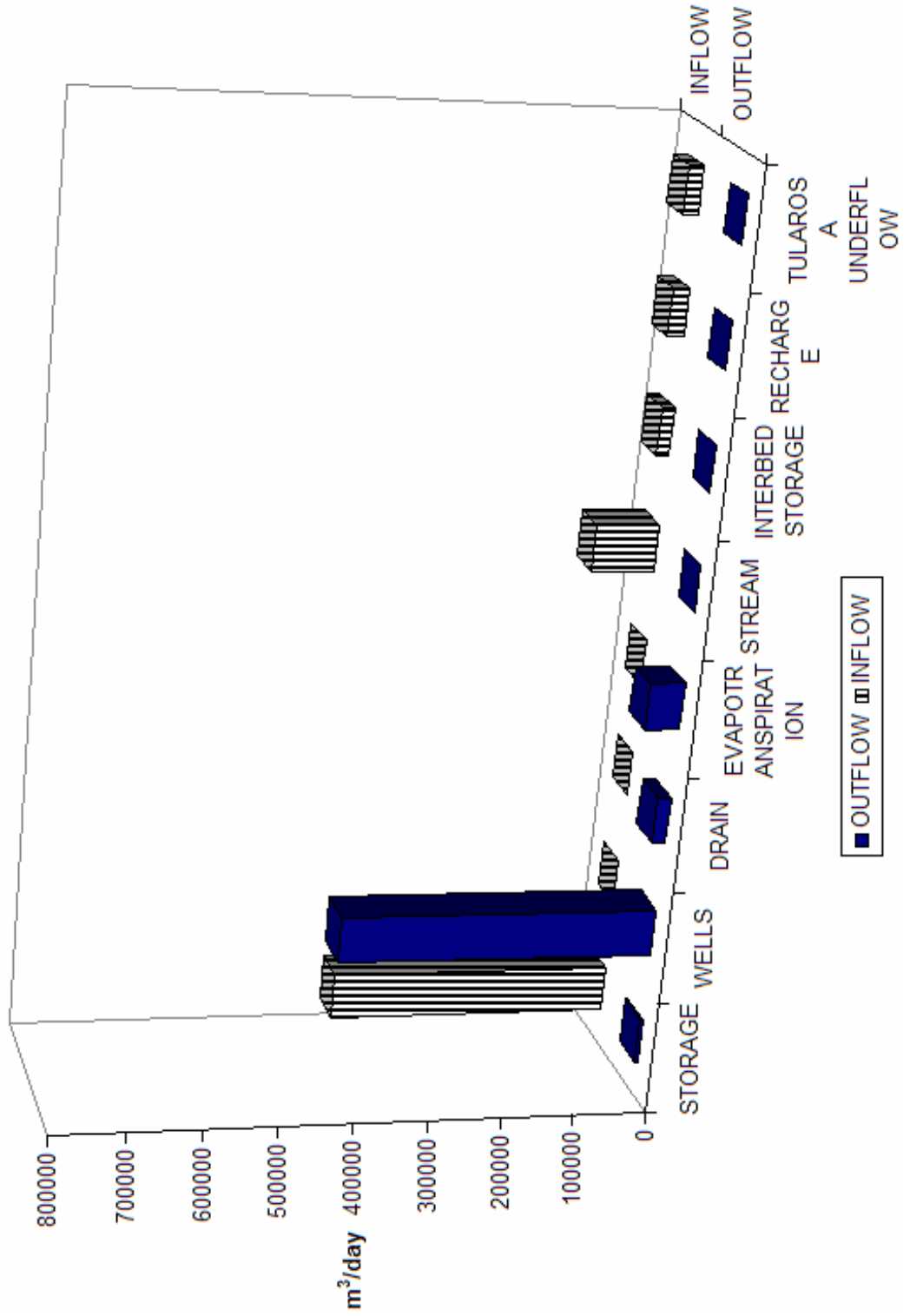

Fig. D- 2. Water budget inflow and outflow components for 1978.

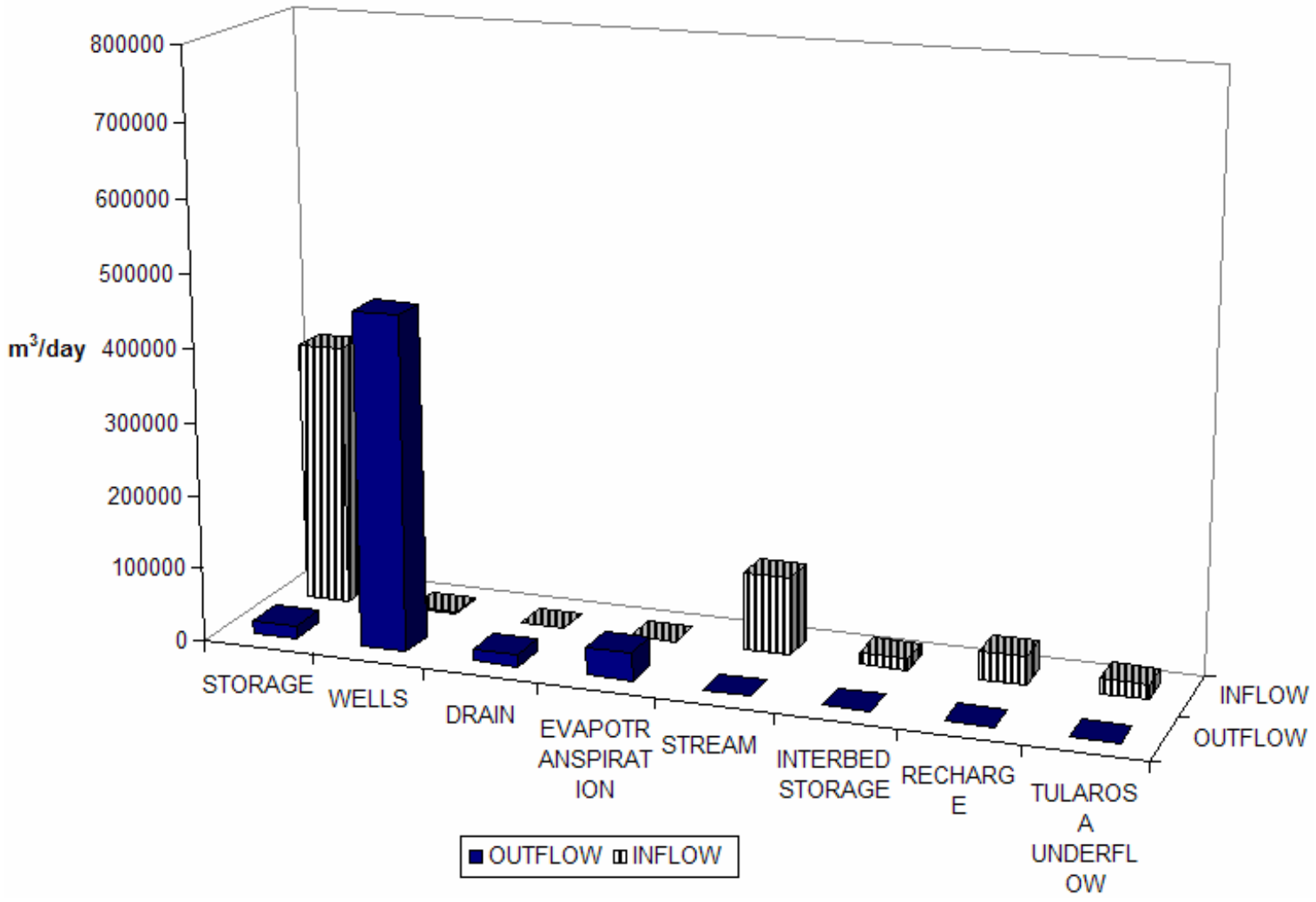

Fig. D- 3. Water budget inflow and outflow components for 1996.

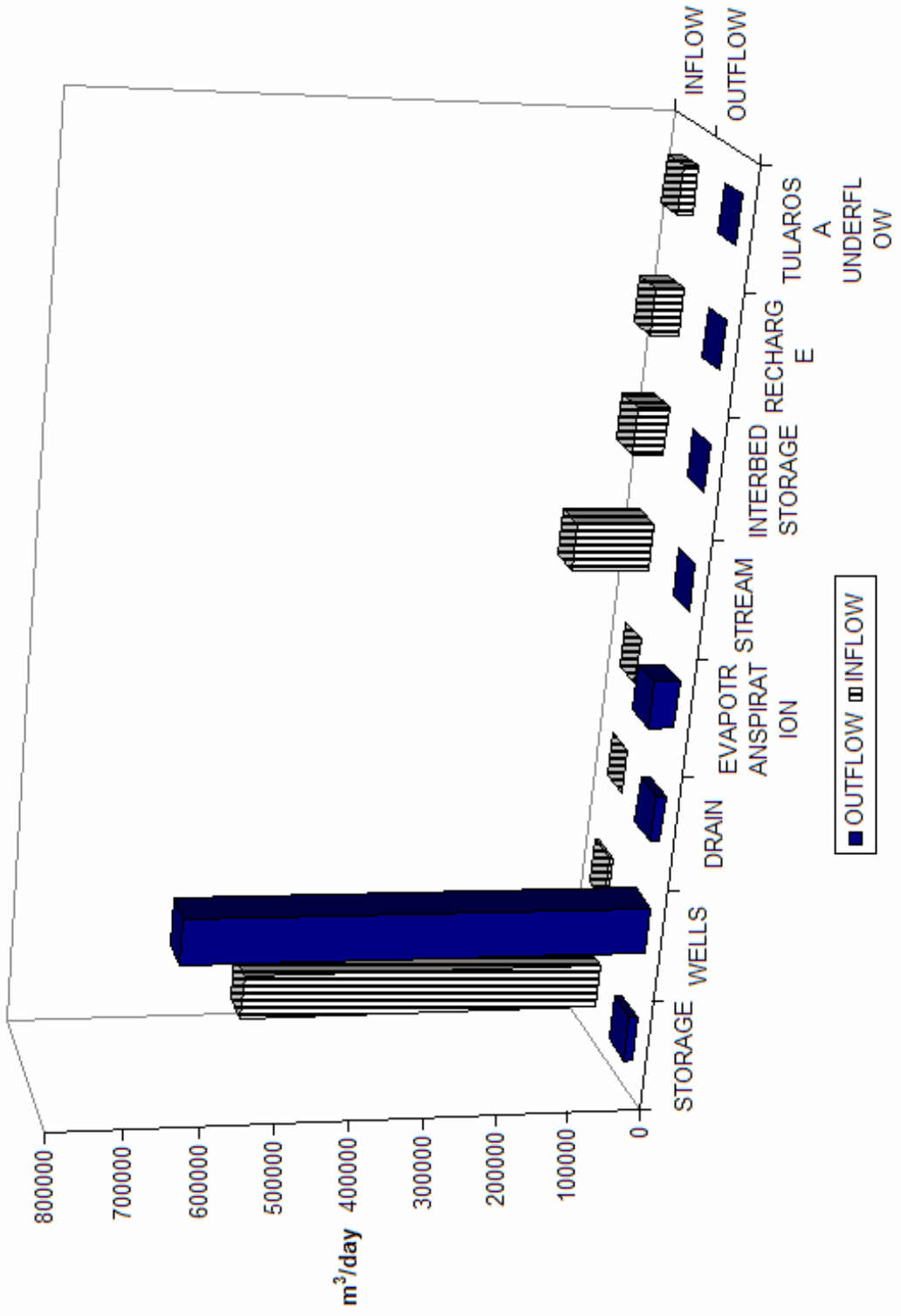

Fig. D- 4. Water budget inflow and outflow components for 2032.

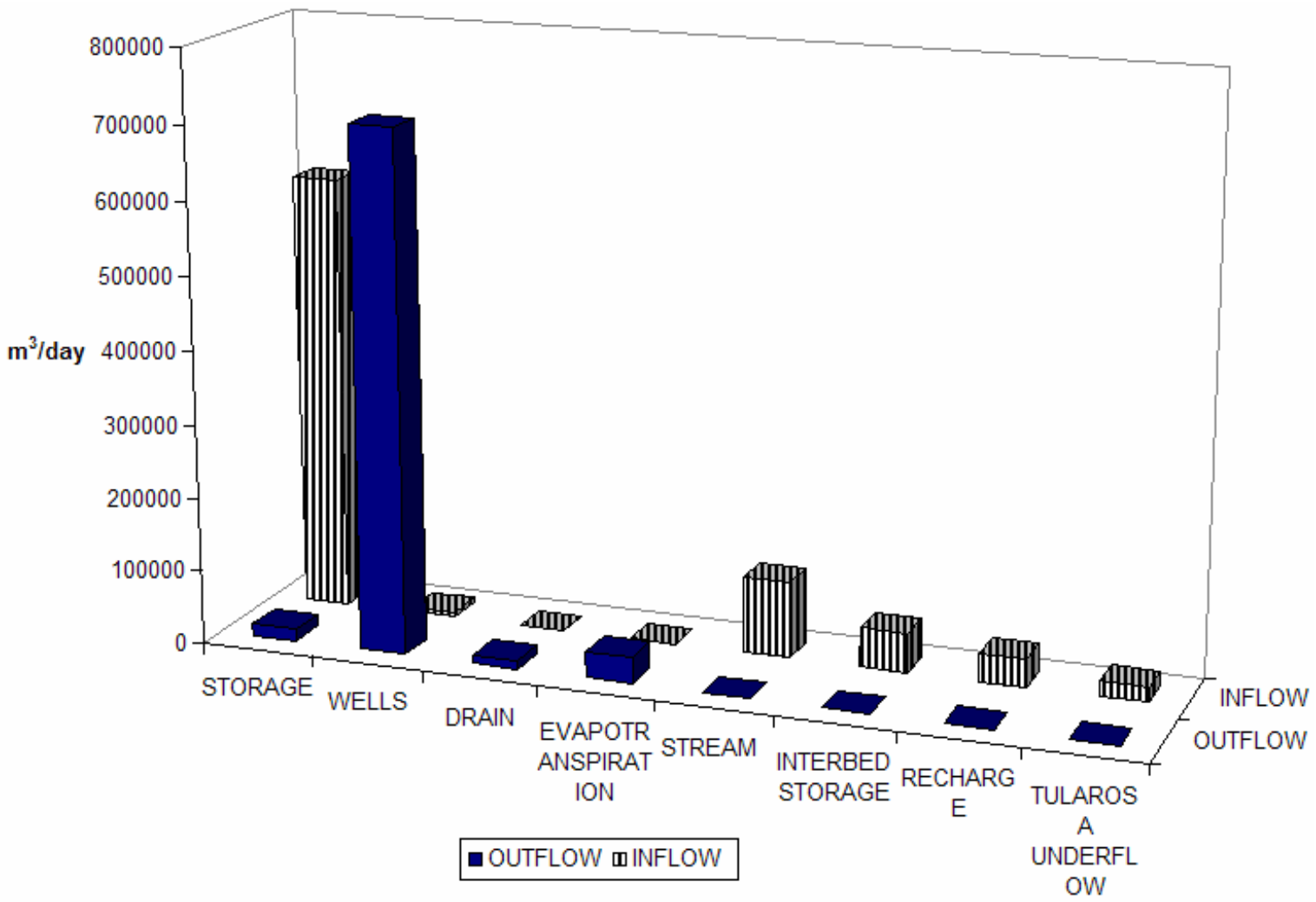

Fig. D- 5. Water budget inflow and outflow components for 2050.

VITA

Okechukwu Nwaneshiudu (Oke), was born in Nigeria, Africa and came to Philadelphia, Pennsylvania, at a very young age, where he grew up, attended, and completed junior and senior high schools in the William Penn Wood School district in Lansdowne, Pennsylvania. Mr. Nwaneshiudu began his college career at Temple University in Philadelphia where he successfully completed his Bachelor of Science in civil engineering in 2002. He then proceeded to obtain his M.S. and Ph.D. degrees at Texas A&M University in environmental engineering and water management and hydrological sciences in 2004 and 2007. In addition to his successful academic career experience, he has also completed several internships at the Shell Oil Company in the Environmental Engineering / Health Safety and Environmental areas and other co-ops and internships in the construction industries. Mr. Nwaneshiudu has completed several research projects in environmental assessment, analysis, and modeling with publications either completed or in progress. Mr. Nwaneshiudu maintains general interests in the fields of energy, environmental remediation, planning and modeling of surface and groundwater water recourses, fate and transport modeling, environmental risk assessment, energy, research, and development. He can be reached at, Department of Civil Engineering, 3136 TAMU, College Station, TX 77843-3136, USA.